N O T I C E

THIS DOCUMENT HAS BEEN REPRODUCED FROM MICROFICHE. ALTHOUGH IT IS RECOGNIZED THAT CERTAIN PORTIONS ARE ILLEGIBLE, IT IS BEING RELEASED IN THE INTEREST OF MAKING AVAILABLE AS MUCH INFORMATION AS POSSIBLE
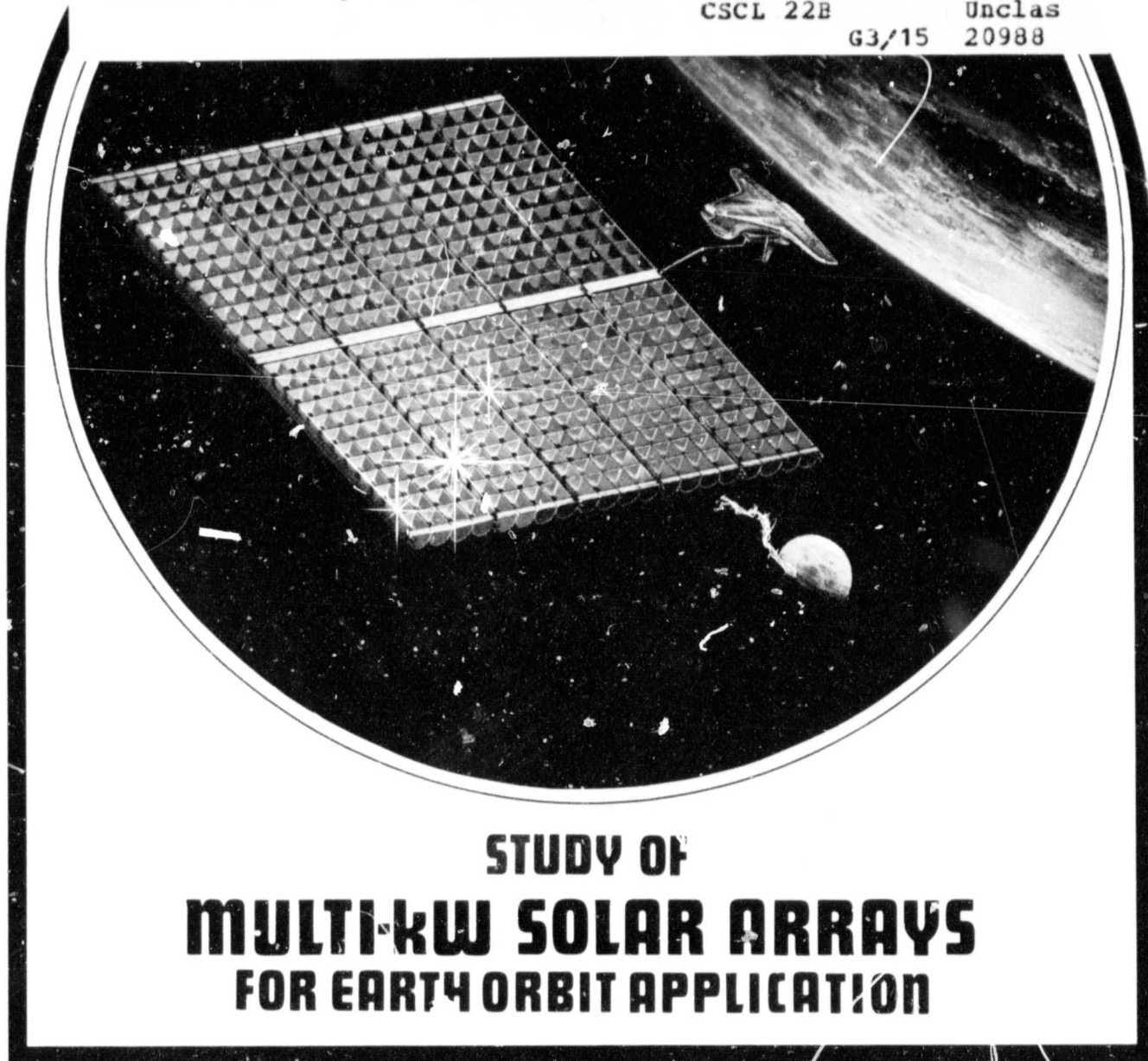
NASA   LOCKHEED

STUDY OF
MULTI-kW SOLAR ARRAYS
FOR EARTH ORBIT APPLICATION

Lockheed   MISSILES & SPACE COMPANY, INC.   SUNNYVALE, CALIFORNIA

prepared for:

MARSHALL SPACE FLIGHT CENTER

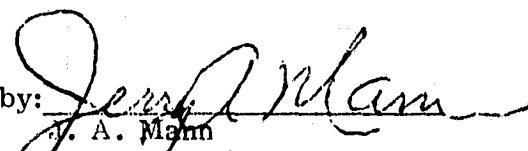National Aeronautics and Space Administration

NAS8-32981

NASA-MSFC STUDY OF
MULTI-KW SOLAR ARRAYS
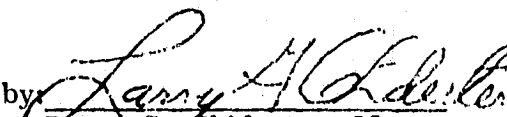FOR EARTH ORBIT APPLICATIONS

FINAL REPORT

April 1980

Approved by: J. A. Mann
Project Leader
NAS8-32981

Approved by: Larry G. Chidester, Manager
Electrical Power Systems

LOCKHEED MISSILES & SPACE COMPANY

FOREWORD

This report documents the work performed by Lockheed Missiles & Space Co., Inc., Sunnyvale, California, for Marshall Space Flight Center of the National Aeronautics and Space Administration under contract no. NAS8-32981 on the Multi-kW Solar Array for Earth Orbit Applications Study.

This report summarizes the full term effort performed on the subject contract over the period of 15 March 1979 to 30 April 1980. Planar and concentrator solar array configurations based on silicon and gallium arsenide solar cells were conceptualized and on-orbit maintainability was addressed. Comparison on-orbit cost to the customer was developed for each of the most promising solar array concepts.
L. Crabtree of the Astrionics Laboratory, Power Systems Branch of NASA/MSFC provided technical direction for this work.

CONTENTS

PRECEDING PAGE BLANK NOT FILMED

LOCKHEED MISSILES & SPACE COMPANY. INC.

CONTENTS (continued)

CONTENTS (continued)

LOCKHEED MISSILES & SPACE COMPANY, INC.

LIST OF FIGURES

LOCKHEED MISSILES & SPACE COMPANY, INC.

LIST OF FIGURES (continued)

LIST OF FIGURES (continued)

LIST OF TABLES

PRECEDING PAGE BLANK NOT FILMED

LOCKHEED MISSILES & SPACE COMPANY. INC.

LIST OF TABLES (continued)

LOCKHEED MISSILES & SPACE COMPANY. INC.

STUDY OF
MULTI-kW SOLAR ARRAYS
FOR EARTH ORBIT APPLICATION

Section 1

Introduction

NASA   LOCKHEED

1.0   INTRODUCTION

1.1   STUDY OBJECTIVES AND DEFINITIONS

Much interest has been generated in large space power systems for a variety of scientific, space base and public service platform missions since the advent of the Space Station concept in 1972. Since that time many relatively large photovoltaic power systems ranging from 10 to 100 kW have been studied with the SEP (Solar Electrical Propulsion) solar array being the only concept to gain flight hardware status. It is appropriate to continue advanced thinking and make the next "step beyond SEP" array technology for conceptualizing larger systems with the experience of today and the prognostication of 1983 technology.

Numerous studies to date have investigated the technical feasibility and comparative cost effectiveness of individual technologies, such as improved silicon cells, GaAs cells, reflector configurations and materials, terrestrial cell processing technologies, etc. The results, while encouraging, were too fragmented to serve as definitive design/development guidelines for the multi-kW space photovoltaic systems which are presently envisioned at NASA for the mid-1980's. Clearly, a systems-level approach was needed at this time. The outcome was a study contract issued in March 1979 by Marshall Space Flight Center (MSFC) to conceptualize a multi-kW solar array system for earth orbiting application whose technology was based on 1983 readiness. This study had two principal tasks:

> Task 1 - To identify by trade study the preferred low cost planar and
>   concentrator solar array concepts.

> Task 2 - To identify on-orbit maintainability conditions and constraints
>   which will enhance low cost power generation.

The output of the study was to conclude with a recommended solar array system capable of producing 300 to 1000 kW at low cost in $/watt/life for 1983 technology readiness. The purpose of this
generated to characterize and select a cost effective solar array power system which in turn will provide answers to certain fundamental questions concerning the use of space concentrators:

1-1

- Are concentrating systems actually more cost effective than planar arrays after considering the increased effort involved in providing adequate structural support, deployment mechanics, and thermal control?

- What energy-cost goals are achievable for various concentrator design concepts?

- Under which conditions will GaAs systems offer cost advantages over silicon systems and can these conditions be achieved for the envisioned mission time-frame?

1.2 STUDY GUIDELINES

General NASA guidelines were given as target parameters for the study:

- Baseline power level – 300 to 1000 kW

- Recurring cost of $30/watt or less

- 3 to 8 year component life

- EVA on-orbit maintenance of life-limiting components

- Practical configurations compatible with Shuttle cargo bay volume and weight and on-orbit operations

- Technology readiness by 1983

- LEO applications

Specific guidelines for Task 1 - trade study between planar and concentrator solar arrays and associated technology were:

LOCKHEED MISSILES & SPACE COMPANY. INC.

- Consider foldup/rollup/erectable systems

- Identify practical concepts for planar and concentrator configurations but examine in depth only the leading planar and concentrator arrays

- Examine both silicon and gallium arsenide solar cell present and projected performance. Consider application of large area, low cost terrestrial cells.

- Consider modular concept configurations.

- Evaluate disposable/returnable considerations.

- Prepare trade study to qualify advantages/disadvantages of planar vs concentrator solar arrays.

Specific guidelines for Task 2 on-orbit maintainability were:

- Identify component lifetime. System lifetime shall not be limited by critical component(s).

- Define on-orbit maintainability and the constraints it places upon the mission.

- Identify one or more concepts for accomplishing 300 to 1000 kW for Low Earth Orbit (LEO).

- Generate specific power and cost estimates

- Recommend a preferred concept for further definition and study.

Reporting

The basic contract required one midterm and final oral presentation and the submittal of a final written report. This was later revised by the contract extension to include an additional midterm and written report. All trade studies, analyses, cost data and recommended technology and system concepts for further development in compliance with the study guidelines are included within this report.
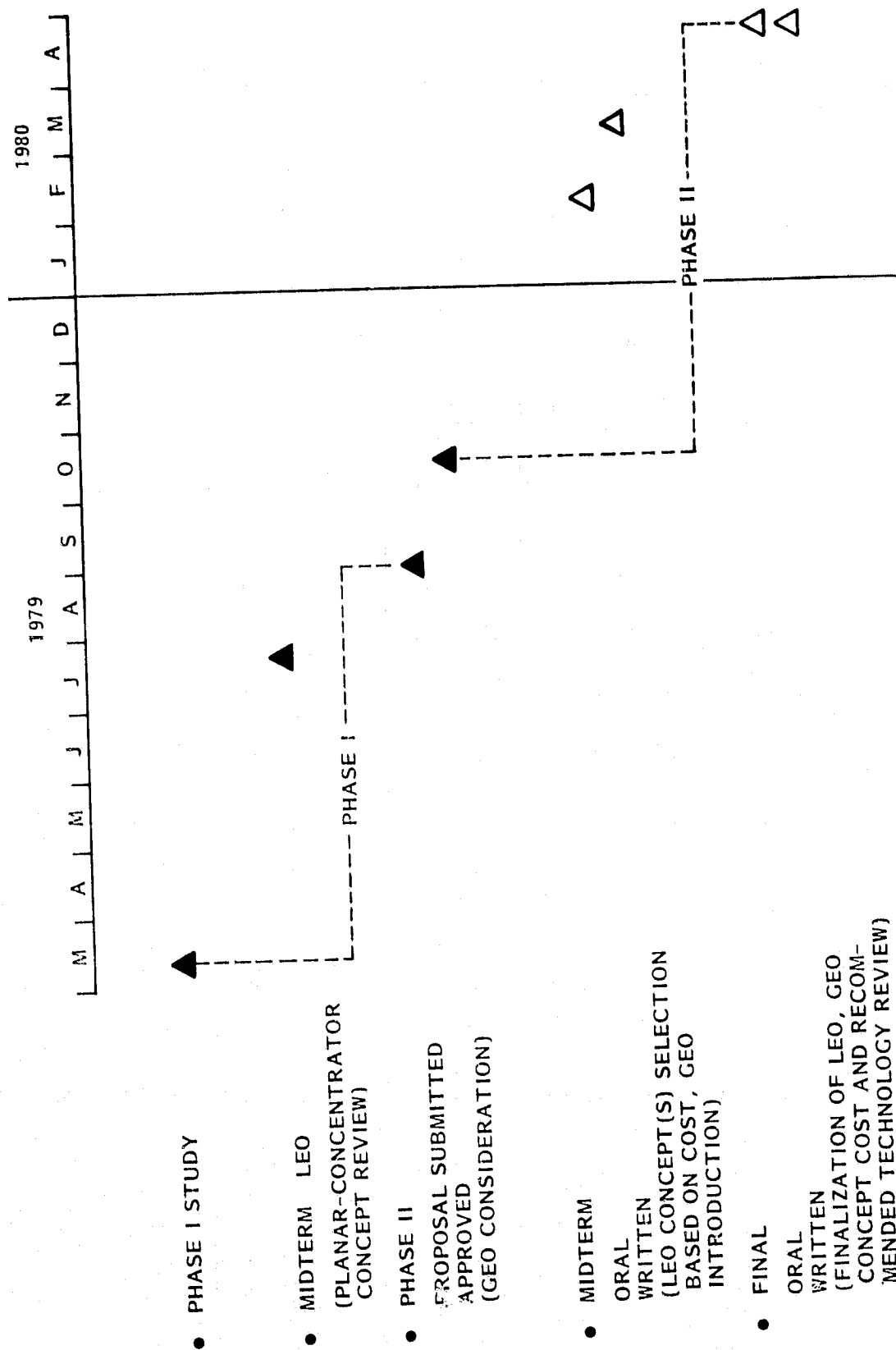
Figure 1-1 Multi-kW Solar Array Study Overview

LOCKHEED MISSILES & SPACE COMPANY

1.3   STUDY SCHEDULE

The term of the basic contract was six months beginning in mid-March 1979 and concluding in September 1979. Shortly after the midterm in July 1979, each contractor was invited to rebid for additional study money that was available to conduct further in-depth analysis necessary to validate the costing effort.

A proposal was submitted on 31 August 1979 for the additional six month study extension and was accepted with a go-ahead on 12 October 1979. As a result of the extension the September final oral and written reports were postponed and a second midterm oral and written report were added. The extension phase also added the new requirements of evaluating the recommended LEO configurations for GEO application and, if required, optimization specifically for a GEO.

Secondarily, the extension required an in-depth thermal analysis of the concentrator concepts and present and projected GaAs and silicon solar cell cost and performance information. Figure 1-1 depicts the time span and schedule relationship of the two phases.

The midterm report was intended to status the study as of the 5 February midterm oral date. This final report will review in depth the tradeoffs conducted, concepts selection, and cost comparisons reached. Recommended technology development required to support the selected design concept will also be discussed.

1.4   STUDY PROJECT ORGANIZATION

The Lockheed team was formed from experienced members of the Electrical Power Systems group managed by L. G. Chidester. The Multi-kW Solar Array Study project is managed by Jerry Mann with Bill Woodcock as technology task leader and Marty Gandel as on-orbit maintainability task leader. Dan Lott has been responsible for the inhouse related technology. See Figure 1-2. This team has been intact during the entire course of the contract to assure proper continuity. Inhouse technical specialists in fields such as thermodynamics, drag make-up, LEO to GEO propulsion systems, etc. have been used as necessary throughout the study term.
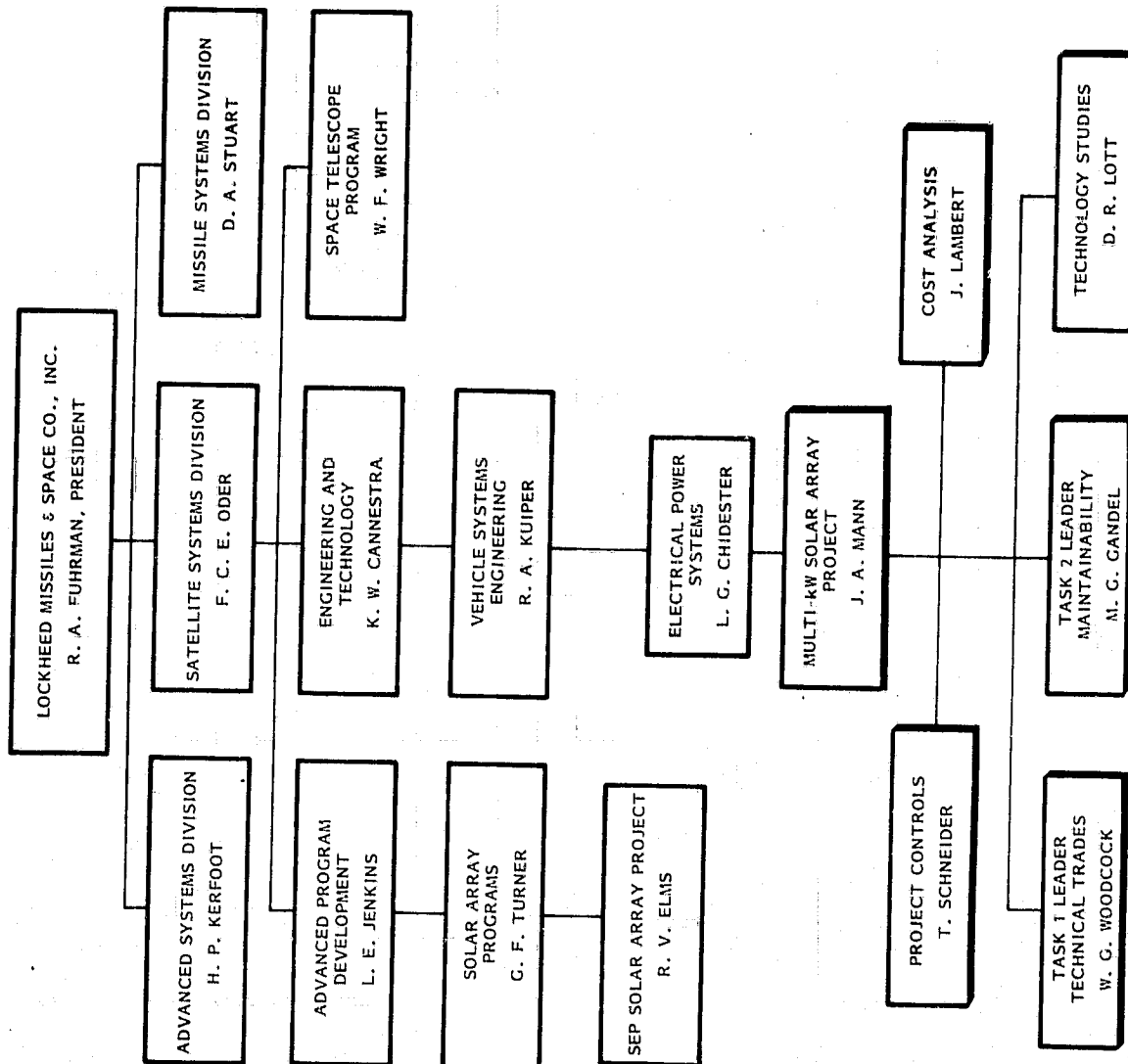
Figure 1-2 Project Organization

1.5 PROGRAM LOGIC FLOW DIAGRAM

In any task where all cost related aspects must be considered to optimize a design concept, a logic flow plan becomes a necessity. LMSC has developed such a plan as shown in Figure 1-3 from which the solar array concepts for both LEO and GEO were configured, performance evaluated and cost derived. Many of the characterizing technologies are common to planar or concentrator and LEO or GEO configurations. Maintainability, orbit environment, orbiter constraints, and growth techniques can be common and unique to specific configurations. The description of these elements of design will be discussed as each solar array configuration is developed.

1.6 SUMMARY OF STUDY

The purpose of the study was to develop workable designs that demonstrate practical concepts without resorting to exotic approaches.

Related inhouse studies and hardware programs and review of pertinent literature provided the background source for the various concepts developed. In order to accentuate the performance differences among several basic system alternates, three levels of concentration were selected based upon the performance characteristics of either silicon or gallium arsenide cells.

Four basic array categories emerged:

1. Planar (non concentrated) with silicon cells
2. Low-CR (concentration ratio = 3.4) with silicon cells
3. Low-CR (concentration ratio = 3.4) with GaAs
4. High-CR (concentration ratio = 62.5) with GaAs

A very High-CR (concentration ratio = 200) was investigated but rejected on thermal grounds.

Shuttle weight and volume (length and width) limitations have been the stimulus for creative thinking in folding and stowing of cell blankets and support and deployment structure. Modular elements evolved with folding blankets and reflectors for the
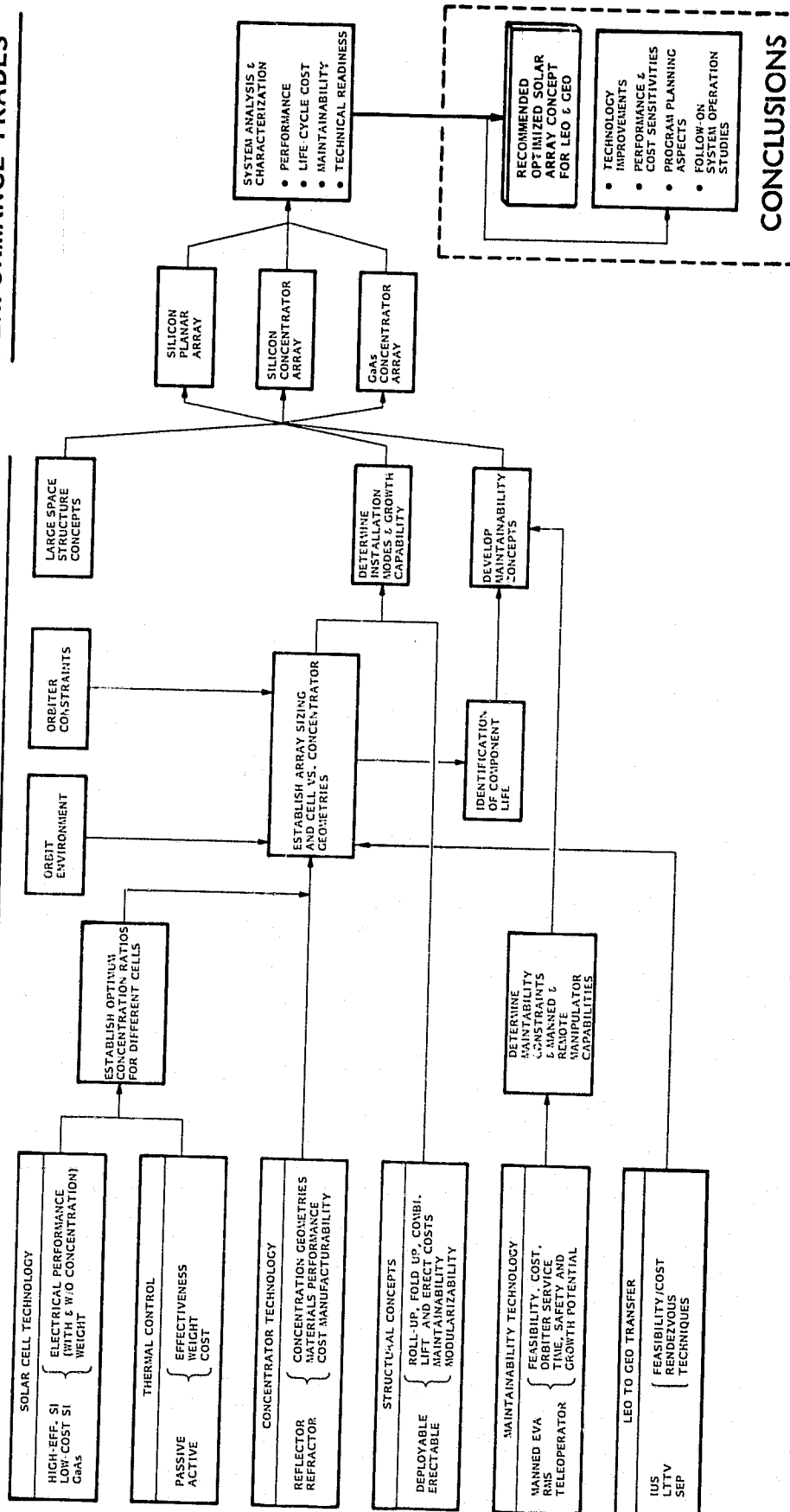
Figure 1-3 Study Logic Flow Diagram

planar and Low CR configuration and spool wraparound reflectors for the Cassegrainian design. The basic deployment structure and mast mechanism was designed to be compatible with the Planar and the Low CR arrays thus simplifying and optimizing a single attractive concept.

Large area wraparound silicon solar cells, 5.9 x 5.9 cm (8 mil) with 0211 (6 mil) covers, bonded with FEP Teflon were selected for common use with either the planar or low CR arrays. The advantage of using large area solar cells over the conventional size cell, 2 x 4 cm, is a 2:1 cost advantage. Further advantage comes from reduced assembly cost of large cells.

The gallium arsenide cell suggested for use in the 1983 time frame is 2 x 2 cm, 12 mils thick. The identical covering used for the silicon cell is recommended.

Once the basic on-orbit maintainability constraints were established the solar array design was implemented. Minimum use of EVA is recommended for the planar and the low CR arrays where self-deployment was feasible. The individual High CR module is also self deploying with the requirement that module clustering must be accomplished by two RMS's with EVA backup. Orbital life extension beyond 1979 technology depends on selection of materials and the use of creative design. LMSC suggests that 15 years is within the realm of 1983 technology. Therefore, non-recurring and recurring cost elements for each of the four concepts selected were compared over a 15 year life cycle. Under conditions where the gallium arsenide cells can be produced for less than $25 per 2 x 2 cm, the Low CR concentrator emerges as the most cost effective configuration. However, the producibility risk remains higher on the gallium arsenide cell.

LEO concept configuration cost and performance summary is shown in Table 1-1.

LOCKHEED MISSILES & SPACE COMPANY

TABLE 1-1
LEO COST AND PERFORMANCE SUMMARY

LEO Concept	Relative Cost	$/Watt	Avg. Power-Watts
Low CR – GaAs	1.00	326	437
Planar – Silicon	1.18	393	311
Low CR – Silicon	1.35	484	380
High CR – GaAs	1.95	736	384

Increased price is based on multiple shuttle launches required.

Specifics relating to both LEO and GEO solar array concepts and conclusions are presented herein.

GEO concept considerations were limited to the Planar Silicon and the Low CR Gallium Arsenide which yielded the highest on-orbit power and the lowest cost per watt. See Table 1-2 for system cost and performance comparisons.

TABLE 1-2
GEO COST AND PERFORMANCE SUMMARY

GEO Concept	Relative Cost	$/Watt	Avg. Power-Watts
Low CR – GaAs	1.00	516	231
Planar – Silicon	1.09	564	206

Dollars per watt (LEO to GEO) increased by approximately 50 percent due to two prime factors: a) added cost of orbit transfer and (b) GEO weight transfer limitation which reduced solar array average delivered power.

The Low CR GaAs configuration, therefore, is the recommended solar array concept. Problems that need to be resolved with GaAs deal more with producibility than technically. Resolution can come by careful and purposeful planning for GaAs in the next three years.

STUDY OF
MULTI-kW SOLAR ARRAYS
FOR EARTH ORBIT APPLICATION

Section 2

Task 1

Technology Trade Studies and Analysis

NASA   LOCKHEED
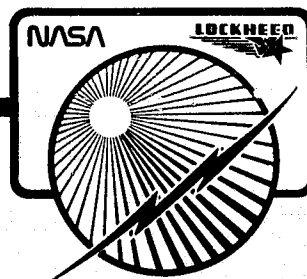
2.0 TASK 1 – TECHNOLOGY TRADE STUDIES AND ANALYSIS

2.1 BASELINE REQUIREMENTS

2.1.1 Shuttle Capability

The maximum Orbiter stowage volume for each multi-kW solar array case was developed using the constraints imposed by the airlock for EVA, the OMS-kit, the overall bay length shown in Figure 2-1, and as derived from the Space Transportation System Handbook. The Remote Manipulator System(s) (RMS) falls outside of the allocated 15 foot diameter payload envelope. Figure 2-1 displays two airlock location options; the airlock can either be located within the cabin or without. It is obvious that having the airlock within uses valuable cabin space; therefore, it may be located in the bay unless the cargo length precludes that.

The need for OMS kits is dictated by cargo weight, and orbit altitude desired as indicated in Figure 2-2, from the STS Handbook. The LEO altitude objective is 400-500 nm; therefore, OMS kits are planned, which limits useful bay length to 567 in. maximum if the airlock is in the cabin or 503 in. if it is in the bay.

GEO flights will use an IUS or other transfer stage from approximately 150 nm to GEO. In this case OMS kits, beyond the integral OMS tankage in the tail section of the Orbiter, would not be required. This allows a maximum cargo length of 674.5 in. which includes a Payload and Orbital Transfer Vehicle. EVA is recommended as a backup to an ejection mechanism or RMS for removal of the solar array/GEO-transfer-stage from the Orbiter. If EVA backup is considered to be an excessive conservatism then a full 718.5 in length could be available.

The design concepts developed all fall within the cargo weight and center of gravity constraints as stated in the STS Handbook. These requirements are most critical for landing conditions and can be relaxed where the cargo will not be returned with the Orbiter; however, a safety argument can be given for always having return capability.
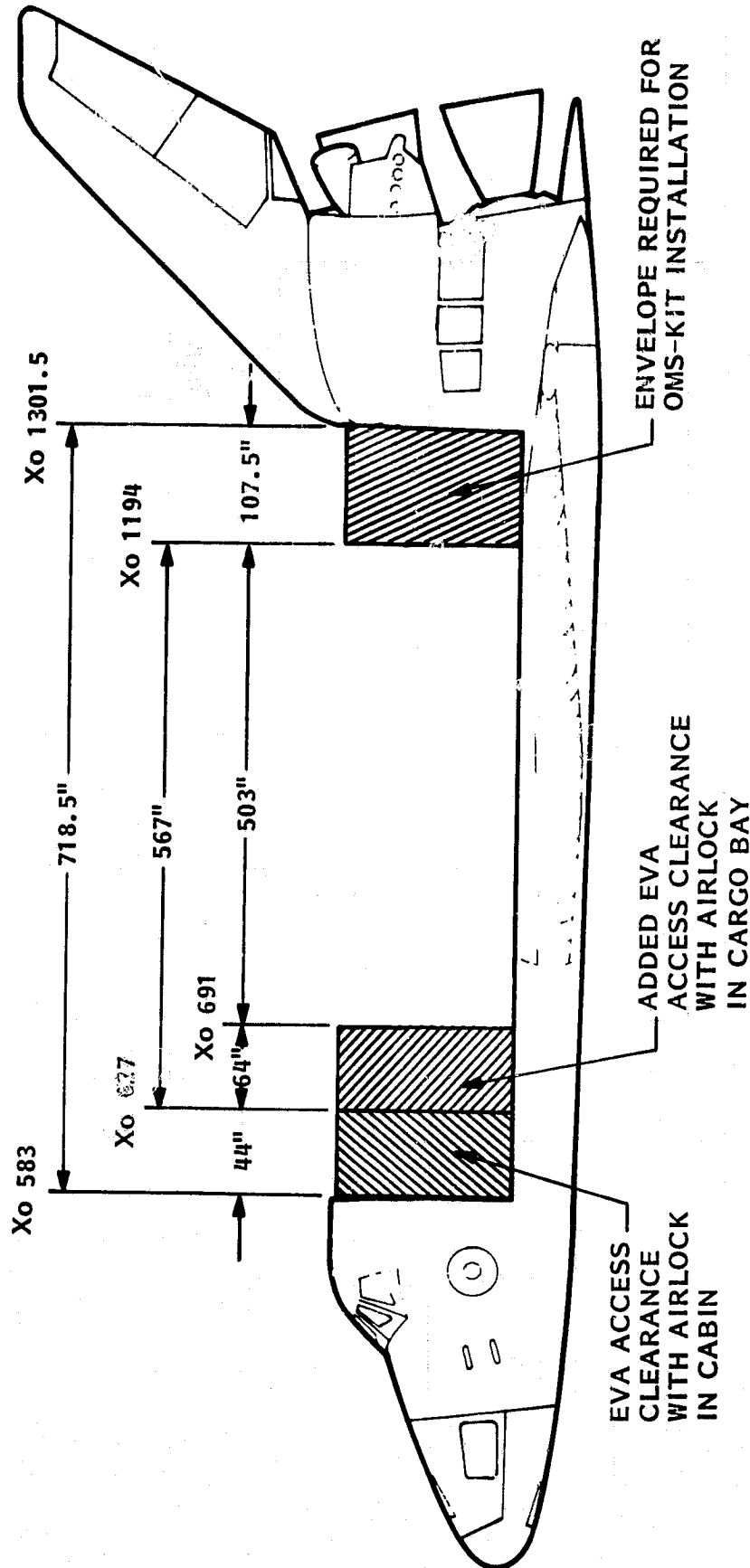
Figure 2-1 Maximum Orbiter Stowage Volume
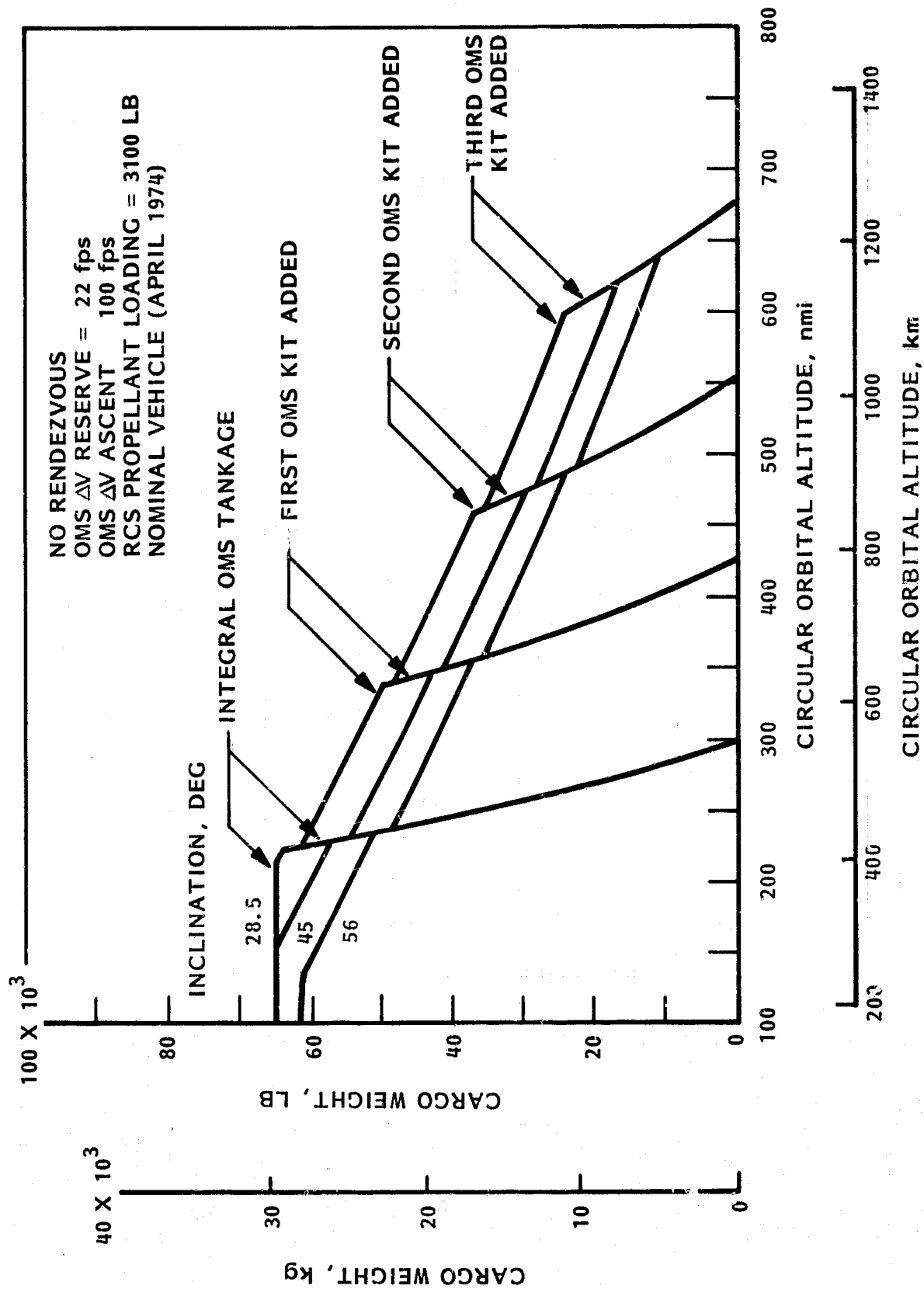
Figure 2-2 Space Shuttle Cargo Weight vs Circular Orbit Altitude
KSC Launch – Delivery Only

2.2   IN-HOUSE SUPPORT STUDIES

The major emphasis of the Multi kW Study is to develop a low cost ($/W-hr) system that can be delivered to space with a high confidence of meeting its goals.

Several aspects of the design could take a variety of avenues, some using the technology of today with known results and others where some portions of the technology need be further developed. Lockheed selected four areas where further study or material evaluation would benefit the multi-kW S/A. The objectives of these studies were to improve overall system performance at a reduced cost. Subcontracts were thus let with Spectrolab- Sylmar, Optical Coating Laboratory, Inc. (now Applied Solar Energy Corporation) - City of Industry, OCLI - Santa Rosa, and Varian - Palo Alto for the following:

   a)   Assess terrestrial cell technology transfer to advanced space cells – Spectrolab

   b)   Evaluate producibility, cost and performance of selective surface reflectors – OCLI

   c)   Evaluate advanced low cost cover technology – Spectrolab

   d)   Perform producibility, cost and performance status of gallium arsenide solar cells – Varian

In conjunction with these subcontracts, personal contacts and literature reviews were made for supplemental information. The overall approach used is shown in Figure 2-3.

2.2.1   TERRESTRIAL CELL TECHNOLOGY TRANSFER

The terrestrial cell has several interesting features which were evaluated to determine its applicability to the space cell. These features and their usefulness in producing space cells are summarized in Table 2-1.
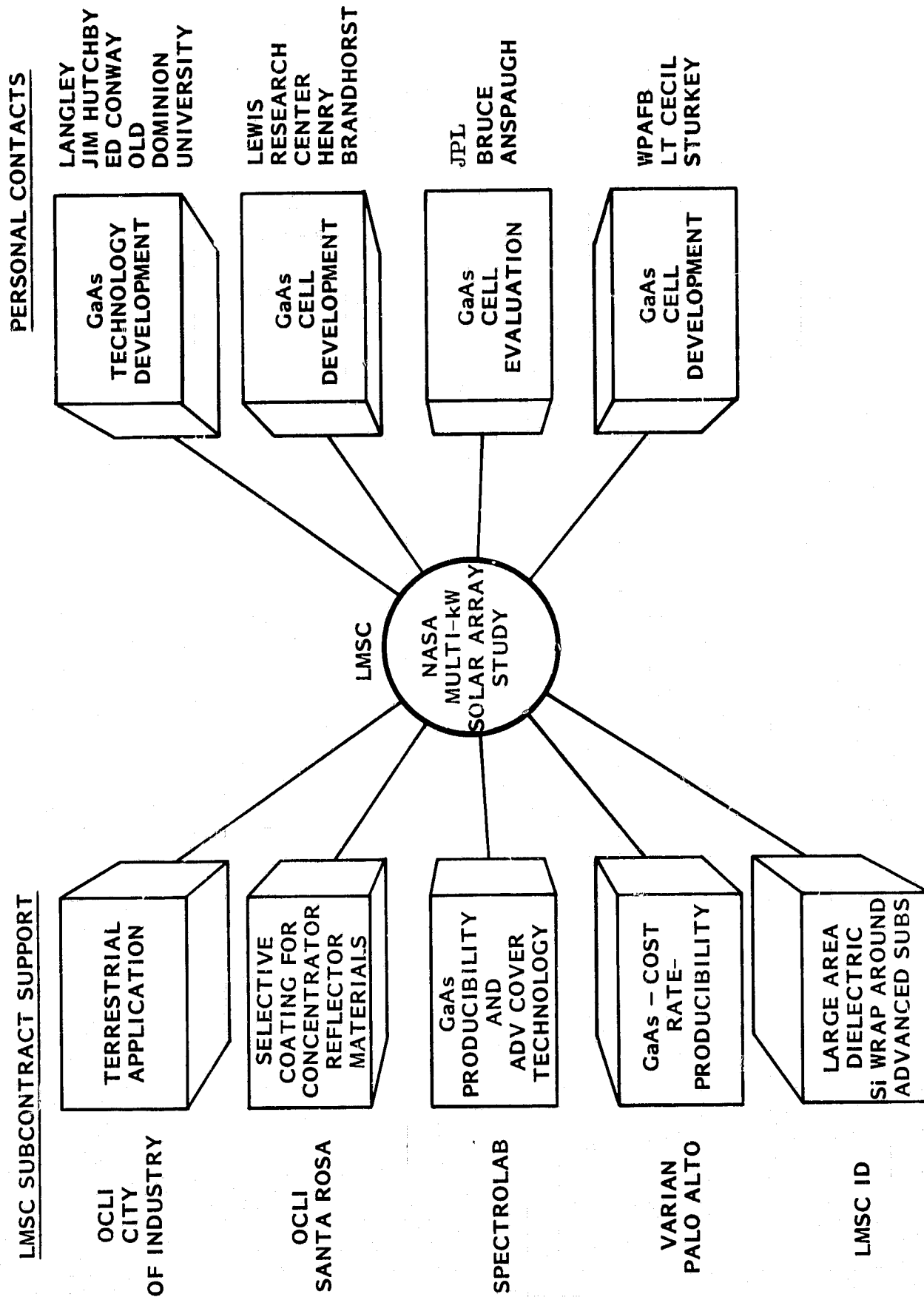
Figure 2-3 In-House Technology Studies

LOCKHEED MISSILES & SPACE COMPANY

TABLE 2-1

TECHNOLOGY TRANSFER SUMMARY

PROCESS	COMMENTS
• Large Area Cells	• Greater utilization of silicon ingot, lower cost, producibility demonstrated (up to 34 cm^2). Further environmental testing at blanket assembly level required.
• Low Cost Polysilicon	• Not available in time frame of study • Unknown BOL/EOL Efficiency

• Sheet Silicon
  – Cast Polysil
  – EFG Ribbon
  – Dendritic Web
	• Not yet competitive for BOL output or throughput

• Low Cost Contacts
  – Screen print pastes
  – Plating
	• Photomasking/electroplating not yet proven for long term stability. Need additional development

• Lower Cost AR Application
  – Spin On
  – Dip
	• Compatibility with space environment not known. Substantially lower cost should make them attractive for near term further development.

• Barrier (Junction) Formation
  – Ion implantation – laser annealing
  – Mis, inversion layer, heterojunction
	• Equipment not available in time frame of study
	• Output or cost advantages not demonstrated

• Simplified Specification	• Mechanical-cosmetic relaxation is practical

The obvious near term technology transfer with the greatest cost reduction potential is the large area cell. Higher utilization of the drawn ingot and fewer pieces to process has demonstrated a 50 percent cost reduction with an increase of 4 times the area--from a 8 cm^2 to a 34 cm^2 cell.

LOCKHEED MISSILES & SPACE COMPANY, INC.

Advantages and disadvantages are summarized for the large area cell.

Advantages

- Results in fewer piece parts through all process steps
- Higher packing factor is achieved for given array area
- Compatible with present trends in growing larger silicon crystals and processing larger slices
- Potential reduction of number of interconnects
- Can be used in combination with larger area, lower cost covers

Disadvantages

- Handling/use damage susceptibility not assessed at this time
- Cells may have to be thicker or used with stiffer substrate causing a weight impact

Conclusions:

LMSC recommends the use of large area silicon solar cells 5.9 cm x 5.9 cm (34 cm^2) wraparound cells with mechanical-cosmetic specification relaxation.

2.2.2   SPECTRALLY SELECTIVE REFLECTOR STUDY, SSR

The specific principle behind the spectrally selective or cold mirror is to reflect onto the cell the visible light portion of the spectrum where the solar cell is responsive (.35 to 1.1 microns) and become transparent where the energy is normally absorbed as heat by the cell. The technique for producing a cold mirror is accomplished by vacuum deposition of various metalization layers on a transparent film such as Kapton or Melinex. The optimum coating must be formulated according to the spectral response of the type of solar cell, silicon or GaAs, considered. The specific response for the cold mirror developed by OCLI, Santa Rosa, is shown in Figure 2-4 comparing typical cell responses of GaAs and Si under visible light (AM0).

It appears that the SSR as shown is optimized toward silicon rather than GaAs; however, taking into account temperature and power gain, GaAs is favored. The design goals established by OCLI for the SSR materials were:

2-7

Primary

- Net power gain over existing reflector materials
- Optimize reflectance/transmittance relative to solar cell response

Secondary

- Space stable
- Low cost

OCLI demonstrated the ability to modify their coating formulization to adapt to a specific cell condition and achieve a net power gain for the system. The trade, however, must be the correct balance between cell temperature and concentration ratio to achieve a net gain. The theoretical comparison between a typical aluminized Kapton reflector and the SSR can be seen in Figure 2-5 a and b. Higher concentration is achievable with the cold mirror and results in an increase in power capability for a unit solar cell. Independently, this appears advantageous; however, when looking for a low cost system reflector complexity and pointing accuracy required must be considered.

Simple reflectors of Al-Kapton and SSR materials were constructed for AM0 performance test comparison of silicon and gallium arsenide cells. The overall results are summarized as follows in Table 2-2.
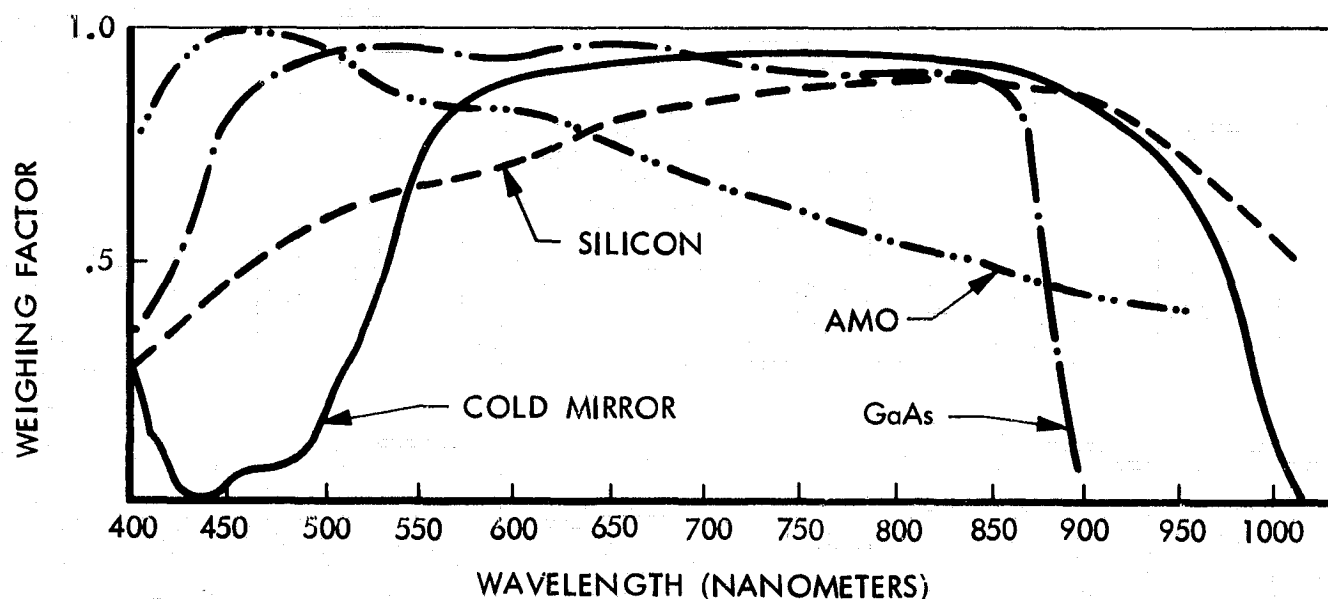
Figure 2-4   Spectral Response Comparison

2-8
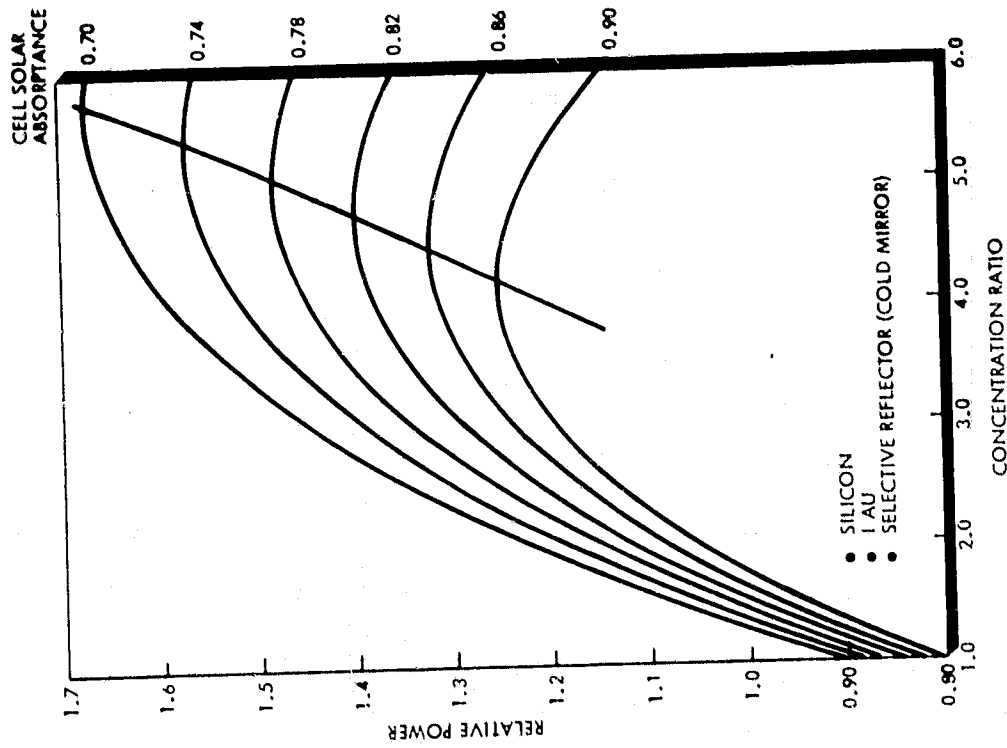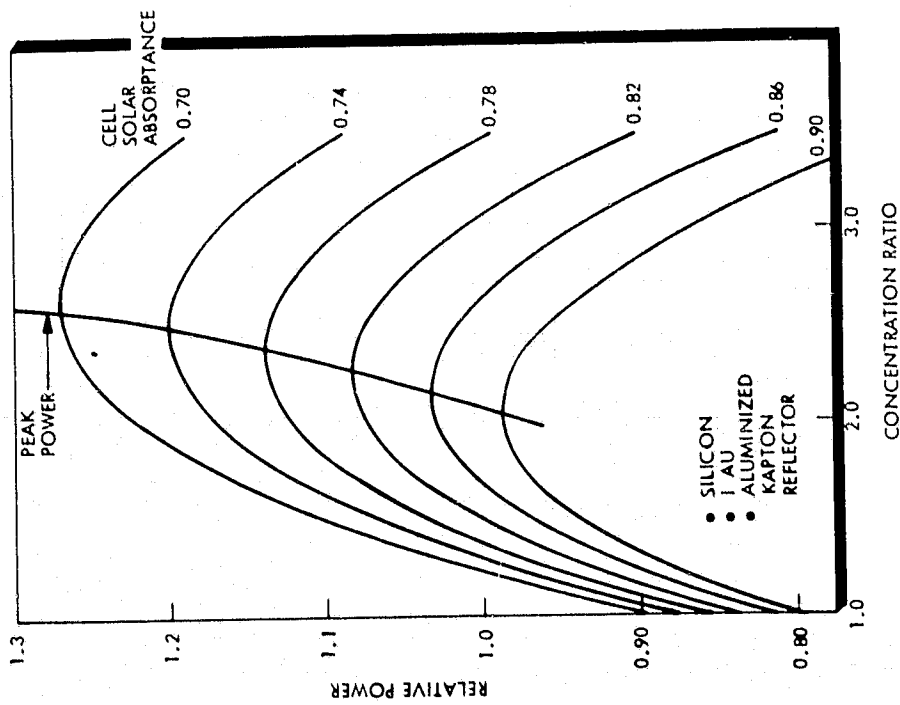
Figure 2-5   Relative Power of Aluminized Kapton and Cold Mirror Reflectors

LOCKHEED   MISSILES   &   SPACE   COMPANY.   INC.

TABLE 2-2
REFLECTOR MATERIAL SUMMARY

<u>Primary Results</u>

	Material	Coating	Cell Temperature °C	Power Gain
<u>Silicon</u>	Melinex	473*	80	1.55
	Kapton	Al	92	1.70
<u>GaAs</u>	Melinex	473	63	2.06
	Kapton	Al	69	2.07

SSR coatings favor spectral response of GaAs over silicon

- SSR demonstrated significant operating temperature reduction as compared to aluminized Kapton

- Analysis indicates SSR is more optimum for higher concentration

- Further development required to 1) optimize spectral response match between SSR and current solar cells and 2) improve incident angle compatibility with cell operating temperature

*Melinex 473 is the material/coating designation from OCLI.

<u>Secondary Results</u>

Radiation and UV testing was postponed as OCLI requested additional time to improve the coating formulation; however, several tests were conducted with the results summarized as follows:

- Passed humidity and adhesion tests
- Passed cloth rub abrasion
- Failed eraser rub test
- Passed 1000 thermal cycle test – 87°C to +82°C

The cost for producing Melinex 473 at the rate of 10,000 m^2/week is $10/$m^2$ and is comparable to Al-Kapton.

Lockheed recommends the use of SSR material for the primary reflectors for the Low and High CR concentrators.

2.2.3   LOW COST SOLAR CELL COVER STUDY

Spectrolab, Sylmar, California, was issued a subcontract to investigate low cost
candidates for near-term and advanced solar cell covering materials and bonding
techniques. This data would be reviewed for its value in terms of usefulness to the
multi kW study. Three near term cover materials emerged as reasonable candidates.

- 0211 microsheet (processed edges to relieve work stresses due to sawing)
- As cut fused silica (7940)
- Ceria doped microsheet (CMS)

FEP teflon was recommended as a cover bonding adhesive for use in the 1983 time
period. FEP offers several advantages as a low cost bonding material over the
conventional DC 93-500. Shelf life is infinitely long as compared to DC 93-500
and it does not degrade under UV exposure. Labor cost to install FEP is lower and
it eliminates the expense of clean up typical of DC 93-500. A disadvantage with FEP
is that once the cure is complete it is impossible to separate the cover and cell in
the event of a damaged or mispositioned cover.

Coverglass AR coatings for the purposes of this study were not considered cost
effective and were not dealt with as a cost factor. Spectrolab did, however, suggest
that further evaluation of Motorola's development of low cost surface-acid etched
or sodium silicate dip AR coatings be considered.   Additional bonding adhesives
and integral cover materials were suggested but would require continued concentrated
development before they could be considered for this application.

The cost of a covered assembly (less cell cost) in $/watt for three cover materials,
three sizes, four thicknesses and 300 and 1000 kW quantities was estimated. A
summary of the results of the study as shown as follows:

- CMS, 93-500 - most expensive combination ⎫
                                              ⎬ 5.5:1
- 0211, Teflon - least expensive combination ⎭
- Coverglass material thickness has relatively little effect on cost
- Larger area covers (5 x 5 cm and larger) are less costly than conventional
  size -- greater attrition requirement included
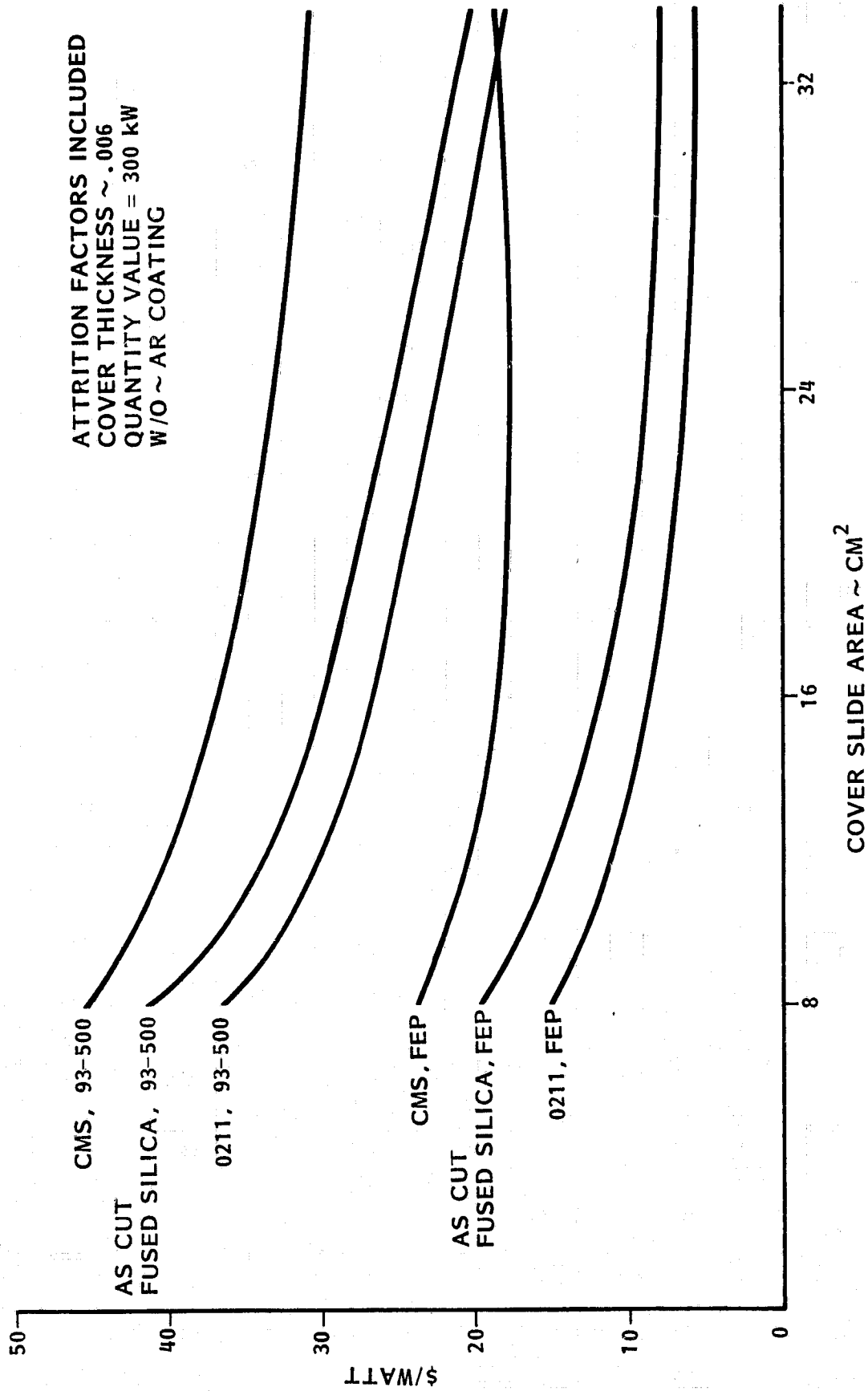
Figure 2-6 Coverslide/Labor/Adhesive Costs

LOCKHEED MISSILES & SPACE COMPANY

- Conventional AR coatings are not cost effective – should consider evaluation of new low cost AR applications
- Automated coverslide installation may decrease bonding labor by factor of 5

A cost comparison of various cover/adhesive combinations vs coverslide area for 300 kW quantity and .006 thick cover material is seen in Figure 2-6.

Conclusion:

Lockheed recommends the use of 0211 microsheet bonded with FEP Teflon. The practicality of this seems most promising. However, it is also realized that appropriate confirming tests be conducted.

2.2.4   GALLIUM ARSENIDE (GaAs) COST AND PRODUCIBILITY STUDY

The merits of the GaAs solar cell have been widely lauded. A review of published cell characteristics would lead one to favor GaAs cells over silicon if they can be produced at a competitive price. GaAs cell advantages make a good case for their use in concentrator arrays, since reflector area is inexpensive (if not too complex) with respect to solar cell area.

Comparing silicon with GaAs the advantages become obvious. See Table 2-3.

TABLE 2-3
GaAs AND Si CELL PERFORMANCE CHARACTERISTICS

	GaAs	Si
• Cell Efficiency 1979	16%	12.8%
1983	18%	14.0%
• Cell Performance f(t)	-.17%/°C	-.5%/°C
• Normalized Power Degradation*		
LEO - 7.5×10^{14} e/cm^2	29%	30%
GEO - 3.0×10^{15} e/cm^2	44%	45%

*EOL Orbital Environment

The relatively low annealing temperature of + 200°C is an additional GaAs bonus as reported in the 14th Photovoltaic Specialists Conference by E. Conway, NASA MSFC. This is within the cell operating temperature in a High CR concentrator. Constant annealing would greatly increase the average power over 15 years and thus reduce the BOL solar array size. Silicon annealing is in the 400°C range which is well beyond its normal operation.

The other side of GaAs is that all data has been taken from non-production-proven laboratory samples. Consequently the cost is high, $500 per 2 x 2 cm cell, and the quantity low. Within industry great interest exists in developing the GaAs solar cell to the point of price competiveness with silicon. The request to evaluate both GaAs and silicon initiated a literature search to determine what really had been accomplished and what was the prognostication for its application. Table 2-4 summarizes the research conducted.

To supplement what was available, Lockheed contracted Varian Associates, Inc. of Palo Alto, California to conduct a 6 month study to establish present and projected 1983 performance and cost of GaAs and to project the effort required to produce such a cell. Varian has had previous experience in gallium arsenide and is already under contract to build and demonstrate refractory-type concentrators, CR=400, focusing on a 1/2 inch diameter GaAs cell of their design and fabrication.

Their contract consisted of two tasks:

Task I: To develop a cell modelling program establishing size, contact design and performance

Task II: To develop the cost of unassembled/assembled cells for quantities of 300 and 1000 kW, assuming a 24 month production span

Results:

Varian optimized their theoretical GaAs cell by developing 29 parameters which define the cell characteristic. A combination of calculations, assumptions and given inputs were considered in the program. Iterations were made until the optimum cell configuration and relative performance were determined for a CR = 125 and 50.

TABLE 2-4

GALLIUM ARSENIDE SOLAR CELL TECHNOLOGY

Sponsor	Supplier	Effort	Comments
WPAFB	Hughes	Cell Development	• 18 percent demonstrated, 20 percent goal • Cost reduction via 8 cell build sets • See hardening – high temp advantages • Future eval flights on NTS-3 and GPS
JPL	Hughes		• JPL eval 30 Hughes cells $800 each • Electron irradiation and annealing tests • Concern on AR coating and contact stability
LMSC	Hughes		• LMSC eval Hughes cells $500 each • 3SR concentrator tests planned
LMSC	Varian	Cell Performance	• Support study for multi-kW
DOE	Varian	Terrestrial Application	• Concentrator cell for Sandia Labs • 23 percent at 300 CR, active cooling
PG&E	Varian	Terrestrial Application	• Terrestrial application for substation
LeRC	MIT	CVD Processes	• Aimed toward lower cost • Jell cost conclusions in 3 years
LMSC	Spectrolab	Study	• Assessment of near term reduction to practice - Device fragility problem - 2.29 x the weight of silicon cells - Need for additional development

LOCKHEED MISSILES & SPACE COMPANY. INC.

TABLE 2-4 (continued)

Sponsor	Supplier	Effort	Comments
LRC	IBM	Cell Development	• Efficiency improvements
	Old Dominion U	Characteristics	• Photovoltaic and Degradation parameters • Spectral response versus temperature
	Carnegie Mellon U	Processes	• Evaluation of MOCVD growth
	A. D. Little	Study	• Cost and producibility on thick GaAs
	-Internal-	Research	• LPE and graded bandgap GaAs cells
Rockwell	Rockwell	IR&D	• LPE work with 18 percent cells • MOCVD on sapphire or GaAs substrate

LOCKHEED MISSILES & SPACE COMPANY, INC.

The work was extremely useful in optimizing a GaAs cell; however, some of the assumptions such as effective CR and cell surface temperature differ from the Lockheed concentrator configurations and could not be used directly.

The important conclusion is that Varian is confident that this solar cell can be produced by the mid 1980's at the present level of effort. A focused, concentrated effort could greatly improve that date.

A comparison of GaAs and Si is interesting and bears out the projection that gallium arsenide holds a definite advantage under high concentration.

- Optimized cell for CR of 125 (100% efficient reflector)

  Cell efficiency* = 14.3% at 175°C (GaAs)

  = 5.8% at 175°C (Silicon comparison)

   *orbital operating conditions

Varian's cost factors were based on the following conditions:

1. 24 months of production beginning in 1983
2. Cell size .8 x 3.0 cm cut from a 1.25 x 1.25 inch wafer
3. Average cell output = 90% of derived theoretical cell efficiency (23.4%)
4. 60.5% yield
5. Capital investment including process equipment and additional floor space
6. 1979 dollars were used but 1983 technology assumed

The cost quotes were for bare cells and cell assemblies. A bare cell was defined as unfiltered after one-sun testing. The cell assembly consists of attaching the cell to a cell support structure, interconnecting and installing a coverglass. The cost also included a 15% attrition from bare cell to cell assembly.

- Cost in $/watt (1983 cell - 1979 dollars)

	300 kW	1000 kW
Cell Assemblies	41	28
Bare Cell	19	13

- Capital Investment - 2.0 to 4.0 million (300 to 1000 kW)

LOCKHEED MISSILES & SPACE COMPANY, INC.

2.3   KEY DESIGN TRADE STUDIES

2.3.1   Concentration Methods (Reflection vs Refraction)

The design of a concentrator system, unlike that of a planar system, must initially address a choice between fundamental alternatives concerning the manner in which concentration is achieved as well as the degree of concentration desired. For space photovoltaic systems there are two practical methods of achieving concentration-- refraction or reflection. The refraction method involves placing lenses in front of the solar cell assemblies; the reflective method involves placing reflectors around the solar cell assemblies.

The use of lenses poses a fundamental dilemma to the designer of a space system. The efficiency of a lense--i.e., the ratio of incident energy to transmitted energy can be quite high for traditional quartz or glass-type lenses. However, the material density and refractive shapes of such lenses lead to systems of prohibitively high weight. Stowage of such traditional lenses into available launch vehicle volumes also becomes a problem, especially for high-CR (concentration ratio) systems.

The requirements for low-weight and low stowage volume virtually mandate the use of plastic-type lenses. Gas-inflatable plastic lenses and thin plastic Fresnel lenses have been contemplated most often in this regard. Plastic lens materials have been the subject of extensive investigations for terrestrial systems. Efficiencies of plastic Fresnel lenses range from approx. 70% - 75% for low concentration (~1.5 - 2.0) to 30% - 40% for high concentration (100 - 200), which make them 10% - 50% less efficient than reflectors, depending upon CR. In addition, many of the materials which are suitable for terrestrial use can be expected to degrade in efficiency upon direct exposure to the space environment. Since thin-foil reflectors (i.e., first-surface metallized plastic foil) exhibit superior efficiencies and more stable material properties, all concentrator design work for this study was performed on reflecting systems.

Although the ultimate design of a concentrating system must reflect a thorough parametric optimization of system concentration ratio in terms of performance, weight, and cost, less emphasis was placed upon this optimization for the present study. The study objective was not to "design-out" a system but rather to identify basic design categories and to optimize them to a degree which permits a clear trade-off among candidate categories.

An inherent decision-driver for the selection of categories is the performance of candidate solar cell types under concentrated light. Silicon solar cells, for example, exhibit a marked decrease in power output with increasing temperature. Thus Si-cells are limited to usage at relatively low concentration ratios. In contrast, GaAs solar cells exhibit significantly less sensitivity to elevated temperatures and are thus particularly suited for usage at high concentration ratios.

Not only from a standpoint of cell type suitability, but also from a standpoint of types of structural configurations needed to achieve various degrees of concentration, a natural threshold has evolved in the concentrator field between low-CR systems (CR $\leq$ 10) and high-CR systems (CR $\geq$ 10).

Figure 2-7 shows a decision tree and major decision criteria surrounding the general aspects of space photovoltaic concentration. Low-CR systems involve simpler structural forms (troughs, petals, pyramids) which must be held at low cost to compensate for the relatively high quantities of (costly) solar cells required under low concentration. For high-CR systems, the structural forms are more complex (typically surfaces of revolution) and can be more costly since the quantities of solar cells required are vastly reduced.

A major objective of this study was to identify, analyze and compare the advantages and disadvantages of planar vs concentrator arrays and of silicon vs GaAs arrays. To meet this objective a planar array, a low-CR array, and a high-CR array were designed, characterized, and compared with each other to determine the most cost effective design approach. The designs were performed to a depth of detail which would permit valid trade conclusions. Since cell performance determines to a large

2-19

CONCENTRATION

REFRACTION

- REFRACTOR EFFICIENCIES TYPICALLY 10%-50% LOWER THAN REFLECTOR EFFICIENCIES
- FOR HIGH CR, MUST BE USED WITH REFLECTORS TO REDUCE SYSTEM DEPTH

REFLECTION

- MOST EFFICIENT METHOD OF CONCENTRATION
- BETTER MATERIAL PROPERTIES LIFETIME

LOW CR (<10)

- SILICON CELLS
- FOCUSSING OR NON-FOCUSSING SYSTEMS
- TROUGHS, PETALS, PYRAMIDS
- RAY DEFLECTION (SINGLE REFLECTION)
- STRUCTURES MUST BE RELATIVELY SIMPLE, LOW COST

HIGH CR (>10)

- GaAs CELLS
- FOCUSSING SYSTEMS
- SURFACES OF REVOLUTION
- RAY REVERSAL (SINGLE, DOUBLE REFLECTION)
- STRUCTURES MAY BE COMPLEX, HIGHER COST

Figure 2-7 Concentrator Decision Tree

LOCKHEED MISSILES & SPACE COMPANY

degree the selection of concentration ratio, which in turn determines system design, two CR's (i.e., CR=5 and CR=125) were selected for further design study. Although the selected CR's do not necessarily represent a precise optimum for their respective design category, sufficient pre- and post-design analysis was performed to indicate that the selected CR's were sound choices for their category.

Figure 2-8 summarizes the logic which led to the selection of CR's. With reference to the low-CR choice, it is widely held that for Si-cell systems a CR in the range of approx. 2.0 to 2.5 is optimum. This view is certainly valid for systems utilizing conventional AM0-reflecting materials, such as aluminized foil. For the spectrally selective (cold mirror) material discussed in a previous chapter, much non-convertible, heat-producing solar IR is rejected through selective transmission, allowing a higher CR with corresponding reduction in cell quantities. With reference to the high-CR choice, CR's of several hundred suns produce extremely high cell operating temperatures, which must be counteracted by the use of bigger, more complex, less efficient heat rejection systems. While this is no inherent difficulty in itself, it leads to higher weight and stowage volume (higher launch costs-per-watt) while yielding an insignificant cost advantage since cell cost is a minor cost component in high-CR systems. This result was verified by analysis of a very-high-CR system (CR = 500) which is included in the discussion in the appropriate section below.

2.3.2   Deployment/Installation Methods (Deployment vs Erection)

The method by which a stowed solar array is removed from the launch vehicle and installed onto orbital station has a major impact on the array design. Selection of a deployment/installation method for the array under study is not governed by such traditional small array concerns as available volume on the spacecraft wall, spacecraft-to-solar array mechanical interface constraints, or array distancing from spacecraft.

A 300-1000 kW array will be the chief or sole occupant of the launch vehicle and must be designed to be removed as a unit directly from the cargo bay and installed onto station directly or through the use of ASE (Airborne Support Equipment) or SSE (Space Support Equipment). In this situation, system maintainability, cost-effectiveness (including ASE and SSE), reliability, human factors, and safety are the paramount concerns.

LOW CR

GEOMETRIC CR = 5

EFFECTIVE CR = 3.4

- LOWER CRs DO NOT TAKE ADVANTAGE OF SPECTRAL SELECTION PROPERTIES OF REFLECTOR MATERIAL

- LOWER CRs PROVIDE NO CLEAR ALTERNATIVE TO PLANAR ARRAY

- HIGHER CRs LEAD TO EXTREMELY COMPLEX REFLECTOR GEOMETRIES

- HIGHER CRs POSE THERMAL DIFFICULTIES FOR PASSIVE THERMAL CONTROL

HIGH CR

GEOMETRIC CR = 125

EFFECTIVE CR = 67.5

- LOWER CRs DO NOT UTILIZE FULLEST CAPABILITY OF GaAs

- HIGHER CRs POSE HEAT REJECTION DIFFICULTIES

Figure 2-8 Selection of Baseline Concentration Ratios

LOCKHEED MISSILES & SPACE COMPANY

For the envisioned mission time-frame (production readiness by 1983; flight by approx. 1987) array installation by erection methods merits consideration over traditional deployment by ground or orbiter-based remote command. Numerous studies have been conducted by NASA to investigate the feasibility of various methods for the erection of large space structures.

One of the two chief methods under investigation involves the use of so-called beam-building machines. A beam-building machine is a self-contained unit which typically takes aluminum or graphite-composite strip materials and, through forming and welding/bonding processes, fabricates them into beams for use as the structural element of an orbiting system. This unit can be installed on-station and supplied with materials to cost-effectively produce large structures on-orbit without the necessity of direct manned involvement.

The second erection method under Agency-investigation utilizes pre-fabricated beam segments and joint-nodes, which are removed from the launch vehicle and assembled into large structural beams on-orbit. Beam assembly involves EVA by suited astronauts with appropriate tools and maneuvering units.

For either method, once the structure is erected, the solar cell panels, wiring harness, and thermal control assemblies must then be installed. This requires a further involvement of suited astronauts and/or maneuvering or manipulating units.

Investigations at LMSC in the field of large space structures have resulted in the development of certain guidelines which govern the implementation of erectable structures. According to these guidelines installation-by-erection can become a cost effective alternative to installation-by-deployment when the size of the structure exceeds approx. 100,000 sq. ft.

As the candidate array design concepts were developed during the present study, it became apparent that the superior basic 300 kW arrays would fall far short of this size-threshold of erectability. This, coupled with the growing industry and Agency sentiments that structure erection methods would not be demonstrated to a

LOCKHEED MISSILES & SPACE COMPANY. INC.

sufficient degree by the production readiness deadline of 1983, led to the choice of self-deployment wherever possible as the guiding philosophy for array structural design. It was further concluded that a retraction capability on-orbit would be neither necessary nor cost-effective. Degraded or defective array modules would not be returned to earth or repaired in-orbit but would be augmented by the addition of new modules. This and other aspects of array maintainability are discussed in the appropriate section below.

2.3.3 Stowage Methods (Fold-Up vs Roll-Up)

The low-volume stowage of large-area flexible solar cell blankets may be accomplished by one of two stowage schemes--foldable or roll-up. In the foldable scheme, the blanket is folded in accordian-fashion and pressurized as a flat-pack between a rigid cover-plate and a rigid base-plate under a pre-determined load. In the roll-up scheme, the blanket is rolled onto a stiff stowage drum under a pre-determined tension applied lengthwise into the blanket.

Both schemes have seen use in previous flight programs so that the advantages and disadvantages of each are understood. The foldable scheme provides a densely-packed stack of panels which is very secure against launch acceleration and vibration loads, regardless of blanket length or solar cell size. It suffers from a slight loss of cell packing factor due to the presence of fold lines in the blanket. The roll-up scheme is not as secure under launch loads, even when the blanket is rolled onto the drum at high pre-tensioning. Lateral blanket slippage under launch loads can be problematic, especially for long blankets. Present stowage drums are typically 8 inches in diameter for solar cells of 2 cm length in the wrapping direction. For this study, the baseline silicon solar cell dimension has been increased to approx. 6 cm in order to drive down cell costs. Stowage drum diameter must be increased to several feet in order to prevent cantilever-type cell breakage. This results in a prohibitively large loss of stowage volume to the hollow of the drum. For concentrator designs, which involve complex out-of-plane configurations, the use of roll-up deployment schemes leads to excessively complicated and structurally unfavorable supporting structures.

Thus, solar array installation-by-deployment utilizing foldable designs has been preferred in the array design concepts presented below. A high degree of expertise is available in-house concerning flat-pack, fold-up stowage and deployment schemes, due chiefly to its use in the design, development, and test efforts associated with the NASA/LMSC SEPS Solar Array Program.

LOCKHEED MISSILES & SPACE COMPANY

2.4   KEY COMMON TECHNOLOGIES

2.4.1   General

Three component technologies play a key role in determining the performance characteristics of the candidate solar array concepts:

- silicon solar cell technology
- GaAs solar cell technology
- spectrally selective reflector technology
- spectrally selective reflector technology

As a supportive effort to the present work, several company-funded studies have been conducted by various silicon and GaAs solar cell vendors and by a major optical coating firm to investigate technological and cost aspects of these key component technologies. As a result of these studies, a realistic projection of achievable performance for the envisioned production readiness time-frame of 1983 was generated. These performance baselines are discussed below.

2.4.2   Silicon Solar Cell Technology

One of the high cost elements of a multi-kW solar array is the solar cell assembly. Thus significant cost and weight savings can be realized by improvement of solar cell production methods, solar array fabrication, and associated cell technologies (e.g., coverslide material and application). This section discusses specific solar cell technology areas which were included in the multi-kW solar array study.

2.4.2.1   Silicon Solar Cell Technology. Ongoing silicon solar cell technology studies can be divided into three main categories--Aerospace, Terrestrial, and Advanced. Aerospace studies tend to have cell efficiency and reliability improvements as primary objectives with low cost a secondary objective. Terrestrial studies usually reverse the order of the Aerospace study objectives. Advanced studies include cells such as GaAs, amorphous cells, ribbon growth, and ultra-thin cells and may have either cost reduction or efficiency improvements as the major goal.

2.4.2.1.1 Aerospace Technology.- Beginning with the introduction of the COMSAT shallow junction "violet" cells in 1973 many solar cell improvements have been made, increasing the AM0 efficiencies of production solar cells from 10%, prior to 1973, to about 14% today.

Junction Depth

The technology for producing shallow diffused junctions on the order of 0.1 μm exists today. Studies correlating junction depth with I_{sc}, short-wave length "blue" response, weldability, and the grid structure technology indicate that a junction depth of between 0.1 μm and 0.15 μm is optimal. No technology improvements are needed in this area.

Back Surface Fields, P+

The back surface field (BSF) or P+ layer has been incorporated into many cell designs and has increased the initial solar cell output by several percent. Unfortunately, the BSF effect is severely degraded by charged particle radiation and any initial power gains have been lost by an equivalent 1 MeV electron fluence of about 4×10^{11} e/sq. cm. The BSF also causes higher cell solar absorptance and cell surface finish roughness (causing welding problems). For this reason, BSF will not be incorporated into the multi-kW array cell design.

Texturing

The technology of texturing or sculpturing a silicon solar cell is well established in the cell manufacturing industry. The sculpturing increases cell efficiency and offers some improved radiation resistance. Sculpturing also drastically increases the cell solar absorptance, which causes increased operating temperature and decreased power. Studies have indicated that the higher solar absorptance is probably not offset by the increased power. Texturing will not be recommended for multi-kW.

Base Resistivity

Currently, most solar cells have either a nominal 2 ohm-cm or 10 ohm-cm base resistivity. The 2 ohm-cm cells exhibit higher initial power than the 10 ohm-cm

cells and retain that advantage until a fluence of 1×10^{15}, 1 MeV e/sq. cm. The 10 ohm-cm cells have a better efficiency from that point on. A 2 ohm-cm base resistivity is the likely choice for a multi-kW array.

Back Surface Reflector

The back surface reflector (BSR) is an innovation in cell technology. Essentially the back of the solar cell is aluminized to form a second surface mirror. The cell appears twice as thick and gains some power from the double pass of the longer wavelengths. More significantly, more than 60% of the light energy with wavelengths greater than 1.2 μm is reflected from the cell. This reflection can lower the cell's solar absorptance by about 10% for a 5-8% power gain at operating temperature. The BSR has undergone space qualification testing and is an important technology for the multi-kW usage.

Antireflection Coating

The relatively new Dual AR coating Al_2O_3/TiO_x has become the standard antireflection coating for high efficiency solar cells. It has high transmission throughout the solar cell response wavelengths and provides nearly ideal optical coupling to the cell's protective cover. A 2% power gain is realized; however, it is partially offset by a 0.02 solar absorptance increase. There is a net power gain of 0.5 - 1.0% with this dual AR coating. This technology does not need development and implementing it is recommended.

Contacts

The current metal system most extensively used is a palladium passivated titanium-silver contact. Gridline densities of 10 to 12 per cm with 0.05 mm grids are routinely produced. These contact systems are very adequate for 1 sun array systems.

With the possibility of concentration ratios of greater than 5:1, new higher temperature, higher gridline density metalization systems will be needed. Photolithography may become the only way to achieve the necessary gridline density. Metal systems such as TaCrPdAg have been under development and show promise as a high temperature

replacement. If high concentration ratios are found to be desirable, some development work will be needed to bring high temperature/high density metal systems to the production readiness needed for multi-kW arrays.

Wraparounds

The wraparound contact cell is a relatively new member of the solar cell family relative to its actual space use. With both N and P contacts on the backside the wraparound enjoys three advantages over its traditional counterpart: 1) the cell can be electrically contacted from 1 side, which is ideal for flexible blanket arrays, 2) the wraparound has more active area than the traditional cell and has a higher efficiency potential, and 3) the cell can be completely covered avoiding coverslide registration problems and increasing radiation resistance.

The wraparound contact solar cell development is continuing, particularly to improve the dielectric isolation employed on the edges and backside to separate the N contact and P material and still minimize P contact giveaway. Although high efficiency wraparound contact solar cells have been made (>14.5%), the current production cells have an average efficiency of 12.8%. With all of the previously mentioned high efficiency cell technology needs to be incorporated into wraparound cells it is predicted that 14% efficiency cells will be available in 1983.

2.4.2.1.2 Terrestrial Solar Cells. The emphasis to develop low cost processes for terrestrial solar cell application was important to examine relative to its use in multi-kW. The value of the continuing emphasis to develop techniques to reduce the terrestrial cell cost is important to examine relative to multi-kW application. Methods of producing low cost cell grade silicon are under investigation. One approach is the carbon reduction of low impurity silica in a plasma heat source. It is technically feasible and is working towards a < $10/kg goal for silicon production. As this technology develops it should be reevaluated for multi-kW incorporation.

Another innovation being investigated is shaped ingot or wafer casting by a directional solidification process. This has been proven feasible and economically attractive.

A third development is ion-implantation. This is not entirely terrestrial as it has an equal attraction to space application. Better p/n junction control and less back surface damage is possible with this technique. It certainly is one which should be watched for possible incorporation when adequate evaluation has been completed.

2.4.2.1.3 Advanced Cells.- The technology status of advanced cell such as ultra-thin or polycrystalline solar cells has been well reported recently. The technology to mass produce 12% (AM0, 28°C), 0.05 mm cells appears to be well developed. The technology for utilizing such thin cells is lagging, however.

Recent polycrystalline work reports solar cell efficiencies 10% being obtained. The environmental stability of these cells has yet to be certified. Considering the 1983 time frame it seems unlikely that any alternate crystal or wafer technology will be able to replace the present single crystal pulling and slicing techniques. The potential for cost reduction in this area is great and for multi-kW array programs it may prove cost effective to develop the technology more rapidly.

2.4.2.1.4 Selected Solar Cell Description.- Figure 2-9 presents the major characteristics of the silicon solar cell which has been taken in this study as a 1983 baseline. The cell is a weldable corner wraparound solar cell of so-called 5.9 cm x 5.9 cm dimensions. These dimensions actually refer to the covered cell assembly size.

A cell thickness of 8 mils has been selected to insure low breakage (high yield) during fabrication and assembly. A reduction of thickness to 4 mils or 2 mils would adversely effect yield of such a large area cell and drive costs upwards unnecessarily. No advantage is to be gained by the use of thin or ultra-thin cells since the stowage of the candidate arrays into the Orbiter cargo bay is limited by volume rather than by weight (i.e., "watts-per-launch" is not increased through a decrease in array weight).

The technology of the cell is consistent with a long mission in low earth orbit. A high thermal input due to the proximity of the earth has dictated a choice of low α/ϵ

- SIZE: 5.9 x 5.9 cm

- THICKNESS: 8 MIL

- TYPE: N-P WELDABLE

- CONTACT MATERIALS: TiPdAg

- CELL AREA: 5.27 IN.^{2} (34 cm^2)

- EFFICIENCY: 14 PERCENT AMO AT 28°C

- THERMAL OPTICAL $\alpha/E = 0.85$

- HIGHLY POLISHED BACK SURFACE REFLECTOR

- BASE RESISTIVITY 1 OHM-cm

- CONTACT TYPE: WRAP AROUND

- ELECTRICAL OUTPUT: 0.64 WATTS

- COVER SLIDE: 6 MIL MICRO SHEET ~ AR COATINGS

Figure 2-9 Silicon Solar Cell Description

LOCKHEED MISSILES & SPACE COMPANY

technologies (Back Surface Reflector) to minimize operation temperature and resulting power loss. A moderate charged particle environment (~ 5×10^{13} 1 MeV el/cm per year equivalent fluence) has led to a choice of low base resistivity. No P+ was included since its marginal effectiveness for the subject radiation levels does not justify its added cost. The added cost of wraparound contact technologies at cell-level is compensated by an overall cost reduction at panel assembly level through more cost-effective cell attachment processes. Cost effectiveness was also the determining factor in the choice of a micro-sheet coverslide combined with FEP glassing techniques.

The choice of silicon cell technologies yields an optimum-performing cell at mission operating conditions. Although alternative technologies are available which provide higher efficiencies on a laboratory basis (room temperatures, unirradiated) in-house analysis has shown the superiority of the chosen cells for similar LEO mission applications. Proton damage concern (GEO) does not dictate a cell change but rather closer attention to cell coverage to protect against any N material exposure.

Development of such large-area cells has begun at LMSC and at NASA for application to the flexible solar arrays of several future programs. In order to begin process testing of the 5.9 x 5.9 wraparound format, preliminary demonstration cells have been recently fabricated (see Figure 2-10) and assembled into blanket coupons.

Figure 2-11 shows the efficiency status of the selected silicon cells (the so-called high-efficiency hybrid) as well as its behavior at elevated temperatures. Present cells are capable of a 12.8% AM0-efficiency. Industry prognoses consistently target an efficiency of 16% for the 1985-1990. The LMSC performance model for the present study assumes a 14% efficiency as being realistically achievable for a 1983 production readiness time-frame.

2.4.3   Gallium Arsenide Solar Cell Technology

Gallium arsenide is a well-known material in the semiconductor industry, where it is used primarily in small switching devices. Its useage in a large power-generating device, such as a solar cell, poses an entirely new set of design
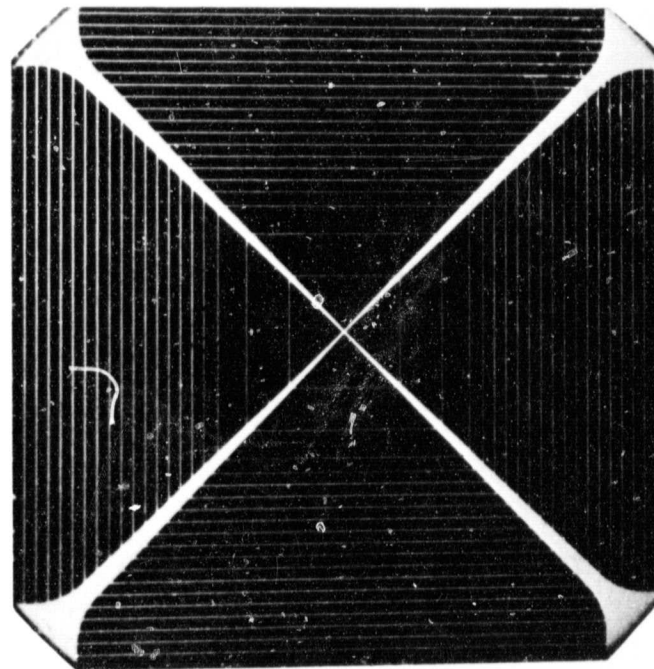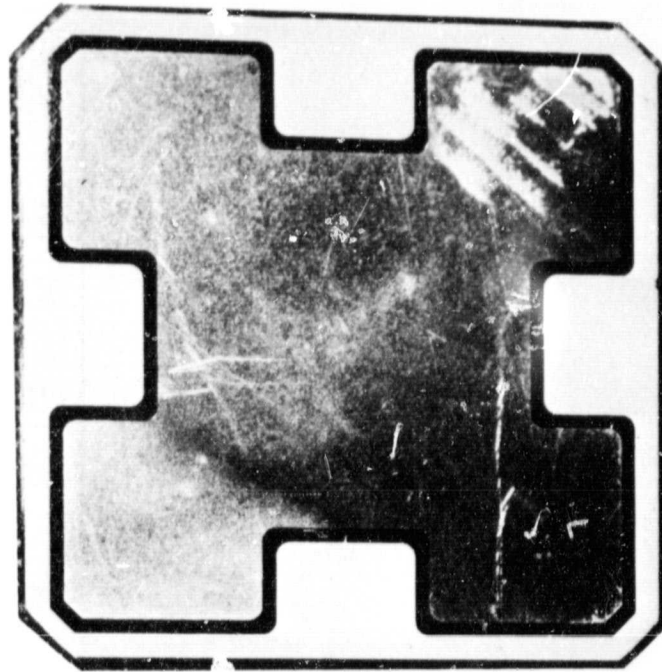
Figure 2-10 5.9 x 5.9 cm Corner Wraparound Solar Cell

LOCKHEED MISSILES & SPACE COMPANY
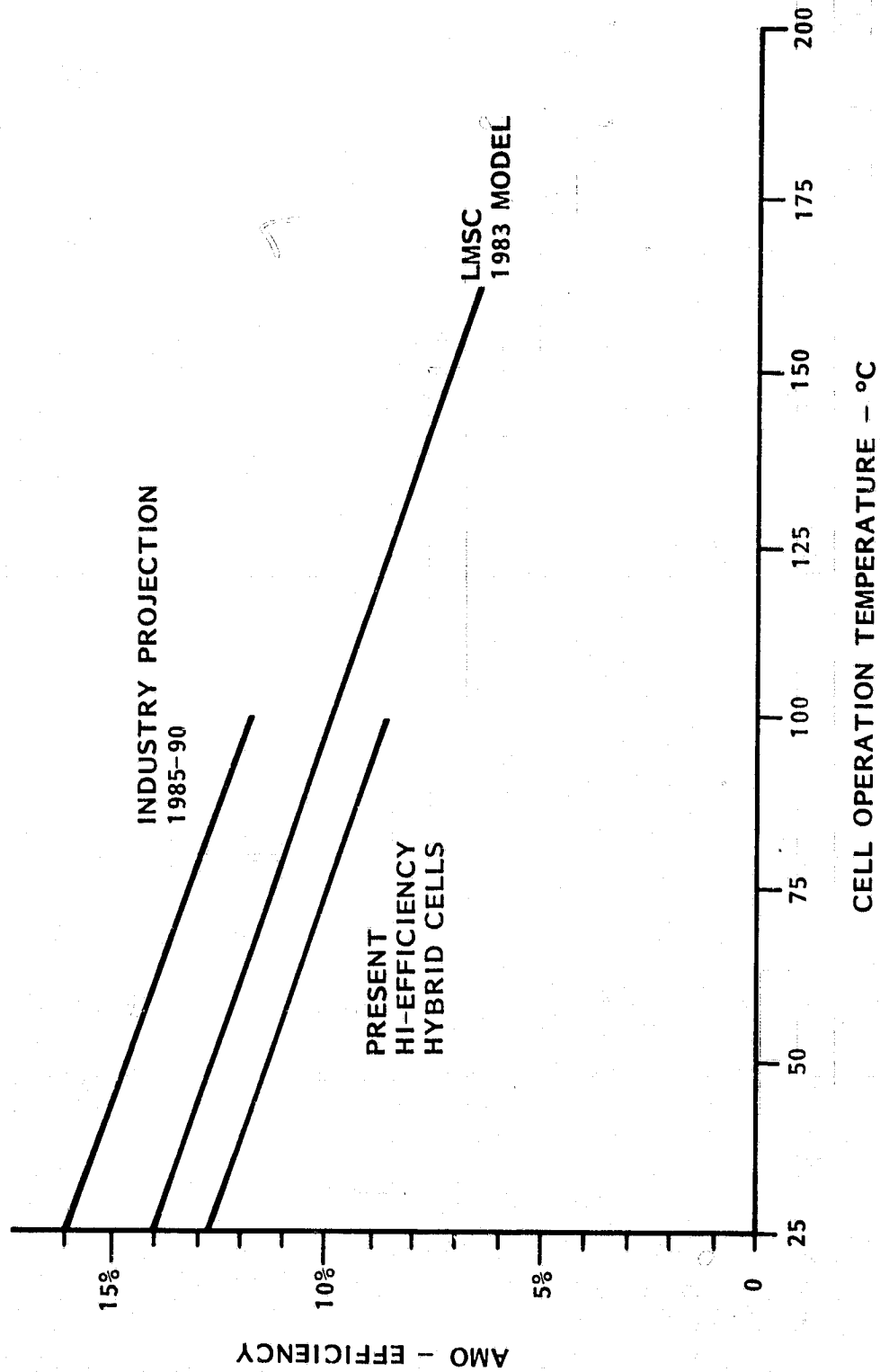
Figure 2-11 Silicon Cell Performance Model

LOCKHEED MISSILES & SPACE COMPANY

and fabrication problems to be solved. Although GaAs solar cell technology is in its infancy, much work is being performed at present to perfect the material technology, optimize cell design, develop fabrication techniques, and demonstrate space and terrestrial applicability. GaAs cells produced to date have flown in space although none have been used as primary power source for a major spacecraft. The chief developmental thrust for space GaAs cells has been for unconcentrated military use, where the superior radiation resistance of the cells is being exploited. Terrestrial development has emphasized useage under high concentration, taking advantage of the cell's superior temperature resistance to offset its high fabrication costs. These efforts form the basis for the design which was selected for this study.

Figure 2-12 presents the major characteristics of the GaAs solar cell which has been taken as the 1983 baseline. The cell is weldable and has a conventional contact system. GaAs material possesses an inherent brittleness which limits its size growth and prevents a reduction of thickness to silicon cell proprotions. Size growth beyond 2 cm x 2 cm and thickness reduction below 12 mils is not considered to be realistic, especially for a 1983 time-frame.

GaAs solar cells have an inherent AMO-efficiency advantage over silicon cells. As Figure 2-13 shows, present GaAs cells are capable of efficiencies in the 13.5% to 16.5% on a lot average basis. Industry projections for a space-configured cell center around the 20% efficiency range. The LMSC performance model for the present study assumes an 18% efficiency as being realistically achievable for the 1983 production readiness time frame. Comparison of Figure 2-11 with Figure 2-13 shows the superior temperature behavior of the GaAs cell over the silicon cell.

2.4.4   Spectrally Selective Reflector Technology

In a prior chapter, in-house supporting technology work has been discussed which pertains to the investigations of reflector materials which separate desirable portions of the AMO spectrum from undesirable portions. An optical coating technology was identified and pursued which reflects wavelengths in the solar cell response region and transmits wavelengths which are not converted in the cell and thus only add power-robbing heat.

- SIZE: 2 x 2 cm

- THICKNESS: 12 MILS

- TYPE: P-N WELDABLE

- CONTACT TYPE: CONVENTIONAL

- EFFICIENCY: 18 PERCENT (AMI AT 28°C)

- THERMAL OPTICAL: $\alpha/E = 0.91$

- COATINGS: MULTI-LAYER AR

- ELECTRICAL OUTPUT: 97.4 mW

- COVER SLIDE: 6 MIL MICRO SHEET ~ AR COATINGS

Figure 2-12 Gallium Arsenide Solar Cell Description
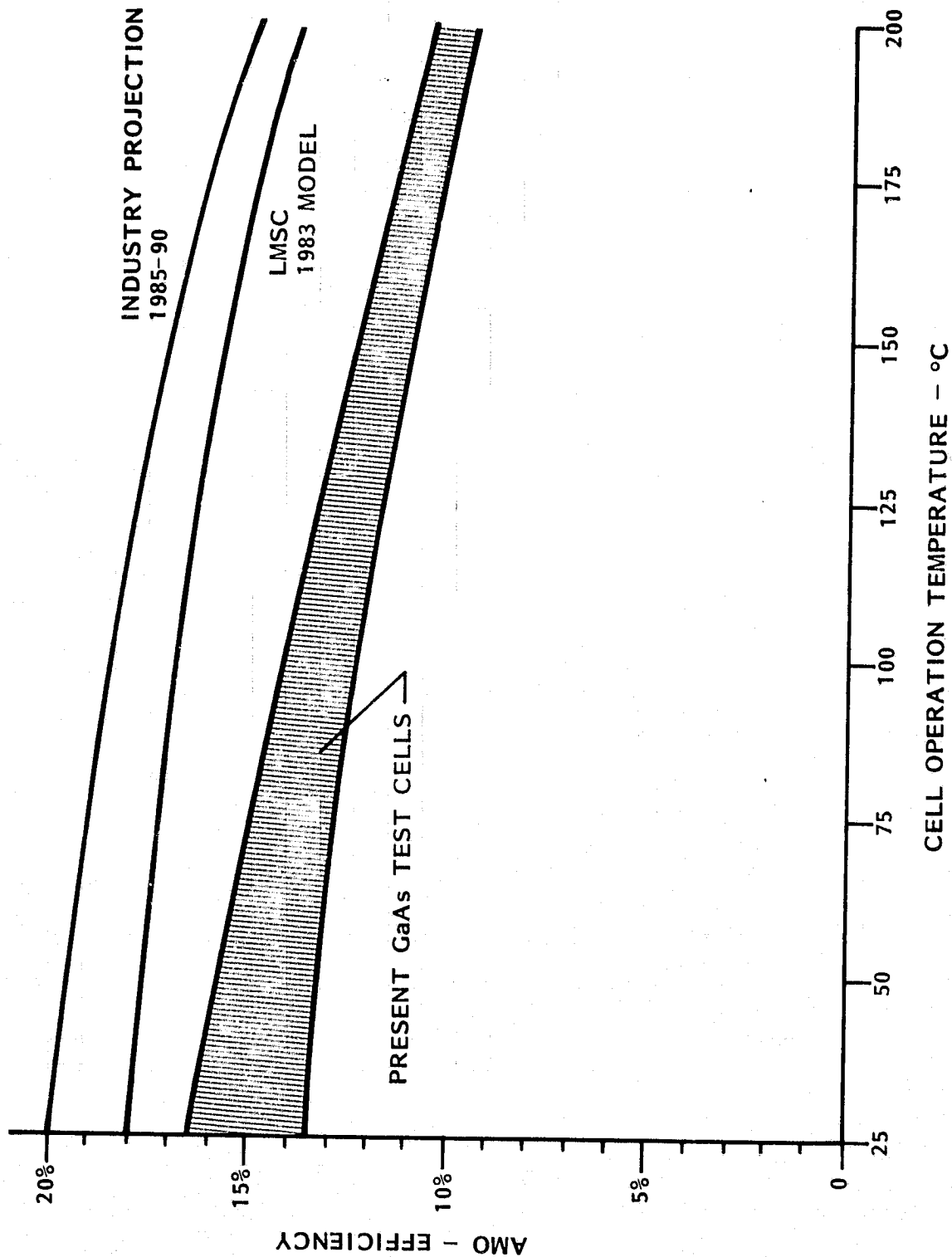
Figure 2-13 GaAs Cell Performance Model

LOCKHEED MISSILES & SPACE COMPANY

Based upon these investigations an achievable reflectance profile was established for this so-called spectrally selective reflector, or "cold mirror." This profile was used to characterize the effect of the mirror on cell performance as shown in Table 2-5. The Table shows the reflective performance characteristics for:

- single reflection from typical aluminized film

- single reflection from the baseline cold mirror as is proposed for the low-CR array below

- double reflection consisting of a single reflection from the cold mirror followed by a single reflection from aluminized film as is proposed for the high-CR array below

The gross average value of reflectance over the AMO spectrum has been measured for both materials. The two "equivalent reflectances" are parameters which characterize the selective properties of the materials. More precisely, when illuminated by an AMO spectrum after single reflection from the subject cold mirror, the cell provides a power output as if it had seen 0.60 suns and establishes a thermal equilibrium as if it had seen 0.40 suns. Since no spectrally selective device is perfect, a certain amount of usable light is being passed unused and some non-usable light is being reflected to the cell. The overall benefit of using the subject cold mirror, however, is substantial, as can be seen roughly by comparing the electrical equivalent to the thermal equivalent.

The equivalent reflectance values are considered to be good approximate values which were derived by integration estimates with typical cell spectral response curves. When done precisely with accurate measured values, the equivalent reflectances will be somewhat different for silicon and GaAs cells. That type of accuracy was not justifiable for the present treatment. A complete detailed analysis of both power and thermal performance would be based upon a complex treatment involving the individual contributions of a large number of small wavelength bands. For the present study the use of "equivalent reflectances" permitted a simple, sufficiently accurate treatment of complex spectrum-shaping effects.

TABLE 2-5

REFLECTOR PERFORMANCE MODEL

	ALUMIZED FILM	LOW-CR COLD MIRROR	HIGH-CR COLD-MIRROR AND ALUM-FILM
GROSS AVERAGE AMO REFLECTANCE	0.92 MEASURED	0.52 MEASURED	0.48
ELECTRICAL EQUIVALENT REFLECTANCE ONTO COVERED SOLAR CELL — ONTO Si	0.90	0.60*	—
ELECTRICAL EQUIVALENT REFLECTANCE ONTO COVERED SOLAR CELL — ONTO GaAs	0.90	0.60*	0.54**
THERMAL EQUIVALENT REFLECTANCE ONTO COVERED SOLAR CELL — ONTO Si	0.93	0.40	—
THERMAL EQUIVALENT REFLECTANCE ONTO COVERED SOLAR CELL — ONTO GaAs	0.93	0.40	0.37

*GEOM CR = 5   EFFECT. CR = 3.4
**GEOM CR = 125   EFFECT. CR = 67.5

Figure 2-14 shows this shaping effect of the cold mirror and compares the shaped-AM0 after single reflection to typical silicon and GaAs spectral response curves. The figure demonstrates clearly that some usable energy is being eliminated in the low wavelength region and some unusable energy has not been eliminated at high wavelengths. A second reflection from a cold mirror (not shown in the figure) would not improve the shaping aspects of the spectrum but would only serve to reduce the reflection in usable regions. For this reason the second reflection in the high-CR array is accomplished by use of traditional aluminized film.

The spectral response curves in the figure apply for room temperature; the shaped AM0 spectrum was derived from cold mirror reflectance profiles for normally-incident light. On an array the cells operate at elevated temperatures, which causes a shifting of their response curves. Furthermore, the reflectors are used at a pre-determined angle to the sun vector, which causes a shifting of their reflectance profiles. (Some measurements of this effect were performed at LMSC). A detailed design and analysis of an array system would have to include such effects. A certain degree of shift-compensation appears to be possible through proper design of reflector layers. In general, however, the use of a cold mirror has significant potential for improving the performance and cost effectiveness of a concentrator solar array.
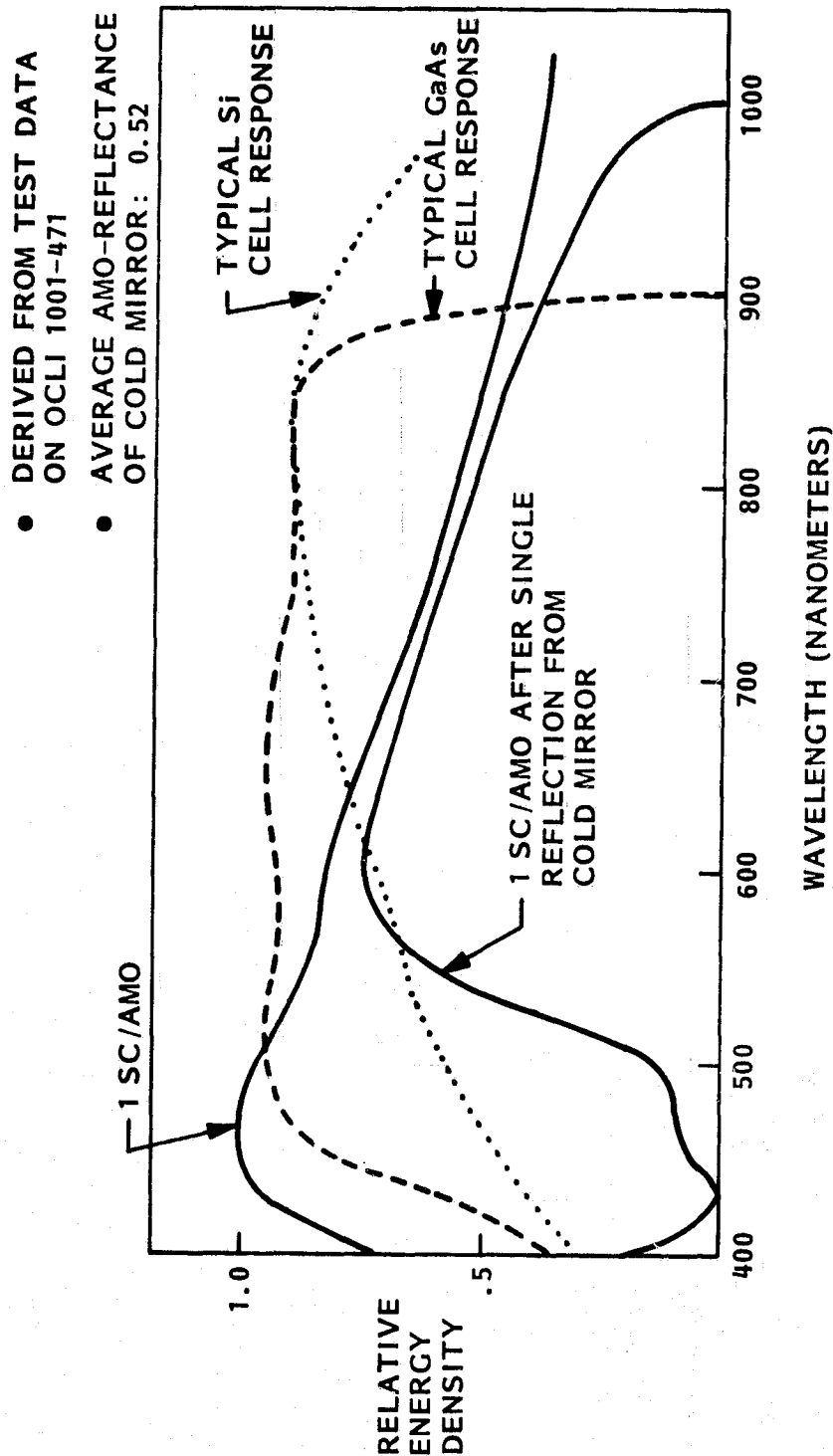
Figure 2-14 Cold Mirror Performance

2.5 PLANAR ARRAY

Many conceptual designs of solar array systems in the multi-kilowatt range have been devised by NASA and industry, extending to several kilometers in basic length dimensions. There are concepts for planar systems which vary as the number of minds which devise them. Figure 2-15 illustrates systems considered. There are planar areas which are rectangular, circular, elliptical, and hexagonal. They are supported by structures which are deployed, erected or fabricated in space.

Although these concepts are generally directed toward systems an order of magnitude or more larger in size than the 1000 kW system in this study, many of the principles are still applicable. General guidelines for determining the techniques for large space structures indicate that structures up to 0.1 km can be deployable, those up to 1 km can be erectable, and those beyond would be fabricated--the size limited by the fabricating equipment. The solar array sizes considered in this study range from approximately 0.03 km to 0.1 km making them applicable to all structural assembly techniques available for consideration. If the projected funding levels are supported, the technology for each category should be available by 1983.

Present-generation large flexible solar arrays are primarily mast/blanket systems which are cantilevered to a "fixed" base. For a planar array in the 300-1000 kW power range, corresponding to ~20 to 100 present-generation-sized wings, such an approach is impractical and dynamically undesirable. The fundamental design task for the planar array of this study consists of devising a deployable frame-type structure which provides good blanket support on-orbit while being collapsible to a low-volume, high-density configuration for stowage in the launch vehicle.

Design alternatives which were investigated in the present study derived their blanket stowage scheme from present generation flexible arrays. All featured solar cell blankets which, for launch, are stowed under pressure between a base plate and a cover plate ("container and cover" in present jargon). Unlike present generation arrays, the containers and covers for this study have been strengthened to serve in a second function as segments of a collapsible space frame. Container and cover frame-pairs are separated on-orbit by a series of extendible masts which provide simultaneous unfolding of the cell blankets.

LOCKHEED MISSILES & SPACE COMPANY

SEGMENTED FLEXIBLY CONNECTED

SEGMENTED STATION KEPT

MONOLITHIC

SEGMENTED RIGIDLY CONNECTED

DEPLOYMENT SCHEMES

FRAME TYPES

TETRAHEDRAL STRUCTURAL BASE

SEPS UTILIZATION

MULTI MEGAWATT CONFIGURATIONS SHOWN TO RELATIVE SCALE
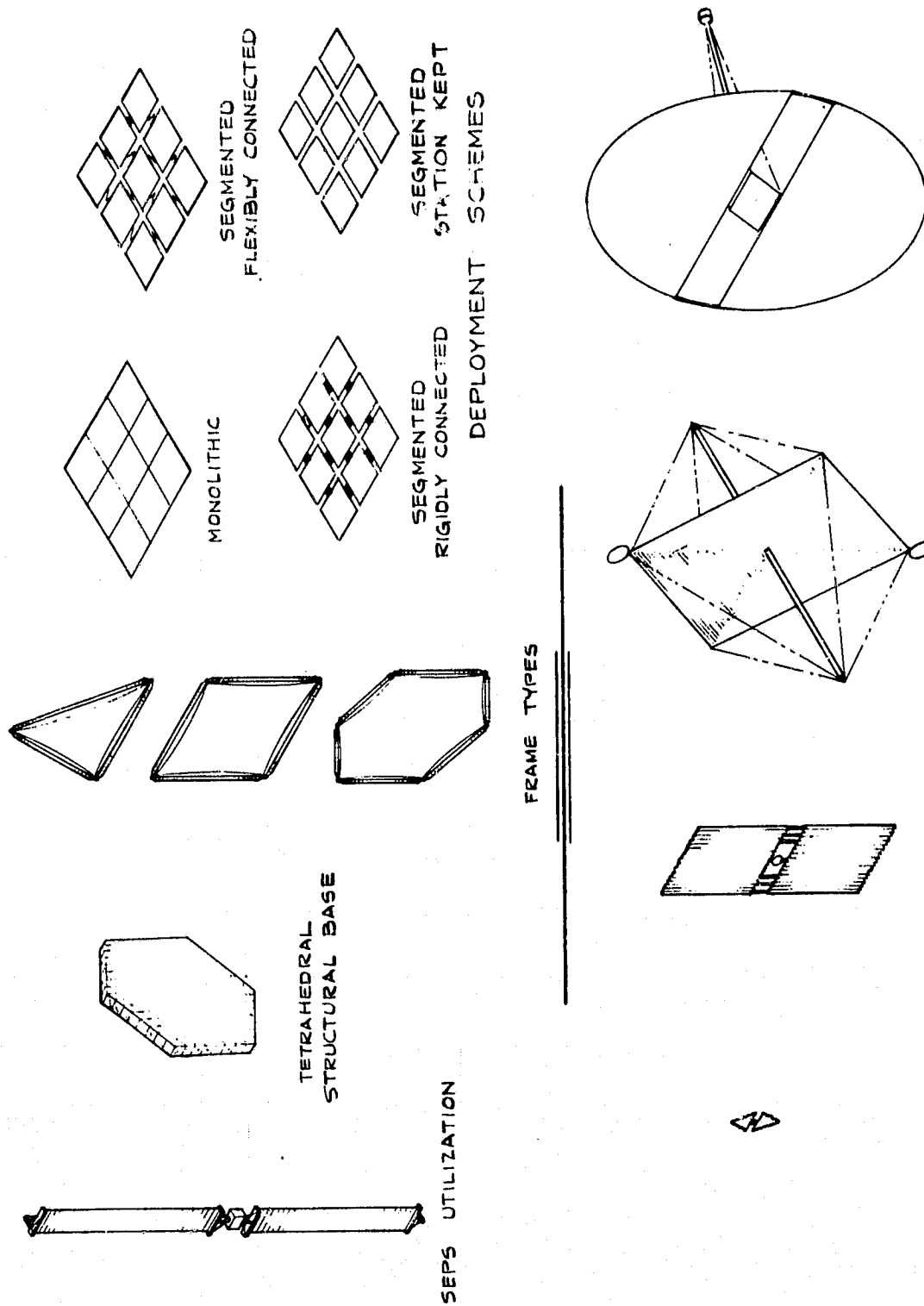
Figure 2-15 Planar Solar Array Concepts

LOCKHEED MISSILES & SPACE COMPANY

Figure 2-16 shows the most attractive of the candidate space-frame designs in its stowed configuration in the Orbiter bay. The canisters containing the stowed masts are tucked away unobtrusively at the front and rear of the stowed package. The end-on view in the figure shows the first 16 of 32 container and cover frame-pairs stowed in the bay, each being 2' x 2.5' and 12.5' long. As the side view shows, two units placed end-to-end occupy 27' of the bay length from canister to canister.

As the performance analysis of Section 4 will show, this array is dimensionally configured to yield a power output at the 300 kW level. The space which is still available in the bay may or may not be exploited for further array segments or for other equipment, depending upon the target altitude and associated weight constraints.

Figures 2-17, 2-18, and 2-19 show the individual stages in the deployment of the array. Though the sequence appears complicated, each separate step is performed with simple, positively driven mechanisms (motors, hinges, etc.) The first step is a rotation about each long edge. Uniform, repeatable angular separation is achieved through the use of cable-loop drives or similar flight-proven methods common to rigid array deployment systems. The second step is a pantograph-type extension which ends by locking in a long double-row of container/cover frame-pairs. The final step is a bi-directional separation of cover-row from container-row through coordinated extension of the row of back-to-back masts. The locked-in cover-rows and container-rows have the properties of a long beam which deploys a set of 10.5' wide solar cell blankets.

A modular unit of the planar array consists of a field of eight 10.5' x 90' blankets which is bounded at each end by extendible masts. The overall gross module size is 50' x 190'.

In the absence of frame stiffness or dynamic requirements which derive from as yet undefined g-loading of the frame (i.e., docking) or from frequency coupling constraints with the user platform, an attempt was made to select a mast weight by similarity with one of two known options from present-generation arrays. The first option is a light mast as designed for use in the SEP solar array. This mast is designed for non-retrieved missions with light propulsion loads and no Orbiter docking. The second

DEPLOYABLE
MAST
CANISTERS

27'

8'

10'

ORBITER
ENVELOPE
15 FEET DIA
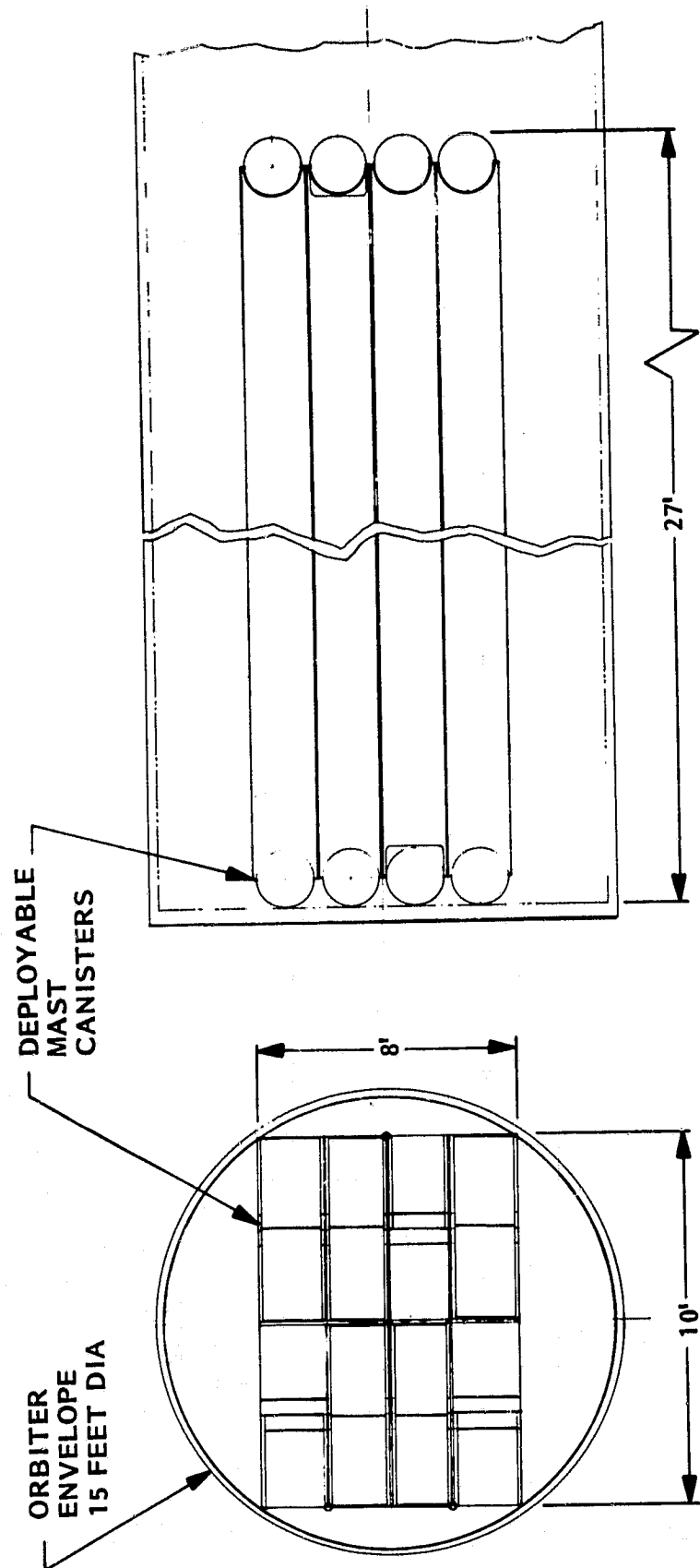
Figure 2-16 Planar Array – Stowed Configuration

2-45

CONT'D

STOWED
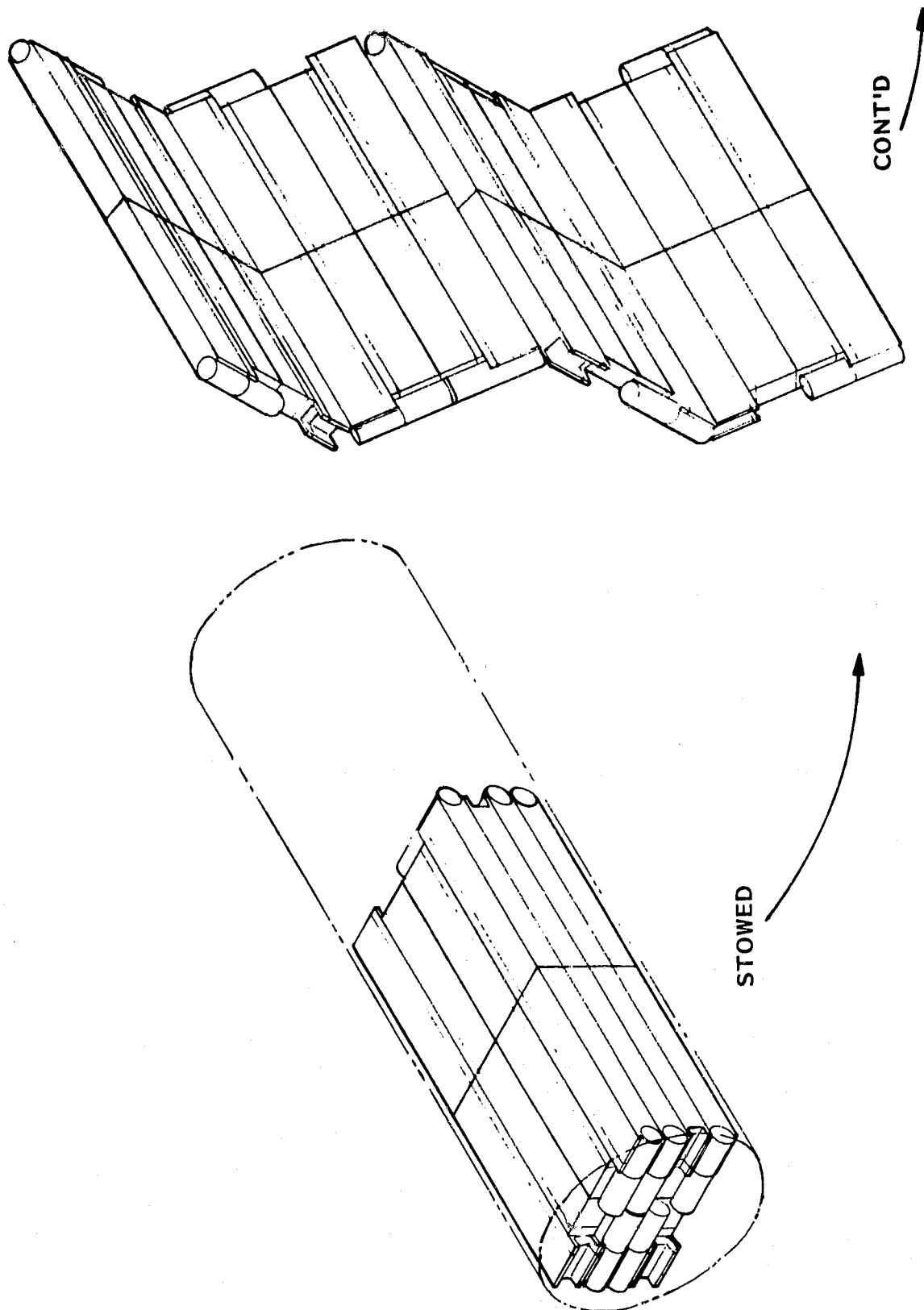
Figure 2-17 Planar Array - Initial Deployment Stages

LOCKHEED MISSILES & SPACE COMPANY
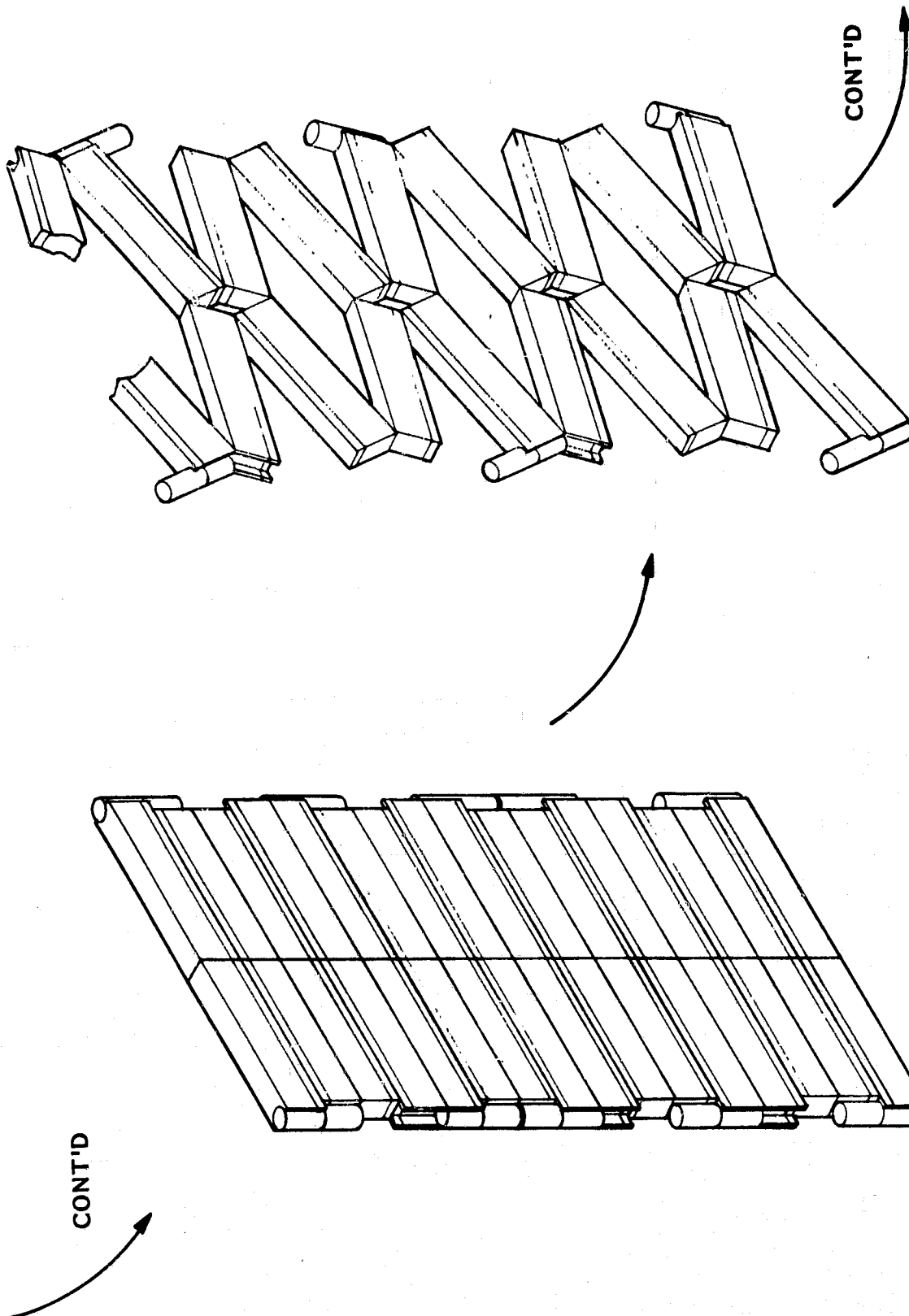
Figure 2-18 Planar Array – Intermediate Deployment Stages

CONT'D

CONT'D

LOCKHEED MISSILES & SPACE COMPANY

FINAL DEPLOYMENT

CONTINUED
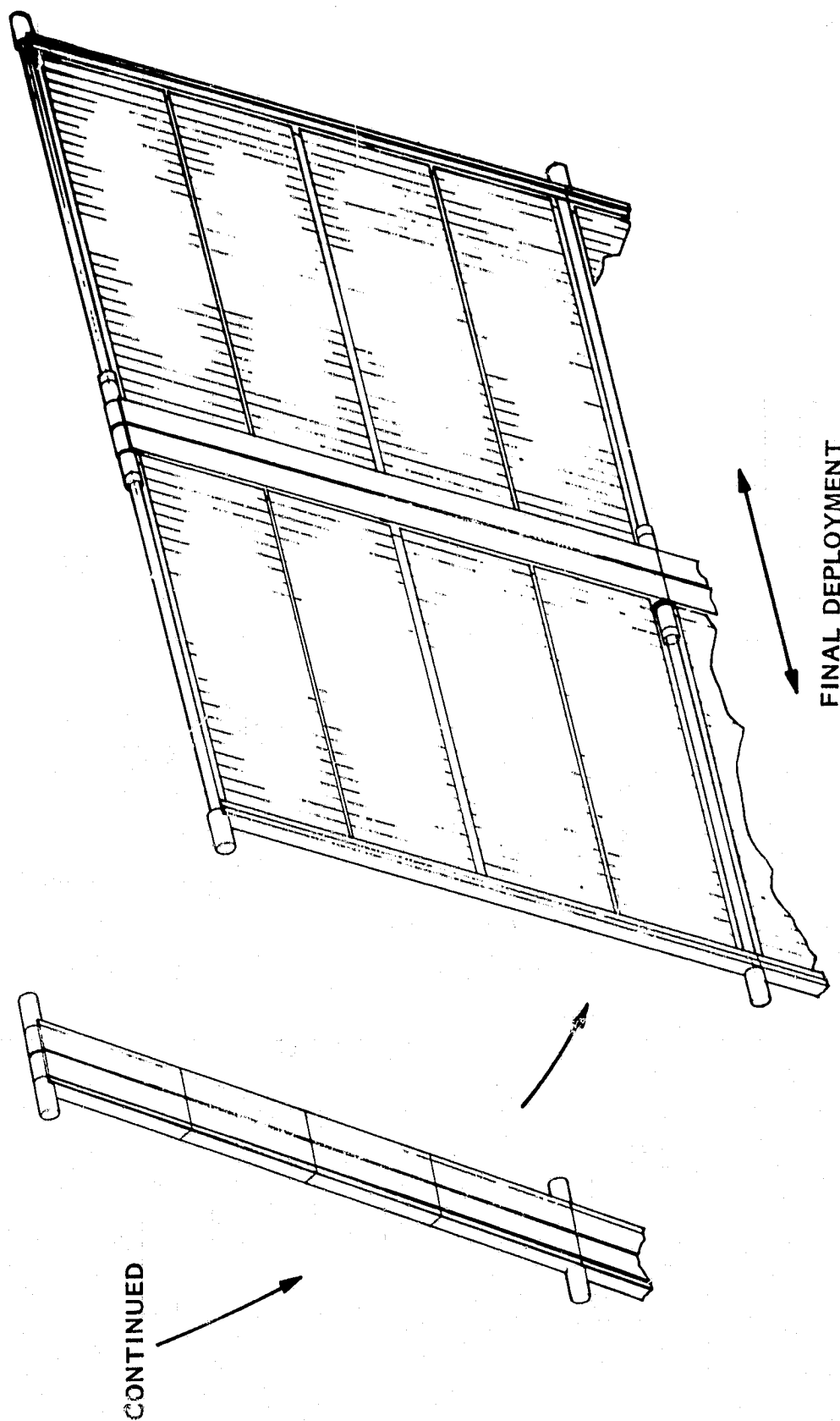
Figure 2-19 Planar Array – Final Deployment Stages

option is a heavy mast as designed for use in the PEP solar array. It is capable of withstanding heavy g-loading from Orbiter thruster accelerations. The heavy mast option was selected for the planar array illustrated here.

Figure 2-20 shows a complete unit of 4 modules after final deployment on-orbit. The performance values shown in the figure are derived in a complete performance analysis in section 4.
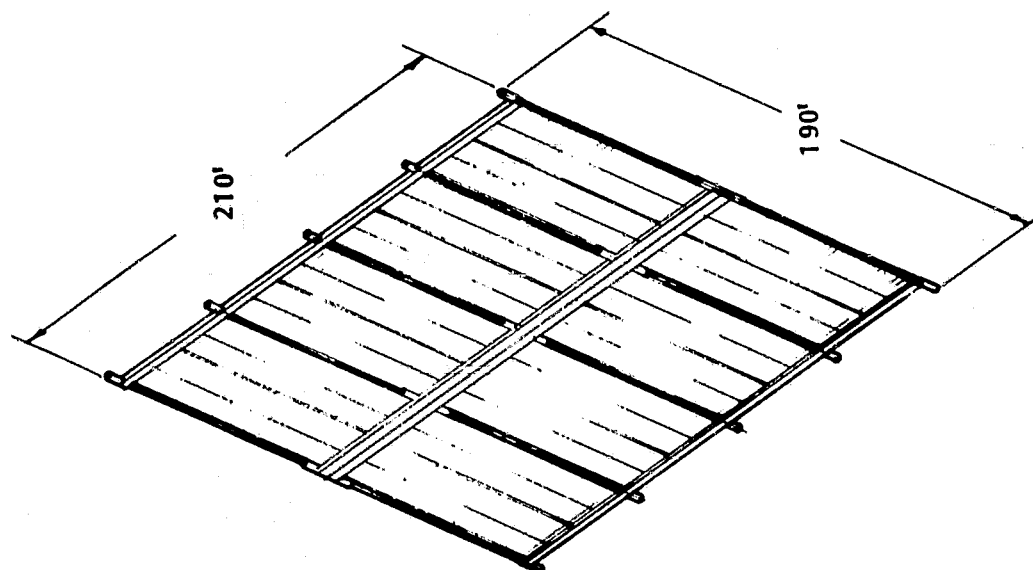
- SILICON SOLAR CELLS
- 427 kW BOL
- 311 kW AVG. (15 YR. LEO)
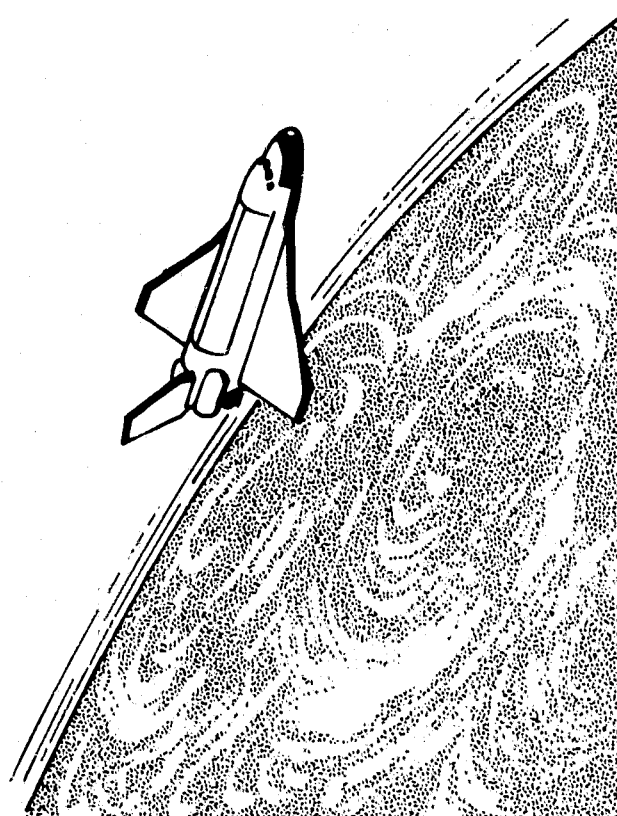
Figure 2-20 Planar Array On-Station

2.6   LOW-CR CONCENTRATOR ARRAY

2.6.1   Reflector Configuration Trades

A trade-off analysis was conducted to determine comparative reflector performance
for front-lit (ray deflection) reflector configurations. Back-lit (ray reversal) con-
figurations are geometrically more complex and would be structurally less stable.
It is felt that they would not offer any compelling advantages for a civilian, low-
earth-orbit mission. Their advantage lies chiefly in their avoidance of direct solar
cell exposure, yielding hardening benefits for potential military applications. Minor
reductions of reflector area ("yardage", weight) through back-lighting will have a
negligible cost advantage.

The analysis of Low-CR reflector configurations began with an investigation of the
concentrating capabilities of fundamental two-dimensional (trough-type) cross-sections,
proceeding from simple planar side-contours to multi-faceted and parabolic contours.
The analysis was then extended to three-dimensional configurations (i.e., petals,
pyramids, and cones) utilizing simple, multi-faceted, and parabolic contours.

Figure 2- 21 shows a matrix of reflector configurations which are suitable for
Low-CR application. Reading downwards in the columns corresponds to increasing
complexity of contour; reading across the rows corresponds roughly to increasing
"dimensionality." Thus, in reading from the top left corner to the bottom right
corner, one is proceeding roughly from lower concentrating power (CR's of 1-3
suns) to higher concentrating power (CR's to 9 suns) and from simple configurations
to complex configurations. The performance comments on the figure will be
developed and elaborated in the discussion below.

Figure 2-21 Low Concentration Ratio Reflector Concepts

LOCKHEED MISSILES & SPACE COMPANY, INC.

Equations were developed to yield the characteristic concentrating properties in terms of reflector angles, contours, and lengths and these equations were analyzed to determine appropriate figures of merit for the performance of candidate reflector configurations. Among the most important figures of merit were:

- uniformity of concentrated beam
- reflector area required to achieve a certain CR
- contour depth required to achieve a certain CR

The first figure of merit above is an indication of how efficiently the solar cell area is exploited by the contour. The other two indicate how large and complex the contours must be to achieve their purpose and can also be thought of as a general indication of structural stability.

Uniformity of the concentrated light beam is a concern because it has a major influence on both the thermal and the electrical performance of the solar cells. If a string of cells is to perform as an optimum power-generating device, then its elements--the solar cells--must not be allowed to experience wide spatial variations of illumination and thus of operational temperature.

Reflectors with straight contours provide a uniform reflected beam. For curved (focussing) contours this is not the case. Figure 2-22 illustrates this point for the case of a parabolic trough. In general, parabolic contours are more efficient collectors of light since they require less area and depth to collect a given number of suns than do straight contours. However, a parabola will concentrate an incident beam into its mathematical focal point. The concentrated rays converge into this point at angles which range from somewhat off-normal to high grazing angles. Point-focussing is ideal for solar-thermal collectors but is inappropriate for photovoltaic systems. Varying degrees of defocussing can be achieved by translating the cell plane upwards out of the mathematical focal plane.
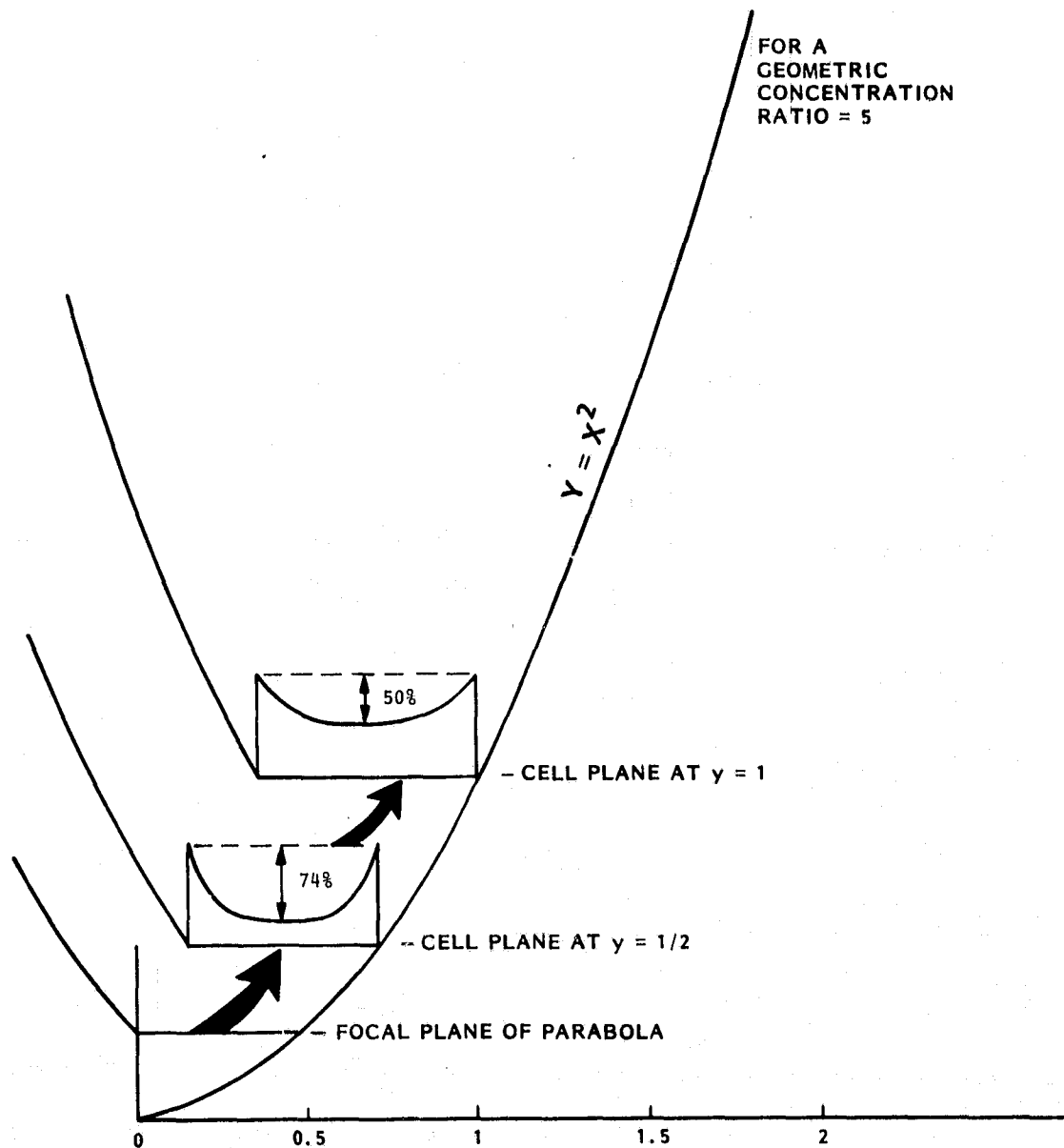
Figure 2-22 Total Beam Distribution in a Parabolic Trough

2-54

LOCKHEED MISSILES & SPACE COMPANY, INC.

The figure shows the effect of such defocussing on the light distribution at the cell plane. The distribution curve includes the directly incident portion of light as well as the reflected portion from parabolic reflectors on both sides. For each of the cell plane locations illustrated, the side reflectors have been extended in length by an amount which provides an overall geometric concentration ratio of 5 suns (direct plus indirect) at the cell plane. As the figure indicates, even after a major translation from the focal plane at $Y = 1/4$ to the plane at $Y = 1$, the illumination at the cell plane still exhibits a peak-to-valley non-uniformity of 50%. A maximum non-uniformity in the 15% - 25% range is felt to be acceptable. At the $Y = 1$ location the curvature of the side reflectors has been reduced so drastically that the parabolic advantage in collector efficiency is virtually lost; the contour nearly resembles a straight trough. For parabolic petals or pyramids the illumination non-uniformities are even more severe.

An important variation of the parabolic contour is the so-called CPS (Compound Parabolic Concentrator), also known as the Winston trough. This configuration is finding wide popularity in terrestrial solar-thermal applications since it is the most efficient collector of all configurations. In essence, CPC contours are obtained by tilting the normal parabolic sides inwards by a certain degree to form an even sharper collection trough. However, studies have shown that the illumination distribution is more highly non-uniform than for normal parabolic contours. Thus all parabolic contours have been eliminated for low-CR applications in this study.

Beam uniformity arguments have also been used to eliminate all cone configurations from further investigation. All cones, including those with straight contours, cast an illumination profile which rises sharply to a point at the center of the cell area. This problem could be avoided by not utilizing a significant center portion of the cell plane. This measure, however, results in an extremely poor collector efficiency for the reflector configuration. Another solution to the problem can be achieved by allowing a gap mid-way up the reflector sides. These solutions are also characterized by either a poor collector efficiency or by structures that are too complex for practical usage in space.

From the previous discussion the selection of appropriate low-CR reflector configurations can be narrowed to simple and multi-faceted troughs, petals, and pyramids. One interesting variation of the basic trough--the "W" trough--was suggested in previous concentrator studies. In the "W" configuration, the outer two legs of the "W" are reflector surfaces, which reflect incident light onto the inner two legs of the "W", where solar cells are laid down. Geometric analysis demonstrates that this configuration offers no advantage in collector efficiency over normal trough configurations and has the disadvantage of an obstructed heat rejection field from the cell area rear surface which lowers cell operating efficiency. In the discussion below, selection criteria for basic trough, petal, and pyramid are developed and analyzed.

The manner in which a multi-faceted contour is configured is shown in Figure 2-23 The leftmost segment of the figure shows the simplest case--a single-facet trough. For each value of the reflector angle θ, there exists a single value of reflector length W, for which the outermost intercepted ray is cast upon the furthermost edge of the cell area X. The projections of W_1 into the plane of the cell area uniquely defines the amount of intercepted light and thus the geometric concentration ratio (i.e., the CR for a 100%-efficient reflector). Stated conversely: the selection of a specific CR-value uniquely determines the geometry (W_1 and θ) of a given reflector configuration-type. The central and rightmost segments show how this conclusion is extended to two- and three-faceted troughs. In every case, each facet is angled such that its intercepted column of light is cast completely (and uniformly) upon the cell area and only upon the cell area. For each configuration, the selection of a specific CR-value uniquely determines a set of reflector angles θ, ϕ, ψ , etc. as well as a set of reflector lengths W_1, W_2, W_3, etc. It is thus possible to uniquely characterize the performance of various competing configurations for a desired CR.

Figure 2-24 shows the manner in which the reflector area increases as the desired geometric concentration ratio is increased for various reflector configurations. The figure of merit which is plotted in the figure is the reflector area ratio, which, as the insert in the figure shows, is the reflector length normalized by the cell area width. This parameter has been adjusted for three-dimensionality of such configurations as the petals and pyramids. The same treatment applies for Figure 2-25 ,

- CR = f(θ, n_{fac})
- UNIFORM BEAM DISTRIBUTION
- W/X = f(θ, n_{fac})
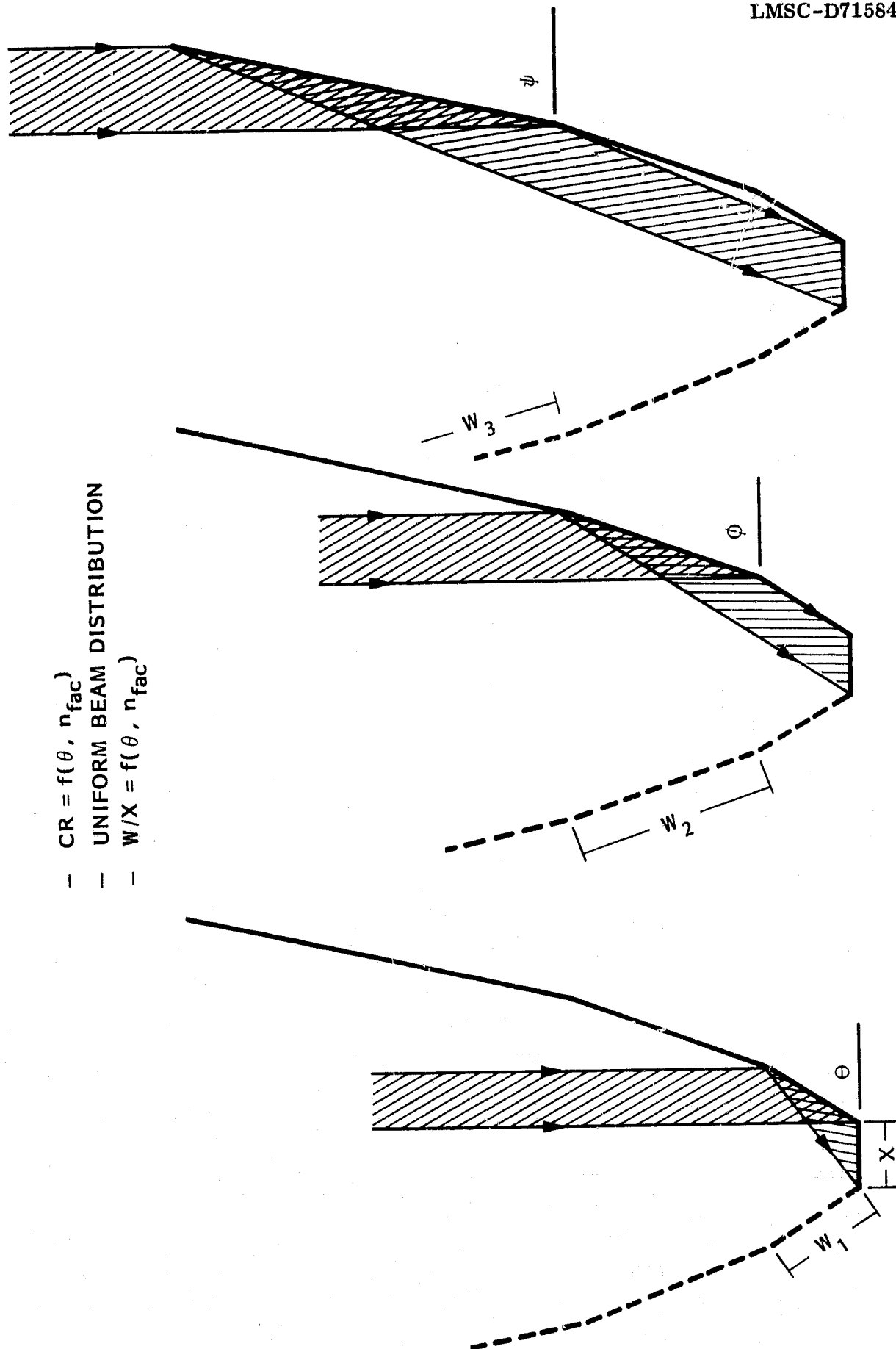
Figure 2-23 Multi-Facet Planar-Trough Concentration

LOCKHEED MISSILES & SPACE COMPANY. INC.
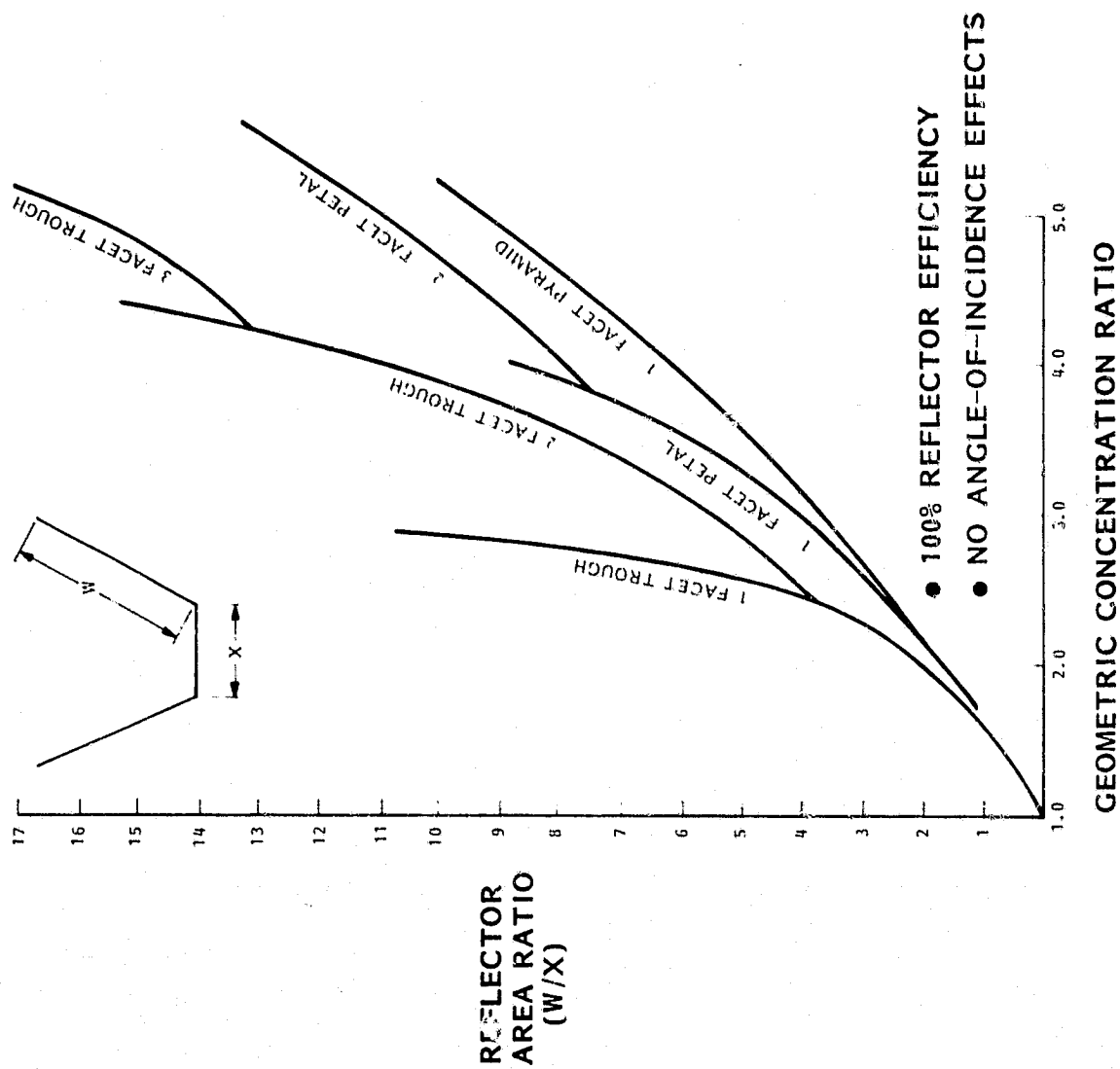
Figure 2-24 Low-CR Reflector Area Comparison

REFLECTOR AREA RATIO (W/X)

GEOMETRIC CONCENTRATION RATIO

- 100% REFLECTOR EFFICIENCY
- NO ANGLE-OF-INCIDENCE EFFECTS

3 FACET TROUGH

2 FACET PETAL

1 FACET PYRAMID

2 FACET TROUGH

1 FACET PETAL

1 FACET TROUGH

LOCKHEED MISSILES & SPACE COMPANY. INC.
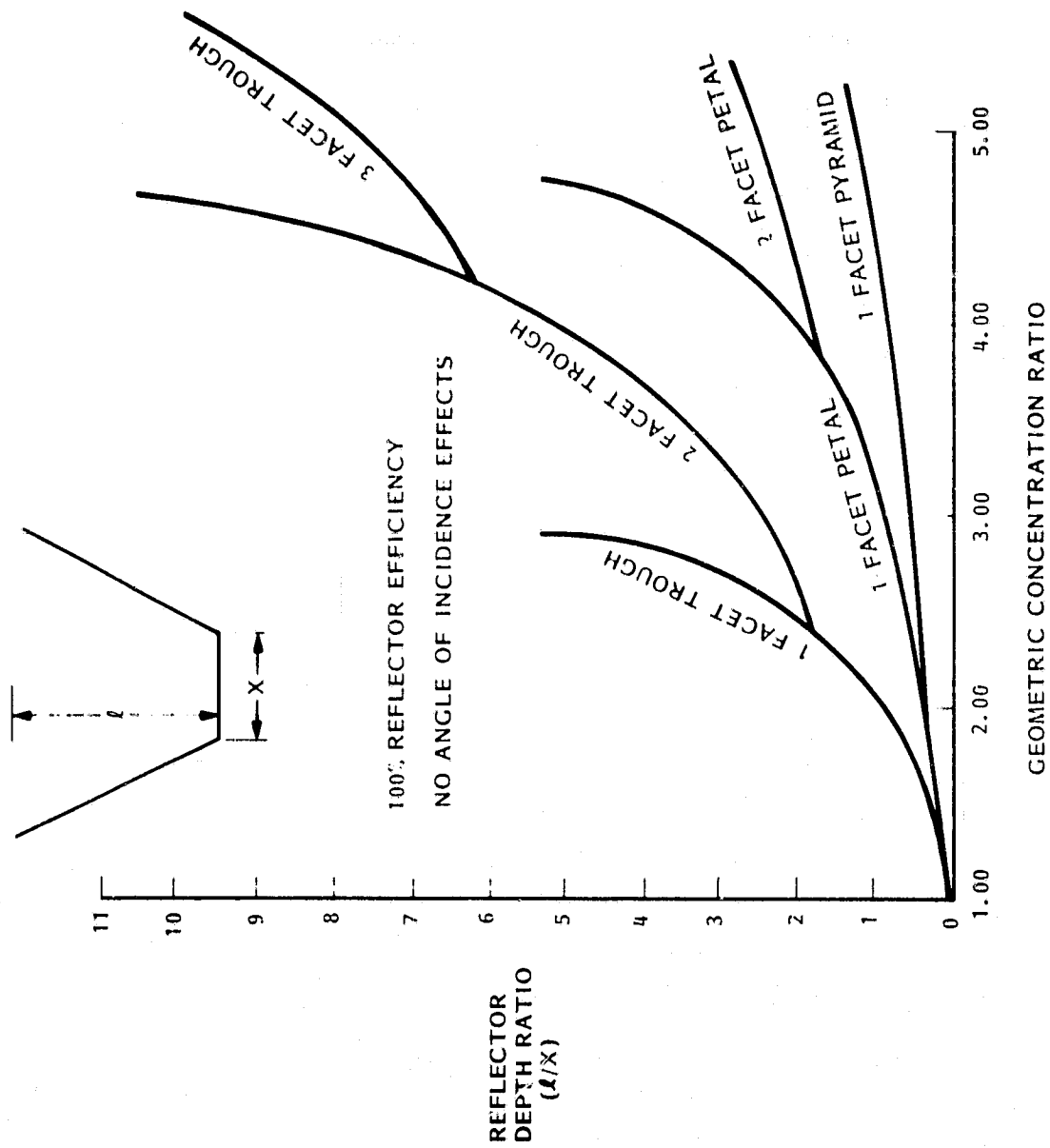
Figure 2-25 Low-CR Reflector Depth Comparison

LOCKHEED MISSILES & SPACE COMPANY, INC.

which shows the reflector depth ratio, i.e., the perpendicular depth normalized to the cell area width. Both figures clearly show the ranges of CR achievable for the various configurations. For example, the single-facet trough curve rises assymptotically to 3 suns; the 2-facet trough and single-facet petal to 5 suns; the 3-facet trough to 7 suns; the single-facet pyramid and 2-facet petal to 9 suns.

The assymptotes discussed above represent a theoretical upper limit achievable, although the structural and weight penalties of driving a reflector configuration into the neighborhood of its limit are too severe. Figure 2-26 shows the cross-sections of three basic options for achieving a geometric concentration ratio (GCR) of 5 suns. The extreme depth of the trough configuration makes a disturbing impression immediately. Reflector misalignment was not investigated analytically for the candidate configurations since a comprehensive treatment of external and internal angular misalignment was beyond the major scope and purpose of the present study. Nonetheless, misalignment of such a trough configuration can intuitively be seen to be a potential problem area. This concern applies to a lesser degree for the 2-facet petal, although its depth ratio appears to be down in an acceptable range. From an analytical point of view the pyramid configuration is superior. However, it is more difficult to design a stowage and deployment scheme for such four-sided reflector configurations than it is for trough types.

In order to get a better feeling for the stowage and deployment difficulties associated with the three reflector configurations of Figure 2-26, preliminary design sketches of representative array segments were generated. Figure 2-27 shows a segment of the 3-facet trough concept. One can visualize several parallel rows of such troughs in some sort of frame structure. As in present day LMSC large flexible arrays, the trough in the figure is suspended in the frame by a series of tensioning cables and negator springs which control the blanket and reflector tensions and prevent major lateral out-of-line motions of the trough. A major difficulty arises when attempting to design a credible stowage scheme. The cell blankets may be folded in present day accordian fashion and the six reflector surfaces may be similarly folded or rolled onto drums for stowage. However, these folded and/or rolled packages must be collapsed in some manner into a dense package in the Orbiter bay. This collapsing sequence presents a kinematic problem of enormous

2-60
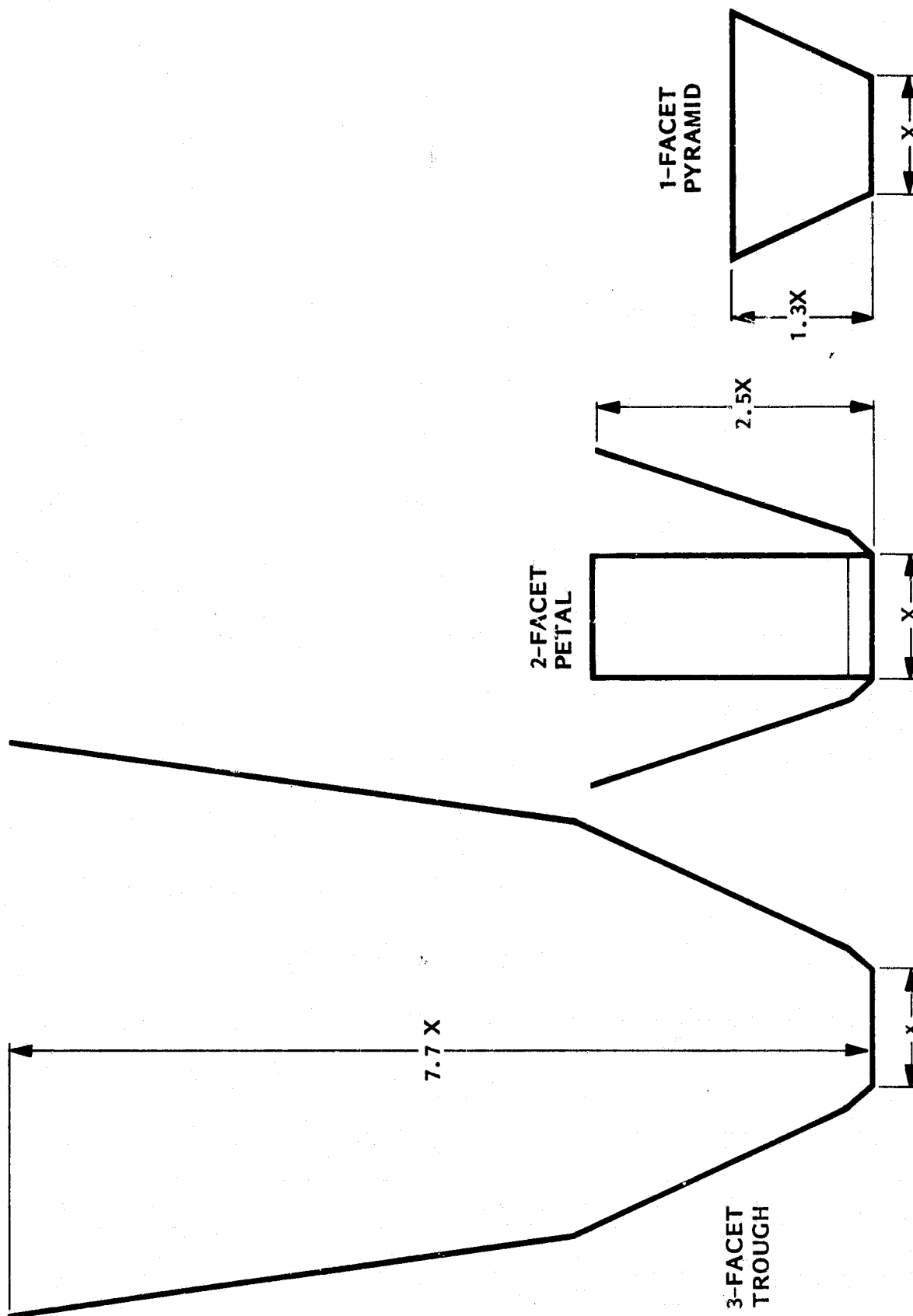
Figure 2-26 Low-CR Reflector Geometries for GCR=5

3-FACET TROUGH
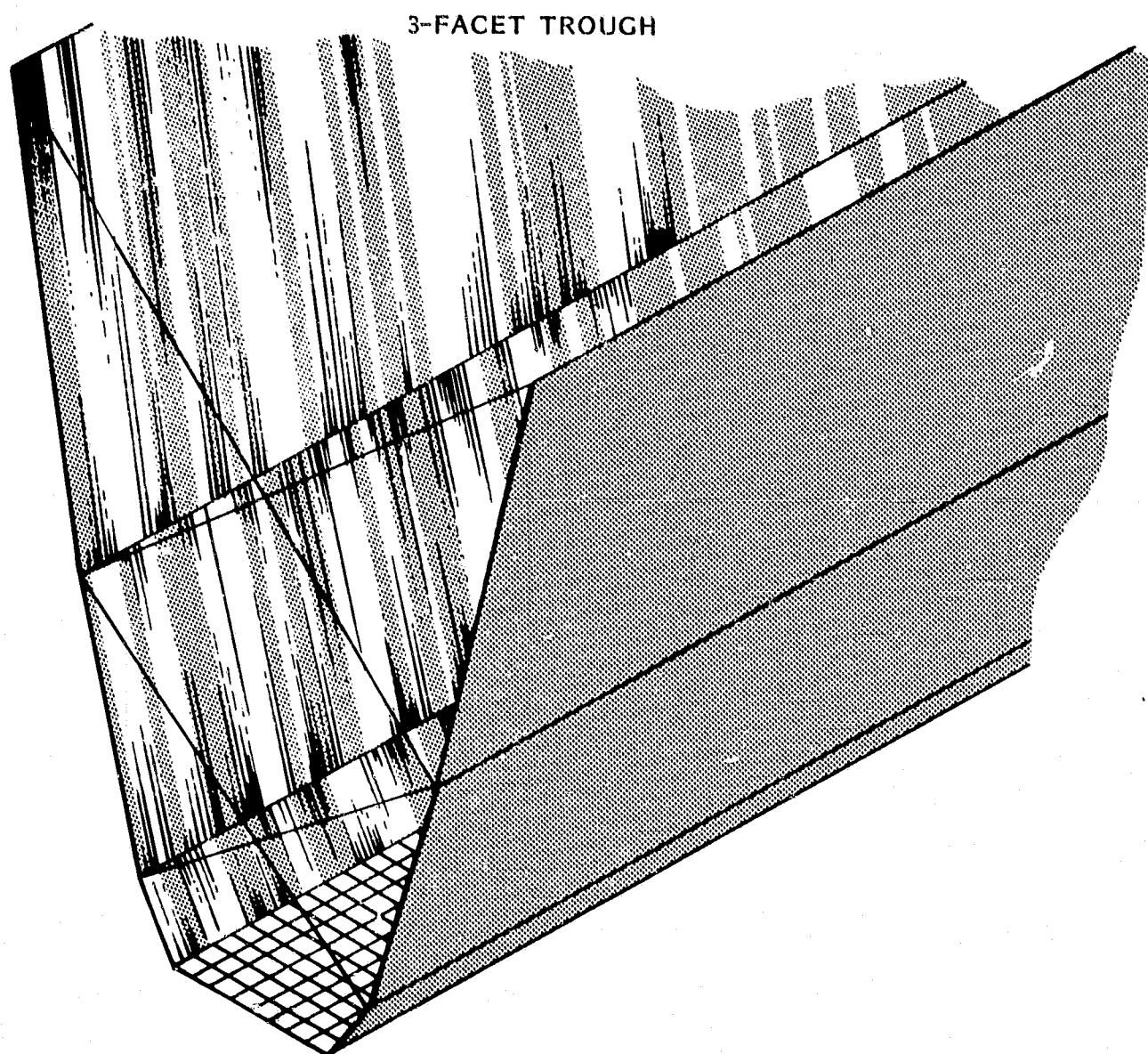
Figure 2-27 Low-CR Reflector Concept 1

2-62

LOCKHEED MISSILES & SPACE COMPANY, INC.

complexity. One would expect, as a minimum, one hinge or pivot at the interface line of each leg of the trough contour. With so many joints coming into play, it is difficult to imagine that such a deep structure can be deployed repeatedly to the designated angular tolerances and then tensioned uniformly without requiring massive structural support.

Figure 2-28 shows a segment of the 2-facet petal concept. As was postulated for the trough case above, here several rows of tandem petals can also be suspended and tensioned in a frame structure. As a result of the smaller dimensions, stowage and deployment of such an array can be achieved with somewhat more credibility than for the trough case. Nonetheless, it is equally difficult to imagine that the surfaces can be deployed repeatedly to the designated angular tolerances and tensioned properly. An added difficulty is posed by the presence of the "back-to-back" reflector segments, which must be brought into position, held, and tensioned with tolerances and tension fields which are perpendicular to those of the side reflectors.

Figure 2-29 shows the pyramid reflector concept. This geometrical shape will be designated by the more precise mathematical term Truncated Pentahedral Pyramid, or TPP. One can visualize a string of tandem TPP's suspended in a frame structure as in the two previous cases. Two advantages are immediately evident. First, a tandem string of TPP's requires a fewer number of tension lines and the positioning of the "back-to-back" reflectors can be controlled at the TPP corners. Second, the number of joints or pivots has been reduced to a minimum, permitting credible repeatability of deployment angles. The major difficulty to be solved is the manner in which such a configuration can be densely packaged and stowed. The solution to this problem will be addressed after a brief discussion of the TPP illumination characteristics below.

While it is clear that the trough and petal configurations yield a uniform reflected beam distribution, it is not immediately obvious that the TPP also does so. Figure 2-29 also shows a typical ray which is incident upon a TPP corner segment at an angle which is normal to the array (i.e. to the cell plane). This ray is reflected onto the adjacent reflector face and from there onto the cell plane. Geometric analysis shows

2-63

2 – FACET INTEGRATED PETAL

OR HALF – PYRAMID (CONTINUOUS SIDE – TROUGH)
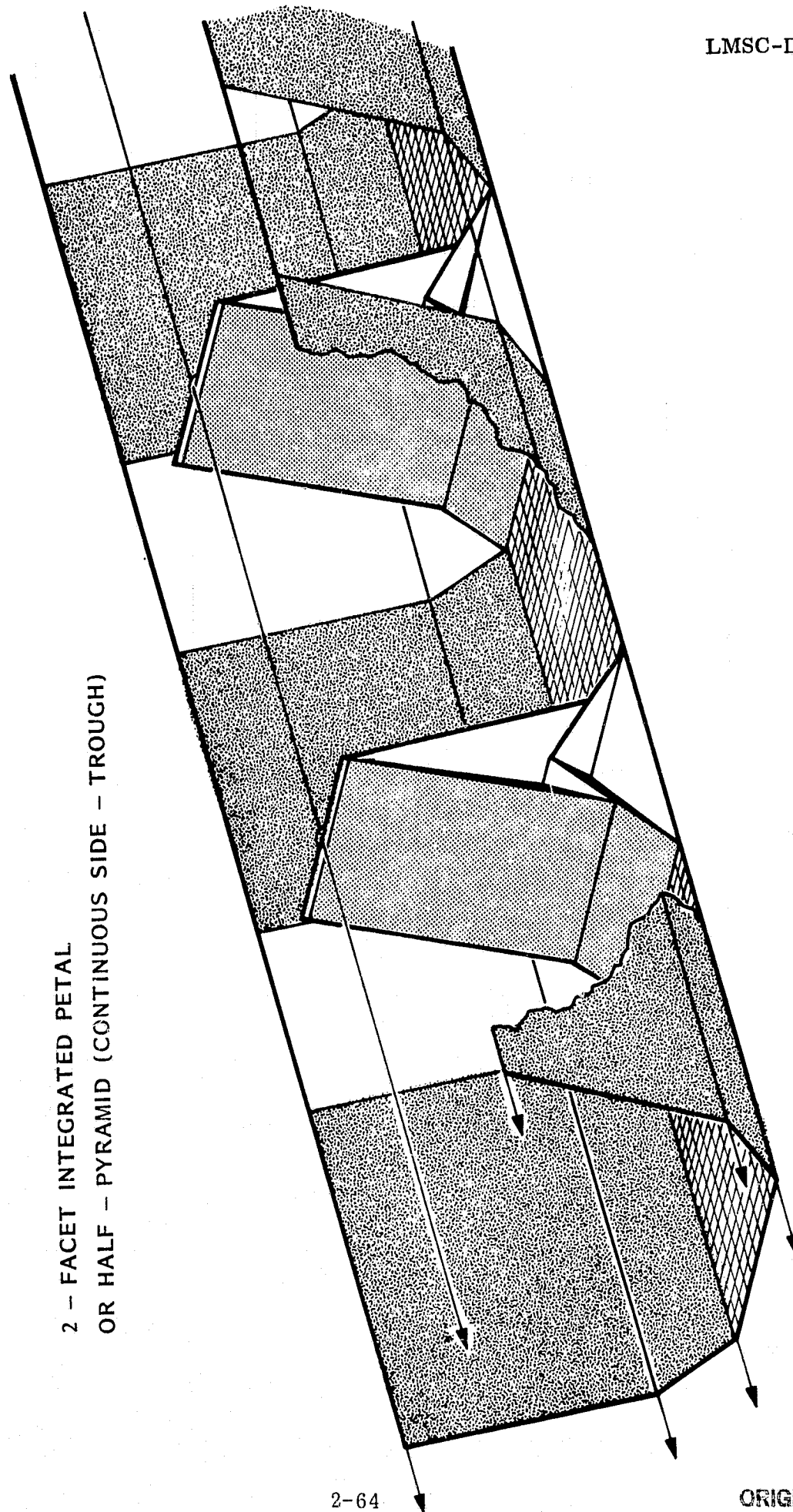
Figure 2-28 Low-CR Reflector Concept II

LMSC-D715841

LOCKHEED MISSILES & COMPANY, INC.

TRUNCATED PENTAHEDRAL PYRAMID
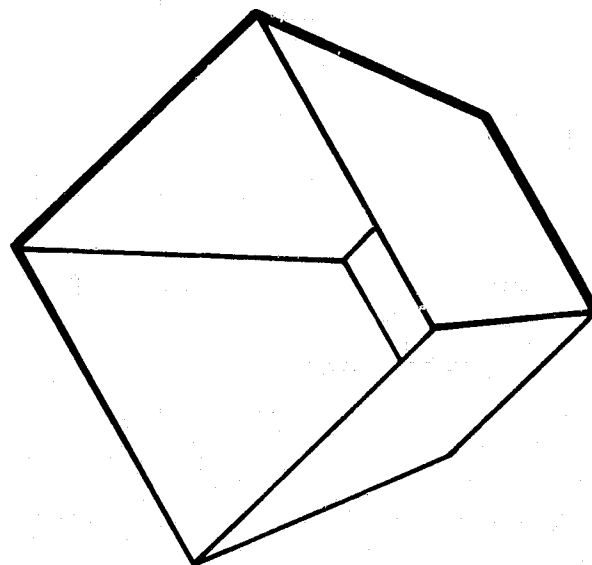
INCIDENT
RAY NORMAL
TO CELL PLANE
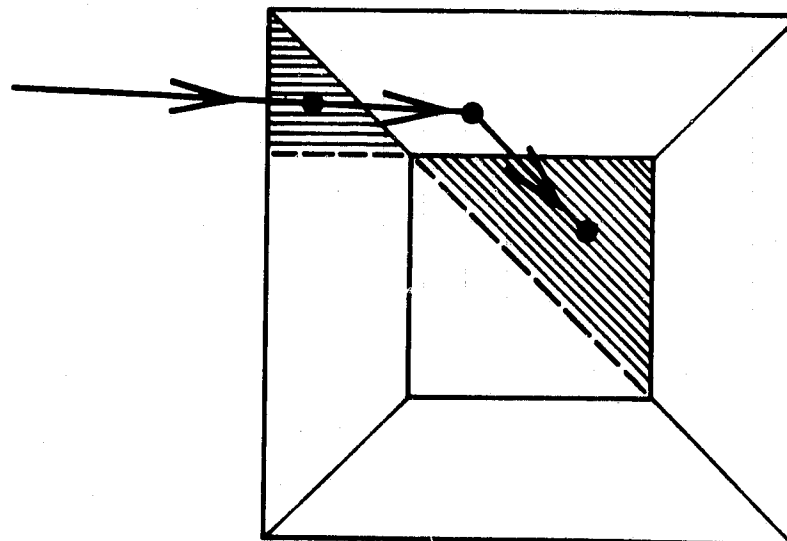
CORNER
REFLECTION
PATTERN

Figure 2-29 Low-CR Reflector Concept III

LOCKHEED MISSILES & SPACE COMPANY, INC.

that a uniform triangular bundle of rays onto the corner segment is reflected uniformly onto the oppositely-situated diagonal-half of the cell plane. Summing up the contributions from all eight corner segments yields a uniform total corner contribution. Actually, a mapping of each separate corner contribution shows that each pair of adjacent corner segments covers the entire cell plane with a different mapping mode, so that corner misalignments do not lead to gross cumulative variations in illumination at a single location on the cell plane.

In order to devise an acceptable stowage scheme for a string of TPP reflector faces, each TPP was considered as an individual inseparable unit. Numerous folding schemes were tested on paper models. Figure 2-30 shows an attractive scheme which resulted from these trials. The illustrated folding scheme is characterized by the following advantages:

- Two opposite reflector faces remain unfolded so that a string of TPP's can be deployed by "pulling" in one direction only.

- A good compromise is achieved between the desire to fold as much material as possible into the smallest frontal area and the counter-acting need to avoid excessive thickness build-up through too many layers at a single point in the stowed package.

- The fold lines are located such that with skeletal struts, a proper choice of hinge location, and 4 to 8 locking pivots, a deployed structure of surprisingly good stability and stiffness is achieved.

At this level of design definition it was appropriate to review the advantages and disadvantages of the three low-CR reflector configurations and to make a single selection for further design at full array level and for detailed performance and cost analysis. Table 2-6 summarizes the appropriate figures of merit for GCR = 5 as discussed previously and adds a further one not discussed previously-- the module packing factor. This parameter gives a ratio of the area (reflector and cell surface) available for intercepting incident light to the gross perimetrical area required by the respective reflector configurations under the idealized conditions of negligible gap between parallel rows. That is, several adjacent rows of troughs

TRUNCATED

PENTAHEDRAL
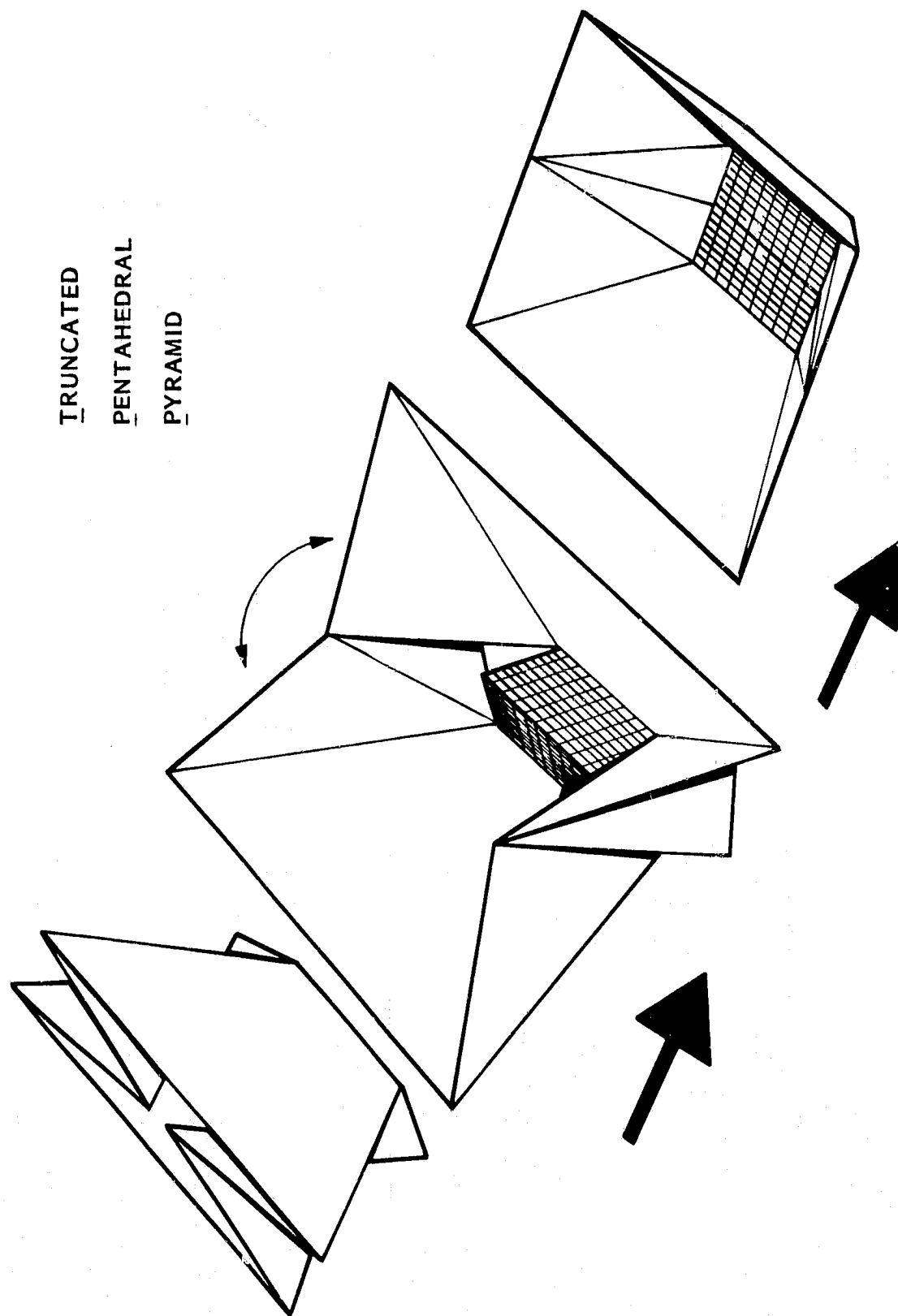
PYRAMID

Figure 2-30 TPP-Reflector, Foldable

LOCKHEED MISSILES & SPACE COMPANY, INC.

TABLE 2-6

LOW-CR REFLECTOR CONCEPT COMPARISON

CONFIGURATION	TROUGH	PETAL	PYRAMID
GEOMETRIC – CR	5	5	5
REFLECTOR AREA RATIO	16.0	10.8	9.2
REFLECTOR DEPTH RATIO	7.7	2.5	1.3
MODULE PACKING FACTOR	1.0	0.56 – 0.83	1.0

LOCKHEED MISSILES & SPACE COMPANY. INC.

or of pyramids (TPP's), with negligible gap between rows, will intercept all incident light. Petals, however, have open corners and thus do not intercept all incident light. Adjacent rows of petals can be butted up to each other in several different ways, as illustrated in Figure 2- 31 . At best they will pass approximately 17% of the incoming light; at worst approximately 44%. This parameter has serious implications for the amount by which the supporting frame structure must be oversized to accommodate an array of a given power level.

Based upon the comparative analysis above and the credibility of the schemes which have been evaluated for stowage and deployment, the TPP reflector concept has shown a clear overall superiority for low-CR application and has been selected for further detailed design and analysis.
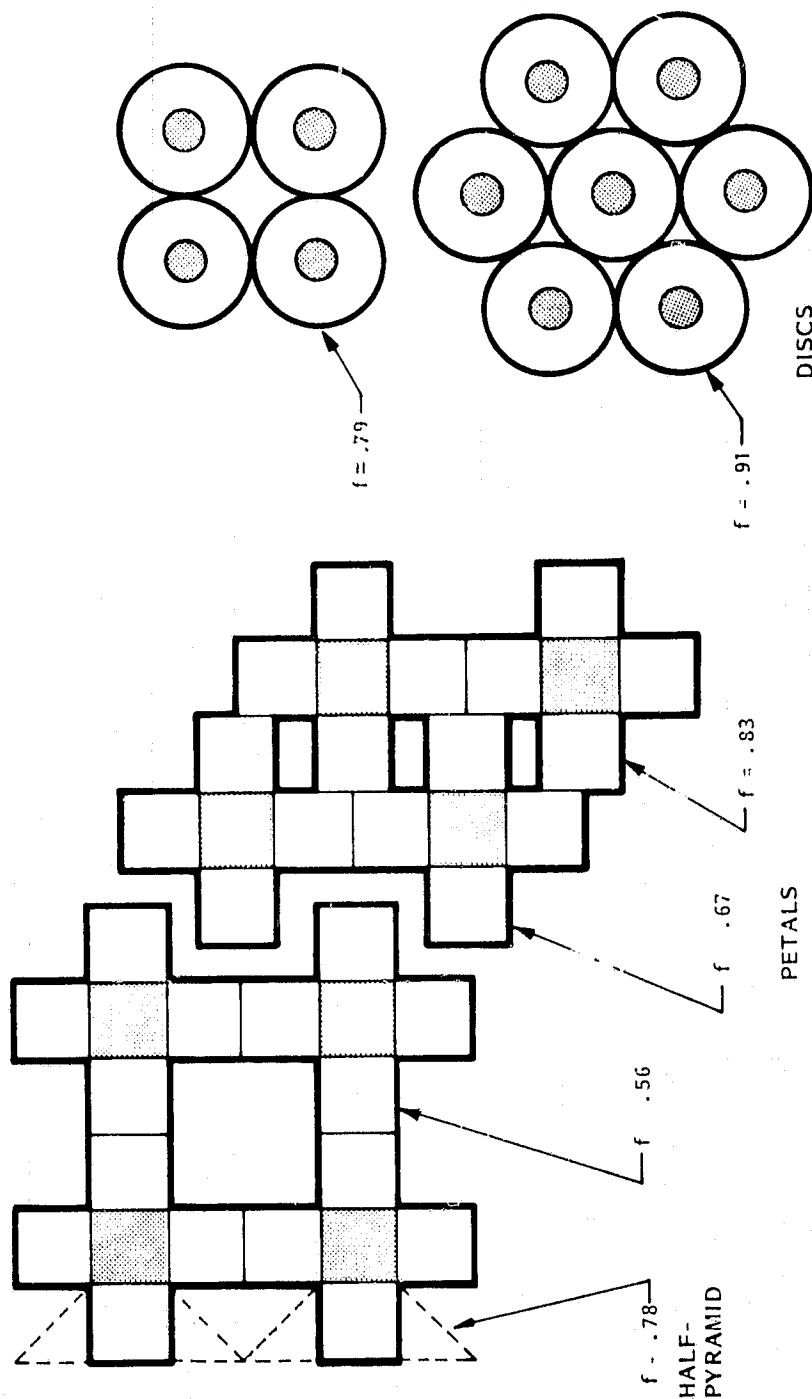
Figure 2-31 S/A Module Packing Factors – f

A string of TPP's in series can be folded up and stowed in several different ways in the Orbiter bay. Since some type of frame structure will be used to deploy and support the TPP-strings, any packaging scheme must seek to position the stowed frame elements in a manner which has the least impact upon TPP density or dimensions. This generally means stowing the frame elements lengthwise along the outer edges of the cargo bay.

Figure 2-32 shows three foldable-TPP schemes as well as a fourth scheme for comparison in which the TPP's are not folded but rather stacked end-to-end along the length of the bay. In the three foldable schemes the trapezoidal packets represent a collapsed string of 12 TPP's each. The three arrangements of these packets in the bay represent basic alternatives which resulted from an investigation of deployment kinematics utilizing a large collapsible beam/extendible mast combination space frame similar to the frame concept for the planar array.

The stacked scheme, while intuitively appealing, emerges as the least attractive of the four. It suffers from the poorest packing density for two reasons. First, a considerable amount of stowage volume is wasted in the interior space of the first TPP in the stack. This space is unsuitable for the stowage of frame structure elements since it offers no access to the side walls for mounting and hold-down. Secondly, the skeletal frame struts of the TPP's are stacked against each other at a high angle. Stacking objects at an angle results in a greater step length between objects (and, consequently, poorer packing density) than for stacking at upright angles.

Aside from the poor packing density of the stackable scheme, once on orbit, the removal of separate TPP's and their installation into a deployed space frame poses an extremely complex problem in manipulation and holding, especially when several hundred TPP's are involved.

The three illustrated foldable schemes are all self-deployable by means of a collapsible frame structure which is stowed and held-down outside the cross-sectional silhouette of the TPP-packets. As the figure indicates, the best

2-71

- MODERATE PACKING DENSITY
- SIMPLEST DEPLOYMENT

- BEST PACKING DENSITY
- COMPLEX DEPLOYMENT

- POOR PACKING DENSITY
- VERY COMPLEX DEPLOYMENT

- GOOD PACKING DENSITY
- COMPLEX DEPLOYMENT
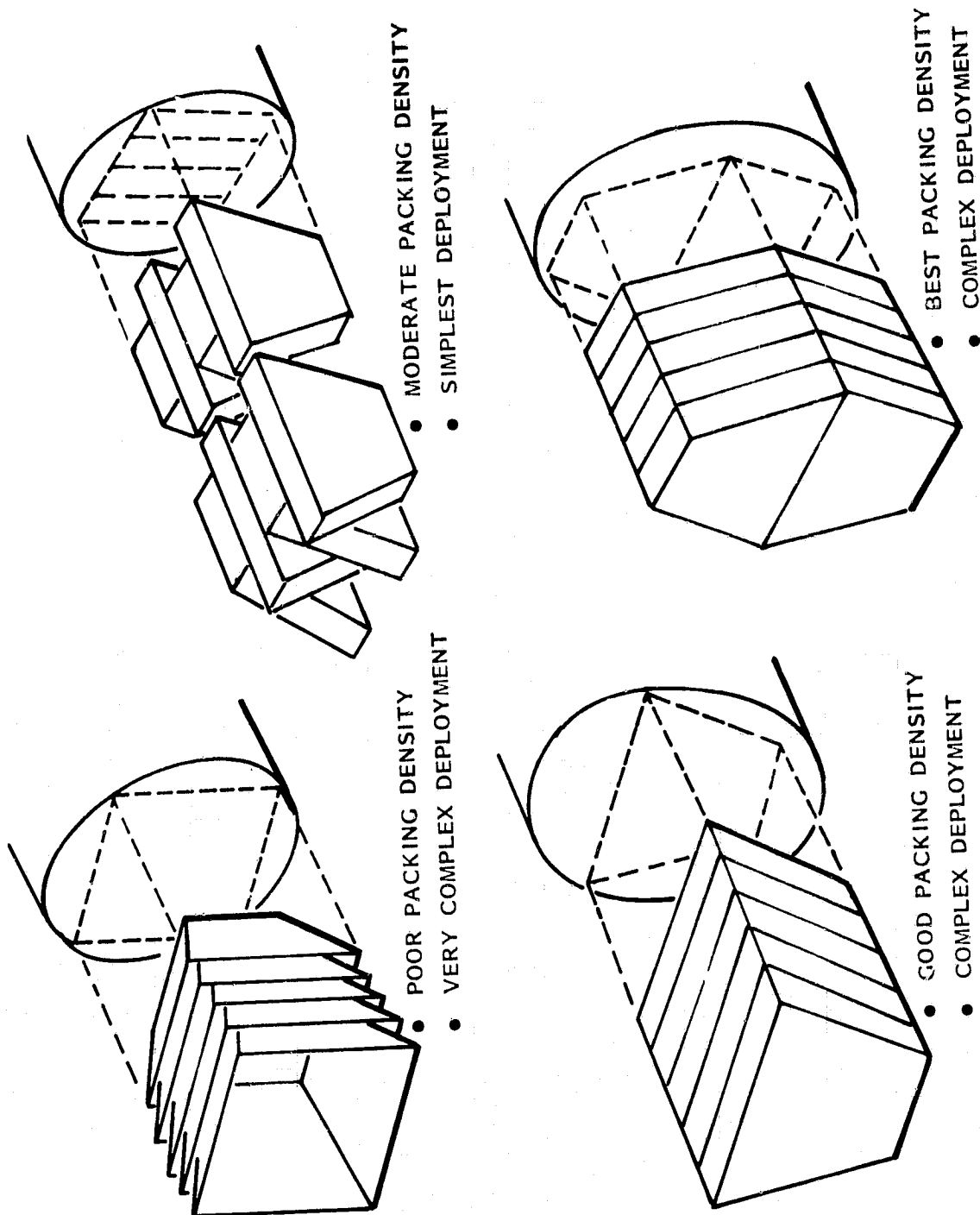
Figure 2-32 Alternative Packaging Schemes/Low-CR

packing density is achieved by the scheme with two rows of TPP's on top of each other (~35% higher packing factor than the adjacent single row scheme). Although this scheme requires more complex deployment kinematics, cost analysis shows that the overriding concern is to offset high launch-costs-per-watt by maximizing packing density.

Figure 2-33 shows a more detailed design of the two-row packaging scheme. Packets of 12 folded TPP's have been enclosed and pressurized in individual gondolas which are graphite-epoxy truss-structures. Each gondola consists of two open-top box-like structures, one of which fits completely inside the other like a box with a deep cover. Gondola separation is ultimately achieved by the deployment of extendible masts. The figure shows the manner in which the mast canisters are located in the available space between the gondolas and the Orbiter side wall. A total of 40 gondolas (x 12 = 480 TPP's) are capable of being stowed in the available cargo bay length defined earlier.

Figures 2-34 and 2-35 show the deployment sequence in steps. Though the sequence appears complicated, each separate step is performed with simple, positively-driven mechanisms (motors, hinges, etc.). The initial "flip-over" places all gondolas in the same plane, followed by a pantograph-type extension which locks all gondolas into a long double-row with properties of a stiff beam. The final deployment step is a coordinated extension of the masts, which separates the mated gondola-halves and deploys the strings of TPP's.

The deployed TPP has a depth of approx. 6 ft. Tension must be applied to the deployed TPP-string at top and bottom. For this reason a frame configuration has been chosen which has depth and which features an upper and lower plane of masts for sufficient overall frame rigidity. Of the two familiar mast options discussed above in relation to the planar array, the light mast option was felt to be adequate here since its stiffness influence on the overall frame is enhanced by its greater numbers (24 vs 10 for the planar array) and by the bi-planar arrangement.

DEPLOYABLE
MAST
CANISTERS

28"

20 GONDOLAS
= 46.67'

13.50'

4.50'

10.06'

ORBITER
ENVELOPE
15' DIA

STOWAGE
GONDOLAS
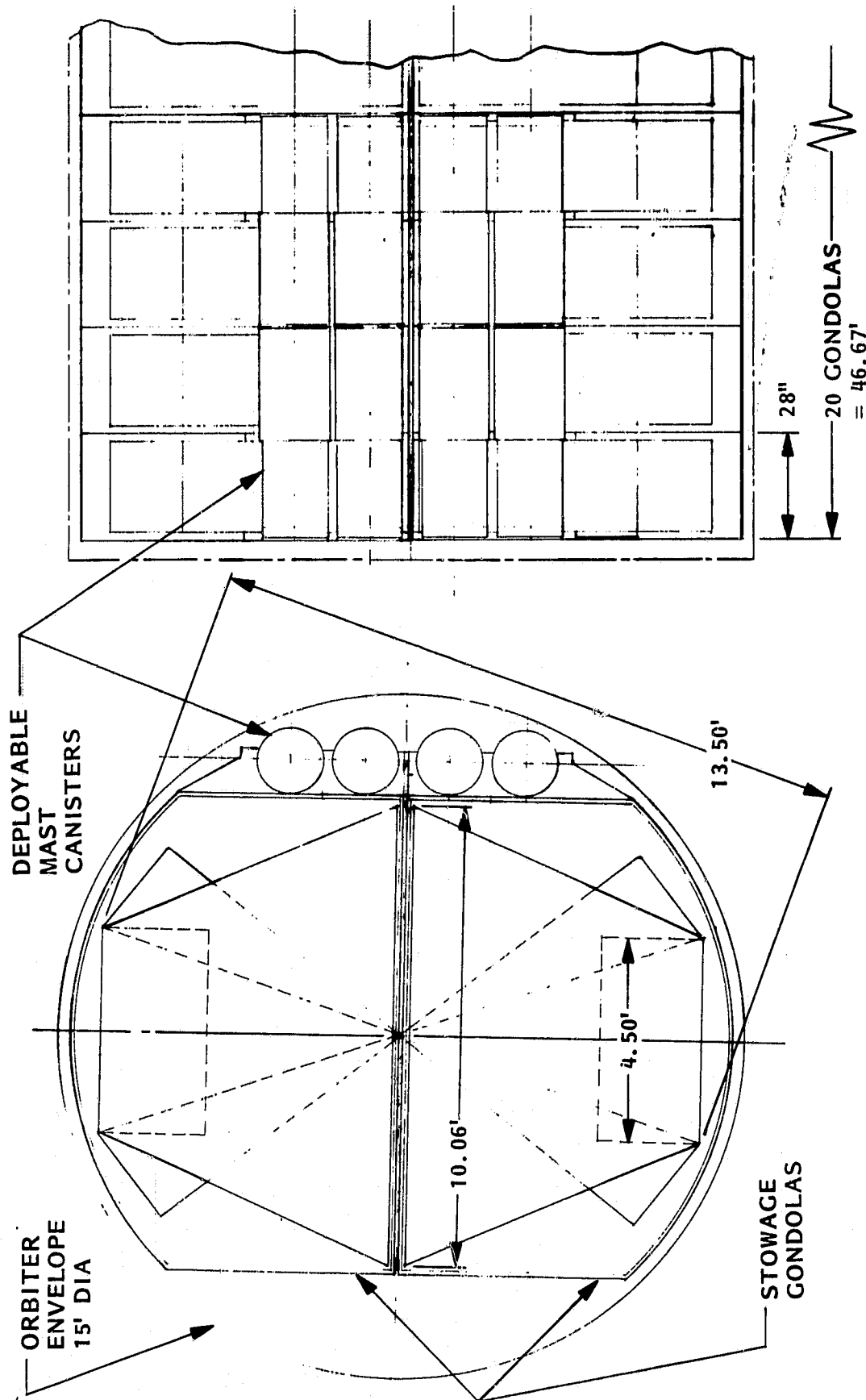
Figure 2-33 Low-CR Array – Stowed Configuration

LOCKHEED MISSILES & SPACE COMPANY. INC.

40 GONDOLAS @ 12 TPPs
= 480 TPPs

STOWED

CONTINUED
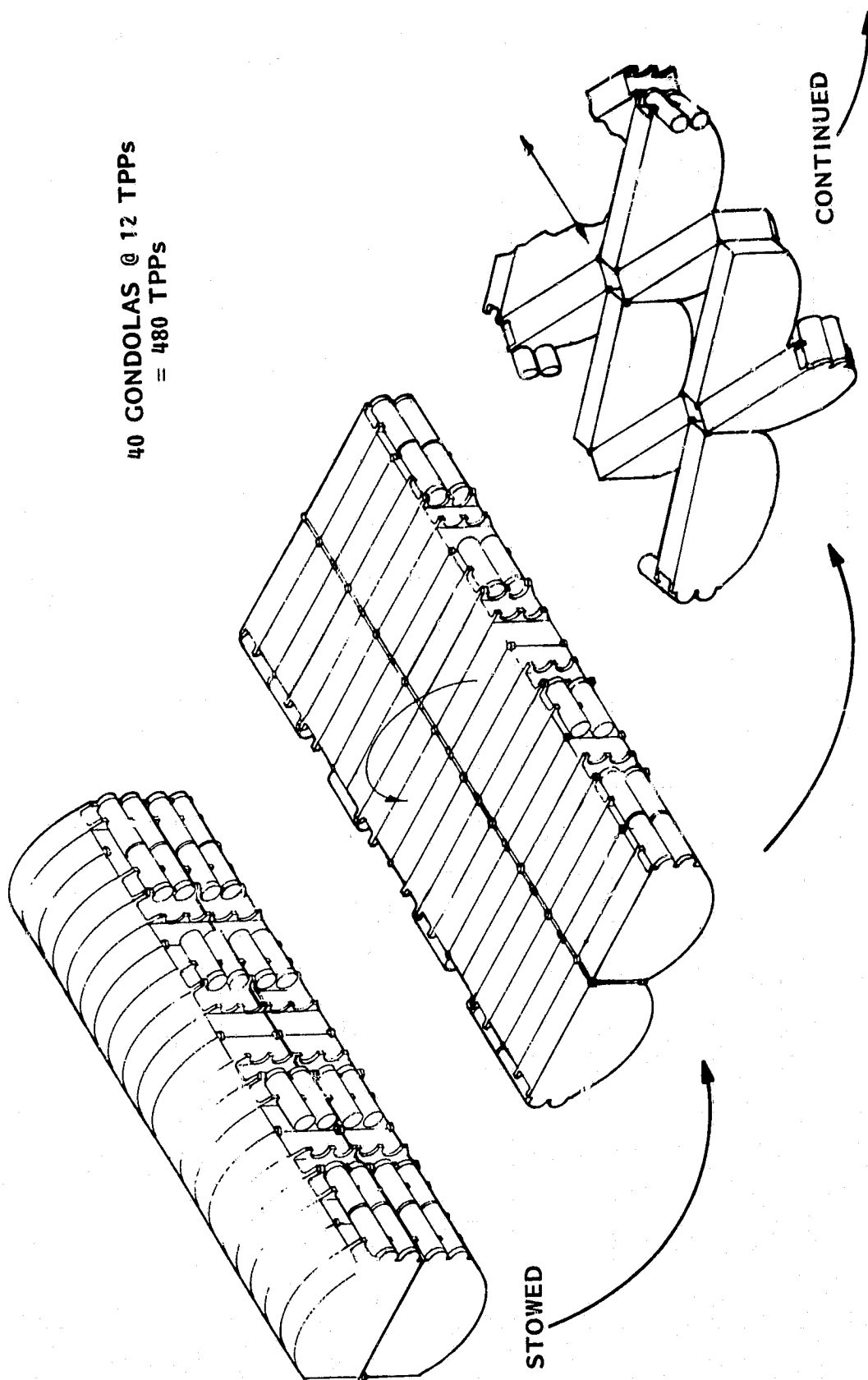
Figure 2-34 Low-CR Array – Initial Deployment Stages

C-2
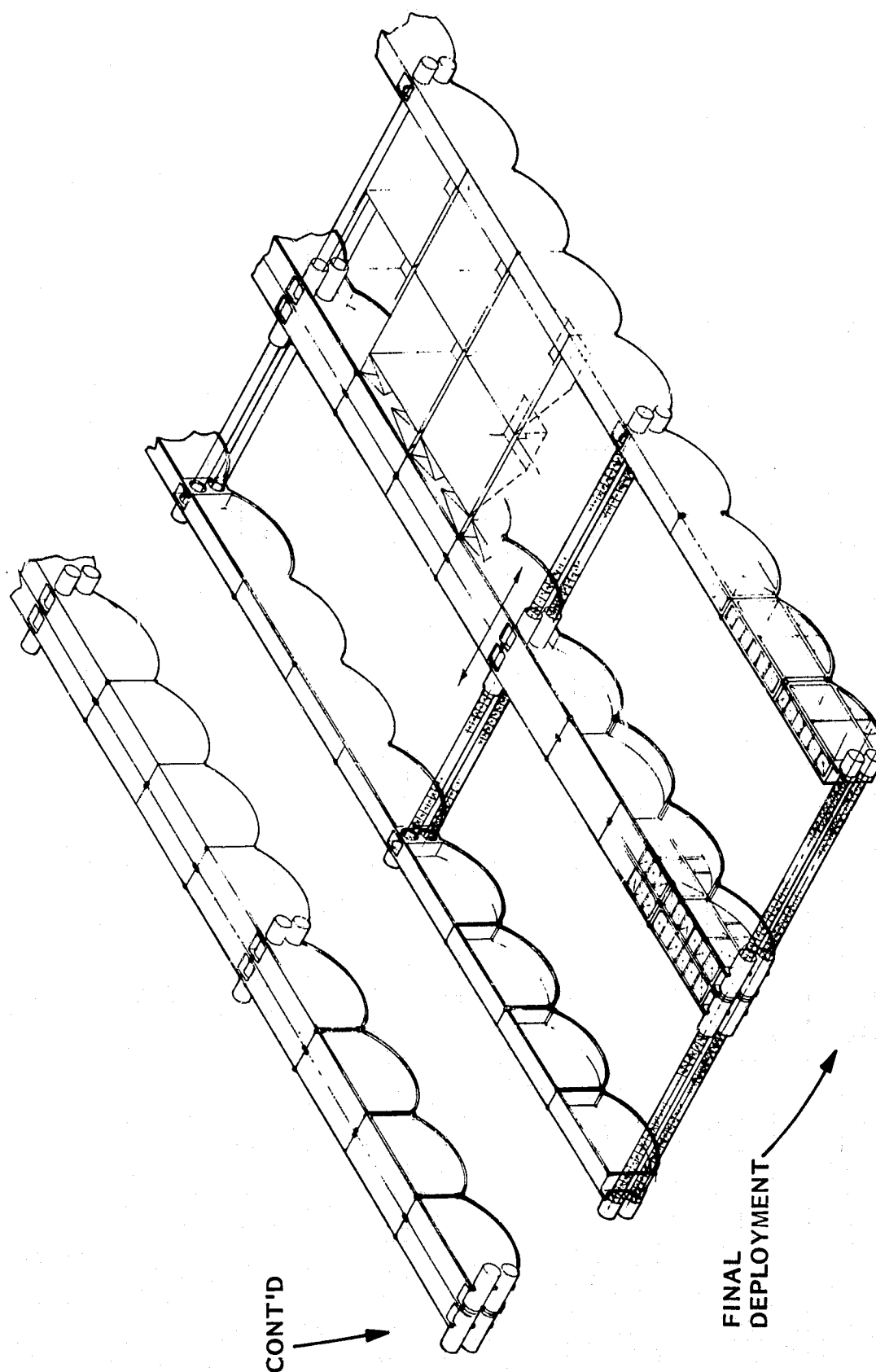
Figure 2-35 Low-CR Array – Final Deployment Stages

CONT'D

FINAL DEPLOYMENT

A modular unit of the low-CR array consists of a field of eight TPP-strings which is bounded at each end by a mast-pair (ref. Figure 2-35   ). A modular unit thus has the gross dimensions of 50' x 250'.

Figure 2- 36   shows a close-up view of a string of TPP's during final deployment. This figure imparts an appearance of massiveness to the TPP skeletal frame which is not intended. The actual frame consists of graphite-epoxy struts which form a hinged frame around the top, around the bottom, and down all four corners. The reflector material is suspended between the struts. In addition, adjacent TPP's are spaced by hinged struts connecting the corners of adjacent bottom planes. Each TPP is approx. 10' x 10' at the top. The actual size of the unit can also be seen in relation to the human figure in the illustration.

Figure 2- 37   shows a complete unit of 5 modules (i.e., one full Orbiter load) after final deployment on-station. The illustrated array design can be utilized with silicon solar cells or with GaAs solar cells. The performance analysis of chapter 2.8 was carried out for both options and shows that two of the illustrated units (i.e., two flights total) are needed to provide power in the 300 kW range if silicon cells are used. If GaAs cells are employed, only one such unit (1 flight) is necessary to achieve the same power range. As the cost analysis in chapter 4 will show, the higher cost of the GaAs cells is more than compensated by the cost savings realized through the elimination of the second flight, resulting in an overall cost advantage for the GaAs version. The performance values cited in the figure, as well as the illustrated array dimensions, apply for the GaAs version only.
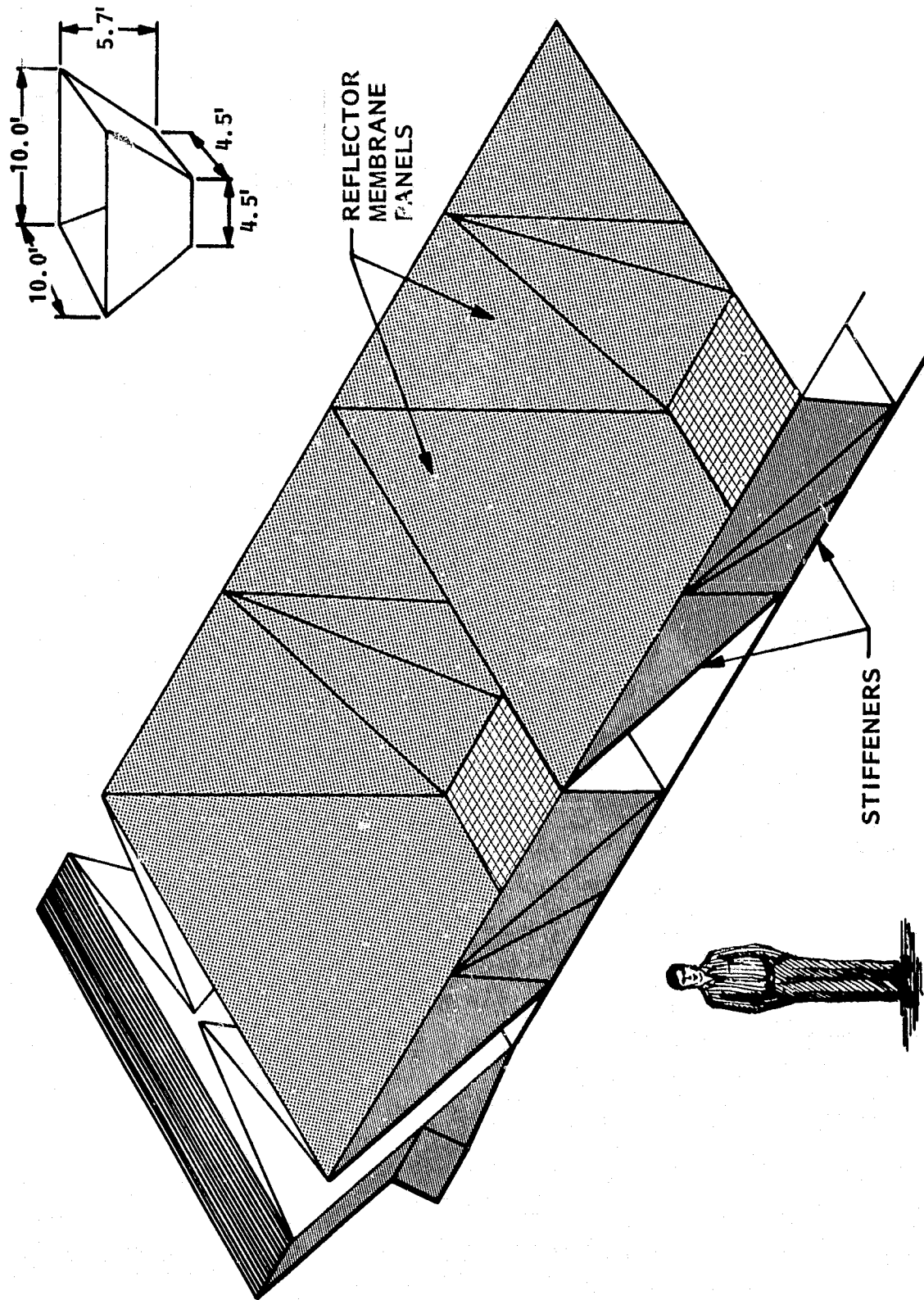
Figure 2-36 Low-CR Array Close-Up View During Final Deployment

REFLECTOR MEMBRANE PANELS

STIFFENERS

5.7'

10.0'

10.0'

4.5'

4.5'

LOCKHEED MISSILES & SPACE COMPANY, INC.

- GaAs SOLAR CELLS
- 606 kW BOL
- 437 kW AVERAGE (15 YEAR LEO)

250 FT

250 FT
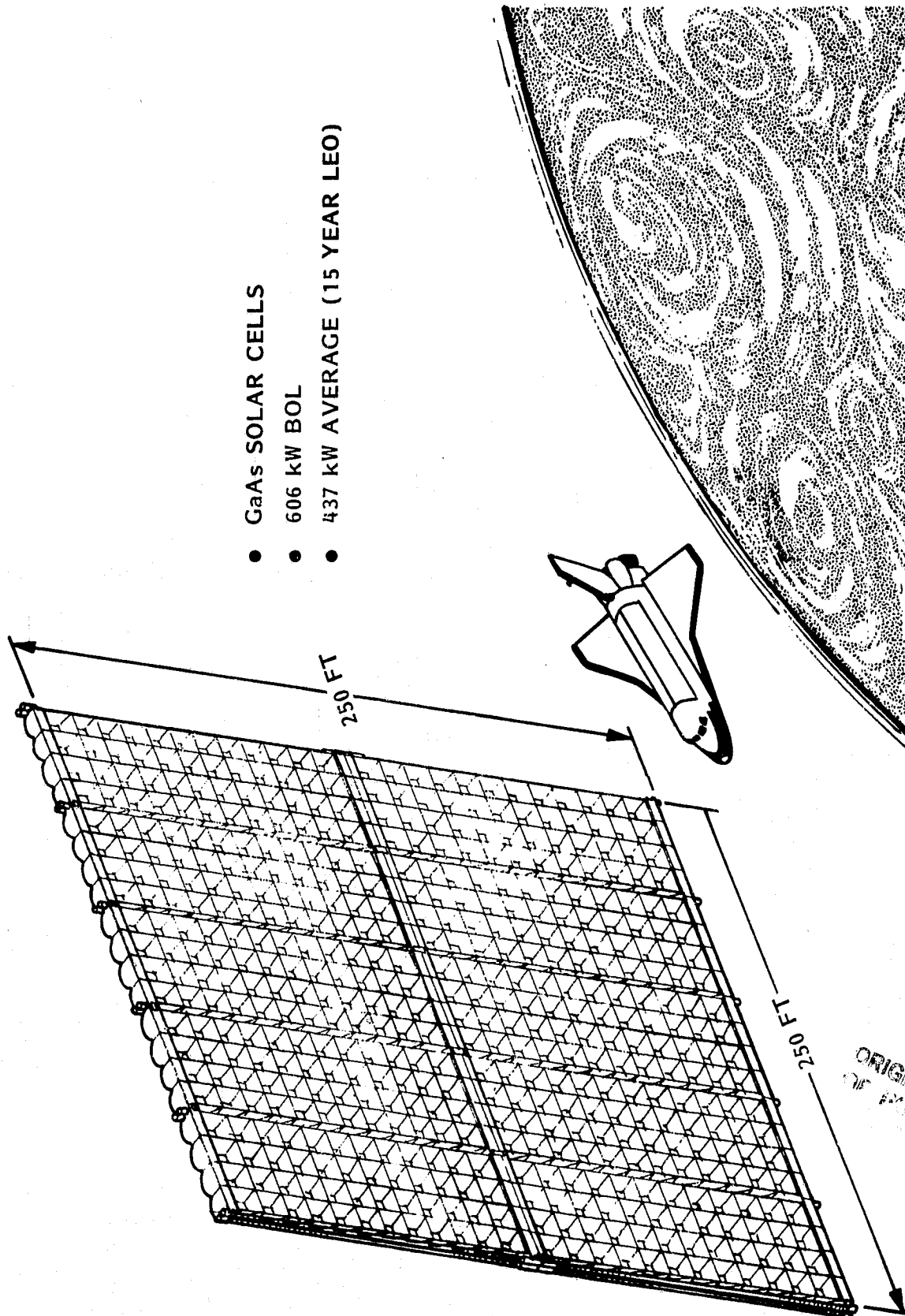
Figure 2-37 Low-CR Array On-Station

2-79

LOCKHEED MISSILES & SPACE COMPANY, INC.

2.6.2 Low-CR Array Thermal Analysis

For the purposes of determining the thermal behavior of the low-CR system, a three-dimensional model was established with radiative-interactive nodes which represent the major parts of a TPP. Figure 2-38 shows a graphic representation of the model used. Nodes representing

- reflectors
- solar cell blanket
- earth
- space

form the basis for the model. Heat inputs to the array consist of sunlight, earth-IR, and albedo. Due to the close proximity of the TPP's, the influence of the neighboring reflector face on all four sides was included in the calculation.

Table 2-7 lists the properties and assumptions made for performing the thermal analysis. Both a silicon cell version and a GaAs version were run. The spectrally selective reflector material (cold mirror) was utilized for all reflector surfaces.

On the basis of reflector studies in section 2.4, the solar cell AM0-efficiency has been converted to an efficiency which applies for the shape of the solar spectrum which actually reaches the cell after single reflection. This "thermal equivalent" efficiency was arrived at through use of the electrical and thermal equivalent reflectances of the reflector material in section 2.4.4. By using this device of a thermal equivalent efficiency, together with the gross average reflectance and absorptance values for the reflectors, a valid set of equilibrium temperatures for all thermal exchange nodes can be reproduced.

Table 2-8 shows the results of the thermal analysis for both silicon and GaAs versions at LEO and at GEO.

It is interesting to note the temperature similarities for both cell versions. Although the GaAs efficiency is higher than that of Si, this effect is almost completely counterbalanced thermally by the GaAs cell's higher solar absorptance.
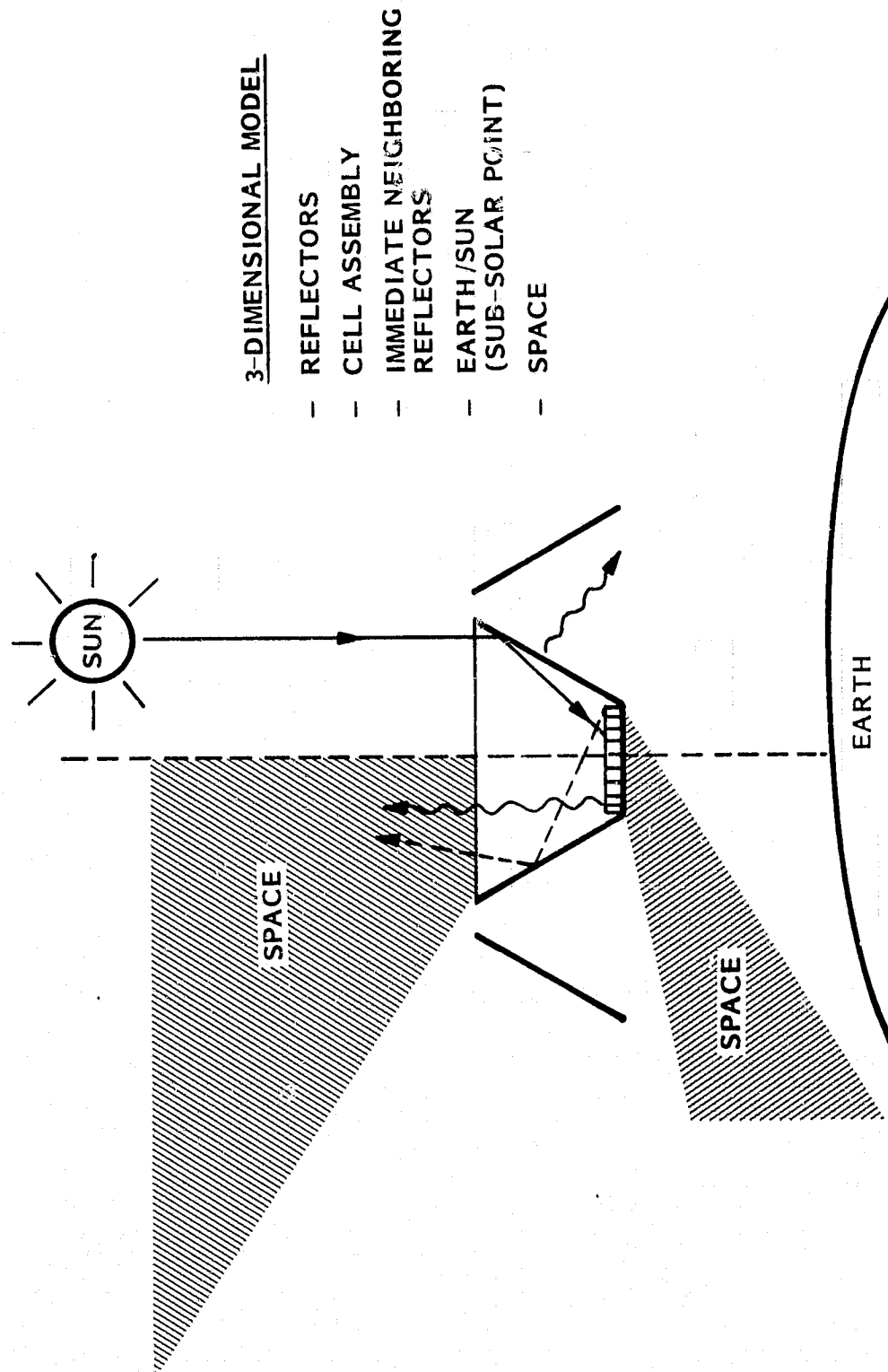
Figure 2-38 Low-CR Petal Thermal Model

TABLE 2-7

LOW-CR THERMAL MODEL ASSUMPTIONS

- STATION: 300 NM SUB-SOLAR POINT

- GEOMETRIC CONCENTRATION RATIO = 5

- Si-CELL EFFICIENCY = 7.5% ON-STATION
  (THERMAL EQUIVALENT: 17.2%)

- GaAs-CELL EFFICIENCY = 16.0% ON-STATION
  (THERMAL EQUIVALENT: 25.2%)

- REFLECTOR
  - FRONT (SPECTRALLY SELECTIVE, COATED REFLECTOR):
    $R = 0.52;$ $\alpha = 0.14,$ $\epsilon = 0.8$
  - REAR
    $\alpha = 0.4,$ $\epsilon = 0.8,$ $\alpha(IR) = 0.8$

- CELL BLANKET:
  - FRONT: $\alpha = 0.70$ (Si) OR 0.75 (GaAs); $\epsilon = 0.82$
  - REAR (E.G. KAPTON):
    $\alpha = 0.4;$ $\epsilon = 0.8;$ $\alpha(IR) = 0.8$

- I. MEDIATE NEIGHBORING REFLECTOR:
  - AS FOR REFLECTOR ABOVE

TABLE 2-8

THERMAL ANALYSIS FOR SILICON AND GaAs VERSIONS
AT LEO AND AT GEO

LEO	SILICON	GaAs
T/REFLECTORS	9°	9°C
T/CELLS	143°C	138°C

GEO	SILICON	GaAs
T/REFLECTORS	-40°C	-40°C
T/CELLS	126°C	121°C

2.7   HIGH-CR CONCENTRATOR CONCEPT

2.7.1   General Configuration Trade Studies

Reflector configurations for achieving a high concentration ratio will necessarily be of the focussing type, which brings with it a certain degree of non-uniformity in the beam distribution. These non-uniformities can be kept acceptably small by choosing a focussing system with long focal length. A long focal length, on the other hand, would normally mean very deep structures of high weight and stiffness and a high vulnerability to internal and external beam misalignment losses. It thus becomes necessary to collapse or fold the converging rays by means of additional reflectors which may or may not be configured (curved) to provide additional focussing action. In any case, a three-dimensional reflector geometry (i.e., surfaces of revolution) provides better useage of space and materials, and thus a higher collector efficiency, than do two-dimensional contours (i.e., curved troughs).

Figure 2-39   shows three representative candidates for such a focussing system. It was assumed from the start that active thermal control techniques will be included in high-CR (CR = 125) system design. The illustrated contours are to be understood as cross-sections of three-dimensional surfaces of revolution. The number of basic configuration alternatives for high-CR application is not as great as for low-CR applications since the collector efficiency of the various low-CR geometries are more sensitive to the choice of CR-range.

The first configuration in the figure--a simple paraboloid--is a non-folded ray system and, as such, has the advantage of only single-reflection losses. As mentioned previously, however, such systems exhibit higher beam non-uniformity or, to reduce non-uniformity, must have deeper, more misalignment-prone structures. The configuration shown suffers mostly from a poor heat rejection capability since the solar cell modules are located with their backs directly in the sun.
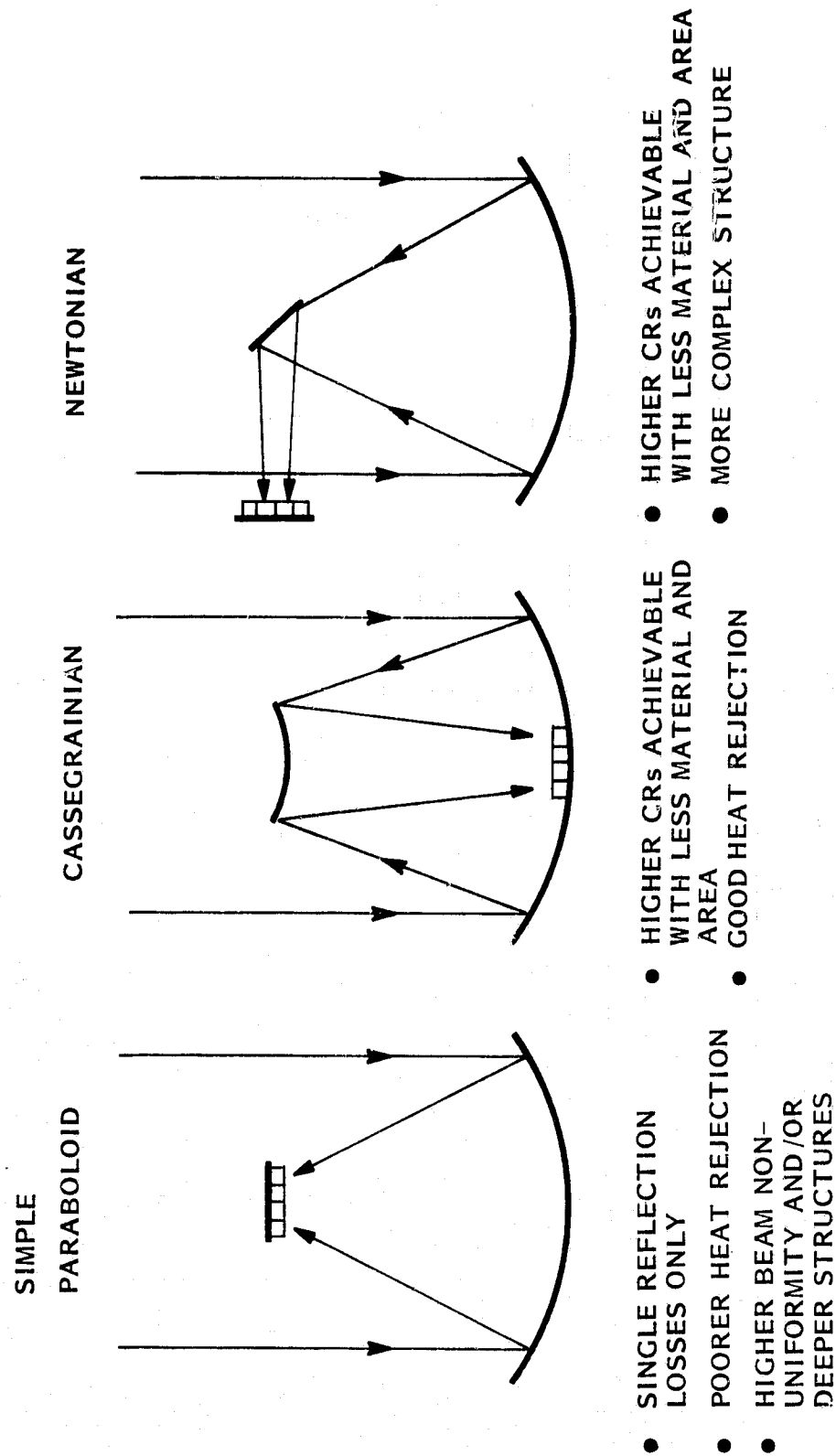
Figure 2-39 High CR Reflector Concepts (CR >10)

LOCKHEED MISSILES & SPACE COMPANY, INC.

The second configuration illustrated--the Cassegrainian system--achieves a
high collector efficiency (less material and area) through the use of a
second focussing reflector. Since the solar cell modules are located under
the secondary reflector and with their backs away from the sun, a good heat
rejection capability is achieved. In addition, stable structural support
for the cells can be provided at their location on the primary reflector.
The structural economy which is inherent in the Cassegrainian system has
been recognized for years in several technological fields of application.
Cassegrainian systems are standard designs for achieving high magnification
in the field of optical telescopy and have found wide useage as high-frequency
radio antennas.

The third configuration--the Newtonian system--also derives from the field
of optical telescopy, where high magnification is achieved. However, by
locating the solar cell modules above and to the side of the primary reflector,
structural support is more difficult to provide. In addition, the heat
rejection capability is not as good due to the greater obstruction of view
factor from the adjacent primary reflectors.

In the case of the above configurations, no quantitative trade-off analysis
was performed as was for the low-CR configurations. The high-CR configura-
tions are characterized by a complex set of configuration parameters which
makes detailed trade analysis extremely tedious and beyond the scope of the
present study. The advantages of the Cassegrainian system were compelling
enough to permit the selection in its favor on the basis of the above qualita-
tive arguments.

Figure 2-40   illustrates the complex set of major geometrical parameters
which characterize a Cassegrainian system. The primary reflector is a
paraboloid and the secondary reflector is a hyperboloid. These two contours
are characterized individually through their respective focal lengths f_p and
f_n as well as their respective diameters ($d = d_p$, which determines d_h).
Reflector separation a is an independent parameter as is the chosen height
of the cell plane h. A given set of these basic parameters will determine
the concentration and focussing characteristics of the system.

- **CONCENTRATOR FEATURES**
  - 3-DIMENSIONAL
  - DOUBLE-REFLECTION, FOCUSSING
  - PRIMARY REFLECTOR: PARABOLOID
  - SECONDARY REFLECTOR: HYPERBOLOID

- **CONFIGURATION PARAMETERS**
  (DETERMINING CR AT CELL PLANE)
  - ECCENTRICITY: f_h/a
  - f_p - VALUE: f_p/d
  - REFLECTOR SEPARATION: a/f_p
  - HEIGHT OF CELL PLANE: h/f_p
    (i.e., DEFOCUSSING)
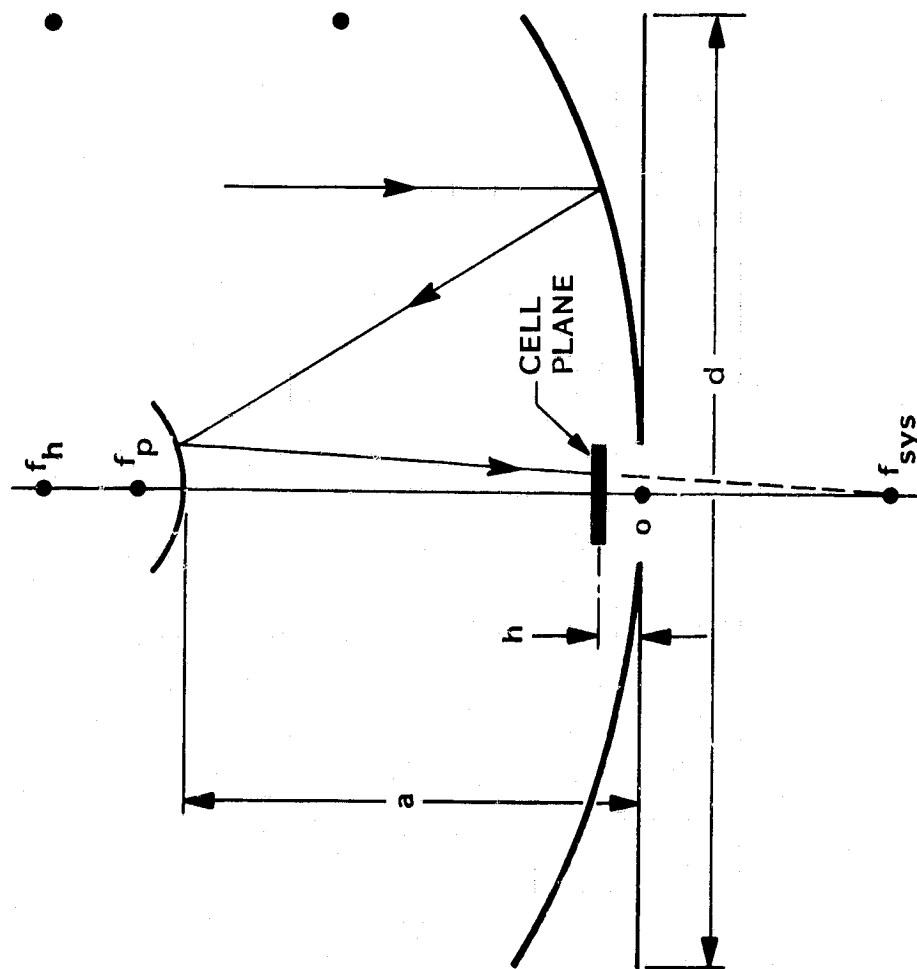
Figure 2-40 Cassegrainian Concentrator Geometry

LOCKHEED MISSILES & SPACE COMPANY, INC.

The general manner in which the system operates can be seen by elementary ray-tracing arguments. The hyperboloid is sized such that a ray which is intercepted at the outermost paraboloid edge is reflected at the outermost hyperboloid edge and received at the outermost edge of the cell area. This leaves a non-contributing annular area on the primary reflector which neither reflects nor receives and which is occulted from the sun by the secondary reflector. The entire area of occultation is occupied by a thermal radiator disc, which, in shadow as it is, can operate at high thermal efficiency. The cell area disc is located concentrically on this radiator disc in the field of illumination, which, as mentioned above, is bounded by the outermost intercepted ray. The areas available for thermal radiation are thus the entire rearside of the occultation disc and the occulted annulus on the frontside surrounding the cell area disc. The innermost intercepted ray just grazes by the secondary reflector to be reflected up and back down onto the cell area disc near its center. The exact center of the cell area disc (and of the secondary reflector) are non-contributing so that a structural support boom for the secondary reflector can occupy this area without obstructing the illumination.

No attempt was made in the present study to optimize the complex set of configuration parameters discussed above for the Cassegrainian system. Computer techniques exist at LMSC for performing this task for high frequency antenna systems. These techniques can be applied to the concentrator array case as a means of achieving an optimum compromise among several conflicting design objectives, such as:

- high collector efficiency through minimal structural effort and low system depth

- good partitioning of the overall concentration ratio (i.e., $CR_{overall} = CR_{primary} \times CR_{secondary}$) to achieve optimum thermal balance of all system elements

- acceptable internal and external misalignment losses

- acceptable beam non-uniformities

- cell plane close to paraboloid vertex for structural stability

- adequate occultation area for thermal radiator performance

As a baseline for further high-CR design and performance analysis, an f-value of approx. 1/2 was assumed (i.e., Cassegrainian module is twice as wide as high) and the cell plane was located at the paraboloid vertex. An acceptable CR-partition ratio (which affects occultation area and thus radiator size) resulted from a series of analyses of system thermal behavior which will be discussed in a separate section.

The wide use of parabolic surfaces for spacecraft antenna systems over the past years has prompted the growth of an entire field of technology devoted to deployable lightweight paraboloidal structures. This technology is directly applicable to the present study; the structures in question can be utilized for solar concentration by replacing their RF-"reflector" (metalized cloth net) by suitable solar reflector films.

Figure 2-41 shows the current leading technologies for large deployable antennas. Several more exotic techniques, such as "maypole" and pressure-e..ected designs for very large structures, are under study at present but are not achievable for a 1983 readiness time-frame.

The wrap-rib concept features a set of radially-directed lenticular ribs of desired reflector contour which are attached to a central hub. For stowage the ribs are wrapped simultaneously around the circumference of the hub until they are positioned snugly spinal-fashion against the side of the hub. Deployment is achieved by allowing the ribs to spiral outwards under the action of their own stored energy with a motor-driven braking system to control deployment velocity. This system is retractable only with the aid of Ground Support Equipment. It has been flight proven with dish diameters of 30 ft., which is roughly the size range for the present study. The major advantages of the wrap-rib concept are its least stowed volume among the three candidate concepts and its provision (via the hub) of a stable location for the plane of focus
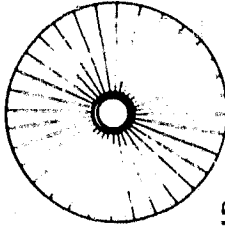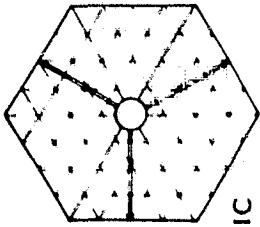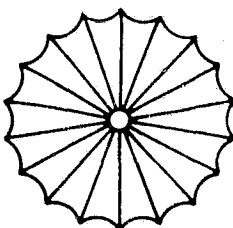
	WRAP RIB	PARABOLIC TRUSS	UMBRELLA
DESCRIPTION	RADIAL RIBS SUPPORT REFLECTIVE MEMBRANE CONTOUR ESTABLISHED BY RIBS.	GEODESIC TRUSS NET WORK. REFLECTING MEMBRANE SUPPORTED BY SERIES OF TIES AND CORDS, WHICH ALSO ESTABLISH THE CONTOUR OF INDIVIDUAL TRIANGULAR ELEMENTS.	RADIAL RIBS AND TENSION TIES SUPPORT REFLECTIVE MEMBRANE, AND ESTABLISH THE CONTOUR.
TECHNOLOGY MATURITY	FLIGHT PROVEN TO 30 FT DIA TECHNOLOGY EXTENDABLE TO LARGER SIZES	UNDER DEVELOPMENT	FLIGHT QUALIFIED TO 16 FT DIA TECHNOLOGY EXTENDIBLE TO LARGER SIZES
ADVANTAGES	• SIMPLE DEPLOYMENT • LEAST STOWED VOLUME • COMPATIBLE WITH CASSEGRANIAN FOCUS	• STIFFEST STRUCTURE • LARGEST NO. OF INDIVIDUAL REFLECTIVE ELEMENTS	• REFURLABLE WITHOUT WEIGHT PENALTY • COMPATIBLE WITH CASSEGRANIAN FOCUS
DISADVANTAGES	• 1G CONTOUR MEASUREMENT DIFFICULT • DIFFICULT TO CONTROL REFLECTIVE SURFACE FOLDS	• DIFFICULT TO INCORPORATE PROVISIONS FOR CASSEGRANIAN FOCUS • MOST DIFFICULT TO CONTROL FOLDS IN REFLECTIVE SURFACE	• POTENTIAL FOCAL POINT VARIATION • LARGEST STOWED VOLUME

Figure 2-41 Reflector Stowage Concept Comparison

(cell area disc). While it is difficult to control the manner in which folds
are induced on the reflector surface; this disadvantage is not considered
to be a major one.

The parabolic truss, or geodesic concept, consists of many triangular structural
segments which are spring-hinged to each other such that they can be folded
into a compact stack. This system is under development at present. Once
deployed, this concept provides the stiffest of the candidate structures,
although it is a major difficulty of the system to achieve a controlled
repeatable deployment sequence in the stack of spring-loaded emerging segments.
A second major difficulty arises when attempting to incorporate a stable focal
area (cells, thermal radiator) into the center of the field of reflector
segments, especially in view of the need for a precisely-position secondary
reflector.

The umbrella concept is the only inherently retractable concept among the
three candidates, although, as mentioned previously, the array maintenance
philosophy does not call for retractability. The system is qualified to
dish diameters of 16 ft. and will be flown in the near future. The umbrella
concept features a set of radially-directed ribs of desired reflector contour
which are attached to a central hub in a geometry similar to the wrap-rib
concept. For stowage the ribs are pivotted at the hub and driven out-of-
plane into a long quasi-cylindrical volume in a manner similar to closing an
umbrella. Deployment is simply the reverse of the retraction sequence.
However, since the pivotting motion is performed in the direction which
establishes the reflector contour, the potential for internal misalignment
(in particular, focal point variation) is high. A further major disadvantage
among the three candidate concepts is its largest stowage volume.

In selecting one of the three deployment concepts, primary emphasis was placed
upon a low stowage volume. For solar arrays of the size for this study,
stowage efficiency is limited by volume, which means that cost-effectiveness
is influenced significantly by number of launches required. This aspect,
together with the necessity to provide a stable Cassegrainian focus with
the least amount of misalignment potential, led to the selection of the wrap-rib

concept as the baseline for the high-CR solar array. Corollary benefits of this choice include a broad base of LMSC experience in wrap-rib systems and, as it turned out, an attractive scheme for stowing large size Cassegrainian modules in the Orbiter bay.

Some aspects of the LMSC wrap-rib experience is documented in Figures 2-42 and 2- 43 . Figure 2- 42 shows an early demonstration model (Diam. 5 ft.) at various stages during the deployment. Most notable in the figure is the controlled unfurling action of the single-lenticular ribs as well as the manner in which the out-of-plane parabolic contour is reduced into the hub-plane at stowage. Figure 2- 43 shows segments of a large-area (Diam. 50 ft.) development unit featuring lightweight graphite-epoxy ribs. The characteristic parameters cited in the figure do not apply for this study.

LOCKHEED MISSILES & SPACE COMPANY. INC.
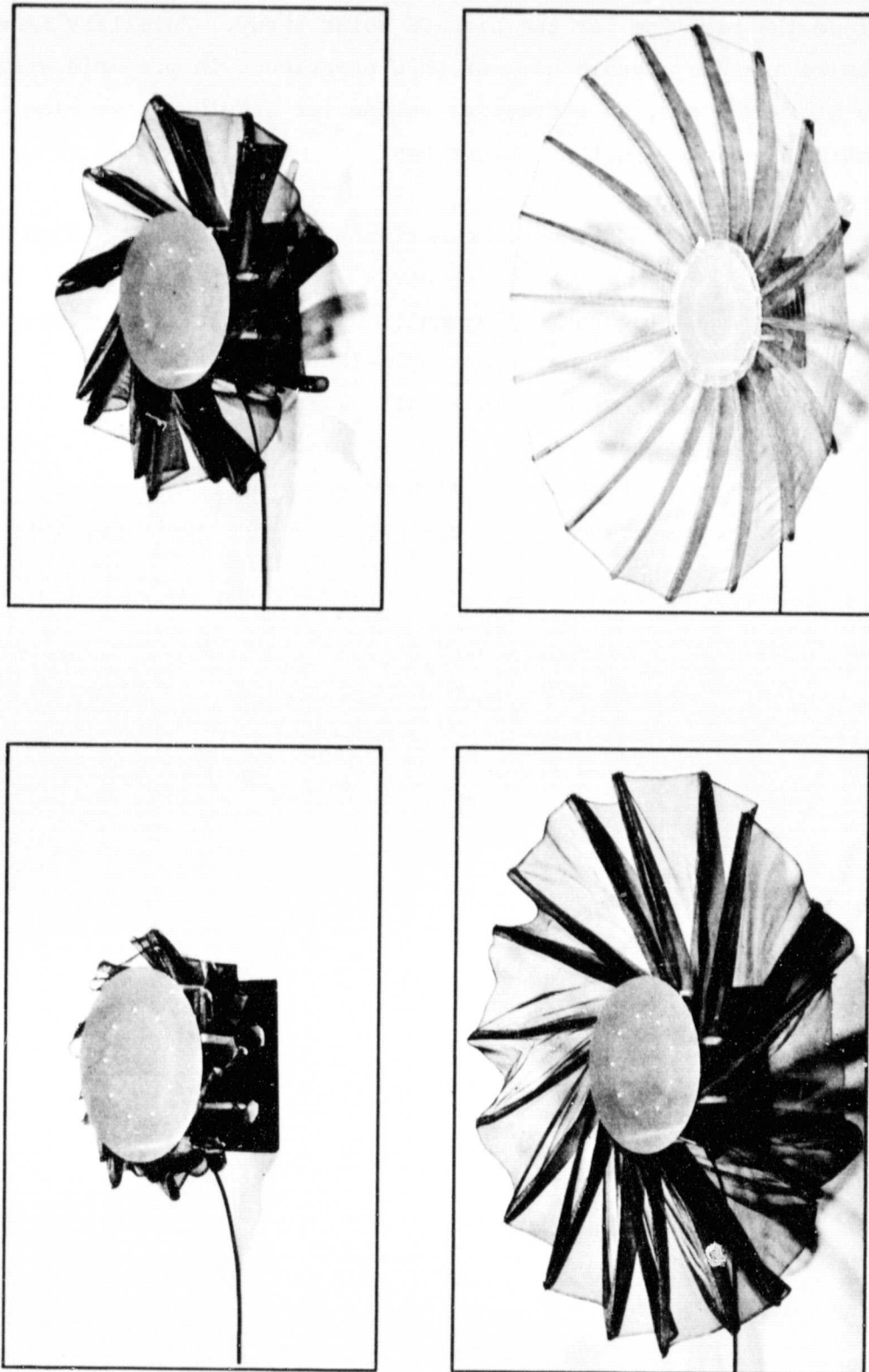
Figure 2-42 Motor-Driven Flex-Rib Antenna Unfurling

LOCKHEED MISSILES & SPACE COMPANY. INC.
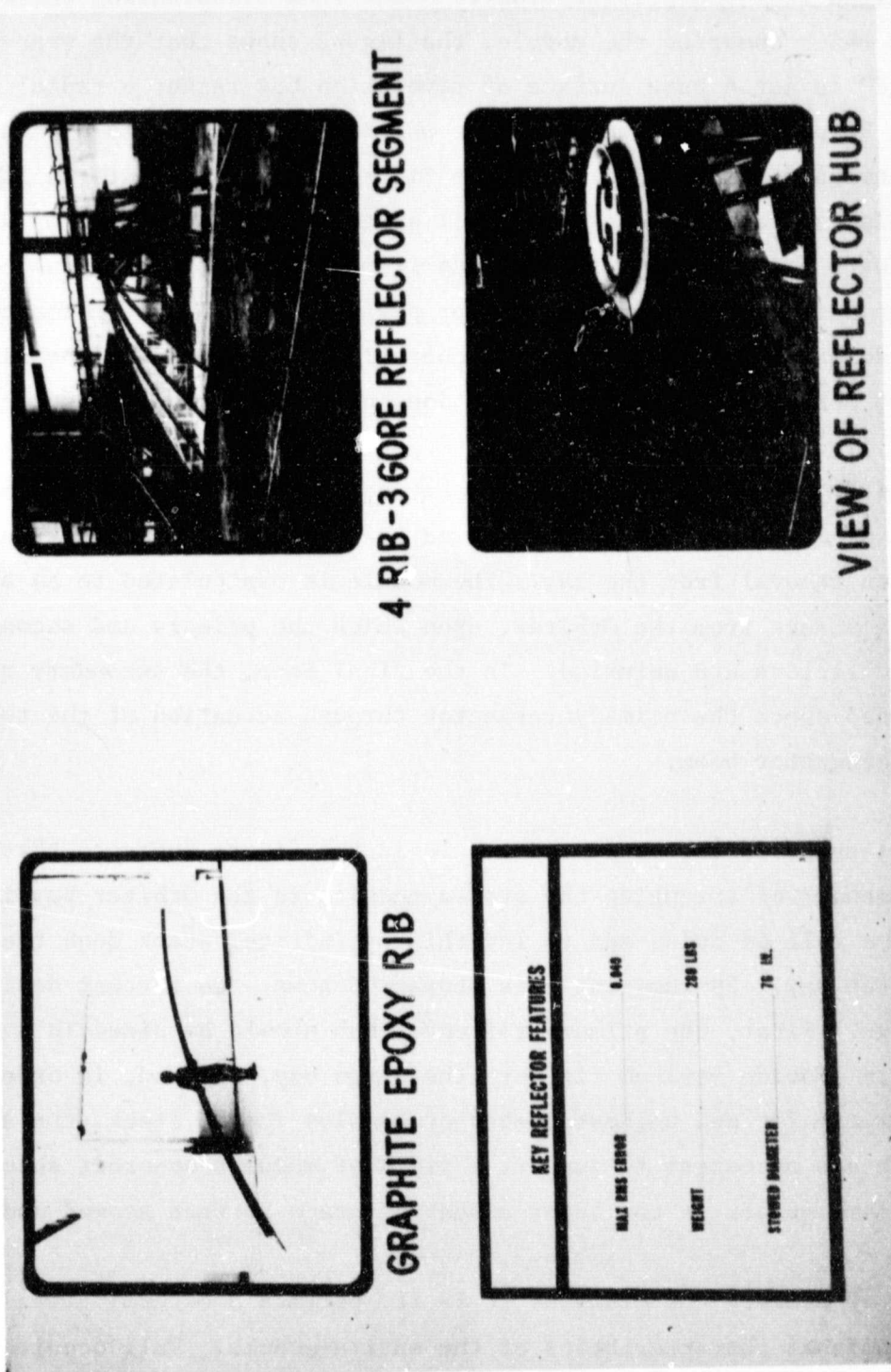
Figure 2-43 LMSC 50 Foot Wrap Rib Reflector

LOCKHEED MISSILES & SPACE COMPANY. INC.

Figure 2-44 shows the design of a high-CR Cassegrainian module (deployed) which resulted from the present study. Aside from illustrating the main assemblies which comprise the module, the figure shows that the wrap-rib "paraboloid" is not a pure surface of revolution but rather a radial assembly of approx. 20 parabolic segments--gores which are tensioned in a parabolic contour between two adjacent ribs. The figure also shows that the main thermal radiator disc surrounding the solar cell area has been augmented by a conical radiator (with heat pipes) which extends from the rear of the module to increase view factor and enhance overall radiator performance. The performance trade-off between modules with and without this conical augmentation will be discussed below. The most cost-effective design does not include conical augmentation.

Figure 2-44 also illustrates the deployment sequence of one high-CR module. The module at lower left is in the stowed state as it is found in the Orbiter bay and upon removal from the bay. The module is manipulated to an adequate clearance distance from the Orbiter, upon which the primary and secondary wrap-rib reflectors are unfurled. In the final step, the secondary reflector is positioned above the primary reflector through actuation of the telescopic reflector separator boom.

The general shape of the retracted module in the figure suggests that the most efficient manner of arranging the stowed modules in the Orbiter bay is to stack them as in a roll of coins and to lay this cylindrical stack down the entire length of the bay. By choosing this stowage scheme, two further design guidelines emerge. First, the primary reflector hub should be sized to a diameter of 15 ft. to provide maximum fit into the cargo bay. Second, in order to achieve maximum fit and highest number of modules in the stack, the structural beams which are necessary to support a field of modules on-orbit should be stowed in some manner in the least amount of space between stowed modules.

The choice of primary hub diameter at 15 ft. permits a determination of the major dimensional characteristics of the entire module. Full occultation of the thermal radiator means a deployed dish diameter of 15 ft. for the secondary reflector. Choice of the CR of 125, along with a CR partition ratio of 8-1/3 / 15 (i.e., 8-1/3 x 15 = 125) yields a primary dish diameter of approx. 44.5 ft. deployed and a cell disc diameter of approx. 3.75 ft.

SECONDARY REFLECTOR

REFLECTOR SEPARATION

TELESCOPIC BOOM

PRIMARY REFLECTOR

GaAs CELLS

THERMAL RADIATOR

REFLECTORS UNFURLING

STOWED
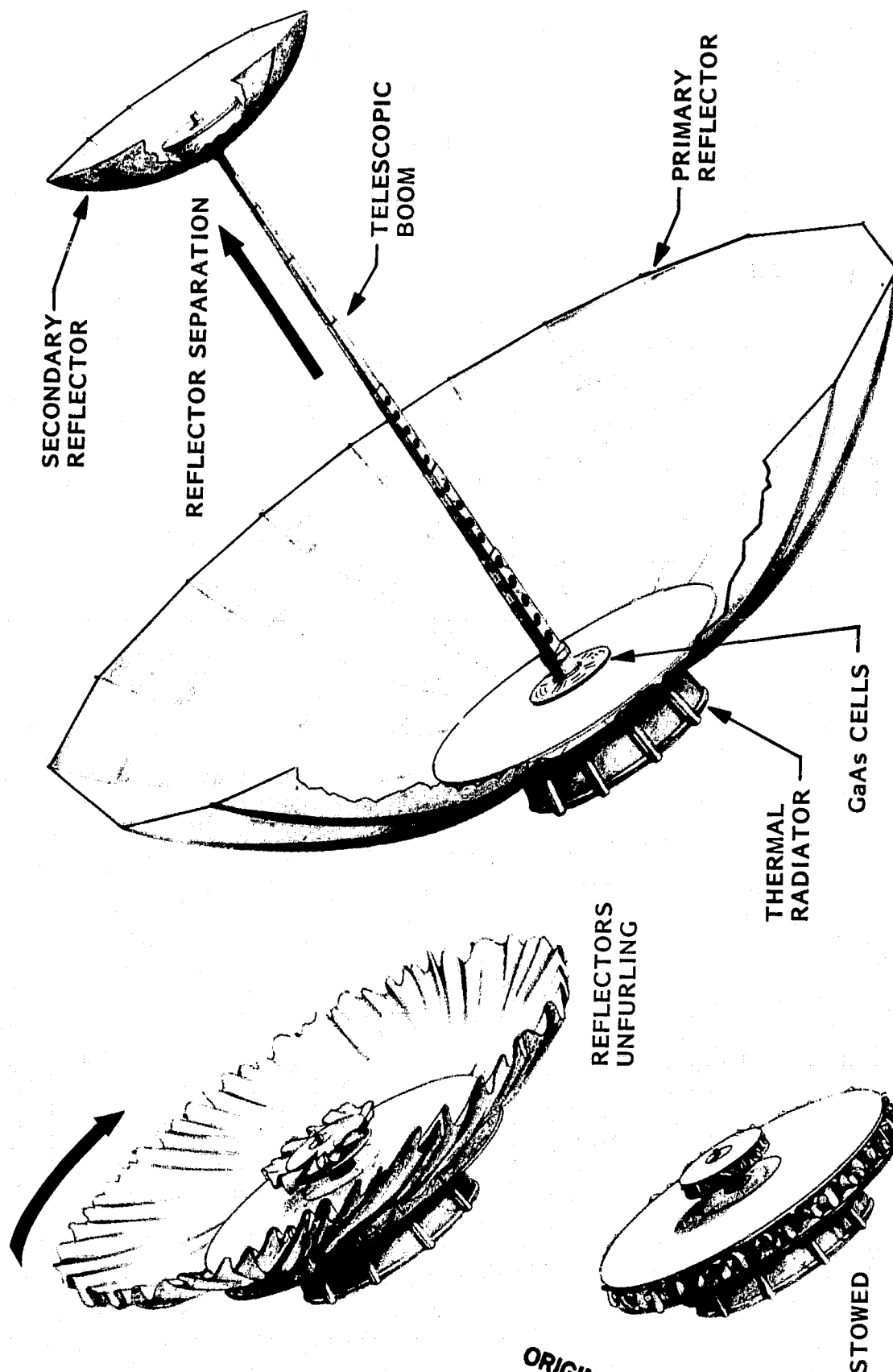
Figure 2-44 Deployment Sequence of a High-CR Cassegrainian Module

2-95

At this point in the design evolution of the high-CR system, the stowage geometry and dimensional configuration has assumed a mature form. It is instructive to note that the exact choice of CR = 125 suns has not played a major role in influencing basic high-CR design choices. Indeed, the Cassegrainian-type system is the logical choice for achieving concentration ratios over a broad range including CR's much lower and much higher than the one chosen. Since the low end of the range overlaps into the sphere of influence of the TPP array (for Si and GaAs cells) discussed in the previous chapter, it remains to be seen if, for completeness of approach, any benefits can be obtained by going to a higher range of concentration ratios.

A very-high-CR option with CR = 500 suns was chosen to analyze the performance sensitivity with increasing CR. The same geometrical constraints were imposed as for CR = 125 (i.e., 15 ft. primary hub diameter). Thermal analysis was performed to achieve a radiator design and acceptable CR-partition ratio which yielded the same target cell operation temperatures as the CR = 125 case. The resulting Cassegrainian module geometry dictated a cell disc area which is 5.7 times smaller (at comparable module weight) than for CR = 125. Thus, despite a 4-fold increase in illumination intensity, the very-high-CR design will generate only 70% of the power output per module as the comparably configured CR = 125 design. This means that for a given power level, the very-high-CR array must contain 41% more modules (higher manufacturing costs, launch costs, etc.) and is not a cost-effective alternative to the CR = 125 design.

With the major module dimensions of the high-CR design determined, the major design problem remaining was to devise a structure which supports a field of deployed modules yet can be collapsed into a form which is compatible with the dense "coin-stacking" stowage mode discussed previously. Figure 2-45 shows the design of a graphite-epoxy dual-lenticular module strut which connects to the base of neighboring Cassegrainian modules and allows the build-up of a large field of densely-packaged modules (hexagonal close-packing). Depending upon location in the field, up to three struts per module (avg. ~ 2.4

2-96
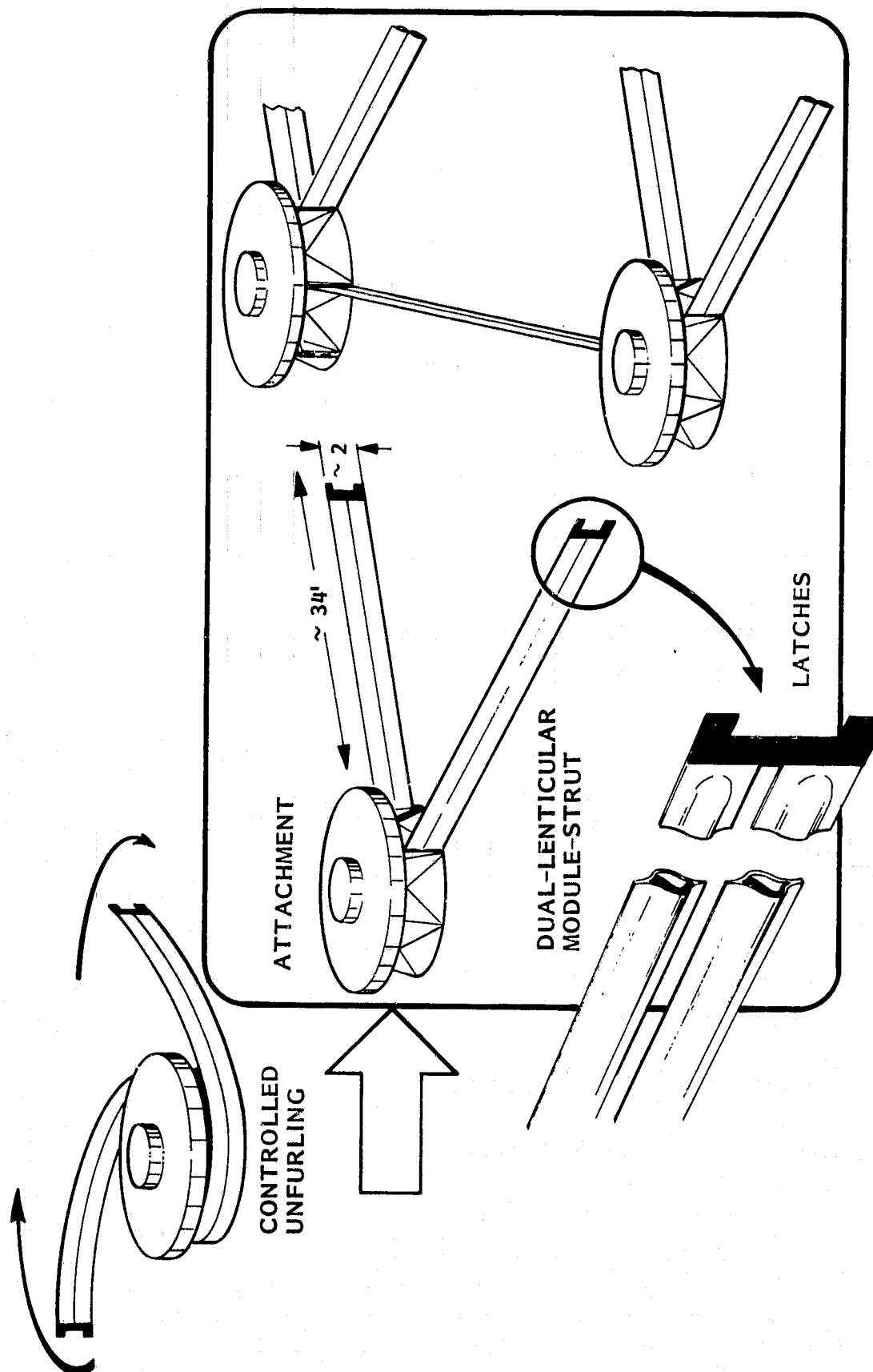
Figure 2-45 High-CR Array Module Integration

~ 2

~ 34'

ATTACHMENT

DUAL-LENTICULAR
MODULE-STRUT

LATCHES

CONTROLLED
UNFURLING

LOCKHEED MISSILES & SPACE COMPANY. INC.

for a large field) are required and these struts can be furled around the module base and unfurled under motor-controlled braking action in much the same manner as for the wrap-rib reflector deployment scheme. This module strut scheme is the only departure from the previously stated installation philosophy of completely self-deploying structures. With this scheme it will be necessary to have an expanded manipulator capability on the Orbiter in order to hold the already deployed field, remove a new module, deploy the struts of the new module, and attach it to the existing field. This operation is discussed in greater detail in the appropriate chapter on build-up and maintainability aspects.

With this lenticular strut scheme it is possible to stack the retracted modules in an uninterrupted stack in the Orbiter bay as shown in Figures 2-46 and 2-47. In the first case the struts (not shown) would be wrapped around the conical augmentation thermal radiator. The size of the cone, which was determined through thermal analysis, is dictating the packing density. In the second case no conical augmentation is included; the struts are wrapped around a support frame. In this option a 50% greater packing density can be achieved (15 modules vs 10 modules per flight) in return for an on-orbit cell temperature increase which causes a 6% loss in power. Thus the non-augmented version is significantly more cost-effective at system level and will be pursued in the detailed performance/cost analysis in a later chapter.

The chief results of that performance analysis are summarized in Figure 2-48. Although the figure shows 29 modules, the array would consist of 45 modules (3 flights) to achieve the required power level.
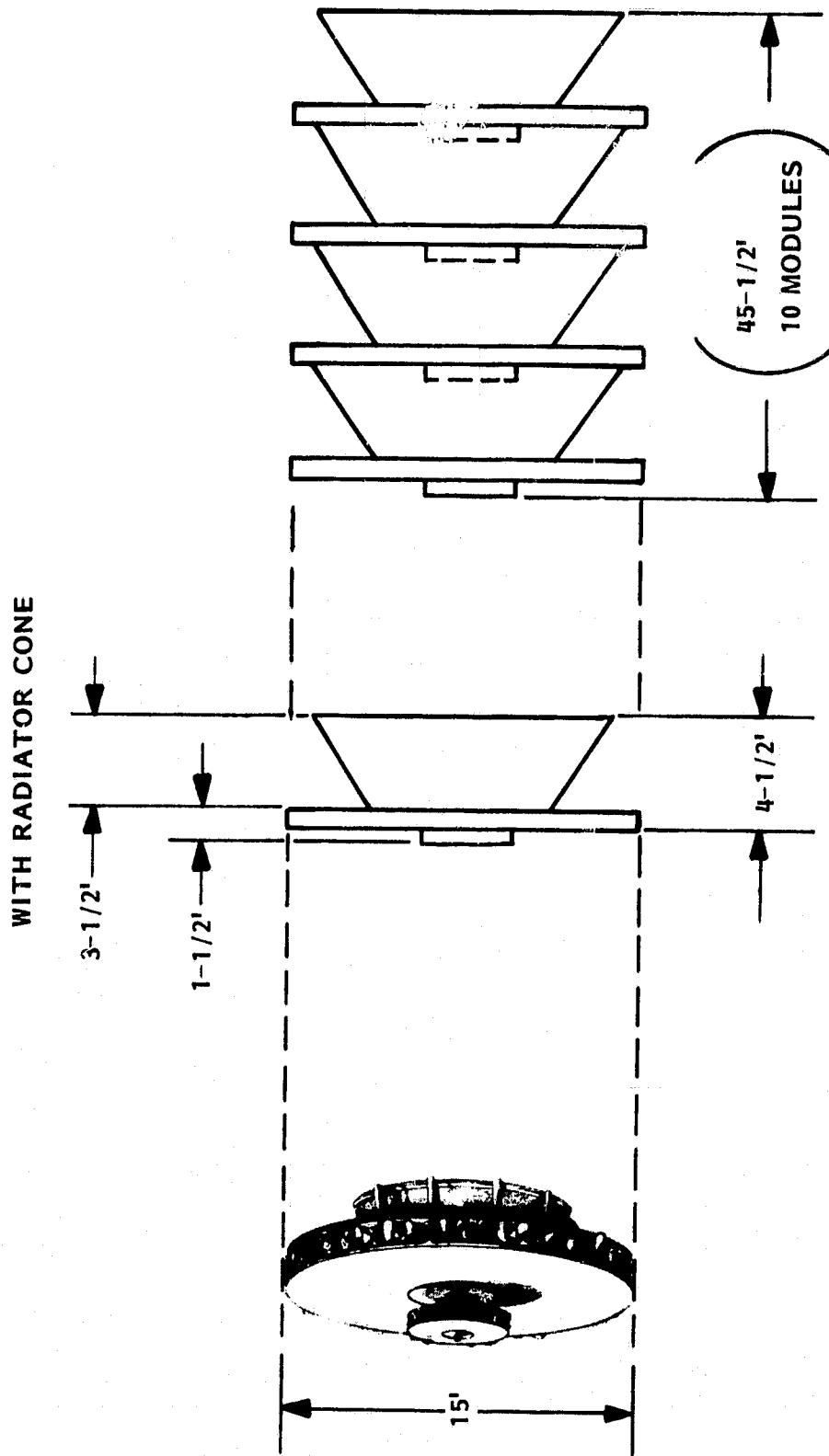
Figure 2-46 Cassegrainian Concentrator – Stowed Configuration

LOCKHEED MISSILES & SPACE COMPANY. INC.

WITHOUT RADIATOR CONE

15'

15 MODULES = 45 1/2'

1/2'

1'

2'
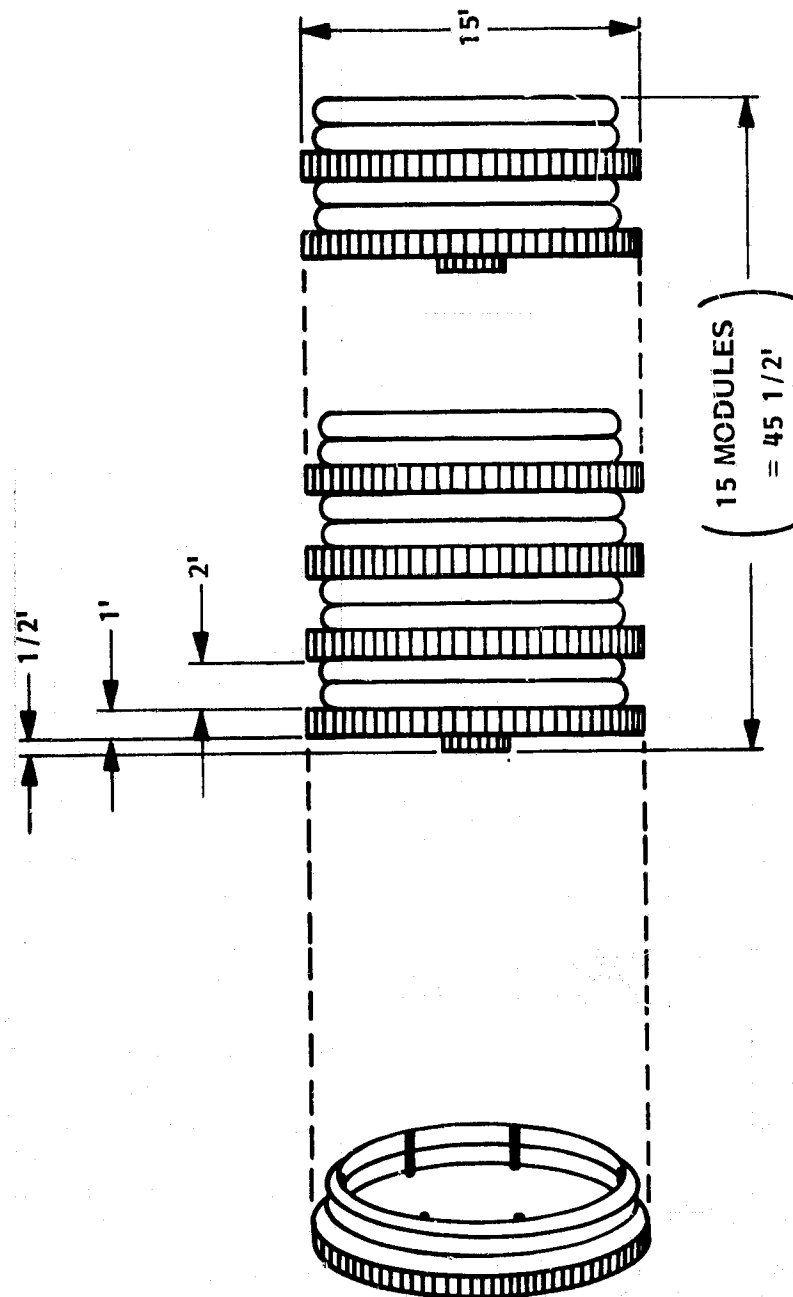
Figure 2-47 High-CR Array – Stowed Configuration

LOCKHEED MISSILES & SPACE COMPANY. INC.

- GaAs SOLAR CELLS
- 576 kW BOL
- 384 kW AVG. (15 YR. LEO)
- 45 CASSEGRAINIAN MODULES
- 82,400 SQ. FT.

44-1/2'
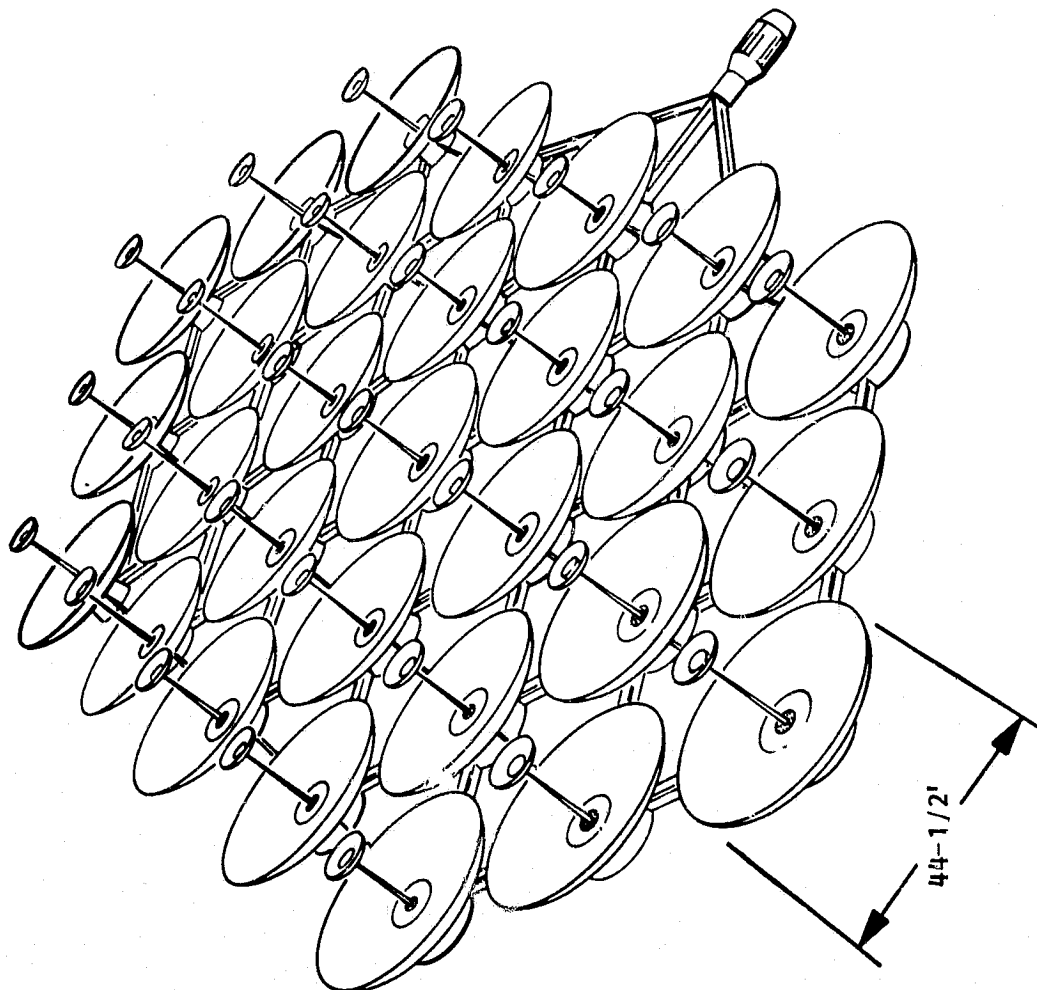
Figure 2-48 High-CR Array On-Station

2.7.2 High-CR Array Thermal Analysis

For the purposes of determining the thermal behavior of the high-CR system, a three-dimensional model was established with radiative-interactive nodes which represent the major parts of a single Cassegrainian module.

Figure 2-49 shows a graphic representation of the model used. Nodes representing

- primary reflector
- secondary reflector
- solar cell module/radiator assembly
- earth
- space

form the basis for the model.

Heat inputs to the array consist of sunlight, earth-IR, and earth albedo. Unlike for the low-CR thermal treatment, the influence of neighboring modules was assumed here to be negligibly small.

In the actual array design the solar cell modules must be electrically insulated from the radiator plate on which they are located. Such an insulation layer will have a significant effect on cell temperature. The effect of this layer has been taken into account by considering the node temperature of the integral solar cell module/radiator assembly node to be the root temperature of the radiator and then determining the resultant temperature at the cells based upon the known thermal conductance characteristics through the layer.

Table 2-9 lists the properties and assumptions made for performing the thermal analysis. Initially, two different CR's were investigated--the baseline CR=125 version as well as a CR=500 version which is discussed in the preceding section. As in the low-CR case, the solar cell AM0-efficiency has, on the basis of reflector studies in section 2.4, been converted to an efficiency which applies for the shape of the solar spectrum which actually reaches the cell after double reflection. This "thermal equivalent" efficiency was arrived at through use of the electrical and thermal equivalent reflectances of the reflector material in section 2.4.4. By

3-DIMENSIONAL MODEL

- PRIMARY REFLECTOR
- SECONDARY REFLECTOR
- SOLAR CELL MODULE
- INSULATION LAYER
- RADIATOR ASSEMBLY
- EARTH/SUN (SUB-SOLAR POINT)
- SPACE

SUN

SPACE

SPACE

EARTH
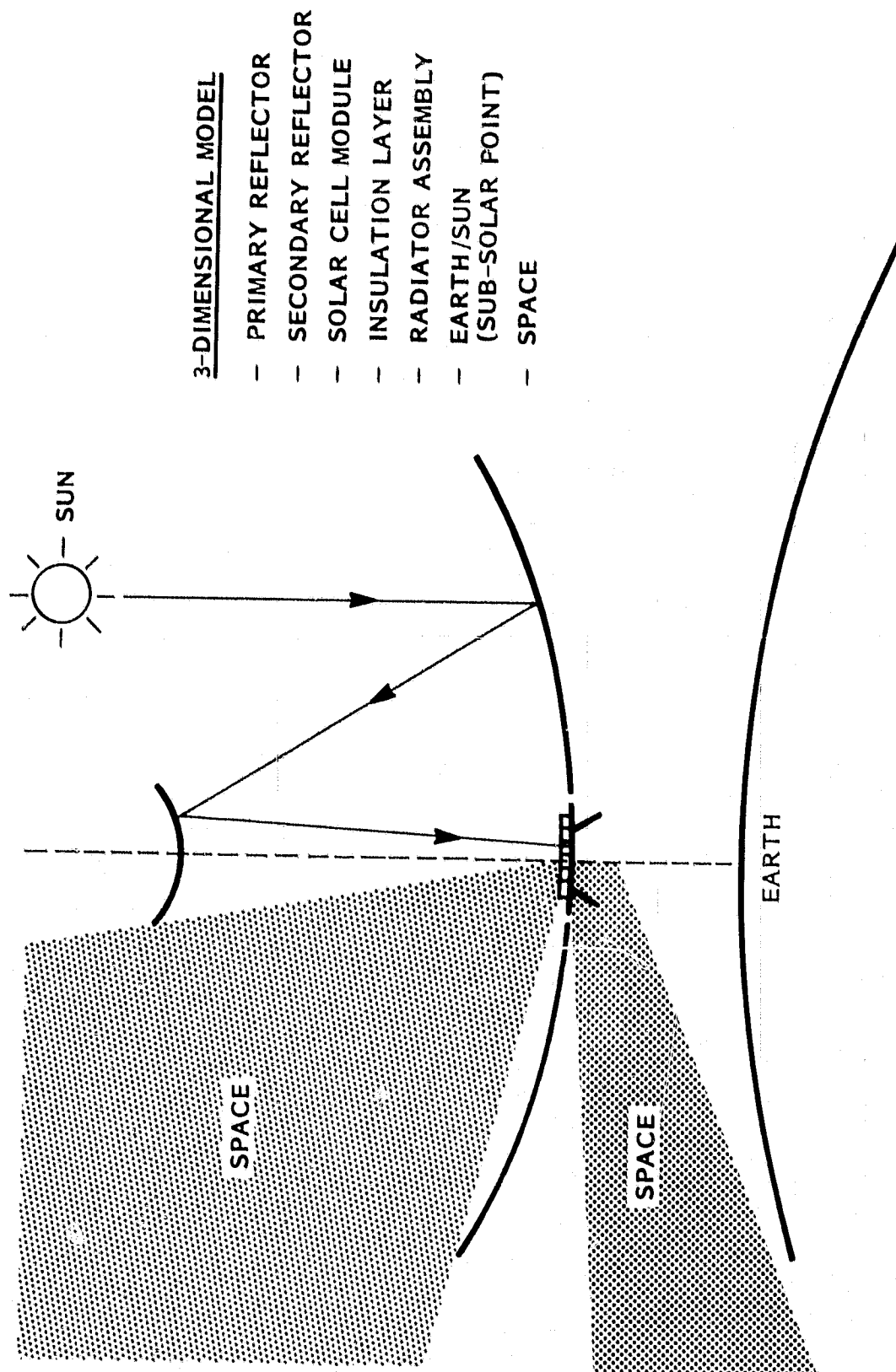
Figure 2-49 High Concentration Ratio Thermal Model

LOCKHEED MISSILES & SPACE COMPANY, INC.

using this device of a thermal equivalent efficiency, together with the gross average reflectance and absorptance values for the reflectors, a valid set of equilibrium temperatures for all thermal exchange nodes can be reproduced.

TABLE 2-9

HIGH-CR THERMAL MODEL ASSUMPTIONS

- STATION: 300 NM SUB-SOLAR POINT
- CONCENTRATION RATIO: VARIED
- CR-PARTITIONING: VARIED
- FULL RADIATOR OCCLUSION BY SECONDARY REFLECTOR
- GaAs-EFFICIENCY: 15% ON-STATION (THERMAL EQUIVALENT: 28.7%)
- PRIMARY REFLECTOR:
    - FRONT (SPECTRALLY SELECTIVE, COATED REFLECTOR):
      $R = 0.52;$ $\alpha = 0.14;$ $\epsilon = 0.8$
    - EARTH-SIDE:
      $\alpha = 0.4;$ $\epsilon = 0.8;$ $\alpha(IR) = 0.8$
- SECONDARY REFLECTOR:
    - FRONT (COATED ALUMINIZED FOIL):
      $R = 0.92;$ $\alpha = 0.08;$ $\epsilon = 0.8$
    - SUN-SIDE (FLEXIBLE SECOND-SURFACE REFLECTOR):
      $\alpha = 0.1;$ $\epsilon = 0.8$
- CELL/RADIATOR ASSEMBLY
    - FRONT (CELL): $\alpha = 0.75;$ $\epsilon = 0.82$
    - INSULATION LAYER (1 MIL KAPTON)
      $k = 0.09$ BTU/HR-FT-°R
    - FRONT + REAR (RADIATOR)
      $\alpha = 0.4;$ $\epsilon = 0.86$ (WHITE PAINT)
    - RADIATOR EFFECTIVENESS = 80 PERCENT

The spectrally selective reflector (cold mirror) was employed for the primary reflector. The inboard reflecting surface of the secondary reflector was chosen to be a typical non-selective aluminized foil for reasons discussed in section 2.4.4. For the insulation layer between cell modules and radiator plate a 1 mil thick Kapton foil was chosen.

The thermal behavior of the module, while not dependent upon overall module size, is very dependent upon the size of its constituent parts relative to each other. That is, a given concentration ratio can equally well be achieved through variously sized combinations of primary reflector, secondary reflector, and cell disc, though each has its own unique thermal behavior. A simple way of expressing such configurational variations for the purposes of thermal analysis is by use of a so-called CR-partition ratio. The CR-partition ratio expresses the amount of sunlight concentration which takes place upon each of the two reflections, and can also be related (though not simply through X^2) to the area ratio of reflectors and cell disc. For example, a concentration of 5-fold from primary reflector to secondary reflector, followed by a concentration of 25-fold from secondary reflector to cell disc, would yield the desired total CR of CR = 5 x 25 = 125 suns; (CR1/CR2 = 5/25).

In the present study, the CR-partition ratio was varied and its effect on various thermal and configurational aspects was investigated. For a given primary reflector size, as CR1 decreases and CR2 increases, the secondary reflector increases in size and the non-contributing annular space between cell disc and primary reflector is increased. At first glance, this trend appears to be desireable since it allows room for a large thermal radiator and results in lower cell temperature. In fact, however, the radiator should be kept as small as possible relative to the cell disc in order to achieve the highest packing density (watts/flight) in the 15' diameter Orbiter bay. Thus the selection of CR-partition ratio has been done to achieve a radiator size sufficiently large to reduce cell temperatures to an acceptable range but not so large that power packing density in the Orbiter is unnecessarily reduced.

A target temperature range of 150°C - 200°C for the cell disc was selected since it was felt that temperatures beyond approx. 200°C would present material-integrity problems, especially for adhesives. Since GaAs is relatively insensitive to elevated temperatures, a lower target range than the one chosen does not yield significant cost benefits.

Table 2-10 shows the results of the thermal analysis which was done for varying
CR-partition ratios. This analysis applies for a flat radiator with and without conical
augmentation. The conical augmentation increases the radiator view factor to space
and thus provides a higher heat rejection capability, resulting in lower cell temperatures.
As the table shows, a CR-partition ratio of 8.33:15 appears to be a good choice for
the present study. Cell temperatures of 172°C and 135°C are achieved for the flat
radiator and the conically-augmented radiator, respectively.

TABLE 2-10

THERMAL ANALYSIS RESULTS FOR CR-PARTITION RATIOS

(a) Flat Radiator Without Conical Augmentation

CR-Partition	9/14 = 126	8-1/3 / 15 = 125	6/21 = 126
T/Prim. Refl.	8°C	--	11°C
T/Sec. Refl.	75°C	--	36°C
T/Radiator	220°C	167°C	139°C
T/Cells	226°C	172°C	145°C

(b) Flat Radiator With Conical Augmentation

CR-Partition	9/14 = 126	8-1/3 / 15 = 125	6/21 = 126
T/Prim. Refl.	11°C	--	14°C
T/Sec. Refl.	73°C	--	34°C
T/Radiator	178°C	132°C	107°C
T/Cells	184°C	135°C	113°C

2.8   COMPARATIVE PERFORMANCE ANALYSIS

2.8.1   General

The major mechanisms of solar array power degradation are identified below and are modeled to reflect the envisioned mission environment. Total mission power profiles have been generated for the four candidate array types:

o   Planar/silicon

o   Low-CR/silicon

o   Low-CR/GaAs

o   High-CR/GaAs

Power add-on during the mission is investigated as a means of improving energy life-cycle cost effectiveness. Mission length and power-rating options are discussed and a comparative summary of array characteristics including size, weight, power, thermal behavior, etc. is given for the candidate arrays.

2.8.2   Power Decay Modes

Table 2-11 lists the major assumptions of the present study concerning the chief mechanisms which cause a decay of solar array power output under the envisioned mission environment. The LEO and GEO charged particle radiation equivalent fluences of 5 E23 and 2 E14 1 MeV el/cm^2 per year, respectively, have been selected by similarity to known missions with similar orbital characteristics. Coverslide erosion due to micrometeorite impact has been taken from a model in use for the Space Telescope program. GEO cover erosion may be somewhat less but has been taken to be equal to LEO erosion for this study. Lack of existing data has prompted the assumption of a similar loss model for reflector erosion by micrometeorites. This is of no disadvantage to the planar array but has been modeled as a two-fold disadvantage for the high-CR array due to double reflection scattering.

TABLE 2-11

SOLAR ARRAY POWER DECAY MODES

SOLAR CELL AND COVERSLIDE

- ASSUME MAXIMUM-POWER OPERATION
- CHARGED PARTICLE RADIATION EQUIVALENT:
  ASSUME 5E13 1 MeV el/cm^2 PER YEAR IN LEO AND 2E14 1 MeV
  el/cm^2 PER YEAR IN GEO
- MICROMETEORITE (MM) - INDUCED LOSSES:
  COVER EROSION SATURATES TO ~5 PERCENT LOSS AFTER 5
  YEARS
- UV: NOT A "DECAY" MODE SINCE SATURATION (1-2%) OCCURS
  AFTER ~1 MONTH

REFLECTOR (REFLECTIVITY)

- PARTICULATE AND UV LOSSES:
  NONE ASSUMED
- MM - INDUCED LOSSES:
  AS FOR COVER EROSION ABOVE

CELL SERIES INTERCONNECT

- 6000 THERMAL CYCLES PER YEAR IN LEO
- 90 THERMAL CYCLES PER YEAR IN GEO
- MEAN FATIGUE LIFE (BREAKAGE):
  ASSUME 100,000 THERMAL CYCLES ACHIEVABLE

THERMAL CONTROL SYSTEM (HIGH-CR ONLY)

- α/ϵ - DEGRADATION OF RADIATOR:
  RESULTANT POWER LOSS FORESEEN TO BE SMALL
- HEAT PIPE PUNCTURE DUE TO MM:
  WILL BE KEPT SMALL BY DESIGN

Degradation of thermal control surface optical properties (α and ϵ) will admittedly cause adverse temperature increases, especially for the high-CR concept. However, the resulting loss in array power output has not been considered as a major decay mode. This assumption is a direct result of the relative insensitivity of the GaAs solar cell to temperature changes.

Figure 2-50 gives the normalized maximum power point degradation $P_{max}(\phi)/P_{max}(0)$ due to equivalent charged particle radiation for the four candidate array concepts. All curves apply for the on-orbit cell operation temperatures established through separate analysis. Sufficient recent test data exists for the GaAs cell (here, for a junction depth of .3 - .5 μm) to allow a degree of confidence which is more than adequate for the purposes of the present study. The figure demonstrates once again the difference in temperature sensitivity of the two solar cell materials.

Cell series interconnect fatigue is potentially the most life-limiting of all array failure mechanisms. Component life-time requirements have been pre-designated as 3-8 years minimum; however, the present study has investigated the optimum mission-life in terms of system cost-effectiveness. Interconnect fatigue modelling has a potentially strong impact upon this optimization. Interconnect to cell technologies exist at present which have been verified to some 30,000 temperature cycles. At LMSC high compliant Moly interconnects have been mechanically flexed $\approx 50,000$ cycles over 2X the equivalent stress (combined bending and elongation) resulting from a $\Delta T = 200°C$. The solar cell test samples, 24 interconnect bonding points were cycled at an ambient temperature of 107°C. No failures occurred at the bond line or within the flexured portion of the interconnect. The samples were soldered which typically in a thermal cycle environment (high and low temperature) tend to become granular (separation of tin and lead) or in other words, brittle. The significant result was that the interconnect withstood 50,000 cycles without failure, indicating that where the cell to interconnect bonding is designed to minimize stress below metallic bond strength the system can survive. The proof can only come through a combination of real time and accelerated life cycling of the proposed system of cell, welding, interconnect pattern and material (adhesive of GaAs) and cell blanket. The difference between 8 years and 15 in terms of Shuttle launch and other associated costs is $\approx \$40$ million dollars. With appropriate developmental planning during these next several years it is realistic to envision a 15 year cell-blanket system in readiness for 1983.
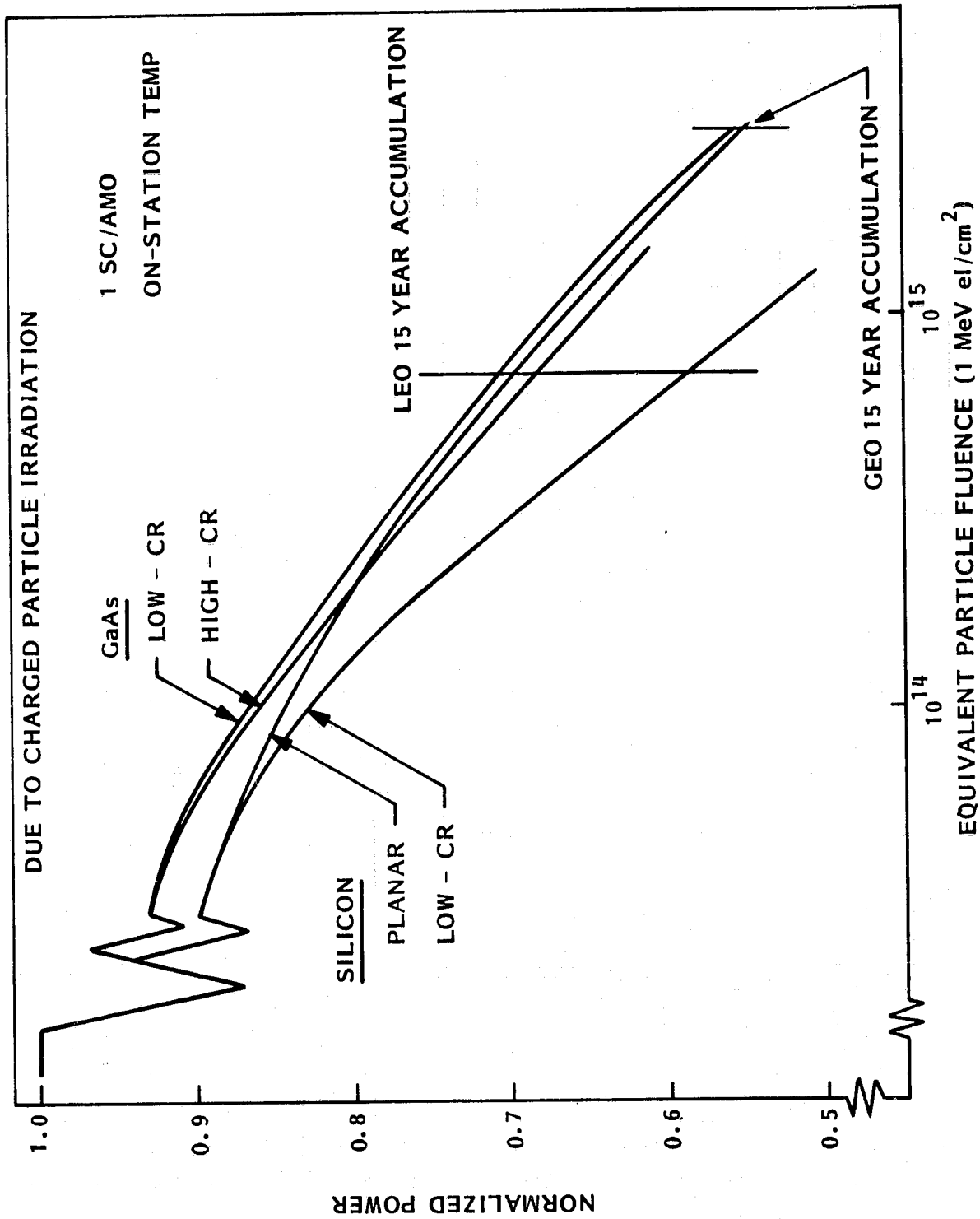
Figure 2-50 Typical Power Degradation Profile

LOCKHEED MISSILES & SPACE COMPANY. INC.

Figure 2-51 shows one possible model for the fatigue behavior of a solar cell series interconnect which is capable of surviving 100,000 temperature cycles. Curves of similar shape and spread-ratio (but lower mean life) have been observed previously for certain discrete interconnect designs. 100,000 cycles corresponds to approx. 16.7 years at LEO ($\sim$6000 cycles/year). According to the model in the figure, losses begin to assume significance at approx. 70,000 cycles ($\sim$11.7 years) and have reached a virtual 100% failure status by approx. 140,000 cycles (23.3 years). Though a detailed interconnect description exceeds the scope of the present study, a certain amount of redundancy has been assumed for the interconnect design. This accounts for the somewhat sharp profile of the fatigue curve. Assuming the plausibility of this fatigue model, Figure 2-51 translates into a power degradation curve (fatigue only) of Figure 2-52.

Figure 2-53 combines into a single LEO profile the effects (at operation temperature) of the major decay mechanisms:

- charged particle radiation
- micrometeorite cover erosion
- reflector erosion (where applicable)
- interconnect fatigue

Three of the four array candidate concepts are shown. The low-CR/GaAs concept is not shown for clarity; its profile runs approximately down the center of the group of curves. This figure provides the basis for all further performance analysis, including concept comparison, mission life-time trades, and power add-on investigations below.

It should be pointed out that in transferring the particle-decay-only curves of Figure 2-50 into the total decay curves of Figure 2-53, the yearly equivalent fluence assumption of Table 2-11 plays a key role. Figure 2-50 shows measured decay under a 1 MeV electron beam. In Figure 2-53 the 1 MeV electron fluence is translated into equivalent years on-orbit under the assumption that a year's bombardment by the orbit particle spectrum is correlatable to a certain 1 MeV electron fluence. A broad, high-confidence data base has evolved over the years for making this correlation for silicon cells. For GaAs cells a similar correlation has not been established. This adds a degree of uncertainty to the GaAs system power profiles.

LOCKHEED MISSILES & SPACE COMPANY, INC.
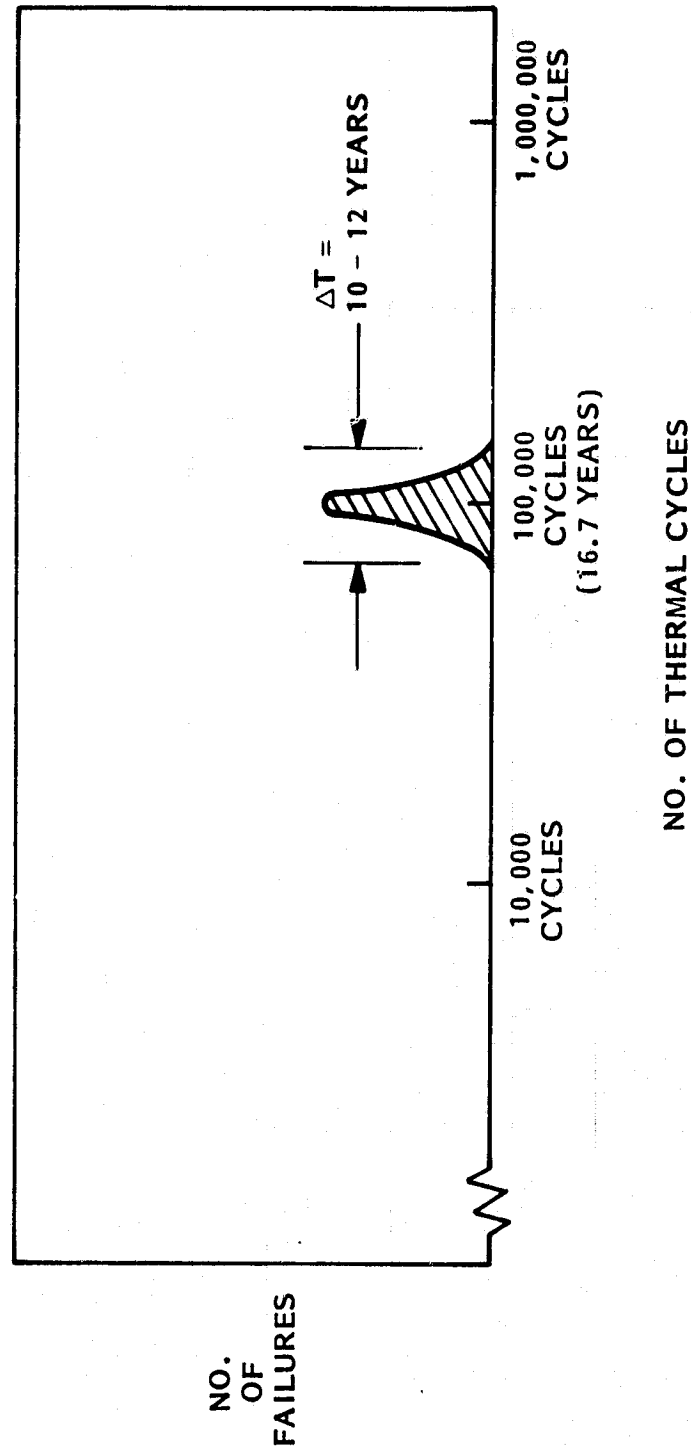
Figure 2-51 Interconnect Fatigue Model

BASELINE MODEL: "100,000 CYCLE" SERIES INTERCONNECT

NORMALIZED POWER OUTPUT

TIME ON-STATION (YEARS)
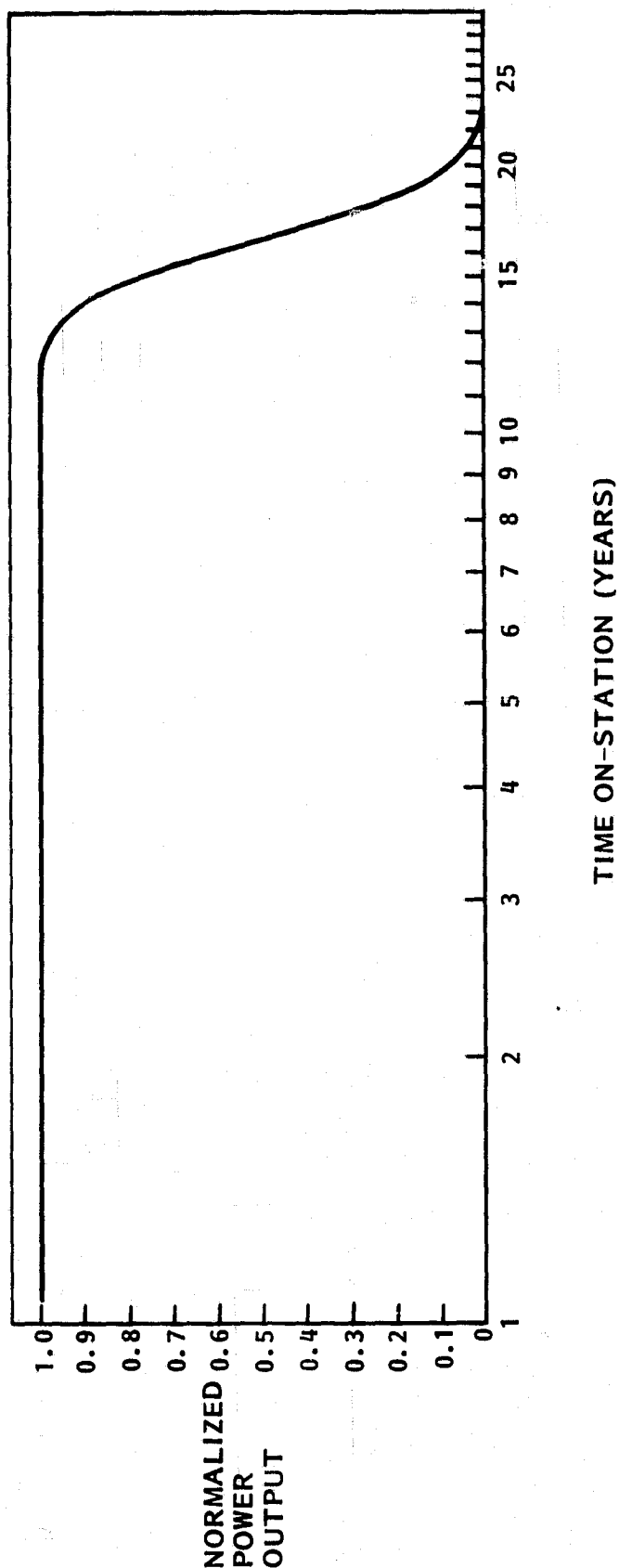
Figure 2-52 Array Power Loss Due to Interconnect Fatigue

RESULTING FROM:

- CHARGED PARTICLE RADIATION
- MM COVER EROSION
- REFLECTOR EROSION (CONCENTRATORS ONLY)
- INTERCONNECT FATIGUE

PLANAR

HIGH-CR

LOW-CR/Si

NORMALIZED ARRAY P_{MAX}

TIME ON–STATION (YEARS)
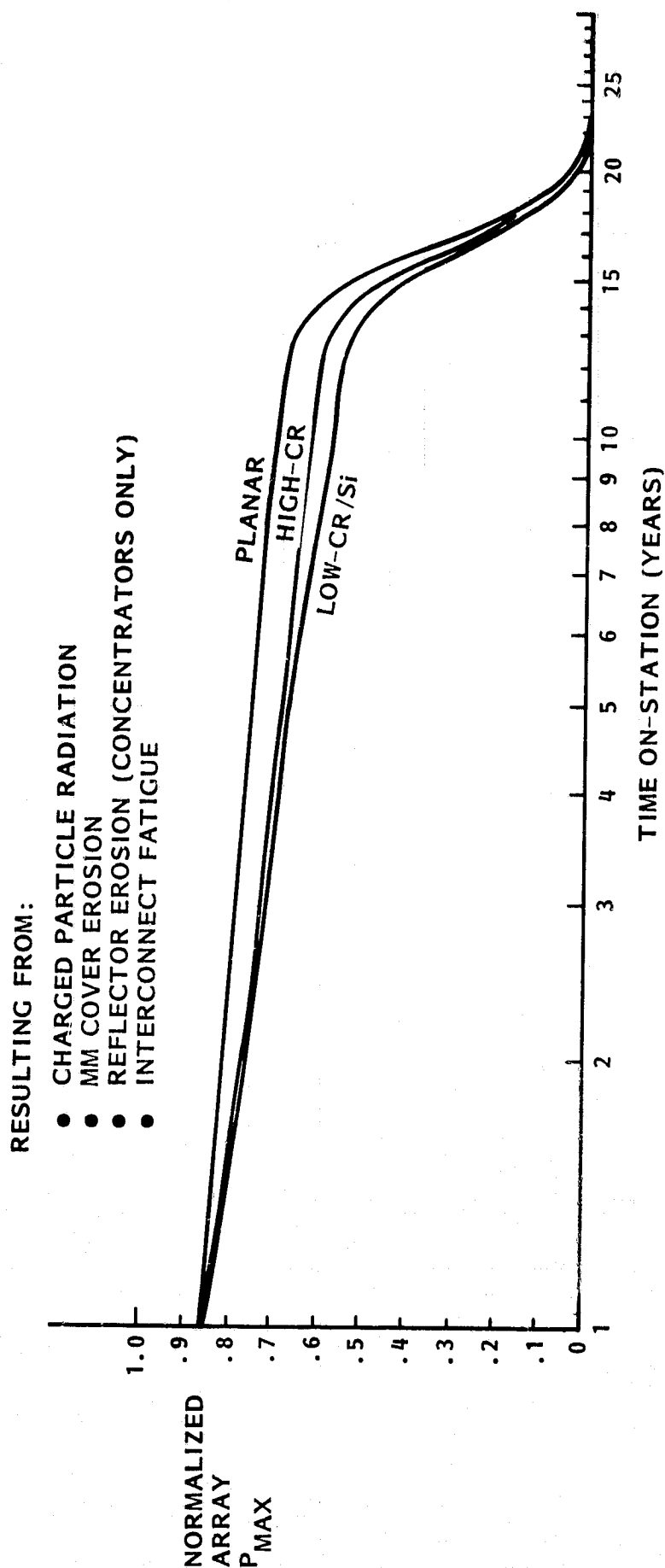
Figure 2–53 Normalized Array P_{max} Degradation Profile (LEO)

LOCKHEED MISSILES & SPACE COMPANY. INC.

2.8.3 Power Lifetime

Now that overall power degradation profiles have been established, it is possible to analyze the manner in which array cost-effectiveness is influenced by the choice of required mission lifetime. If, for example, the required power level is specified as an average power available over lifetime, two counteracting tendencies combine to determine the optimum cost-effectiveness lifetime. On the one hand, lengthening the designated life serves to drag down the value of average power. This drives up the initial size, and consequently, cost of the array. On the other hand, on an energy (kW-hr) cost basis, lengthening the designated life increases the total energy available over the total mission.

The top set of curves in Figure 2-54, labeled "BOL Power Oversize," show how the required size of the planar/Si array at LEO is affected by choice of mission length. The bod curve applies if, as is likely, average power over life is specified; the broken curve applies if minimum power during life (i.e., EOL power) is specified. If, for example, n kW avg. is required, the array must be sized to approx. 1.2 n kW BOL (temp.) for a 5 year design-life and to approx. 1.4 n kW BOL (temp.) for a 15 year design-life. This oversize factor is a valid comparative cost-indicator, since it reflects not only manufacturing and assembly costs but also launch and maintenance costs. In fact, since the curves apply for unity specified power, they reflect costs on a per-watt basis. Conversion of this $/W indicator into an indicator of energy life-cycle cost ($/kW-hr)--the primary figure of merit--is achieved by simply dividing by the chosen mission length. The bottom set of curves in the figure, labeled "Relative Energy Life-Cycle Cost," accomplishes this by taking the top set of curves and dividing by the designated mission time in years.

As expected, the bottom curves exhibit a strong hyperbolic component (i.e., via division by the independent variable) but will also exhibit an upwards tendency at higher life-times due to the "fatigue-tail" of the top curves. In fact, for the case of a minimum power requirement (the $P_{min} = 1$ curve), the energy-cost indicator reaches an optimum for a mission life of approx. 13 years and then rapidly deteriorates upwards.
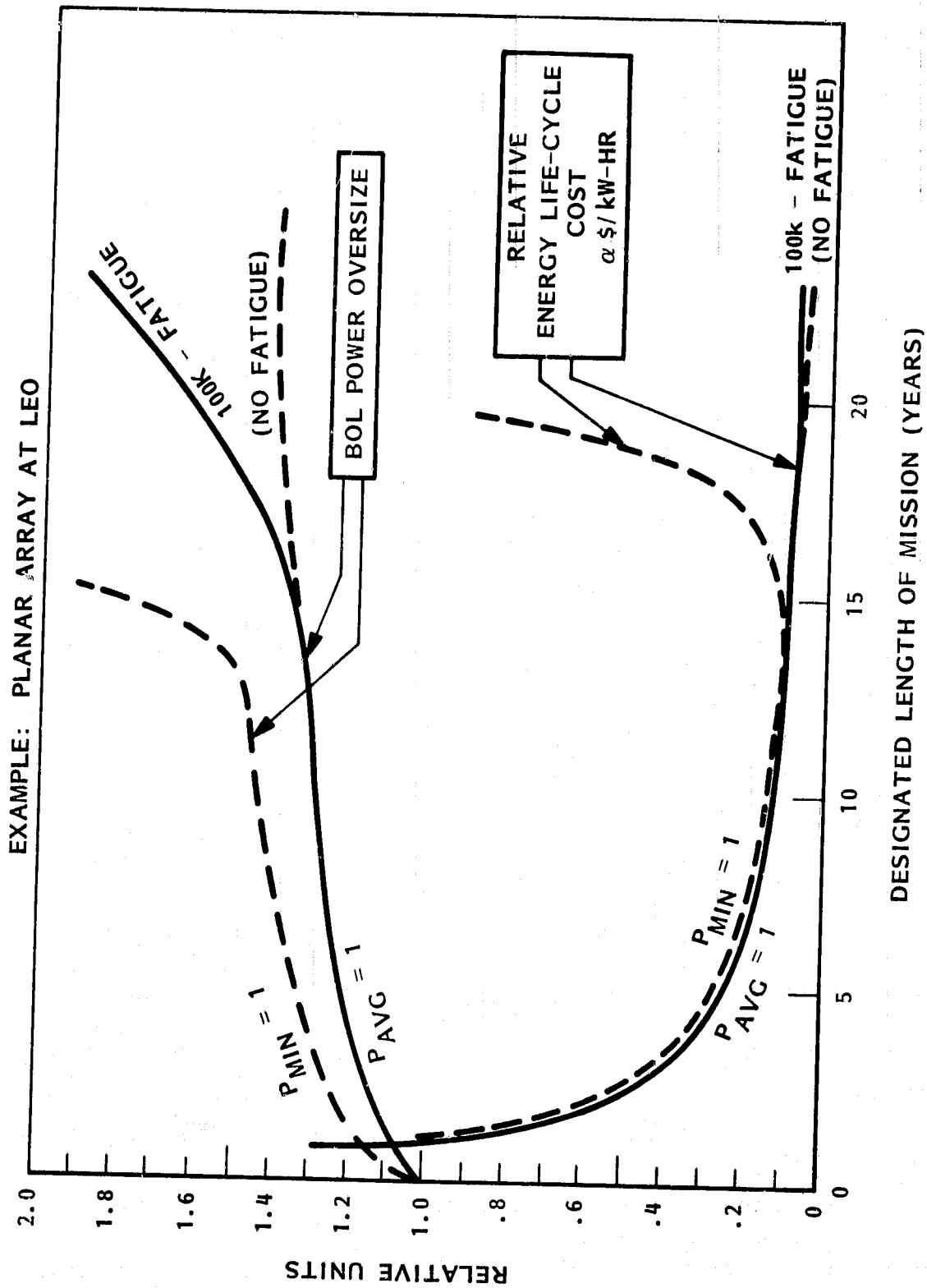
Figure 2-54 Size and Cost Impact of Increasing Mission Length

LOCKHEED MISSILES & SPACE COMPANY, INC.

For the most probable case--requirement of an average power (the $P_{avg} = 1$ curve)--
the upwards tendency is much weaker and cannot be distinguished after a 20 year life.
Between 10 and 15 years a yearly kW-hr cost gain of a few percent per year is still
being gleaned from the system, thus providing a significant total cost gain by extending
the mission-life requirement from 10 years to 15 years. Beyond 15 years modest
cost gains appear to still be achievable. However, since the instantaneous power is
dropping rapidly, it hardly appears to be prudent to extend the mission beyond 15 years.

It is instructive to investigate the influence of the "fatigue tail" upon the curve form.
At approximately the 18 year point the $P_{avg} = 1$ energy cost indicator curve splits into
two curves--one which includes the 100,000 cycle interconect model (labeled "100K-
Fatigue") and one which includes no fatigue decay at all. The split tail has been exaggerated
in the figure for clarity. It is nonetheless clear that the 100K-fatigue influence is not
significant. This result is not surprising in view of the overpowering hyperbolic
tendency of the curve.

As Figure 2-53 has shown, the power profiles of the four candidate concepts are
sufficiently similar to permit the conclusion that a 15 year mission-life is appropriate
not only in the planar case treated above, but also for all candidate concepts. A 15
year life, while technologically ambitious, is thought to be realistic for the envisioned
1983 time-frame and will provide significant cost benefits.

2.8.4   Power Add-On

Utilizing the 15-year result from above, an analysis was performed to determine
potential cost benefits to be achieved through periodic add-on of array power instead
of the traditional one-time array installation at BOL. Figure 2-55 shows the 15 year
power profile for the planar array at LEO after renormalization for unity average power
and a re-scaling to a linear time scale. The top curve shows the 1.37 array oversize
factor at the BOL point. The bottom curve illustrates a typical power add-on profile
for comparison. After 5 and 10 years, respectively, add-ons are performed such that
a unity mission average emerges. By totalling the initial oversize and the two sub-
sequent add-ons, a total "build-size" of 1.53 is obtained, which is 12% greater than for the
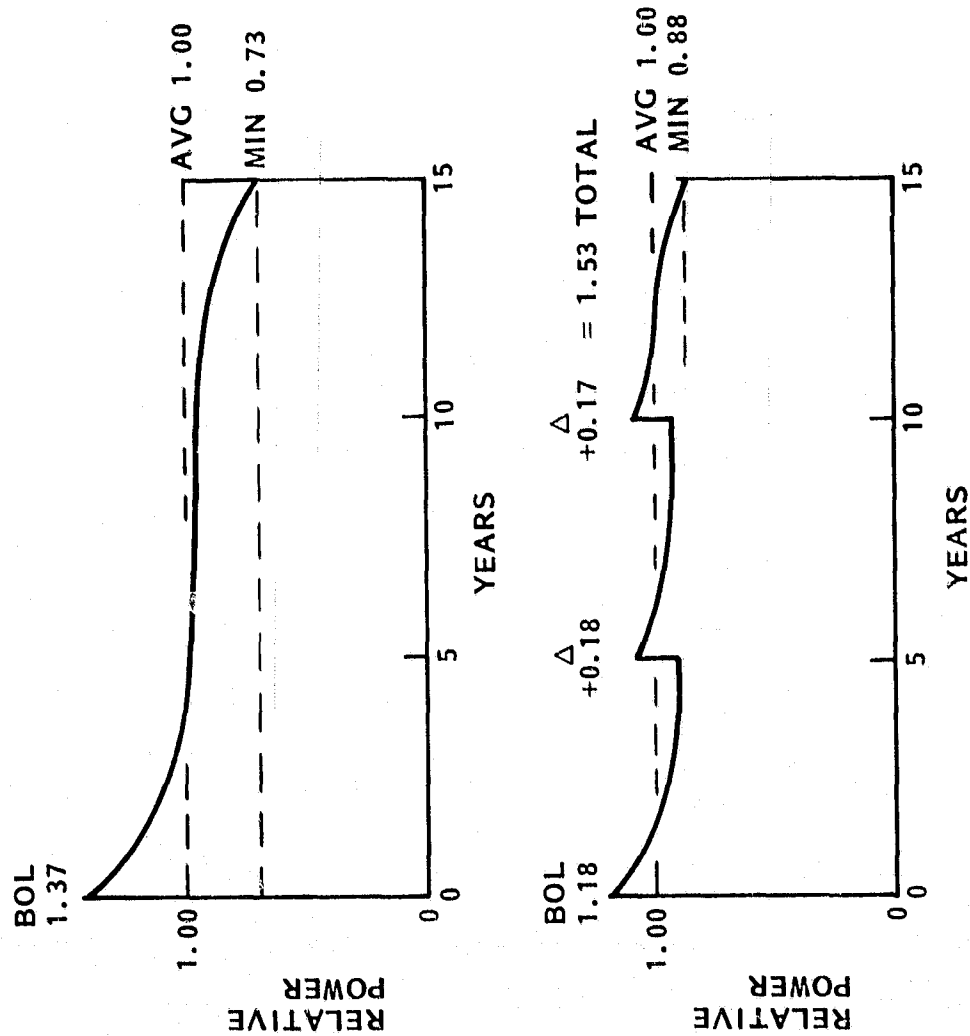
Figure 2-55 Power Add-On Impact for $P_{avg}=1$ (Planar in LEO)

LOCKHEED MISSILES & SPACE COMPANY, INC.

non-add-on case and is thus significantly more costly. This basic result is
not peculiar to the chosen add-on profile. Analysis shows that the total
"build-size" can be reduced by increasing the initial oversize, reducing
subsequent add-ons, and lengthening the add-on intervals until the limiting
case is reached--namely, no add-on at all. Indeed, this result appears to
be a fundamental characteristic of a decaying system, when average perfor-
mance is the objective.

Figure 2-56   repeats the same exercise for the less likely case of requiring
a minimum power during the mission. Here a double add-on profile was chosen
where unity minimum power is achieved at 5 years, 10 years, and at EOL. The
total build-size is 9% less than for the non-add-on case and thus significantly
more cost-effective. Here too, analysis of several profiles showed the validity
of the basic result for minimum power requirement.

The oversize factors seen in the figures above are significant amounts of energy
at system sizes considered in this study. The first case above specifies an
average power (i.e. unity) and presumes that this power--essentially all
available power--will be utilized by the payloads. The second case above
specifies a minimum power (i.e., unity) but, by using resultant BOL oversize
or total build-size as a cost indicator, presumes that only the minimum power
is the cost basis for utilization by payloads. This utilization philosophy is
not likely, whereas the utilization philosophy of case one is highly likely.
A third alternative exists whose likelihood is also high. Reference to Figure
2-56   will illustrate this third case. The minimum power is specified (i.e.
unity) however, the intent is to use all available power--essentially the
average power. In this case the two average values (i.e. 1.38 and 1.11) are
cost-indicated by using them to normalize the oversize or build-size factors.
For the profiles of Figure 2-56   this results in a 14% cost advantage for
the non-add-on case, which is indicative of the general result for this type
of power specification.
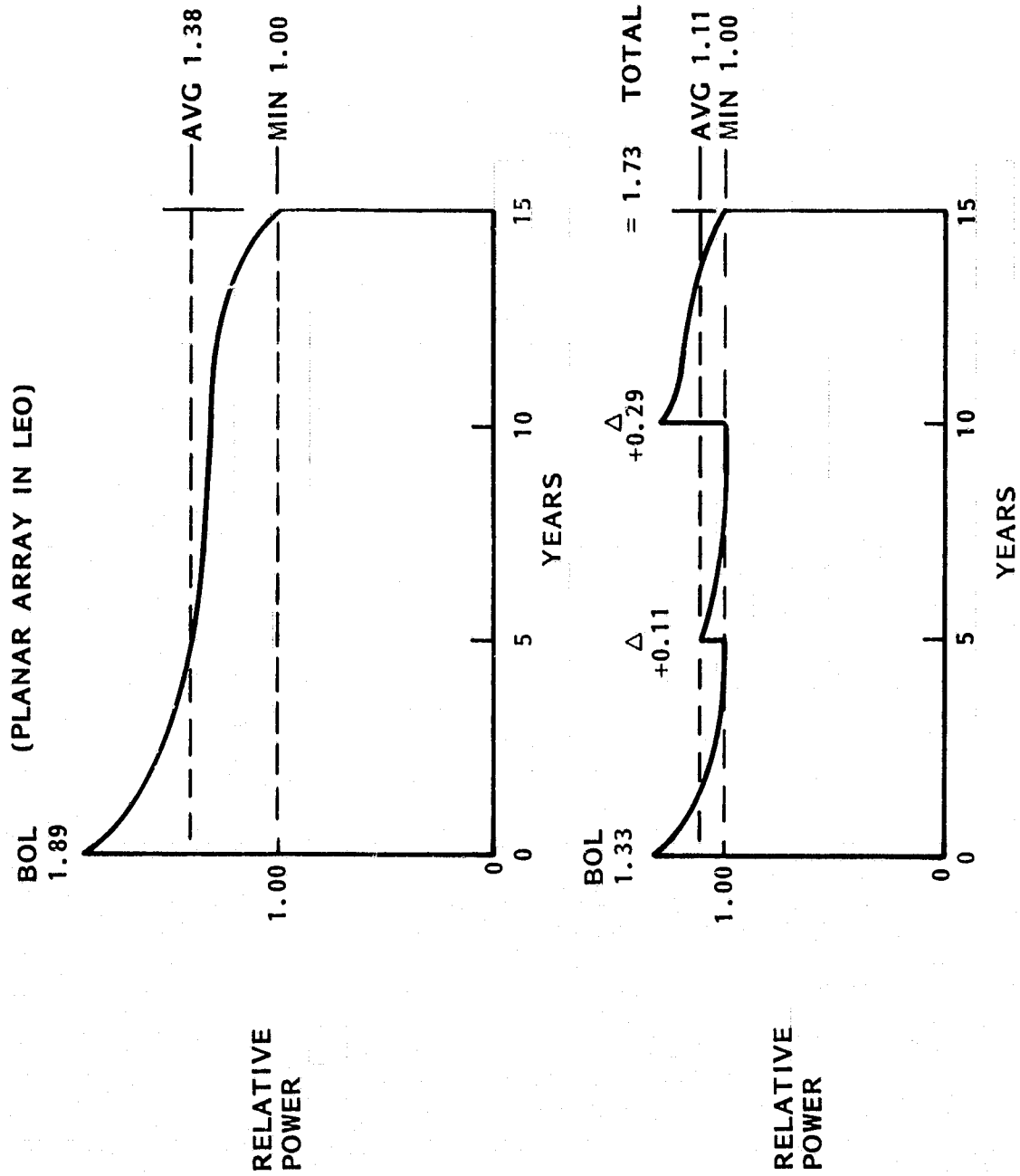
Figure 2-56 Power Add-On Impact for $P_{min} = 1$

LOCKHEED MISSILES & SPACE COMPANY, INC.

The general results from all cases above are summarized in Table 2-12 and illustrate an obscure but significant finding: the power add-on philosophy influences cost-effectiveness significantly, and this philosophy depends strongly upon how the system power requirement is specified in relation to how system power is utilized.

2.8.5   System Performance Comparison

The LEO power profiles of the four candidate array concepts are shown in Figure 2-57 normalized to unity average power. The similarities are striking, with the exception of the low-CR/silicon array, which is degrading more rapidly due to increased silicon radiation sensitivity at elevated temperatures.

Table 2-13 shows a weight breakdown for the candidate arrays. This breakdown is based upon a detailed weight analysis of all major components and assemblies. The planar array weight distribution shows the expected high percentage of cell and coverslide contributions. In proceedings to the low-CR arrays, the support structure percentage remains, while half the cell/cover percentage is shifted to the reflector structure. In the high-CR array the cell/cover percentage is negligible, while the reflector structures and the thermal control system have both assumed the major weight burdens. On an absolute weight scale the low-CR/ silicon array weighs more than twice as much per watt as the low-CR/GaAs. (The values in the figure are not normalized). This is due to the poor Si-efficiency at elevated temperatures. This fact is reflected again in Table 2-14, which shows the gross size of the low-CR/silicon array to be roughly twice as large as the low-CR/GaAs array. It is significant to note the number of Orbiter flights necessary to install these arrays of roughly the same power level. This number will have a significant impact upon the cost comparison of the array candidates, since, unlike traditional array costing, launch costs are to be fully included in the cost trade analysis for this study.

TABLE 2-12

POWER PROFILE AND ADD-ON/CONCLUSIONS

- 15 YEAR MISSION:

    LOW ENERGY LIFE-CYCLE COSTS. TECHNOLOGICALLY
    AMBITIOUS, YET REALISTIC FOR 1983 TIME FRAME

- IF P_{AVG} SPECIFIED AND P_{AVG} UTILIZED (COSTED):

    NO POWER ADD-ON. LOWEST COST THROUGH ONE
    INITIAL POWER INSTALLATION

- IF P_{MIN} SPECIFIED AND P_{MIN} UTILIZED (COSTED):

    POWER ADD-ON REDUCES ENERGY LIFE-CYCLE COST

- IF P_{MIN} SPECIFIED AND P_{AVG} UTILIZED (COSTED):

    NO POWER ADD-ON. LOWEST COST THROUGH ONE
    INITIAL POWER INSTALLATION

As a final note, it is revealing, although not significant to the study objectives, to compute the resultant BOL power-to-weight ratios:

- planar/Si   44 W/lb
- low-CR/Si   23 W/lb
- low-CR/GaAs   45 W/lb
- high-CR/GaAs   14 W/lb

The first and third array types have thus advanced into power-to-weight regions beyond present flexible array technology (SEPS Array: 30 W/lb), despite the virtual disregard for low weight in the present study (emphasis on cost, not weight). If, however, the planar/Si and low-CR/GaAs concepts above were equipped with 2 mil cells and 2 mil covers (an apparent lower boundary), BOL power-to-weight ratios of 81 W/lb and 60 W/lb, respectively, would result.
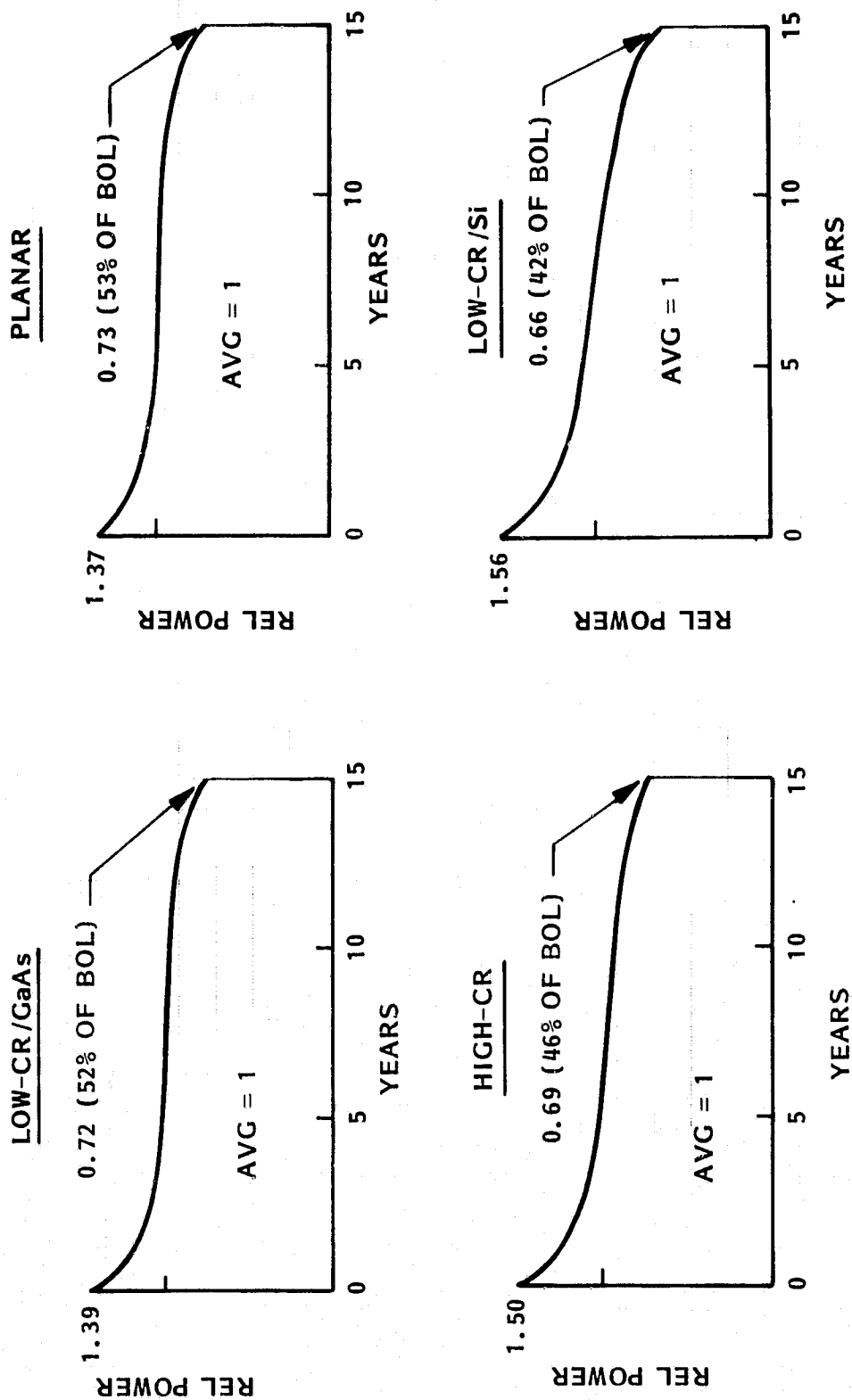
Figure 2-57 LEO Power Profile Comparison

TABLE 2-13

ARRAY CONCEPT WEIGHT COMPARISON

SOLAR ARRAY TYPE	PLANAR	LOW – CR		HIGH – CR
SOLAR CELL TECHNOLOGY	Si	Si	GaAs	GaAs
CELL BLANKETS	6,470 LB (66%)	8,320 LB (32%)	4,665 LB (35%)	240 LB (1%)
REFLECTORS (STRUCTURE AND MATERIALS)	–	7,680 LB (30%)	3,840 LB (29%)	20,160 LB (48%)
STRUCTURE (STOWAGE, DEPLOYMENT, AND SUPPORT)	3,320 LB (34%)	9,800 LBS (38%)	4,900 LB (36%)	6,050 LB (14%)
THERMAL CONTROL	–	–	–	15,400 LB (37%)
TOTAL WEIGHT	9,790 LB	25,800 LB	13,405 LB	41,850 LB
POWER (15 YR AVG)	311 kW	380 kW	437 kW	384 kW
NO. OF FLIGHTS TO INSTALL	1	2	1	3
LBS PER FLIGHT	9,790 LB	12,900 LB	13,405 LB	13,950 LB

LOCKHEED MISSILES & SPACE COMPANY, INC.

TABLE 2-14

SYSTEM PERFORMANCE SUMMARY – LEO

	PLANAR	LOW-CR	LOW-CR	HIGH-CR
SOLAR CELL	Si (5.9 x 5.9)	Si (5.9 x 5.9)	GaAs (2 x 2)	GaAs (2 x 2)
GEOM CR/EFF CR	1/1	5/3.4	5/3.4	125/67.5
CELL OPERATION TEMP	65°C	143°C	138°C	172°C
CELL EFFICIENCY BOL (1983)	28°C: 14% ORBIT: 11.3%	28°C: 14% ORBIT: 7.5%	28°C: 18% ORBIT: 16%	28°C: 18% ORBIT: 15%
THERMAL CONTROL	PASSIVE	PASSIVE	PASSIVE	ACTIVE
GROSS PLANE AREA	39,900 FT^2	125,000 FT^2	62,500 FT^2	82,400 FT^2
ARRAY WEIGHT	9790 LB	25,800 LB	13,405 LB	41,850 LB
MODULARITY	4 MODULES	10 MODULES	5 MODULES	45 MODULES
POWER/BOL	427 kW	594 kW	606 kW	576 kW
POWER/15 YR AVG	311 kW	380 kW	437 kW	384 kW
NO. FLIGHTS TO INSTALL	1	2	1	3

2.8.6   System Performance Comparison - GEO

It becomes obvious when one reviews the average LEO power at End of Life (15 years), Table 2-14, that the Low CR Si and High CR GaAs are not cost effective to be continued in the GEO performance discussion. This is due to 1 and 2 extra shuttles required to deliver equivalent power systems into orbit. As such only the Planar-Si and Low CR-GaAs will be discussed in this section. Figure 2-58 is the resulting combination of particle decay-only curves of Figure 2-50 and the solar array decay modes of Table 2-11. The same concerns hold true as described in the LEO discussion. Normalization has coincidentally overlaid the Planar and the Low CR. The absolute difference would spread the two apart but parallel with the Low CR GaAs being the upper curve based on higher cell efficiency at operating temperatures.

The GEO power profiles of the Planar and Low CR GaAs configurations are shown in Figure 2-59 normalized to unity average power. The same reasons for the similarities exist as previously described.

Table 2-15 details the weight breakdown of major components for both GEO configurations. GEO sizing was established by LEO to GEO transfer vehicle payload capability. The nearest whole LEO module to payload capacity of a LTTV 2 stage vehicle was selected. In the case of the planar the GEO size is 3/4's that of the LEO configuration (4 to 3 modules). The Low CR GaAs was restricted by volume before weight to be 3/5's of the LEO size. Weights for each concept were simply scaled down since full modules were used in each case and thus the same cell to blanket weights percentages exist for GEO as did for LEO.

The GEO system performance comparison is extremely matched for both the Planar Si and Low CR-GaAs Solar Arrays (Figure 2-60). The planar may be slightly improved by enlarging the basic blanket width which would increase the overall design and cost. The effect of a major modification to the basic design was not considered cost effective at this time.

Power to weight ratio is slightly improved at GEO due to:

        Planar/Si   46 watt/lb
        Low CR/GaAs   47 watt/lb
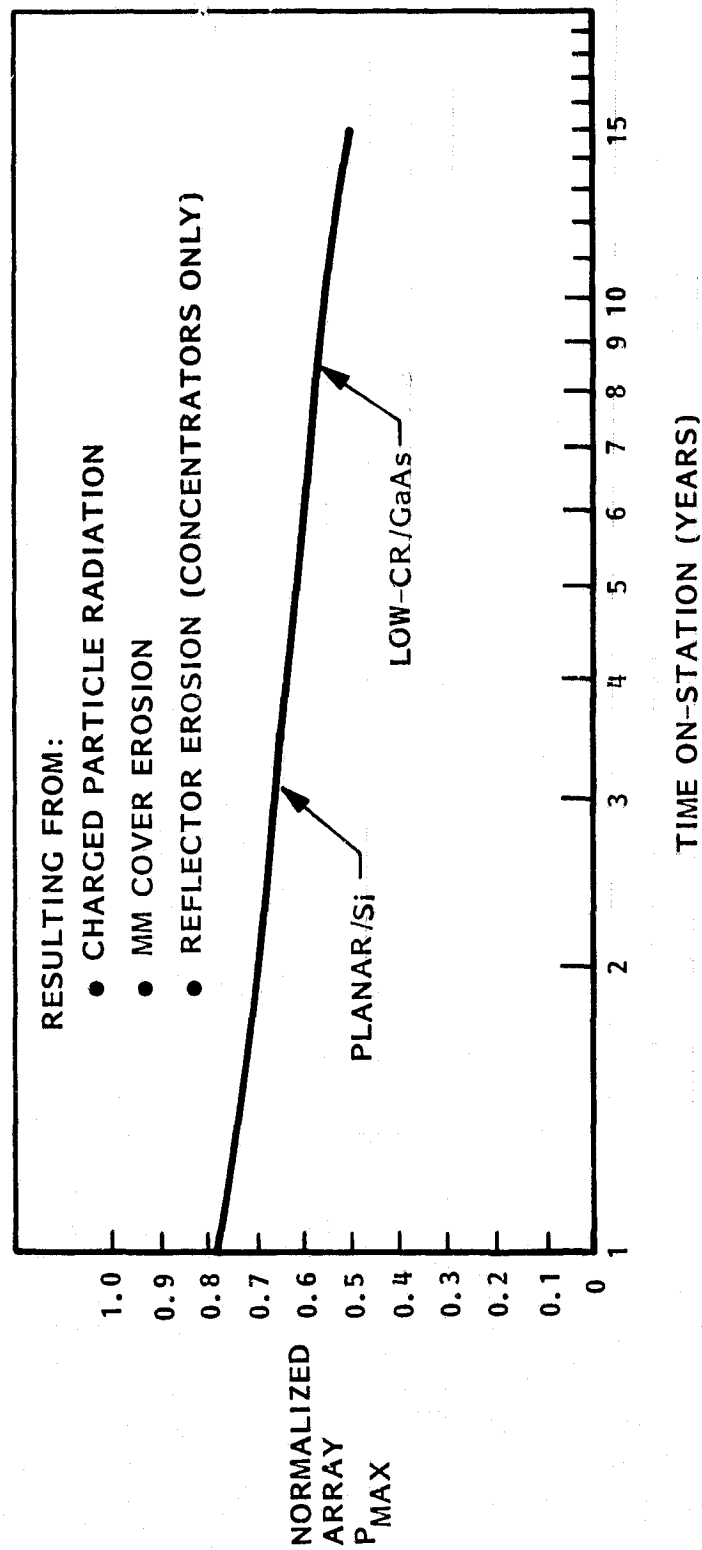
Figure 2-58 Normalized Array P_{max} Degradation Profile – GEO
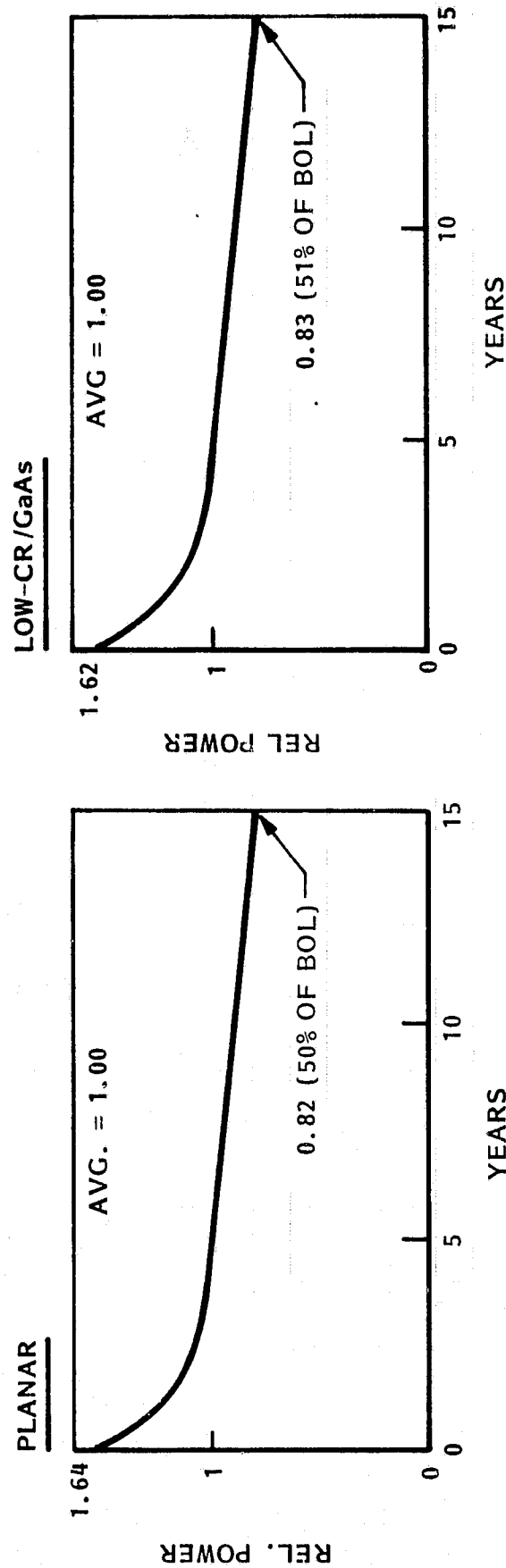
Figure 2-59 GEO Power Profile Comparison

LOCKHEED MISSILES & SPACE COMPANY. INC.

TABLE 2-15

ARRAY WEIGHT COMPARISON – GEO

PARAMETER	PLANAR/SILICON	LOW-CR/GaAs
CELL BLANKETS	4855 LB (66%)	2800 LB (35%)
REFLECTORS (STRUCTURE AND MATERIALS)	–	2305 (29%)
STRUCTURE (STOWAGE, DEPLOYMENT, AND SUPPORT)	2490 (34%)	2940 (36%)
TOTAL WEIGHT	7345 LB	8045 LB
POWER (15 YEAR AVERAGE)	206 kW	231 kW
NUMBER OF FLIGHTS TO INSTALL	1	1

PARAMETER	PLANAR	LOW-CR
SOLAR CELL	Si (5.9 X 5.9)	GaAs (2 X 2)
GEOM CR/EFFECT CR	1/1	5/3.4
CELL OPERATION TEMP	55°C	121°C
CELL EFFICIENCY BOL (1983)	28°C: 14% ORBIT: 12.4%	28°C: 18% ORBIT: 16.5%
THERMAL CONTROL	PASSIVE	PASSIVE
GROSS PLANE AREA	29,925 FT^2	37,500 FT^2
ARRAY WEIGHT	7345 LB	8045 LB
MODULARITY	3 MODULES	3 MODULES
POWER/BOL	337 kW	375 kW
POWER/15 YR AVG	206 kW	231 kW
*NUMBER OF LAUNCHES	1	1

* WITH TRANSFER BY LTTV/2 STAGE

Figure 2-60 System Performance Summary – GEO

STUDY OF
MULTI-kW SOLAR ARRAYS
FOR EARTH ORBIT APPLICATION

Section 3

Task 2

On—Orbit Maintainability

NASA LOCKHEED
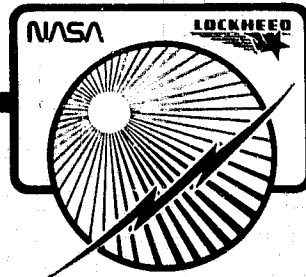
3.0 TASK II – ON-ORBIT MAINTAINABILITY

3.1 Maintainability Philosophy

The intent of the task is to examine what benefits might accrue from using the on-orbit maintenance services available from the Orbiter and to consider those factors in arriving at the design concepts developed in Task I.

The philosophy of on-orbit maintainability is to improve cost effectiveness by being able to correct equipment deficiencies or malfunctions by direct on-orbit service. This approach will be made possible by manned Shuttle flights to low earth orbit. In this study we have applied those tools and services available from the Orbiter to the tasks of building and maintaining multi-kW solar array systems in low earth orbit. Application of the multi-kW systems to geosynchronous orbit will require development of a new generation of remote controlled equipment which will enable rendezvous and docking of solar array systems with solar powered user stations and their deployment.

3.1.1 Guidelines for Low Earth Orbit (LEO) and Geosynchronous Orbit (GEO) Application

LEO

The multi-kW solar array package launched to LEO must either be directly mated to an existing platform or it must carry with it in orbit and attitude maintenance module containing avionics, attitude control, drag makeup and electrical power for housekeeping. A segment of the first solar array launched could be dedicated to housekeeping power.

As the concepts for planar and concentrator designs were developed, the first trade was between erection and deployment of the solar arrays. Discussions with LMSC's large space structures group led to our favoring deployment, because of their statement that a structural platform of less than 10,000 sq. meters (corresponding to a 1 MW planar S/A) would not justify automated erection machines and furthermore, none were currently under development. Present manned extravehicular activity (EVA) is limited by the Manned Maneuvering Unit (MMU) capability of 220 lbs.

The next resultant LEO trade is between manned and unmanned buildup and maintenance for the Multi-kW S/A. Since the deployed structure approach was favored, EVA will be minimized; however, where required, the Extravehicular Mobility Unit (EMU) which is the astronaut's space suit or the MMU will be used. The latter is an astronaut back-pack which permits free translation with its self-contained propulsion and electrical power systems.

The primary remote controlled Orbiter system which can be used to remove and deploy equipment from the Orbiter bay is the Remote Manipulator System (RMS). One RMS is standard with each Orbiter and a second RMS is optional. Since the RMS is attached to the Orbiter and has a maximum reach of 50 feet, a remotely controlled transport vehicle (RCT) was conceived to enable buildup or maintenance of a Multi-kW S/A system without physically coupling to the Orbiter. If remotely controlled equipment is used, it would still be backed up by manned EVA.

There are a number of reasons for limiting manned involvement in maintenance and primary buildup to backup functions only. First, two astronauts are limited to 6 hours of EVA per day and the maximum Orbiter mission is 7 days; therefore the maximum work time is 84 manhours per mission. Each EVA day is a very full one for an astronaut which makes a sequence of 7 days very impractical.

EVA must be based on full artificial illumination because up to 0.6 hours per 1.5 hour orbit is in solar eclipse. Also, when the Orbiter is in the sun the astronaut will be working in the shadow of the solar array being erected, because it is undesirable to have the astronaut in a position where he can damage cell and reflector area or be exposed to concentrated sunlight. Artificial illumination will be required during remote controlled operations as well, because they will be observed from the Orbiter.

Backup EVA to remote controlled operations will include tasks such as using a hand drill drive powered by the MMU to operate a mast deployer mechanism which may have stuck and exhausted its battery or had a motor control failure.

LOCKHEED MISSILES & SPACE COMPANY, INC.

The S/A design concepts were developed using modular building blocks for efficiency of Orbiter bay packaging and ease of deployment. Guidelines for maintenance were devised and include the following:

(1)   The module used during buildup of the S/A would be the same used to replace a defective module or to augment power output.

(2)   Addition of modules is favored over replacement, because hazards are less and so long as a module is generating power, even though degraded, it is probably worth operating.

(3)   Since deployed structures were favored over erected and (2) above, EVA functions were minimized.

(4)   To maximize reliability and minimize weight and cost, deployed structures were not made retractable. Recovery, refurbishment and redelivery to orbit was not deemed cost effective where solar cell degradation and cell interconnect failure are the most probable cause of power loss. Hardware would be either destructively recovered by the Orbiter or by controlled deboost.

(5)   The S/A is assumed to be docked to a power user station which contains drag make-up and attitude control subsystems and the necessary avionics.

3.1.2   Identification of Component Life

The major assemblies and components which were used in the concepts developed in Task 1 have been identified in Table 3-1. Wherever feasible, materials having demonstrated long-life characteristics were selected. Where test data was lacking, engineering judgment was applied to arrive at "expected" performance. Cell to blanket interconnecting was discussed under Task 1.

TABLE 3-1

MULTI-KW S/A MATERIALS LIST

(Page 1 of 4)

ITEM DESCRIPTION	MATERIAL OF CONSTRUCTION	ENVIRONMENTAL STABILITY UNDER:			COMMENTS	USEFUL LIFE-YRS
		THERMAL CYCLING	U-V RADIATION	PARTICLE RADIATION		
PRIMARY STRUCTURE						
Main Support Beams						
Planar	Graphite/ Epoxy	Good (Expected)	Good (Expected)	Good (Expected)		>15
Low CR	"	"	"	"		
Heat Sink-High CR	Aluminum/ St. Steel	Excellent	Excellent	Excellent		
Lenticular-High CR	Graphite/ Epoxy	Good (Expected)	Good (Expected)	Good (Expected)		
REFLECTORS						
Low CR	Melinex 471/473	Good (Expected)	Good (Expected)	Good (Expected)		>15
High CR	" & Aluminized Kapton	" "	" "	" "		

LOCKHEED MISSILES & SPACE COMPANY, INC.

MULTI-KW S/A MATERIALS LIST

ITEM DESCRIPTION	MATERIAL OF CONSTRUCTION	ENVIRONMENTAL STABILITY UNDER:			COMMENTS	USEFUL LIFE-YRS
		THERMAL CYCLING	U-V RADIATION	PARTICLE RADIATION		
MAST						
Cannister	Aluminum	Excellent	Excellent	Excellent		>15
Bearings	Steel	"	"	"	Only critical during deployment	
Lubricant	MIL-L-81329(AS)	Good	N/A	Good (Expected)		
Deployment Section	Fiberglas/Epoxy	Good	Good	Good	"	
Guide Rails	Delrin (Acetal)	Good	Good	Good	"	
Boom						
Longerons	Fiberglas/Epoxy	Good (Expected)	Good (Expected)	Good (Expected)		
Battens	"	"	"	"		
Adhesive	EA934 Hysol	"	"	"		
Fittings	Aluminum	Excellent	Excellent	Excellent		
Cables	St. Steel	"	"	"		
Motors	Space Qual.	"	"	"	Only critical during deployment	
Lubricant	MIL-L-81329(AS)					
MECHANICAL LINKAGE						>15
Mast Tip Fitting	Aluminum	Excellent	Excellent	Excellent		
Adhesive	TBD					
Locking Levers	Aluminum/Steel	Excellent	Excellent	Excellent		
Guide System	"	"	"	"		
Lenticular Assy	Aluminum	"	"	"		
Turnbuckle	St. Steel	"	"	"		

MULTI-KW S/A MATERIALS LIST

ITEM DESCRIPTION	MATERIAL OF CONSTRUCTION	ENVIRONMENTAL STABILITY UNDER:			COMMENTS	USEFUL LIFE-YRS
		THERMAL CYCLING	U-V RADIATION	PARTICLE RADIATION		
COVER ASSEMBLY						
Padding	Kapton-Covered	Good (Expected)	Good (Expected)	Good (Expected)	Only critical through deployment	
Cover	Glass Cloth Composite over Ar. Honeycomb	"	"	"	"	
Turnbuckle Pin	St. Steel	Excellent	Excellent	Excellent		>15
BLANKET ASSEMBLY						
Leader Assy	Kapton/Aluminum	Good (Expected)	Good (Expected)	Good (Expected)		
Adhesive (2 Faced Tape)	Silicone	"	"	"		
PANEL ASSEMBLY						
Laminate Substrate	Copper (Interconnect)	Excellent	Excellent	Excellent	Eventual Delamination of copper from Kapton not critical	>15
	Kapton	Good	Good	Good		
Hinge	Kapton	"	"	"		
Interconnect	Moly.Ag Plated	Excellent	Excellent	Excellent	For use with GaAs solar cell	
Solar Cells	Silicon	Good (Use & Test)	Good (Test)	26% Deg. in 15 Yrs.	Initial Oversizing required	>15
	GaAs	Good (Expected)	Good (Expected)	25% Deg. in 15 Yrs.	"	

3-6

MULTI-KW S/A MATERIALS LIST

(Page 4 of 4)

ITEM DESCRIPTION	MATERIAL OF CONSTRUCTION	ENVIRONMENTAL STABILITY UNDER:			COMMENTS	USEFUL LIFE-YRS
		THERMAL CYCLING	U-V RADIATION	PARTICLE RADIATION		
Coverslide W/	0211 Microsheet SiO2	Good (Expected)	Good	Good (Expected)		
AR Coating	MgF2	Excellent	Excellent	Excellent	Micrometeorite Erosion Only	
Cover Adhesive	FEP Teflon	Good (Test)	Good (Test)	Good (Expected)		>15
Cell Assy. Adhesive	600 Series	Good	Good	Good	Bonding Adhesive for GaAs solar cell	
HINGE PIN	Fiberglass/Epoxy					
HARNESS					Even eventual delamination of insulator from conductor is not critical	
Flat Conductor	Copper	Excellent	Excellent	Excellent		
Insulator	Kapton	Good	Good	Good (Exp'd)		
Stranded Conductor	Copper	Excellent	Excellent	Excellent		
Insulator	Kapton	Good	Good	Good (Exp'd)		
Connectors	Space Qual.	"	"	Good		
Adhesive (On 2 Faced Tape)	Silicone	Good (Expected)	Good (Expected)	Good (Expected)		
INNER TENSIONING	Aluminum	Excellent	Excellent	Excellent		>15
Distribution Box	Sping Stl. Wire	"	"	"		
	Kapton	Good (Expected)	Good (Expected)	Good (Expected)		
GUIDE WIRE RETAINERS	Polycarbonate	"	"	"		>15
CONTAINER						
Planar	Graphite/Epoxy	"	"	"		>15
Low CR	"	"	"	"		>15
STRUCT ASSY	Aluminum	Excellent	Excellent	Excellent		>15
Fasteners	St. Steel	"	"	"		

3.1.3 Shuttle Deployment and Maintenance Techniques

The techniques available for buildup and maintenance of multi-kW solar arrays from the Orbiter can be divided into manned and unmanned or remotely controlled systems. These systems can be used in combination, singularly or backup mode.

Manned operations can be accomplished using the Extravehicular Mobility Unit (EMU). While in the EMU, the astronaut can work for up to 6 hours in the proximity of the Orbiter. No life support umbilicals are required, but tethers, handholds and work stations can be provided for stability. Mass translation capability is limited, but the Remote Manipulator System (RMS) can be used for this purpose at the Orbiter.

Translation of manned activities away from the Orbiter can be accomplished by use of the Manned Maneuvering Unit (MMU) which has the following characteristics:

    (1)   Attaches to EMU as backpack

    (2)   6-degree-of-freedom control

    (3)   automatic attitude - hold capability

    (4)   2 amperes at 28V for tools, lights, etc.

    (5)   220 lbs cargo carried by astronauts

    (6) N_2 propellant exhaust gas will not contaminate solar array

    (7)   Weight - 243 #

The MMU can be carried at little sacrifice in Orbiter weight and volume; therefore, whether or not it is used for planned work functions, it is an economical backup system. Furthermore, two 6.5 hour, 2-man EVA periods are provided within the normal Shuttle charges.

Remotely controlled systems fall into two categories; those attached to the Orbiter and those which are operated in a free-flying mode. The former is exemplified by the RMS which is existing and the latter by the Teleoperator or the RCT. The Teleoperator development was discontinued. The RCT is purely conceptual and has been sized for the largest solar array package conceived in this study; it can therefore be smaller than the Teleoperator. While at this time the RCT would only require rendezvous and docking capability, it could later have a remote manipulator added.

Figure 3-1 illustrates how buildup and maintenance could be achieved using two RMS's or RCT in LEO applications. In the first case one RMS would secure the Orbiter to the existing system while the second RMS would remove the new solar array module from the Orbiter bay and dock it to the existing array docking port. Array deployment would be activated after Orbiter separation.

An alternate to the RMS method is the use of an RCT to transport the new solar array package to the existing system or platform and accomplish rendezvous and docking. The RCT/solar array package could employ either a rotation and ejection mechanism or an RMS to exit the Orbiter bay. Following rendezvous and docking, the RCT could be either recovered by the Orbiter with an RMS or deboosted. Array deployment would be activated either from the Orbiter or the existing system.

A comparison of the above manned and remote controlled equipment is listed in Table 3-2. The payload capability of an EMU or EMU/MMU is small with respect to replacement for buildup module size; therefore remote controlled equipment is a necessity whether or not manned EVA is planned. The RCT payload capability of 14,000 lbs. was selected to exceed the largest S/A module weight now contemplated. The major advantage the MMU provides is range; and even if not a planned requirement it greatly increases manned EVA backup capability at a modest cost ($1M) and slight volume impact. A trade between the RMS and the RCT shows the major difference to be range, because the RMS can only extend 50 feet. Volume and cost for the RCT are significant, but not prohibitive especially if the RCT is recovered and reused.

The Remote Manipulator System capability is briefly summarized below:

(1)   Only one of the two RMS's can be operated at a time. One RMS can hold item in position while 2nd RMS performs active function.

(2)   The RMS has a reach of 50 ft with:
   - Shoulder – pitch and yaw
   - Elbow – pitch
   - Wrist – pitch, yaw and roll
   - 2 ft end effector extension

RCT METHOD

EJECT OR
RECAPTURE
BY ORBITER
USING STD
RMS

ADD-ON

EXISTING S/A
SYSTEM

RENDEZVOUS
AND DOCK

ROTATION
& EJECTION
FROM ORBITER

SHUTTLE
TO LEO

2 – RMS METHOD

EXISTING S/A
SYSTEM

ADD-ON

SHUTTLE
TO LEO
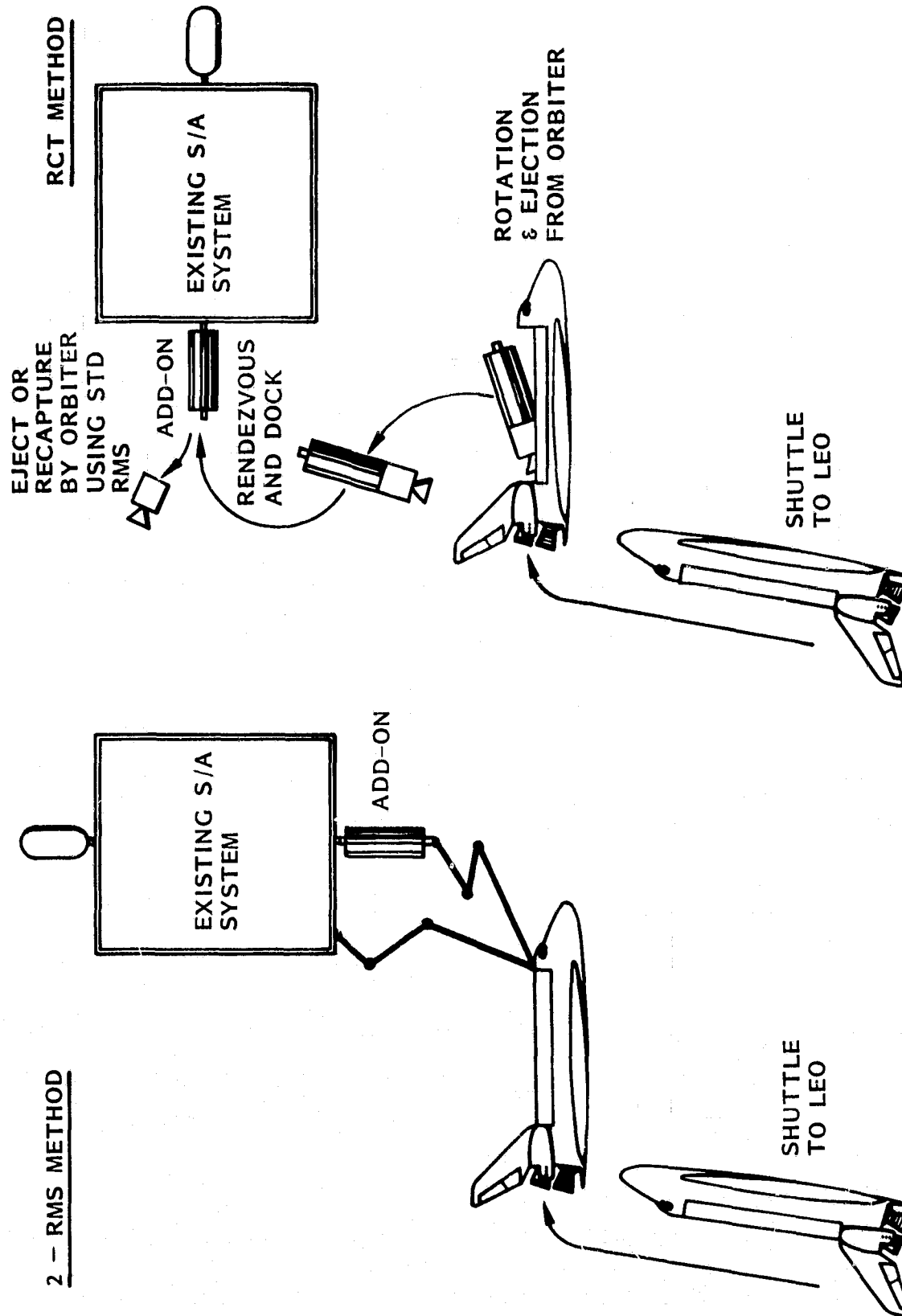
Figure 3-1 Remote Controlled Buildup & Maintenance for LEO

LOCKHEED MISSILES & SPACE COMPANY, INC.

TABLE 3-2

EQUIPMENT CONSIDERED FOR LEO BUILDING & MAINTENANCE

PARAMETER	EQUIPMENT			
	MANNED		REMOTE CONTROLLED	
	EMU	EMU/MMU	RMS	RCT
PAYLOAD CAPABILITY, LB	180	220	65,000	14,000
RANGE (FROM ORBITER), FT	0	3390	50	>>MMU
ΔVELOCITY, FT/SEC	–	66	–	200
WEIGHT, LB	–	243	933	1028
VOLUME IMPACT	–	–	–	3' x 15' DIA
NON-RECURRING COST, $M	0	0	0	38
RECURRING COST, $M	0	1	1	9

RCT – REMOTE CONTROLLED TRANSPORTER

(3)   The placement accuracy with a 65,000 # P/L is:

- Attitude within 1°
- Position within 2"

(4)   Velocity varies from 0.2 ft/sec with 32,000 # to 2 ft/sec with no load.

The RMS is capable of removing payload from the Orbiter bay and translating it up to 50 feet from the bay. Using two RMS's adds the capability of holding one structure while coupling a second structure to the first.

Removal of the solar array package from the Orbiter bay could be accomplished using either the RMS (one or two) or a rotation and ejection mechanism; the latter is suggested from a reliability standpoint, but would cost weight and volume.

The RMS vs RCT trade-offs for LEO buildup and maintenance are summarized in Table 3-5. At this time the two RMS method is favored because of economy and volume.

Manned backup is planned to assure proper deployments, dockings and connections, to correct structural deficiencies and to make general repairs.

A general philosophy is that as solar array performance falls off or components fail, it would be cost effective to add modules to augment power output rather than attempt repair. In large, light-weight S/A systems only a limited number of components might be serviceable. Safety considerations will limit manned exposure to high solar array voltages, concentrated light, elevated-temperature radiator surfaces, or large-area dielectric foils.

3.1.4   LEO Maintainability Approaches, Trade-Offs and Conclusions

Planar S/A System

The Orbiter can deliver a 311 kW (15 year average) planar S/A to LEO which is made up of 4 modules. One module at a time can be added to the basic 4 module system. It is assumed that a solar powered user station (SPUS) has already been placed in orbit and can be controlled for rendezvous with the Orbiter. This plan is depicted in Figure 3-2. The S/A is removed from the bay with the RMS and the "W" structure

TABLE 3-3

RMS VS RCT TRADE-OFFS FOR LEO BUILDUP & MAINTENANCE

	2-RMS METHOD	RCT METHOD
ADVANTAGES	• SLIGHT IMPACT ON ORBITER BAY VOLUME AND WEIGHT	• REMOVES OPERATION FROM CLOSE PROXIMITY TO ORBITER • PROVIDES FLEXIBILITY IN DOCKING TO OR SERVICING SOLAR POWERED USER STATION • REMOTE MANIPULATOR COULD BE ADDED TO RCT
DISADVANTAGES	• MAXIMUM REACH OF 50 FEET REQUIRES CLOSE PROXIMITY OF S/A TO ORBITER	• RCT CONSUMES ORBITER BAY VOLUME AND WEIGHT • REQUIRES DEVELOPMENT • MORE COSTLY

PRESENT CHOICE

LOCKHEED MISSILES & SPACE COMPANY. INC.
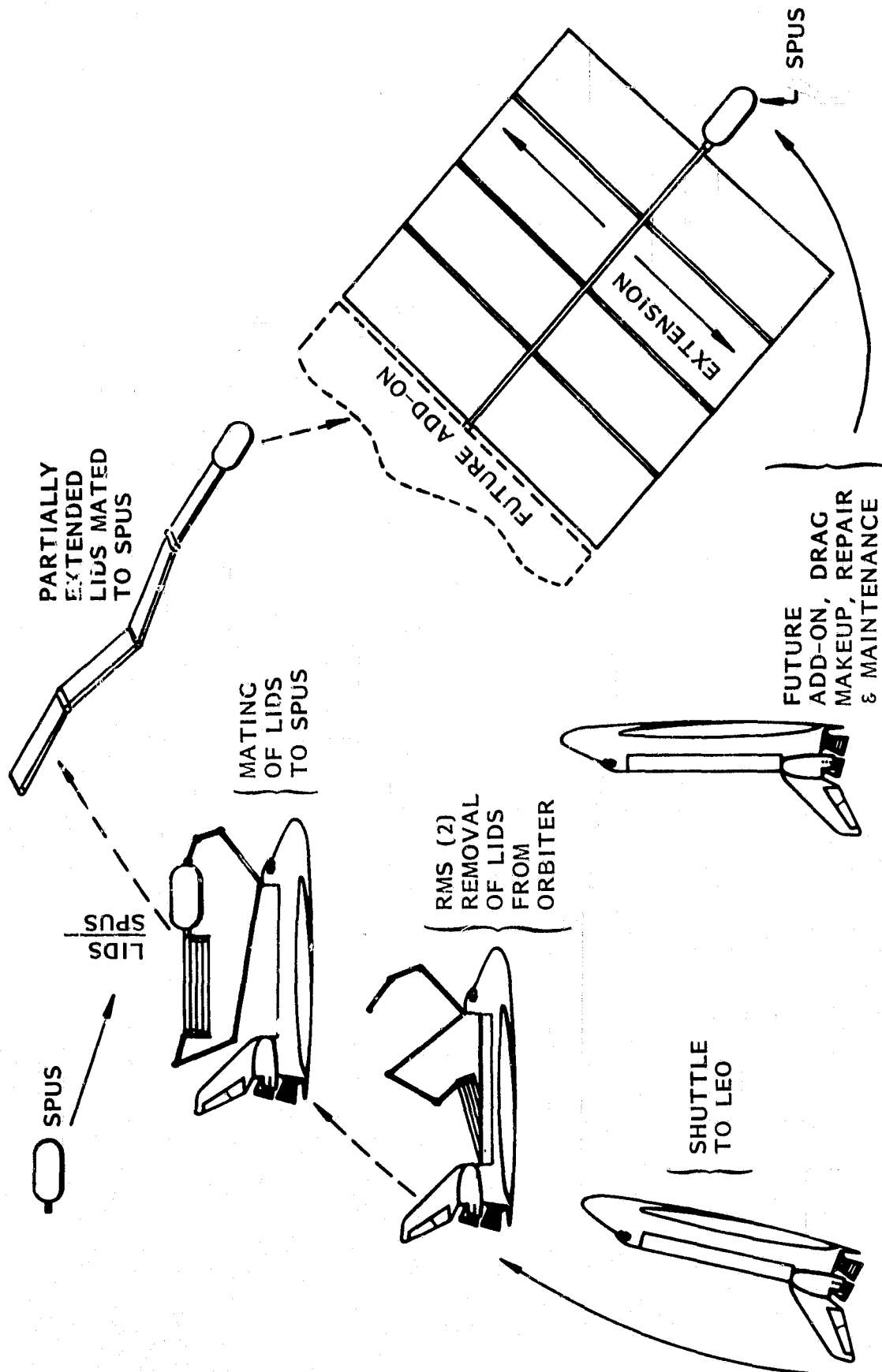
Figure 3-2 Buildup and Maintainability of Planar S/A for LEO

opened at the hinges. It is then docked to the SPUS. Array blankets are then deployed by the masts.

Augmentation flights would carry additional modules which would be docked to the existing S/A central structure with the RMS's. Mast and blanket deployment would follow.

Repair and maintenance flights may follow if required. Drag makeup propellants would be resupplied by docking to or transferring tanks to the SPUS.

Plan for Low CR S/A

Figure 3-3 depicts a plan for building up and maintaining a low CR system. The SPUS is assumed to be in orbit and equipped with a docking port to interface with the S/A core structure. Each Shuttle launch during buildup could carry 10 modules with each module containing 48 TPP's which are folded and attached to 24 packaged mast assemblies, connected to a folded core structure. The Orbiter, when in docking range, would deploy the RMS's and remove the full package from the bay. The core structure would be docked to the SPUS interface and the Orbiter moved away. Next, the core structure would be deployed, then masts would be extended to unfold each concentrator module. As in the planar case drag makeup and maintenance would require dedication of some partial Shuttle cargos.

High CR S/A Buildup and Maintenance Plan

Figure 3-4 indicates the buildup and maintenance approach for the high CR concept. An RMS would remove each S/A module from the Orbiter bay and as indicated in Figure 3-4 hold it while its lenticular struts are unfurled to provide an interface with the SPUS. A second RMS would attach one strut to the SPUS. One RMS would remove a second module from the Orbiter bay and unfurl its struts. Using the other RMS, the 2nd module's struts would be secured to the SPUS and the first module. Subsequent modules would be added in a like manner.

Reflector dishes would not be deployed until the last module is added. Astronauts equipped with MMU's would be available to secure the structural couplings and electrical interconnections. Electrical cabling would be designed into the lenticular strut assemblies.
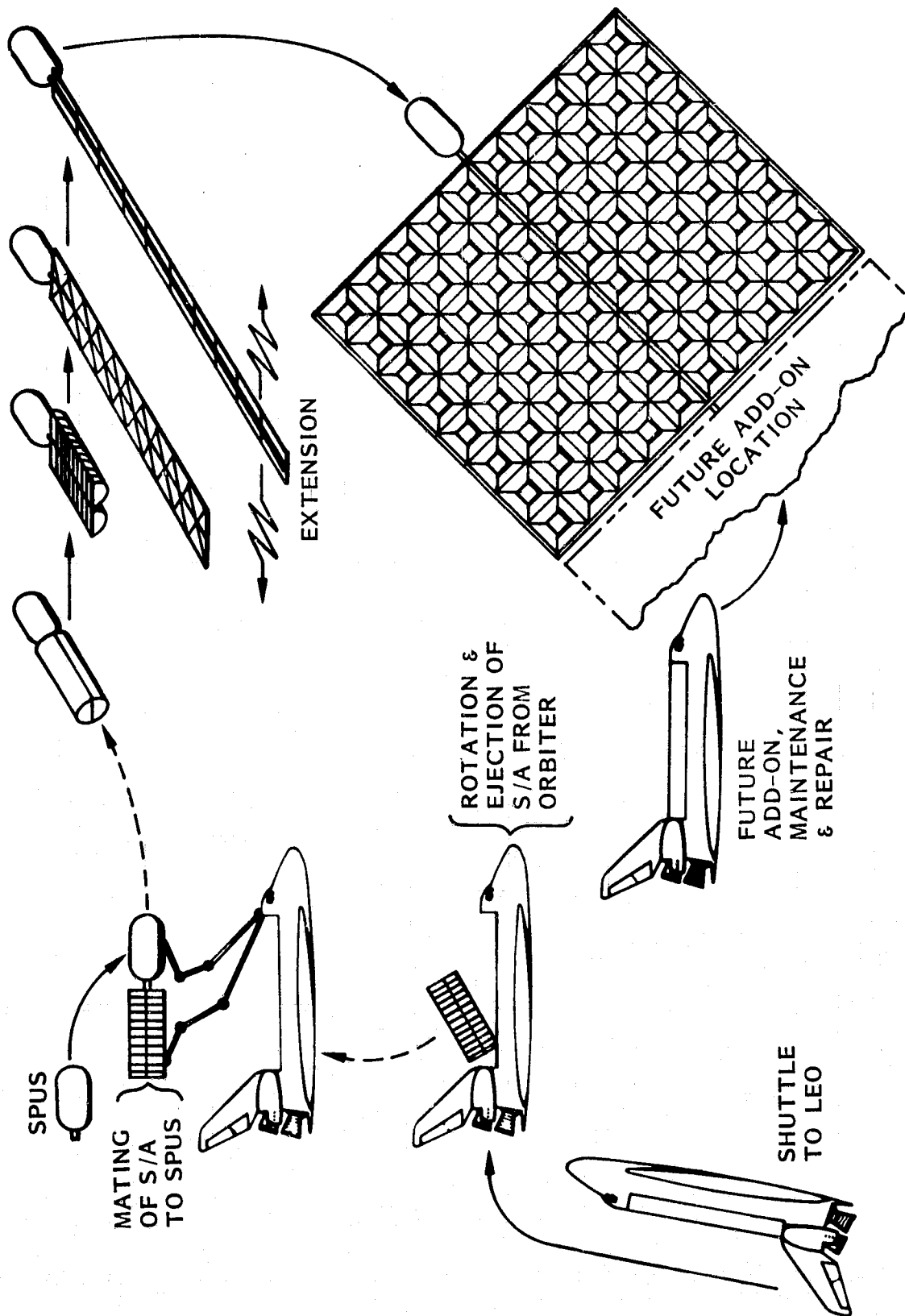
Figure 3-3 Low CR S/A LEO Buildup and Maintenance Plan

LOCKHEED MISSILES & SPACE COMPANY. INC.
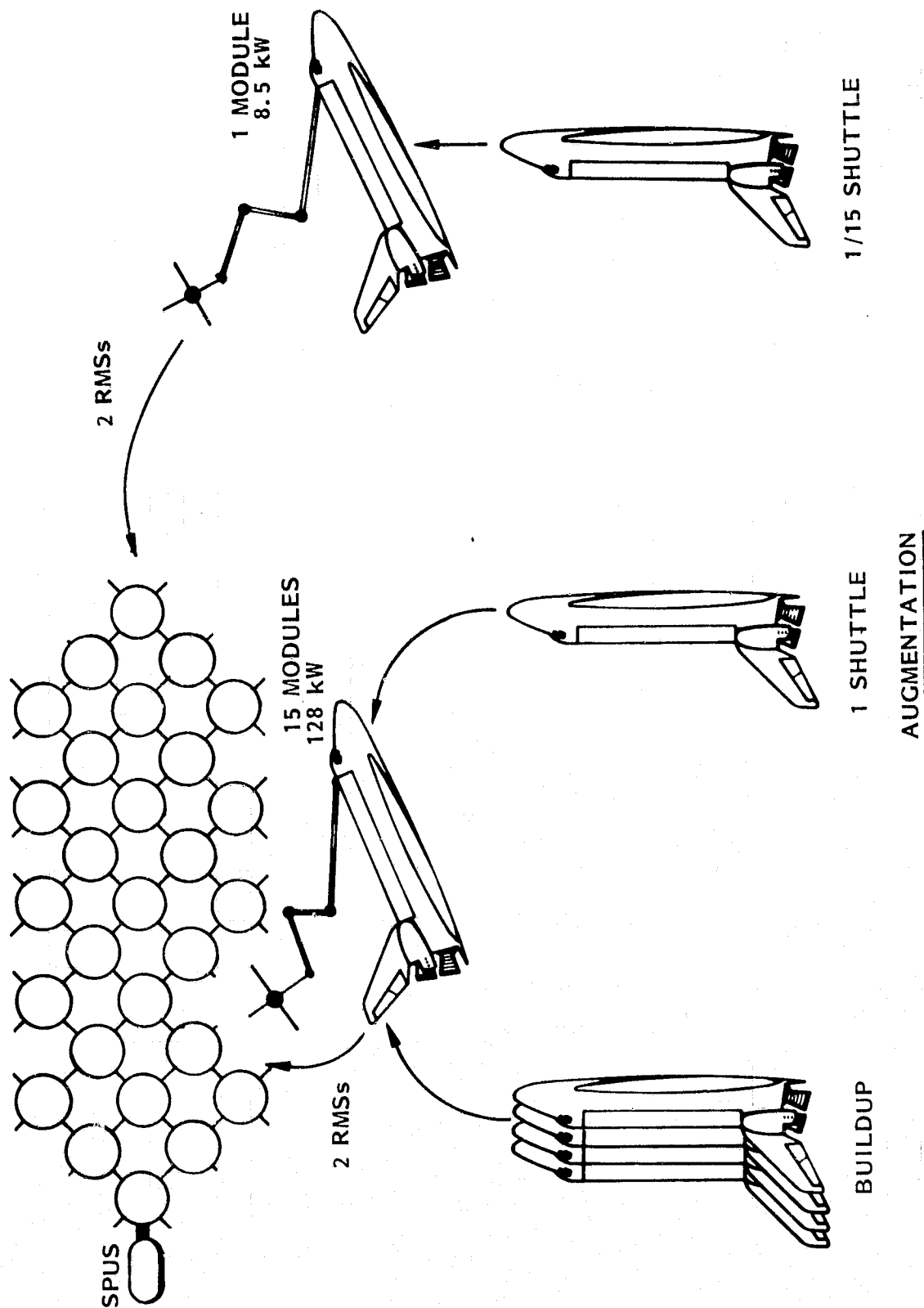
Figure 3-4 High CR S/A LEO Buildup & Maintenance

LOCKHEED MISSILES & SPACE COMPANY. INC.

The astronauts with MMU's would be returned to the Orbiter, the RMS would release the platform and the reflectors would then be deployed remotely. The SPUS would orient the arrays to the sun and switch to solar array power for station keeping.

Power augmentation could be done on a single module basis. Repair and maintenance of this system would be limited to structural and electrical problems which can be handled from the backside of the S/A.

Conclusions for LEO Maintainability

A second RMS should be provided to accomplish removal of the packaged S/A from the Orbiter, the mating of the packaged S/A to the SPUS and to accomplish drag makeup resupply to the SPUS/SA system.

Manned backup using the MMU should be provided, but would be limited to mechanical servicing where loads are small, troubleshooting and the modification of electrical cabling only where high voltage, static charge or concentrated light hazards are precluded.

3.1.5   GEO Maintainability Approaches, Tradeoffs and Conclusions

The requirements imposed by applying a multi-kW S/A in geosynchronous orbit are as follows:

(1)   The system will be transported to 150 NM minimum by the Space Shuttle.

(2)   Transport to GEO will be accomplished using the Interim Upper Stage (IUS) vehicle or an alternate.

(3)   The multi-kW S/A package must be delivered to GEO and must rendezvous with the SPUS.

(4)   The S/A must be fully deployable.

(5)   All buildup and maintenance functions must be remotely controlled.

The guidelines for maintenance at GEO are:

(1)   A failed or low performance module will not be replaced--a new module will be added to maintain capability.

(2)   Recovery from orbit is impractical and no retraction capability will be provided.

(3)   Long-life materials are dictated.

The use of the IUS for transport from LEO to GEO will require a supplemental spacecraft in order to achieve rendezvous and docking since the IUS has an injection accuracy of ± 92 nm. Figure 3-5 shows outline dimensions and descriptive data for the IUS; also shown is a hypothetical remote control transporter (RCT) stage which could affect rendezvous and docking. The derived velocity requirement for the RCT is 200 ft/sec. The estimated weight of the RCT is shown in Table 3-4.

TABLE 3-4

ESTIMATED RCT WEIGHT BREAKDOWN

Guidance, Navigation and Control	163
Communications	80
Thermal Control	25
Structure	50
Electrical Power	25
Docking Guidance	55
Propulsion Dry	83
Propellants	157
Total Weight	638 lbs.

The IUS P/C capability was assumed to be 5000 lbs placed in synchronous orbit. This, with the estimated weight of the RCT, resulted in an allowable weight for the solar array system of 4362 lbs. The IUS error corrections used for this study were: a radial error of 50 nm, an inclination error of 40 nm, and an intrack error of 66 ft/sec. The total RCT velocity requirement of 200 ft/sec was broken down as follows:

91.0 IN. DIA

16.4 FT

18.5 FT

3 FT

RCT
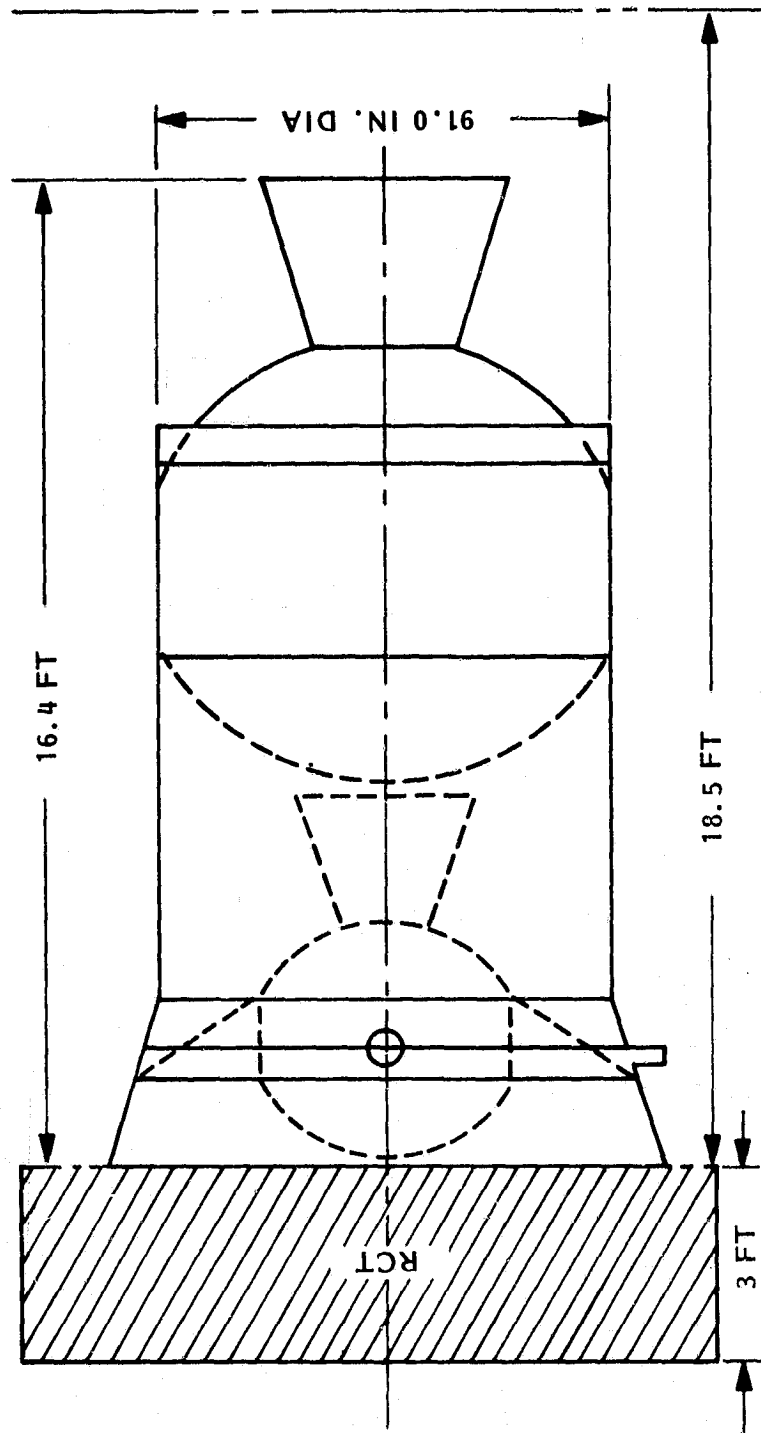
CHARACTERISTICS

- S/C SEPARATION CONSTRAINTS
  - 14 MIN AFTER 2ND STAGE BURN OUT IF ROTISSERIE DURING TRANSFER
  - 10 MIN IF DON'T ROTISSERIE
- INJECTION ACCURACY ±92 nm (RSS)
- PAYLOAD ~4362 LBM

FEATURES

- TWO STAGE CONCEPT
  - ONE LARGE SRM FIRST BURN
  - ONE SMALL SRM SECOND BURN
- TWELVE 26 LBF HYDRAZINE A/C THRUSTERS

	Mp (LBM)	AVG F∞ (LBF)
− FIRST STAGE	21,400	45,000
− SECOND STAGE	6,000	18,000

- ASE MASS = 9100 LBM

Figure 3-5 IUS − Two Stage Vehicle

IUS radial error correction of 11 ft/sec, IUS inclination error correction 35 ft/sec, IUS intrack error 66 ft/sec, docking allowance 33 ft/sec, separation 25 ft/sec, and attitude control equivalent to 30 ft/sec.

Figure 3-6 illustrates how a new S/A assembly-RCT-IUS system might be transported to LEO by the Shuttle Orbiter, rotated and ejected from the Orbiter bay, and then propelled to GEO by the IUS. At GEO the spent IUS is separated and the RCT propulsion system is used to transport and guide the S/A to the SPUS/existing array for rendezvous and docking. The RCT is then separated and the array deployed.

An objection to the above plan is that an RCT is spent on each resupply visit to the SPUS. Therefore a plan which applies a reusable rendezvous stage was examined and is illustrated by Figure 3-7. It is called a GEO Retrieval System (GRS). The initial GRS with a propellant storage and dock rack would be launched with the first S/A assembly and attached to the SPUS when not in operation. Because GRS chemical propellant would be depleted after each mission, a resupply propellant rack would be brought up with each new S/A. Applying this concept, Figure 3-8 shows the IUS transporting a GRS propellant resupply rack/SA package to GEO, the IUS separation and retrieval of the package by the GRS. Next, the GRS would transport the new S/A and rack to the SPUS/existing S/A system. After docking the new S/A to the existing, the GRS and propellant resupply rack would reattach to the SPUS. The last stage would be deployment of the S/A.

The estimated velocity requirements for the GRS are 146 ft/sec from the existing array to the new array and 146 ft/sec back to the old array. For the first 146 ft/sec the GRS only has to accelerate itself. The estimated weight of the propellant supply module is 250 lbs. The estimated weight of the GRS is 627 lbs including propellant. The performance of the IUS with the GRS is 4372 lbs in synchronous orbit, and 4750 lbs for the case where the IUS only brings up the propellant supply module.

Another alternative for accomplishing S/A retrieval, rendezvous and docking in GEO would use an ion engine, or solar electric propulsion (SEP) system. This system illustrated in Figure 3-8 would use the IUS to propel the S/A package to GEO; an attitude control system, with a probable battery power source, would stabilize the package while the SEP system would propel the SPUS/existing S/A system to
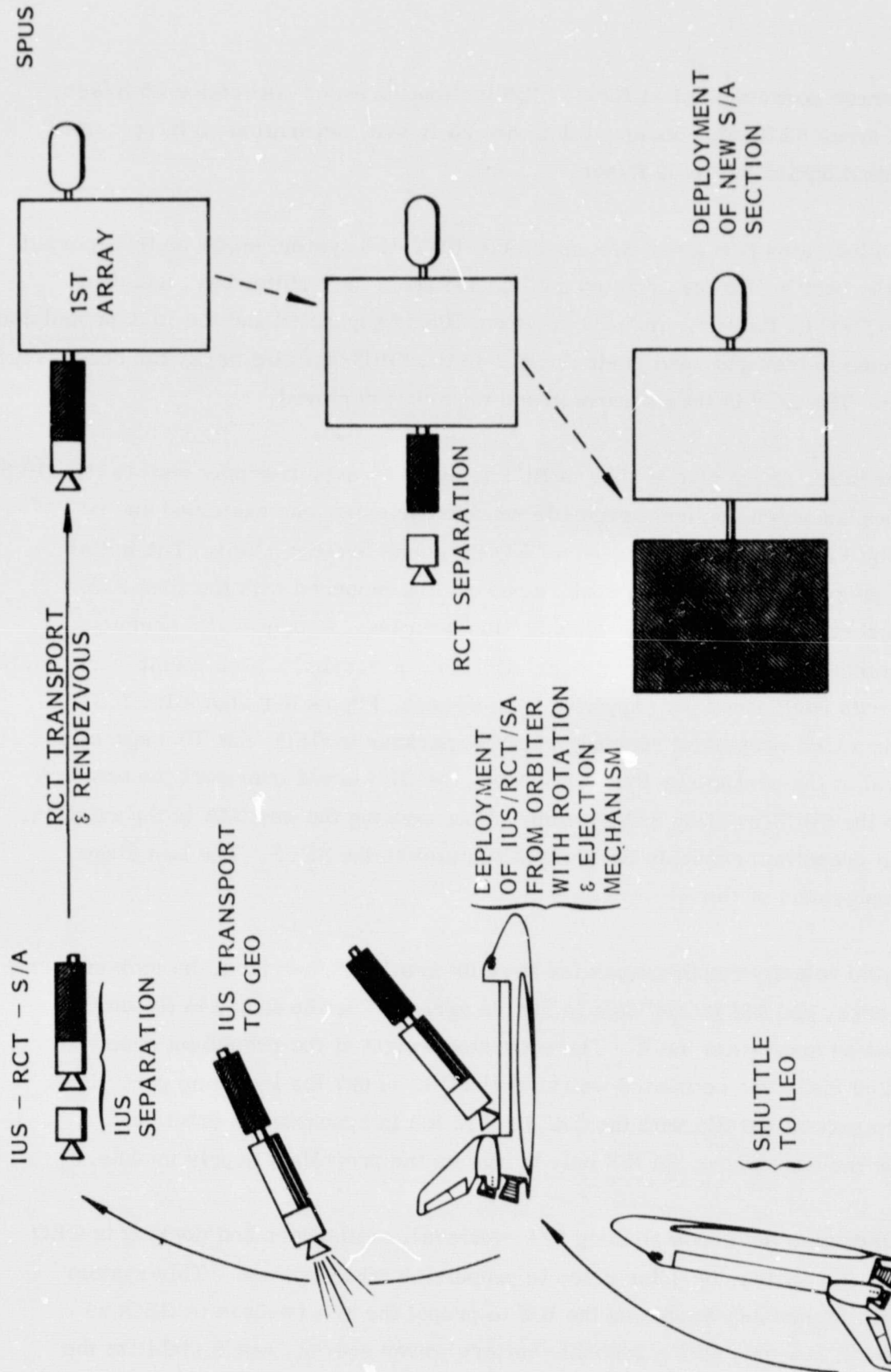
Figure 3-6 Buildup and Maintainability for GEO Applications - RCT Alternative

LOCKHEED MISSILES & SPACE COMPANY. INC.
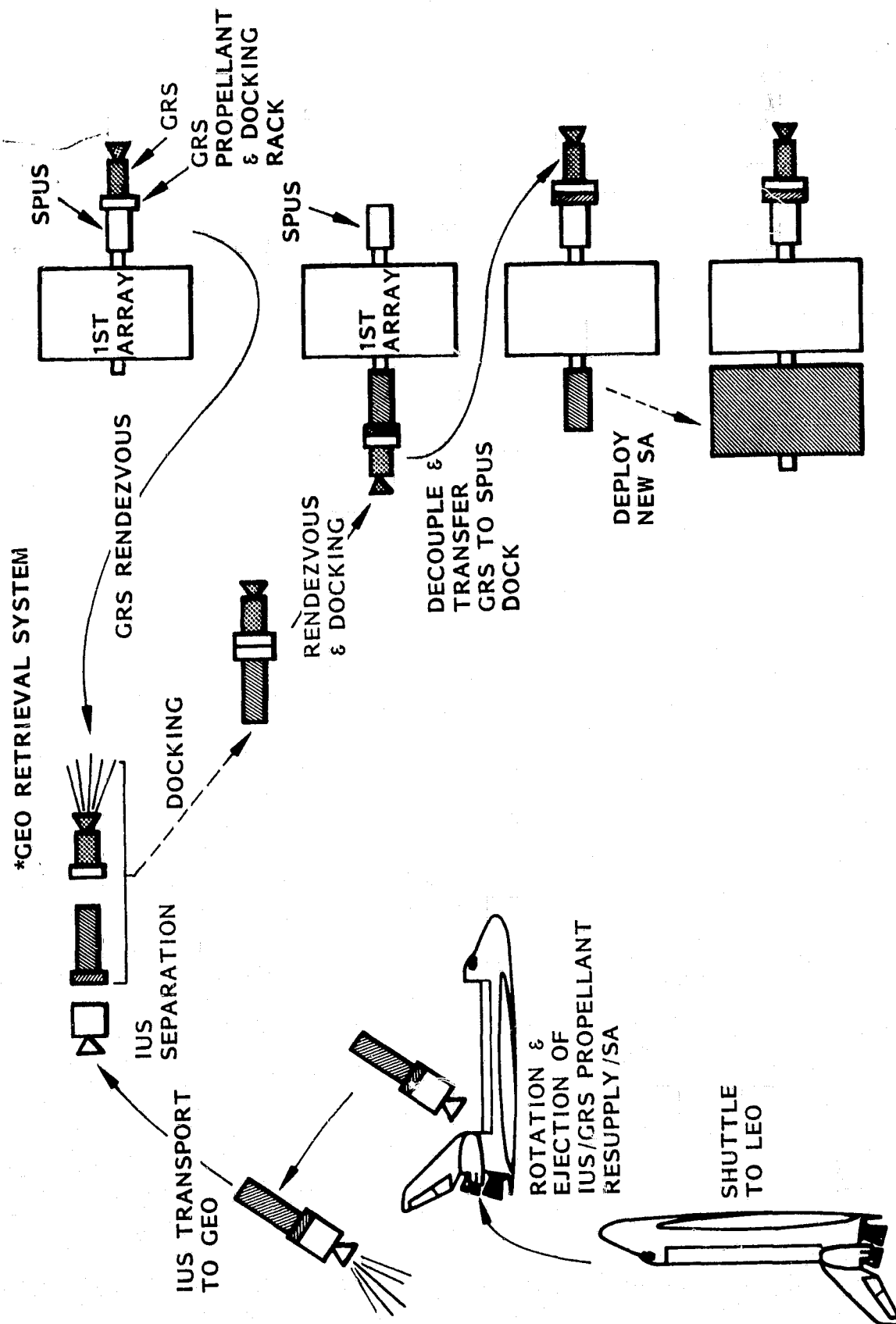
Figure 3-7 Buildup and Maintainability for GEO Applications–
GRS* Alternative
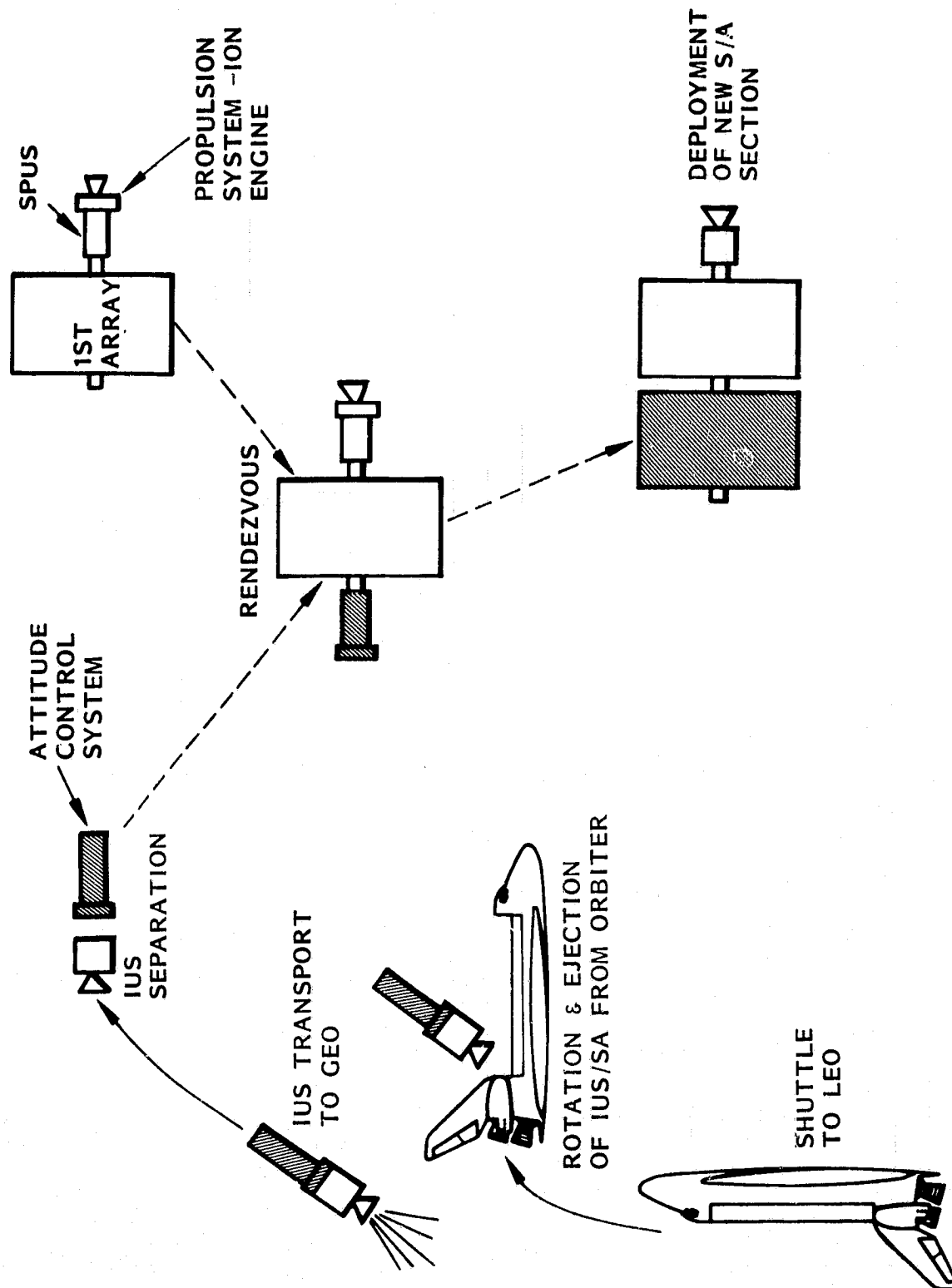
Figure 3-8 Buildup and Maintainability for GEO Applications – SEP Alternative

LOCKHEED MISSILES & SPACE COMPANY, INC.

rendezvous and docking. Two thrusters aft and two thrusters forward could propel, orient and brake the system. The new S/A would be deployed after docking. The estimated weight of the SEP module is 711 lbs. The IUS that brings up the SEP module can only provide a solar array weighing 4289 lbs.

The GEO buildup and maintainability plan based on IUS LEO to GEO transport, are compared in Table 3-5. From a functional standpoint the SEP system is very attractive, because one long-life SEP system could satisfy attitude control and propulsion needs for rendezvous. SEP is projected to be very expensive, however. Use of an RCT or GRS appears to be a close trade and very mission dependent. A reusable system may not be advantageous if it is only used once or twice. The above alternatives are based on IUS transport to GEO; however, there are other options which will change if a different LEO to GEO transport stage is used.

A study was made to determine the GEO weight capabilities for the above solar array launch and deployment methods using the IUS and other vehicle concepts. These other vehicles include solar electric, and chemical stages using both solid and liquid propellant.

Volume and weight requirements for candidate systems were developed. Figure 3-9 shows the maximum spacecraft length of 480 inches that can be accommodated in the Orbiter bay with an IUS .

An alternative to the IUS, which dispenses with a separate low thrust RCT, GRS or SEP stage, would be a low thrust chemical or a solar electric transfer vehicle, respectively called LTTV and SETV. These concepts utilize vehicles which do not exist at this time. These concepts and their performance were taken from reference (1). The performance was adjusted down for the necessary propellant required to accomplish the required docking, in-orbit maneuvers, and additional systems required, in particular the docking adapter and docking guidance.

The first method studied was a single stage pressure fed system and modified for docking, etc. This stage is illustrated in Figure 3-10. This stage has the capability to place an array weighing 7363 lbs in final orbit and docking with an existing array. In effect this stage can do the same tasks as the IUS and the RCT combined, with greater capability.

TABLE 3-5

GEO BUILDUP AND MAINTAINABILITY TRADES

ALTERNATIVE	ADVANTAGES	DISADVANTAGES
RCT – REMOTE CONTROLLED TRANSPORTER	• CAN DELIVER P/L AND S/A TO PASSIVE SPUS	• USES ORBITER VOLUME AND WEIGHT EACH LAUNCH • DISCARDED AFTER ONE USE
SPUS/SEP – SOLAR POWERED USER STATION/ SOLAR ELECTRIC PROPULSION	• ONLY IUS IS REQUIRED TO SUPPORT BUILDUP AND MAINTENANCE AFTER FIRST FLIGHT • NO RESUPPLY • STATION CAN BE MAINTAINED OR TRANSLATED	• FULL SPUS WITH DEPLOYED S/A IS PROPELLED BY SEP • S/A PACKAGE BEING DELIVERED REQUIRES ATTITUDE CONTROL SYSTEM • SEP SYSTEMS ARE COSTLY
GRS – GEOSYNCHROUS RETRIEVAL SYSTEM	• USES COLD OR HOT GAS PROPELLANT SYSTEM • GRS WITH PROPELLANT RESERVE IS KEPT WITH SPUS • SPUS WITH DEPLOYED S/A IS NOT DISTURBED DURING S/A ADD-ON • GRS IS A REUSABLE RCT AND REQUIRES LESS ORBITER VOLUME	• PROPELLANT RESUPPLY RACK MUST BE CARRIED UP WITH IUS AND S/A • GRS MUST BE INITIALLY LAUNCHED WITH SPUS
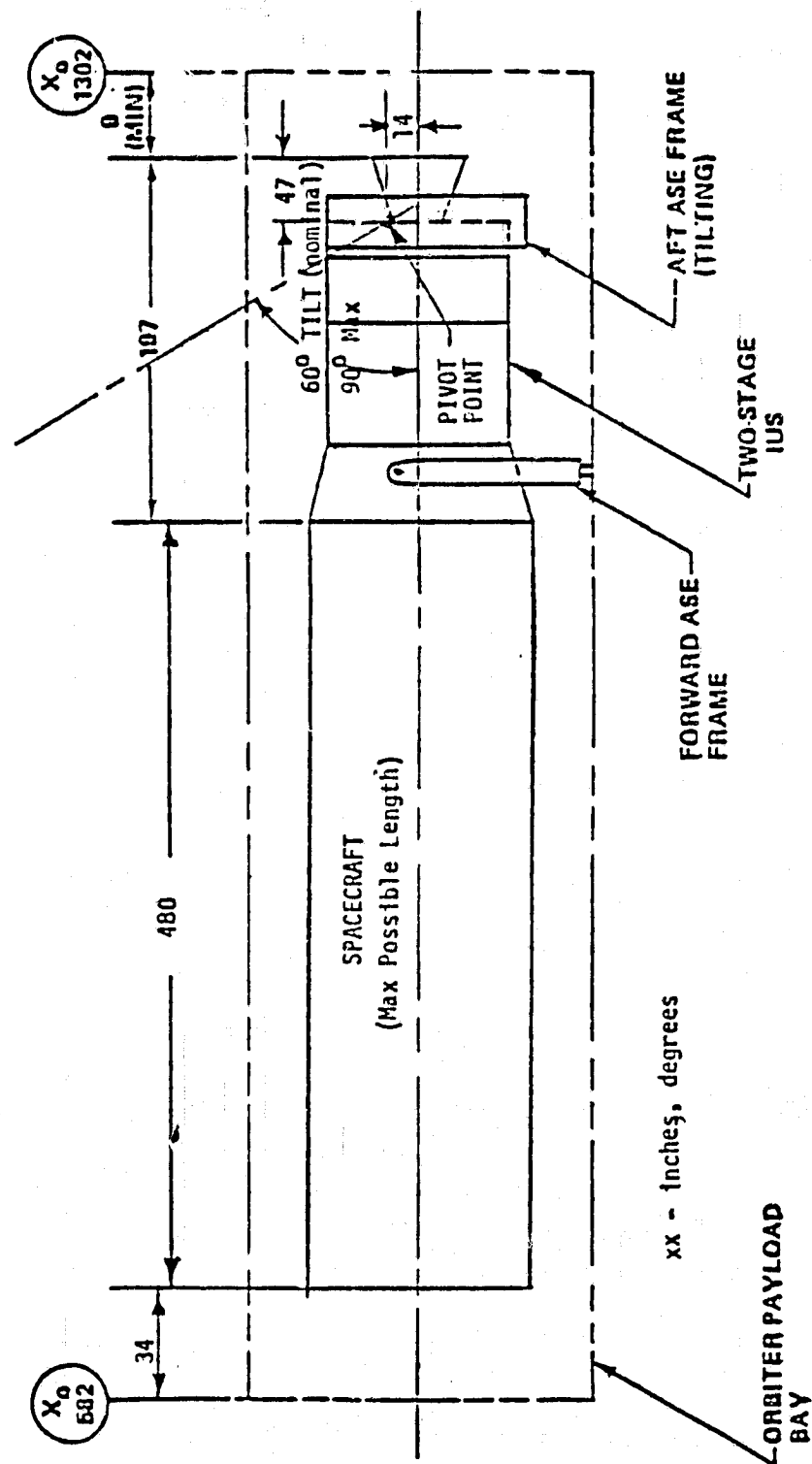
Figure 3-9 IUS/Spacecraft Installation

CHARACTERISTICS

- PAYLOAD–7363 LBM
- $Mp = 44,220$ LBM
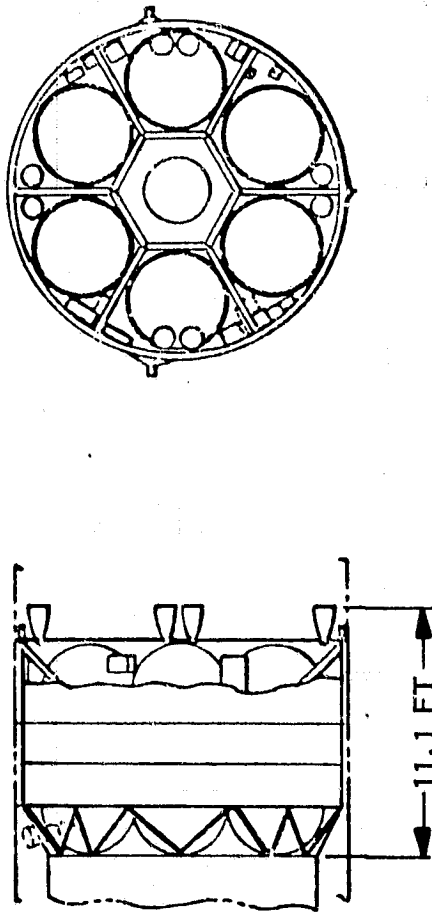
FEATURES

- SINGLE STAGE–NTO/MMH PROPELLANTS
- EIGHT 100 LBF MARQUARDT ORBIT ADJUST THRUSTERS
  - $I_{SP} = 303$ SEC
- TWELVE 5 LBF MARQUARDT A/C THRUSTERS
  - INTEGRATED FEED
- SIX TITANIUM PROPELLANT TANKS
- COMPOSITE PRESSURANT TANKS
- HELIUM PRESSURANT
- ASE MASS = 1500 LBM

11.1 FT

Figure 3-10 Low Thrust Pressure Fed Transfer Vehicle
(Single Stage)

LOCKHEED MISSILES & SPACE COMPANY, INC.

The two stage pressure fed low thrust transfer vehicle is illustrated in Figure 3-11. This system is a two-stage version of the system described above and can perform the same functions as the IUS and RCT combined. The capability of this system is 8382 lbs docked to an existing array in synchronous orbit. This system is also taken from reference (1) and modified for docking and maneuvers.

The single stage pump fed low thrust transfer vehicle is illustrated in Figure 3-12. This system is taken from reference (1) and modified for docking. This system can also perform the same functions as the IUS and the RCT and has the capability to place 8632 lbs, docked array weight, in synchronous orbit.

The solar electric transfer vehicle is illustrated in Figure 3-13. This system uses solar electric power to transfer to synchronous orbit. The performance of this vehicle is determined by the time allowed for the transfer. For a 250 day time the array weight placed in final orbit is 8000 lbs; and the maximum weight is 9519 lbs in a volume limited configuration which requires 280 days. The performance data for this stage taken from reference (1) and modified for the case where the payload solar array is utilized for ascent stage power during the ascent and docking maneuvers.

The chemical low thrust systems take 12 days for LEO to GEO transit and the SEP systems from 250 to 280 days as opposed to 6 hours for the high thrust chemical systems. Two high thrust transfer vehicle (HTTV) system concepts are included as alternatives to IUS and each would require an RCT (or GRS or SEP) stage, one uses solid and the other uses liquid propellant.

The HTTV, solid propellant vehicle uses the IUS motors in a combination that increases the on-orbit payload capability. This vehicle is illustrated in Figure 3-14. The capability of this vehicle is 6765 lbs of array docked in orbit.

The HTTV, liquid propellant vehicle uses the Agena engine. This vehicle is illustrated in Figure 3-15. The capability of this vehicle is 7907 lbs of array docked in orbit. This HTTV configuration is volume limited for the Planar/Silicon array concept.

(1) LMSC-D668638 Transfer Orbit Optimization Study

CHARACTERISTICS

- Mp = 21,289 LBM EACH STAGE
- PAYLOAD–8382 LBM

13.9 FT
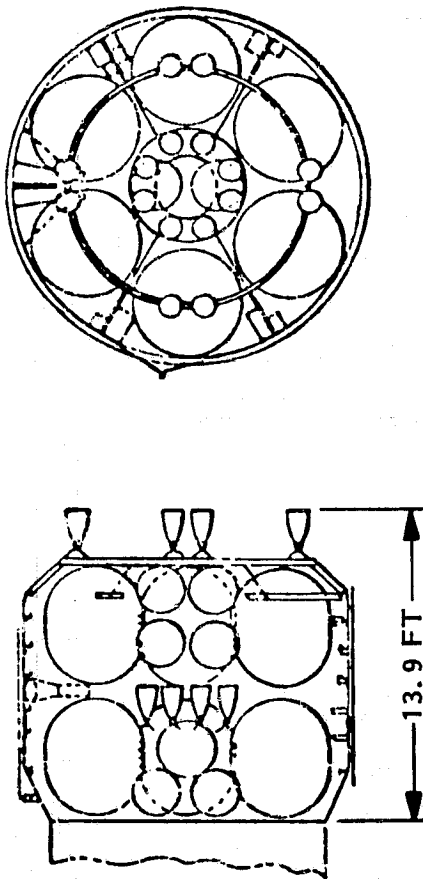
FEATURES

- TWO STAGES–NTO/MMH PROPELLANTS
- FIRST STAGE–8–100 LBF MARQUARDT ORBIT ADJUST THRUSTER
  - I_{SP} = 303 SEC
- SECOND STAGE
  4–100 LBF MARQUARDT ORBIT ADJUST THRUSTERS
  12–5 LBF MARQUARDT ATTITUDE CONTROL THRUSTERS
- TITANIUM PROPELLANT TANKS
  SIX FIRST STAGE
  SIX FIRST STAGE
- COMPOSITE HELIUM TANKS
- HELIUM PRESSURANT
- ASE MASS = 1500 LBM

Figure 3-11 Low Thrust Pressure Fed Transfer Vehicle (Two Stage)

CHARACTERISTICS

- M_p = 44,200 LBM
- PAYLOAD-8632 LBM
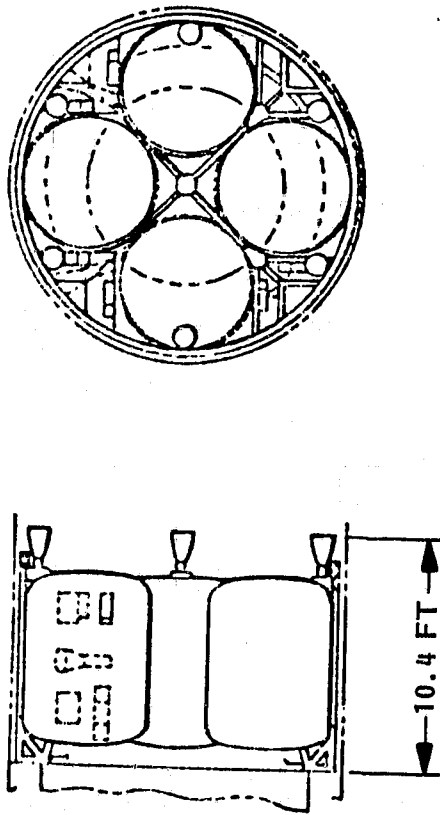
FEATURES

- SINGLE STAGE-NTO/MMH PROPELLANTS
- SIX 100 LBF MARQUARDT ORBIT ADJUST THRUSTERS
- TWELVE 5 LBF MARQUARDT ATTITUDE CONTROL THRUSTERS
- SIX EMPAs FOR PROPELLANT FEED
- TWO BELLOWS ACCUMULATORS FOR ATTITUDE CONTROL FEED DURING COAST
- USE OF PUMPS ALLOWS USE OF 6:1 BLOWDOWN PRESSURIZATION
- FOUR ALUMINUM TANKS – ELLIPTICAL DOMES
- 50 PSIA INITIAL TANK PRESSURE
- ASE MASS = 1500 LBM

10.4 FT

Figure 3-12 Low Thrust Pump Fed Transfer Vehicle

CHARACTERISTICS:

- NO BALLAST REQUIRED

- M_p = 3860 LBM

- PAYLOAD – 8000/9519 LBM
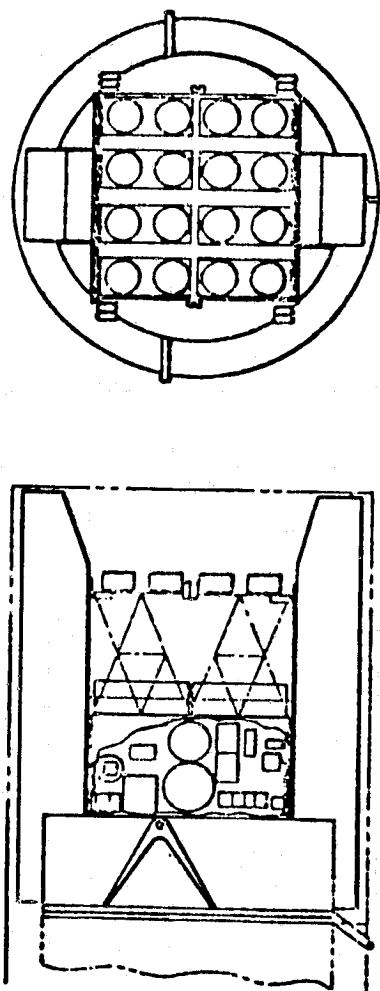
FEATURES:

- SIXTEEN HUGHES 30 CM ION ORBIT ADJUST
  THRUSTERS

  - I_{SP} = 3000 SEC

  - F_∞ = .030 mLBF

  - ALL THRUSTERS GIMBALLED FOR 3 AXIS
    CONTROL DURING THRUSTING

- TWELVE 1 LBF HYDRAZINE ATTITUDE CONTROL
  THRUSTERS

- TWO SS MERCURY STORAGE TANKS

- TWO TITANIUM HYDRAZINE STORAGE TANKS

- ASE MASS = 1500 LBM

Figure 3-13 Solar Electric Propulsion Transfer Vehicle

CHARACTERISTICS:

● PAYLOAD – 6,765 LBM
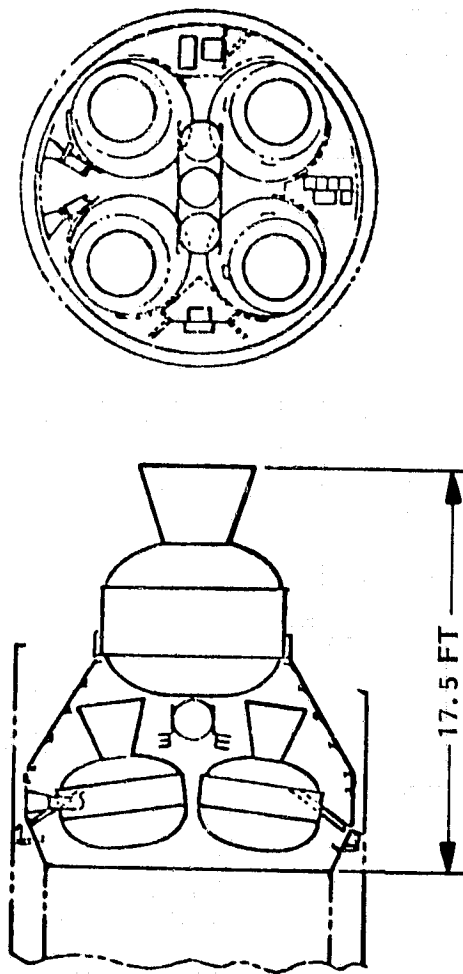
FEATURES:

● THREE-STAGE CONCEPT:

   – ONE LARGE IUS SRM FIRST BURN
   – TWO SMALL IUS SRMs SECOND BURN
   – THREE SMALL IUS SRMs THIRD BURN

● TWELVE 26 LBF HYDRAZINE ACS THRUSTERS

●

	M_p (LBM)	AVG F_∞ (LBF)
– FIRST STAGE	20,400	45,000
– SECOND STAGE	12,000	36,000
– THIRD STAGE	11,017	36,000

● ASE MASS = 1500 LBM

Figure 3-14 Three Stage SRM Transfer Vehicle

17.5 FT

LOCKHEED MISSILES & SPACE COMPANY, INC.

CHARACTERISTICS:

- Mp = 43,425 LBM
- PAYLOAD – 7907 LBM
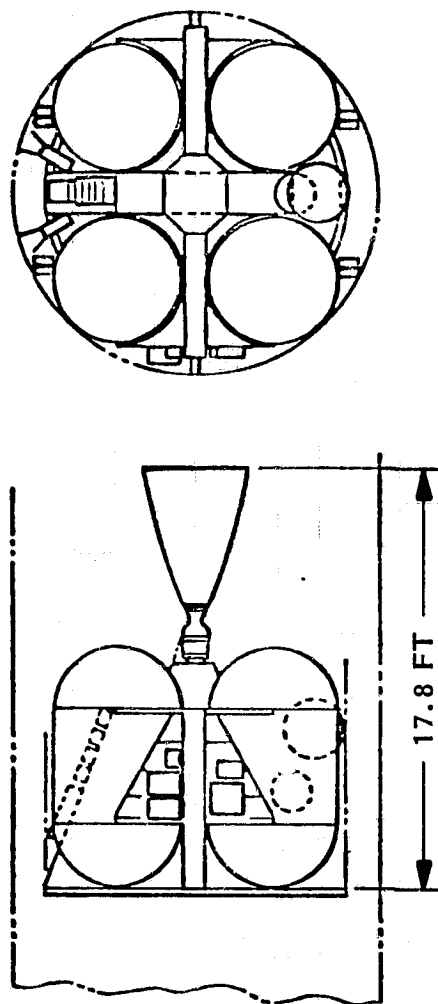
FEATURES:

- SINGLE STAGE – HDA/MMH PROPELLANTS
- BELL 8096 ENGINE – MODIFIED FOR MMH
  - I_{SP} = 321 SEC
  - THRUST = 16000 LBF
- GIMBALLED ENGINE FOR REDUCED RCS REQUIREMENTS
- TWELVE 26 LBF HYDRAZINE A/C THRUSTERS
- FOUR 60-IN. DIAMETER x 112 IN. LONG ALUMINUM PROPELLANT TANKS
- ASE MASS = 1500 LBM

17.8 FT

Figure 3-15 High Thrust Pump Fed Transfer Vehicle

Analyses were made of all concepts to assure that the longitudinal center of mass met the STS requirements. The results of these analyses are shown in Table 3-6.

A comparison of concepts is shown in Table 3-7. This table includes the allowable solar array weights, the gross weights including payload, the cargo bay weights, the number of ascent burns, the time for transfer from LEO to GEO, and the ROM estimates for nonrecurring and recurring costs.

Two systems in Table 3-7, the higher capability SETV and the liquid fueled HTTV, are precluded because of volume limits. The solid HTTV approaches the weight limit of the Orbiter and represents a "larger IUS," but has less capability than the LTTV. SETV is highest in cost, risk and the long transit time through the Van Allen belt is degrading to the solar arrays required to power the ion engines. The estimated recurring cost of the SETV does not include the cost of larger arrays to compensate for Van Allen belt degradation.

The LTTV, 2 stage, pressure fed system shows 4,000 lbs more S/A payload capability than the IUS systems at higher NR cost, but lower recurring cost. As stated above, the LTTV can achieve rendezvous and docking without a separate stage; this system's operation is illustrated in Figure 3-16. The trade between the IUS and the LTTV is summarized in Table 3-8.

Conclusions

The conclusions for how buildup and maintenance might best be accomplished in the context of 1983 technology readiness are summarized as follows:

(1)   Rendezvous in GEO will require the development of an RCT, GRS or SEP vehicle using an IUS booster or a low thrust transfer vehicle.

(2)   The LTTV could deliver 8382 lb of solar array P/L as opposed to 4372 lb for the IUS-GRS. The longer transit time of 12 days as opposed to 6 hours does not seem significant.

3-35

TABLE 3-6

CENTER OF MASS ANALYSES RESULTS

CONCEPT	TOTAL LENGTH INCHES	ALLOWABLE CM LOCATION CARGO BAY STATION		CM LOCATION STATION	FORWARD CLEARANCE INCHES	AFT CLEARNACE INCHES
		FORWARD	AFT			
IUS WITH RCT	468.5	989.44	1116.97	1052.0	133.4	118.06
IUS WITH GRS	469.0	989.44	1116.97	1052.1	133.09	117.91
IUS WITH SEP	500.6	989.44	1116.97	1048.6	236.8	118.0
LTTV SINGLE STAGE, PRESSURE FED	531.0	1013.45	1114.76	1114.2	109.0	80.0
LTTV TWO STAGE, PRESSURE FED	619.5	1012.91	1114.81	1115.0	52.8	47.7
LTTV PUMP FED	597.0	1013.45	1114.76	1094.5	33.96	89.04
SETV (8000)	595.0	875.86	1112.41	989.5	34.0	91.0
(9516)	677.0	891.16	1126.0	1039.9	34.0	9.0
HTTV SOLID	612.0	1012.91	1114.81	1114.7	66.4	41.6
HTTV LIQUID	677.0	1012.55	1114.84	1097.4	34.0	9.0

TABLE 3-7

LEO TO GEO TRANSFER CONCEPT COMPARISONS

CONCEPT	ALLOWABLE S/A WEIGHT LB	GROSS WEIGHT/LB	CARGO BAY WEIGHT/LB	ASCENT TIME	ROM COST NR/R $M
IUS WITH RCT	4362	37400	46400	6 HOURS	18/20
IUS WITH GRS	4372	37400	46400	6 HOURS	18/20
IUS WITH SEP	4289	37400	46400	6 HOURS	60/42
LTTV SINGLE STAGE, PRESSURE FED	7363	58500	60000	12 DAYS	23/13
LTTV TWO STAGE, PRESSURE FED	8382	58000	60000	12 DAYS	25/16
LTTV PUMP FED	8632	58500	60000	12 DAYS	24/14
SETV	8000 9516*	18423 19942	19923 21442	250 DAYS 280 DAYS	100/67 100/67
HTTV, SOLID WITH RCT	6765	58000	60000	6 HOURS	36/23
HTTV, LIQUID WITH RCT	7907*	57677	59155	6 HOURS	52/32

IUS — INERTIAL UPPER STAGE
LTTV — LOW THRUST TRANSFER VEHICLE
SETV — SOLAR ELECTRIC TRANSFER VEHICLE
HTTV — HIGH THRUST TRANSFER VEHICLE
RCT — REMOTE CONTROLLED TRANSPORTER
GRS — GEOSYNCHRONOUS RETRIEVAL SYSTEM
SEP — SOLAR ELECTRIC PROPULSION

*VOLUME LIMITED CONFIGURATIONS

LOCKHEED MISSILES & SPACE COMPANY, INC.
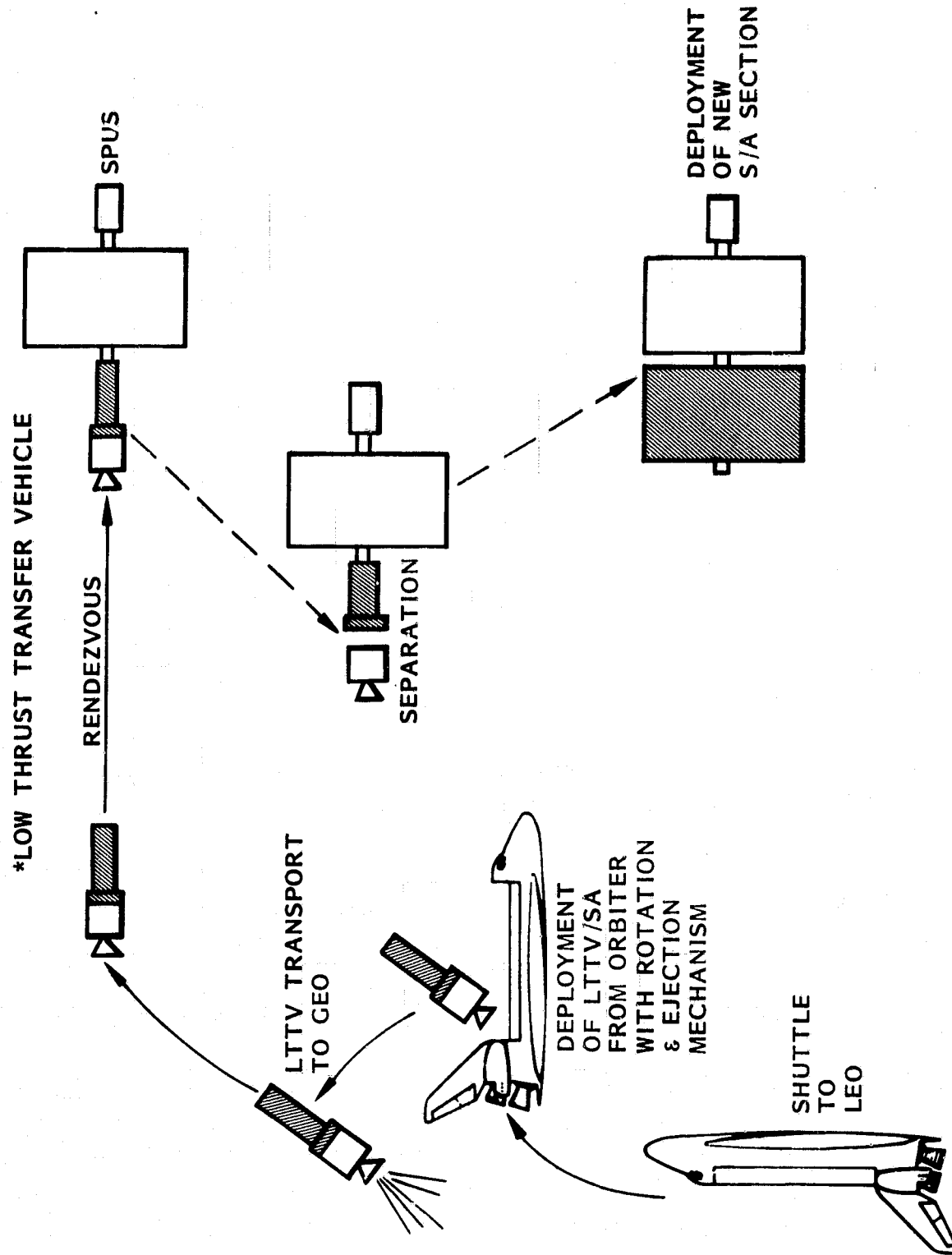
Figure 3-16 Buildup and Maintainability for GEO Applications – LTTV* Alternative

TABLE 3-8

IUS VS LOW THRUST BOOSTER TRADE

	ADVANTAGES	DISADVANTAGES
LOW THRUST BOOSTER	• CAN TRANSPORT P/L TO GEO AND RENDEZVOUS • > P/L CAPABILITY	• REQUIRES NEW DEVELOPMENT • 12 DAY TRANSIT TIME
IUS	• WILL BE AVAILABLE • 6 HOUR TRANSIT TIME	• REQUIRES ADDED RENDEZVOUS STAGE – RCT, GRS OR SEP – ALL OF THESE REQUIRE DEVELOPMENT

(3)   The trade between the RCT, GRS and SEP is very dependent upon the number of launches, solar array size and the solar powered user station application, since P/L capability is equal.

(4)   The SETV is expensive, but it accomplishes attitude control for the SPUS; therefore it could be cost effective for some applications in the long term.

(5)   The final trade will consider the solar array packaging designs which may favor one system over another.

Section 4

Cost Analysis

NASA   LOCKHEED
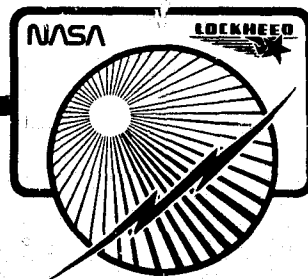
4.0   COST ANALYSIS

4.1   GENERAL - LEO/GEO

The ultimate objective of the present study was to determine the type of solar array and solar cell technologies which are capable of achieving the greatest cost-effectiveness in the 300-1000 kW range. Major systems trade-offs include planar vs concentrator designs and silicon cells vs GaAs cells, whereby the selection of appropriate concentration regimes plays a key role. The LMSC approach has been to identify basic technology influences (reflector capabilities, cell capabilities under concentration, Orbiter and operations constraints, etc.) and to utilize them in selecting and designing a limited number of arrays to represent the basic relevant design categories. The categories which emerged are:

- Planar/Silicon
- Low-CR/Silicon
- Low-CR/GaAs
- High-CR/GaAs

In each category a baseline design was generated in sufficient detail to permit a valid prediction of performance (power, size, weight, etc.) and a credible cost breakdown for a power level of approx. 300-400 kW (15 year avg. at LEO).

In the sections below, a cost model has been established which shows the inter-relationship among contributing cost elements and defines the figures of merit to be used for array concept selection. A detailed cost breakdown by major assembly groups is given and comparative cost/performance conclusions are drawn. A short technical discussion is included for the purpose of establishing a, for LEO only, costing baseline for reboosting operations after loss of altitude through drag forces on the arrays.

LOCKHEED MISSILES & SPACE COMPANY, INC.

4.2   DRAG MAKE-UP (LEO Only)

For long-term missions in a low-earth orbit, a large-area solar array will experience drag forces due to the residual atmosphere which can lead to catastrophic orbit decay. The mission (user platform) for which the arrays of this study are envisioned is likely to be positioned in the 400-500 nautical mile altitude range.

Figure 4-1 shows the results of an analysis of altitude decay for two different indicative circular orbits--400 n.m. and 500 n.m., both with inclination of 28.5°. The effects of two nominal solar cycles were included in the 15 year mission length. As the figure shows, at 400 n.m. none of the array candidates can survive without reboost. At 500 n.m. no reboost is necessary over the 15 year period. For inclinations up to 90° no major difference in drag behavior were seen.

Despite the above results, a 400 n.m. orbit may be more appropriate for the envisioned mission. Although the arrays can be launched and installed into higher orbits, the user platform will need to be frequently revisited for payload installation, exchange, or retrieval. These user-payload launches may be densely packaged modules which impose weight limitations upon the attainable altitude. Thus a 400 n.m. orbit has been selected for the costing baseline.

It is unrealistic to perform all-inclusive costing for the drag make-up of the solar array by itself. The array is a subsystem of a large-area user platform, which also experiences drag and must be reboosted. The choice of a reboost propulsion unit, required amount of fuel expenditures, as well as launch volume and frequency for the reboost package will be determined by the entire platform system. In view of this situation, neither the reboosting propulsion unit (or vehicle) nor its launch to station will be charged to the solar array budget in the present study. Charges to the solar array will consist of:

- cost of 15 year propellant supply and tank for the amount of fuel required for the solar array alone
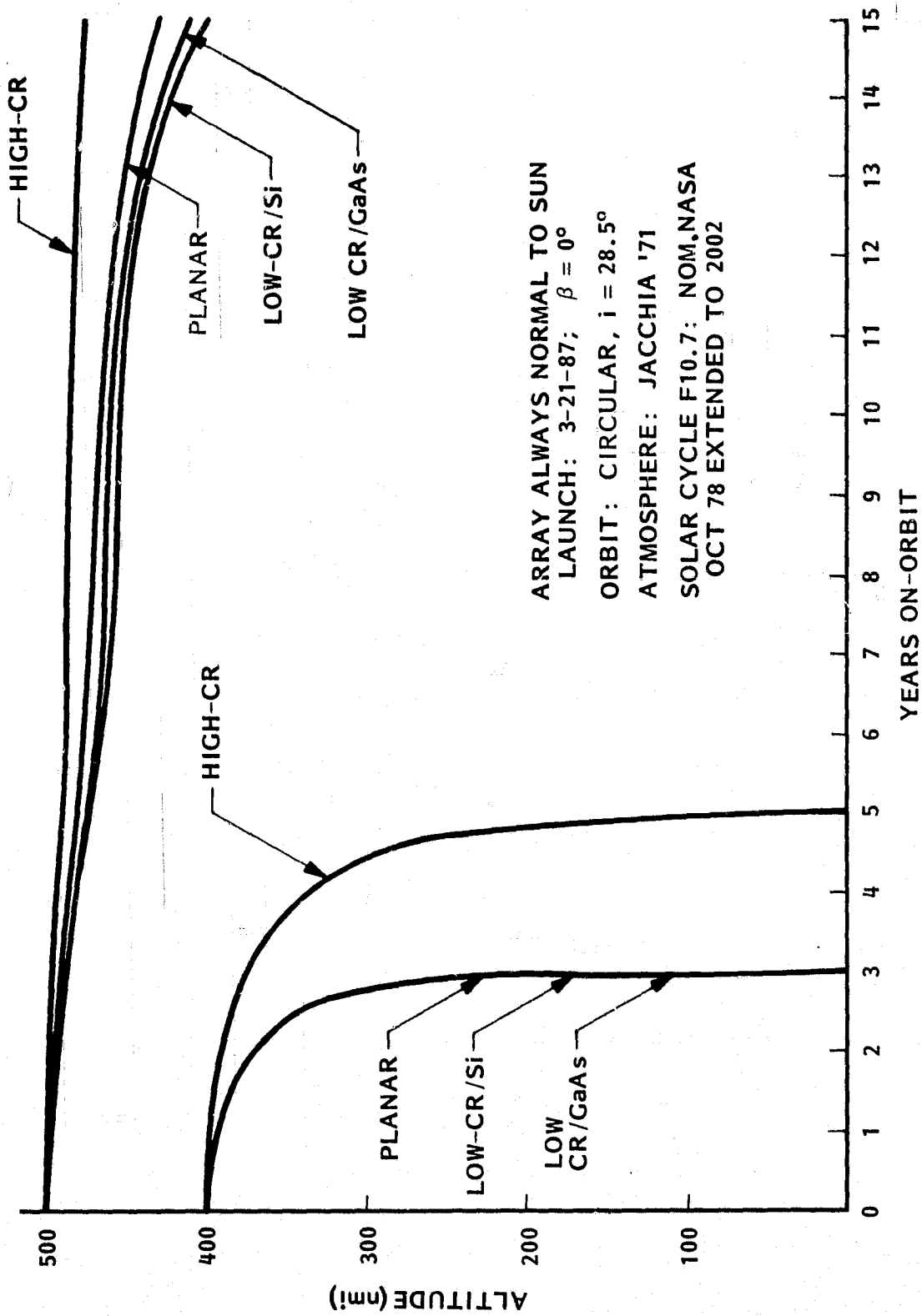
Figure 4-1 Solar Array Altitude Decay

LOCKHEED MISSILES & SPACE COMPANY, INC.

- one single launch (partial payload) of tank and 15 year fuel supply

Table 4-1 shows the results of the drag make-up costing exercise. Two reboost modes were considered in order to investigate cost sensitivity. For the first mode, labeled "400-20" in the table, decay by 20 n.m. from 400 n.m. was permitted, followed by reboost back to 400 n.m. For the second mode, labeled "400-5", decay was permitted by 5 n.m., followed by reboost back to 400 n.m. As the table shows, the number of reboosts required over 15 years is significantly higher for the 5 n.m. decay case. However, since fuel expenditure back to 400 n.m. is significantly less, no great differences in fuel expenditure is seen.

Tank costs were obtained from existing in-house tank designs; hydrazine fuel was costed at the GFE rates instead of at open market prices, which is approx. 10 times higher. Even so, the cost of the single partial payload launch dominates overwhelmingly. For such low payload volume and weight, a minimum charge factor of 0.067 was applied to an escalated 1979 basic flight and rendezvous charge plus integration, operations fees, second RMS, and OMS kits fees, yielding a launch cost of $2.3 million. When combined with fuel and tank costs, the total drag make-up cost amounts to $2.6 million for all array concepts.

The above analysis was performed for arrays in the 300-400 kW range. The decay curves of Figure 4-1 are valid for all power levels since decay is determined by ballistic coefficient, a specific quantity in array area-per-weight. Fuel expenditure per reboost, however, is dependant upon array weight only, which makes it size, or power-level dependant. Thus the drag make-up costs belong in the recurring cost category.

4.3 COST MODELING

Figure 4-2 illustrates the cost model established in the present study, showing the basic cost components and the manner in which they combine to influence the relevant cost figures of merit.

TABLE 4-1

DRAG MAKE-UP COMPARISON

| | PLANAR | | LOW-CR | | | | HIGH-CR | |
	SILICON		SILICON		GaAs		GaAs	
BALLISTIC COEFFICIENT*	130 FT^2/SLUG		155 FT^2/SLUG		149 FT^2/SLUG		63 FT^2/SLUG	
NO. OF REBOOSTS IN 15 YR (INDEPENDENT OF POWER LEVEL)	400-20 / 12	400-5 / 42	400-20 / 14	400-5 / 50	400-20 / 14	400-5 / 48	400-20 / 5	400-5 / 20
WEIGHT OF FUEL AND TANK (15 YRS SUPPLY/I$_{SP}$ = 230)	1190 LB	1030 LB	3915 LB	3080 LB	1810 LB	1550 LB	2385 LB	2065 LB
FUEL AND TANK COST (GFE FUEL)	$304K	$303K	$312K	$310K	$306K	$305K	$308K	$307K
LAUNCH COST (ONE PARTIAL PAYLOAD)	2.3 MILLION							
TOTAL DRAG MAKE-UP COST (1979 DOLLARS)	$2.6 MILLION							

*LMSC CONVENTION. NASA CONVENTION IS THE RECIPROCAL OF THE ABOVE.

ARRAY ALWAYS NORMAL TO SUN
400 nmi CIRCULAR ORBIT
i = 28.5°/LAUNCH 3-21-87
ATMOSPHERE: JACCHIA '71
SOLAR CYCLE F10.7: NOM NASA 10-78

4-5
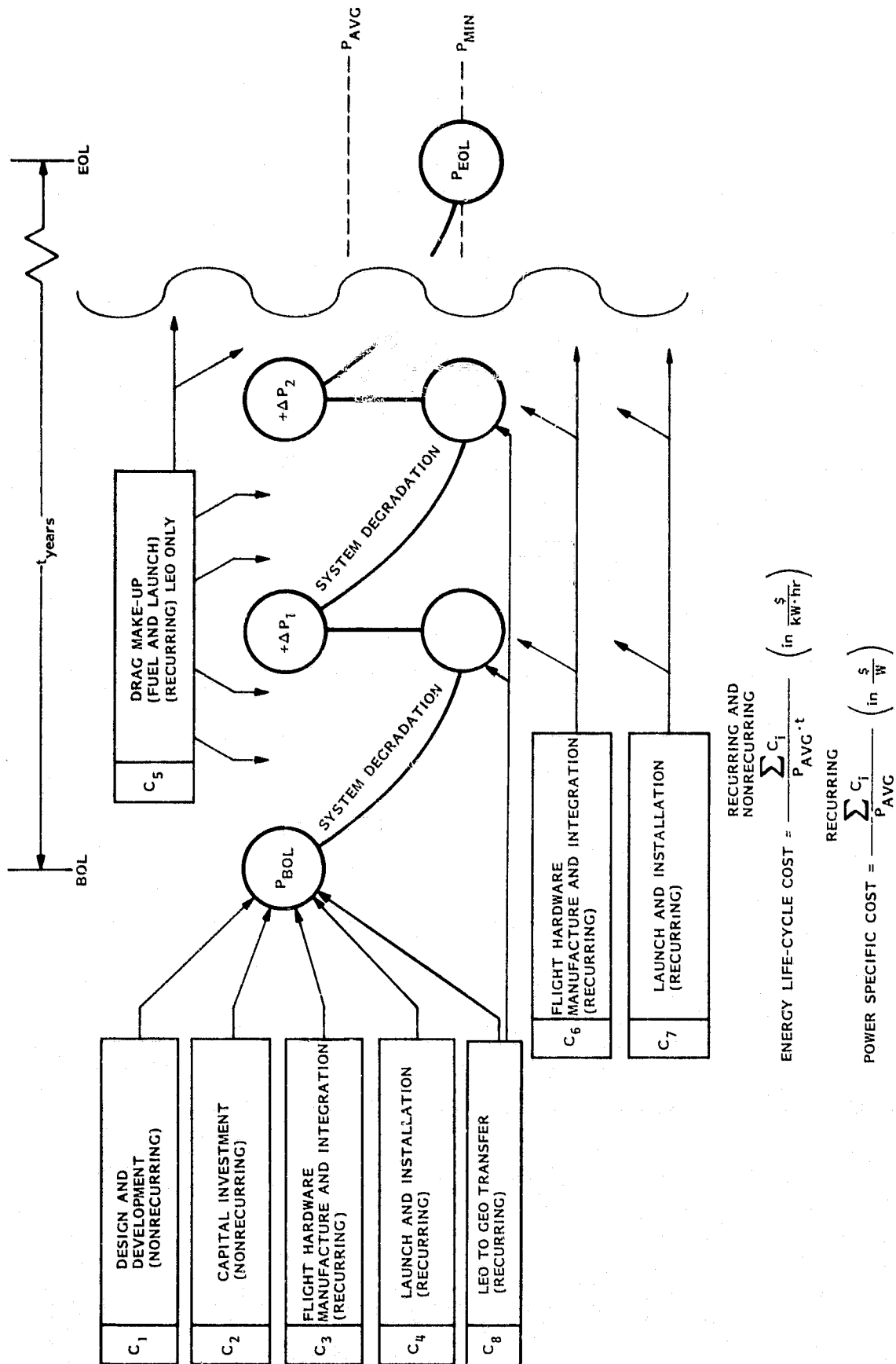
Figure 4-2 Solar Array Cost Model

$$\text{ENERGY LIFE-CYCLE COST} = \frac{\displaystyle\sum \frac{c_i}{P_{AVG} \cdot t}}{\text{RECURRING AND}} \quad \left(\text{in } \frac{\$}{kW \cdot hr}\right)$$

$$\text{POWER SPECIFIC COST} = \frac{\displaystyle\sum \frac{c_i}{P_{AVG}}}{\text{RECURRING}} \quad \left(\text{in } \frac{\$}{W}\right)$$

LOCKHEED MISSILES & SPACE COMPANY, INC.

A certain power level P_{BOL} is installed through the expenditure of non-recurring funds for

- design and development
- capital investment (equipment)

and recurring funds for

- flight hardware manufacturing and integration
- launch and installation
- orbital transfer cost (GEO only)

The system is kept on-orbit through the expenditure of recurring funds for

- drag make-up (LEO only)

The installed system degrades in power over the mission life t, during which additional recurring funds may or may not be expended for manufacturing, integration, launch, and installation of add-on units.

Two relevant cost figures of merit are cited in the figure:

- Power Specific Cost ($/W), which sums all recurring costs and normalizes this sum to an appropriate power value (here P_{AVG}). This is the traditional approach to solar array costing with the important exception that here it includes launch cost also.

- Energy Life-Cycle Cost ($/kW-hr), which sums all non-recurring as well as recurring costs and normalizes this sum to the average energy available during the mission (P_{AVG} x mission life). This approach is reminiscent of a power plant approach to costing and is thought to be more relevant to the type of mission and size of array under study here.

In all cases, costs have been expressed in 1979 dollars.

4.4   COST ANALYSIS

As the cost model in the previous figure indicates, non-recurring cost elements consist of design and development costs and capital investment (equipment) costs. Experience in previous programs has served as a guideline in arriving at a rough estimate of the costs foreseen for the design and development of a system of this magnitude.   The Planar was burdened at $15M being the least complex based on previous development while the High CR having the least experience and being more complex was burdened at $22M.

The amount of capital investment required for a system of this magnitude has been a major subject of concern, particularly in the area of solar cell production. Table 4-2 shows a breakdown of anticipated capital investment requirements for the four LEO candidate array concepts. Table 4-3 is the anticipated capital investment breakdown for the two GEO candidate arrays. Vendor inputs have been solicited in arriving at the solar cell production facility capital requirements. In no case was the feasibility of tooling up to the production rates required for 1983 readiness regarded as questionable. No capital investment is required for coverslide production or for reflector material production; our capacity demands are slight to the glass and film vendors. The remaining four areas involve in-house processing. Capital requirements in these areas could be accurately estimated as a consequence of LMSC's active involvement in all of them.

The total results in the figure are not surprising in view of the magnitude of the envisioned program. It is noteworthy that the LEO low-CR/GaAs concept requires approximately twice as much capital investment as the other concepts due to the large quantities of 2 x 2 cm^2 GaAs cells required.

Of the various recurring cost elements in the cost model, drag make-up costs (LEO) have been estimated above and power add-on costs have been eliminated since power add-on has not been selected as a cost-effective maintainability option. Manufacturing and integration costs have been modeled after well-established cost guidelines of

4-8

TABLE 4-2

CAPITAL INVESTMENT REQUIREMENTS - LEO

300 kW/LEO BASELINE IN 1979 $.	PLANAR	LOW – CR		HIGH – CR
	SILICON	SILICON	GaAs	GaAs
SOLAR CELL PRODUCTION FACILITY	$4M (~0.8 M CELLS)	$3M (~0.5 M CELLS)	$12M (~2.5 M CELLS)	$2M (~100 K CELLS)
COVER SLIDE PRODUCTION FACILITY	NO MAJOR OUTLAY FORSEEN	NO MAJOR OUTLAY FORSEEN	NO MAJOR OUTLAY FORSEEN	NO MAJOR OUTLAY FORSEEN
REFLECTOR MATERIAL PRODUCTION FACILITY	✕	NO OUTLAY NECESSARY	NO OUTLAY NECESSARY	NO OUTLAY NECESSARY
CELL BLANKET MANUFACTURING FACILITIES*	$3M	$2M	$2M	NO MAJOR OUTLAY FORSEEN
STRUCTURE, MAST, OR DISH MANUFACTURING FAC	$1M	$2M	$2M	$3M
HEAT PIPE/RADIATOR MANUFACTURING FACILITIES	✕	✕	✕	$1M
ARRAY ASSEMBLY, INTEG AND TEST FACILITIES	$2M (INCL TV-CHAMBER)	$3M (INCL TV-CHAMBER)	$3M (INCL TV-CHAMBER)	$3M (INCL TV-CHAMBER)
TOTAL	$11M	$10M	$19M	$9M

*INTERCONNECTION, PANEL FABRICATION, ETC.

TABLE 4-3

CAPITAL INVESTMENT REQUIREMENTS – GEO

	PLANAR	LOW-CR
	SILICON	GaAs
SOLAR CELL PRODUCTION FACILITY	(~0.65 M CELLS)	(~1.4 M CELLS)
COVER SLIDE PRODUCTION FACILITY	NO MAJOR OUTLAY FORSEEN	NO MAJOR OUTLAY FORSEEN
REFLECTOR MATERIAL PRODUCTION FACILITY	X	NO OUTLAY NECESSARY
CELL BLANKET MANU- FACTURING FACILITIES*	$3	$2
STRUCTURE, MAST, OR DISH MANUFACTURING FACILITIES	$1	$2
HEAT PIPE/RADIATOR MANUFACTURING FACILITIES	X	X
ARRAY ASSEMBLY, INTEG AND TEST FACILITIES (TV)	$3 (INCL TV- CHAMBER)	$3 (INCL TV- CHAMBER)
TOTAL	$11	$15M

previous and current programs, including the SEPS development program, reflector dish antenna programs, and active thermal control system manufacturing activities. Launch and installation costs have been generated through reference to the applicable Orbiter user's manuals.

Table 4-4 shows the baseline LEO and GEO assumptions used for purposes of establishing a real, all-inclusive Shuttle launch fee. A second RMS is included for a full holding and manipulating capability when removing from the Shuttle or installing solar array segments. After inclusion of the various facility rental fees, integration fees, operations and documentation fees, a first LEO flight, for instance, has been costed at $39.0 million (1979 dollars) and subsequent reflights at $34.0 million each.

Table 4-5 shows the resulting costs for each array concept broken down into major assembly groups. The values in the figure are not normalized to power but rather apply for the 15 year average power values given in the top line. Compared to the planar/silicon array, the low-CR/silicon array is burdened primarily by the necessity of two launches. The cost figures reflect once again the fact that a low-CR/silicon array must be approx. twice the size of the low-CR/GaAs array. However, the low-CR/ GaAs suffers in the cell cost category due to the large quantities of 2 x 2 cm^2 GaAs gcells. The low quantity of cells for the high-CR/GaAs array provides a drastic reduction in the cell cost category. However, the dish reflector structures impose an overwhelming cost burden, which combined with the cost of three required launches, render the high-CR concept unacceptably costly.

GEO system cost breakdown comparison is shown in Table 4-6. Both GEO systems have comparable average power over a 15 year period in the range of 200 kW. This specific power size was a function of transfer weight capability (neither concept exceeded this value) and existing LEO modules which were sized by shuttle stowage or by baseline blanket widths (automated manufacturing limitations). Nevertheless, it does provide a good means of direct comparison. The blanket/cell assembly for both configurations is essentially the same with different emphasis on cell price and blanket assembly costs. Three areas appear to make up the Δ cost difference between the planar and the Low CR. 1) A more complex reflector structure, 2) Greater capital investment in manning up to produce GaAs cells and 3) Increased development cost.

LOCKHEED MISSILES & SPACE COMPANY, INC.

TABLE 4-4

LAUNCH COSTING BASELINE

- 1979 DOLLARS

- LAUNCH AND RENDEZVOUS

- FROM ETR INTO 400 nm CIRCULAR, i = 56°

- SECOND RMS

- TWO OMS KITS

- 1-DAY TIME-ON-ORBIT

- LAUNCH FACILITY RENTAL FEES

- INTEGRATION FEES

- FLIGHT AND POST-FLIGHT OPERATION FEES

- DOCUMENTATION FEES

- 47 FEET OF CARGO BAY AVAILABLE FOR ARRAY

TABLE 4-5

SYSTEM COST BREAKDOWN – LEO

	1979 DOLLARS/IN $M	PLANAR SILICON 311 KW AVG	LOW-CR SILICON 380 KW AVG	LOW-CR GaAs 437 KW AVG	HIGH-CR GaAs 384 KW AVG
RECURRING	COVERED SOLAR CELLS	15.4	10.0	31.7	3.0
	CELL BLANKETS (INCL. CELL ATTACHMENT, PANEL ASSY)	18.6	12.6	7.7	0.5
	STRUCTURES (INCL. MASTS, REFLECTORS, ASSEMBLY)	29.2	62.4	39.6	115.7
	THERMAL CONTROL SYSTEM	–	–	–	16.4
	PROGRAM SUPPORT (MGMT, ENG, QA, INTEGRATION, TRANSP)	17.4	23.4	21.7	37.3
	LAUNCH AND RENDEZVOUS	39.0	73.0	39.0	107.1
	DRAG MAKE-UP	2.6	2.6	2.6	2.6
	TOTAL RECURRING	122.2	184.0	142.3	282.6
NON-RECURRING	CAPITAL INVESTMENT	11.0	10.0	19.0	9.0
	DESIGN AND DEVELOPMENT	15.0	20.0	20.0	22.0
	TOTAL NON-RECURRING	26.0	30.0	39.0	31.0

TABLE 4-6

SYSTEM COST BREAKDOWN – GEO

1979 DOLLARS/IN $M		PLANAR SILICON 206 kW AVG	LOW CR GaAs 231 kW AVG
RECURRING	COVERED SOLAR CELLS	12.2	22.9
	CELL BLANKETS (INCL CELL ATTACHMENT, PANEL ASSY)	14.0	4.6
	STRUCTURES (INCL MASTS, REFLECTORS, ASSEMBLY)	21.9	23.8
	THERMAL CONTROL SYSTEM	—	—
	PROGRAM SUPPORT (MGMT, ENG, QA, INTEGRATION, TRANSP)	13.1	13.0
	LAUNCH TO 15 nmi	39.0	39.0
	LEO TO GEO TRANSFER AND RENDEZVOUS*	16.0	16.0
	TOTAL RECURRING	116.2	119.3
NON-RECURRING	CAPITAL INVESTMENT	11.0	15.0
	DESIGN AND DEVELOPMENT**	40.0	45.0
	TOTAL NON-RECURRING	51.0	60.0

*GROUND CONTROL OF TRANSFER AND RENDEZVOUS COSTED TO SPUS
**SOLAR ARRAY = $15M, LTTV ORBITAL TRANSFER VEHICLE = $25M

These cost trends are reflected more accurately in Figure 4-3, which shows the recurring costs normalized to 15 year average power ($/avg. watt). Drag make-up costs are seen to be virtually negligible. Blanket costs appear larger than covered cell costs since they include not only substrate fabrication and cell attachment, but also blanket assembly and panel-level testing. The single largest cost factor is the launch costs. If launch costs were excluded, the figure shows that the cost spread between the planar and low-CR concepts would be very close. As it is, the planar/silicon and low-CR/GaAs arrays demonstrate superior cost-effectiveness.

Figure 4-4 converts Table 4-6, recurring cost/watt numbers into graphic representation for the two GEO solar array concepts. Overall costs from LEO to GEO are decreased due to the smaller array sizes delivered to GEO.

The significant increase in overall $/watt (LEO to GEO) can be attributed to added orbital transfer cost ($\approx 15\%$) and higher array degradation due to particle radiation ($\approx 13\%$).

Figures 4-5 and 4-6 show a comparison of energy life-cycle costs ($/kW-hr) for the candidate arrays, GEO and LEO, including all costs, whether recurring or non-recurring. As an indication of array cost-effectiveness, this figure totally reinforces the conclusions of the previous figures. For the two superior candidates, the planar/silicon array and the low-CR/GaAs array, non-recurring costs are seen to contribute a maximum of 20% (LEO) and 30% (GEO) of total costs for a power level of 300-400 kW (LEO) and 200 kW (GEO). This percentage will decrease somewhat for higher power levels.

The exact values of the calculated figures of merit in the above two figures are given below.

LOCKHEED MISSILES & SPACE COMPANY, INC.
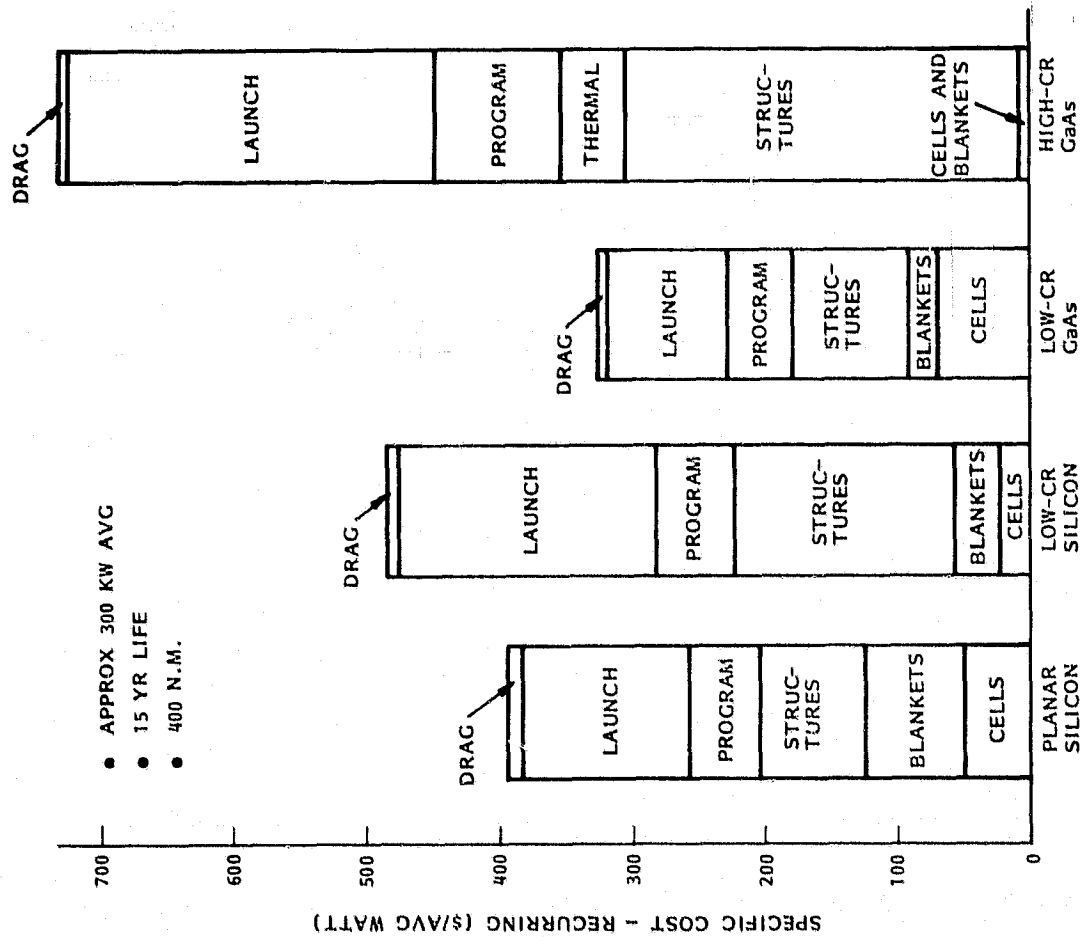
Figure 4-3 Solar Array Specific Cost-Recurring – LEO
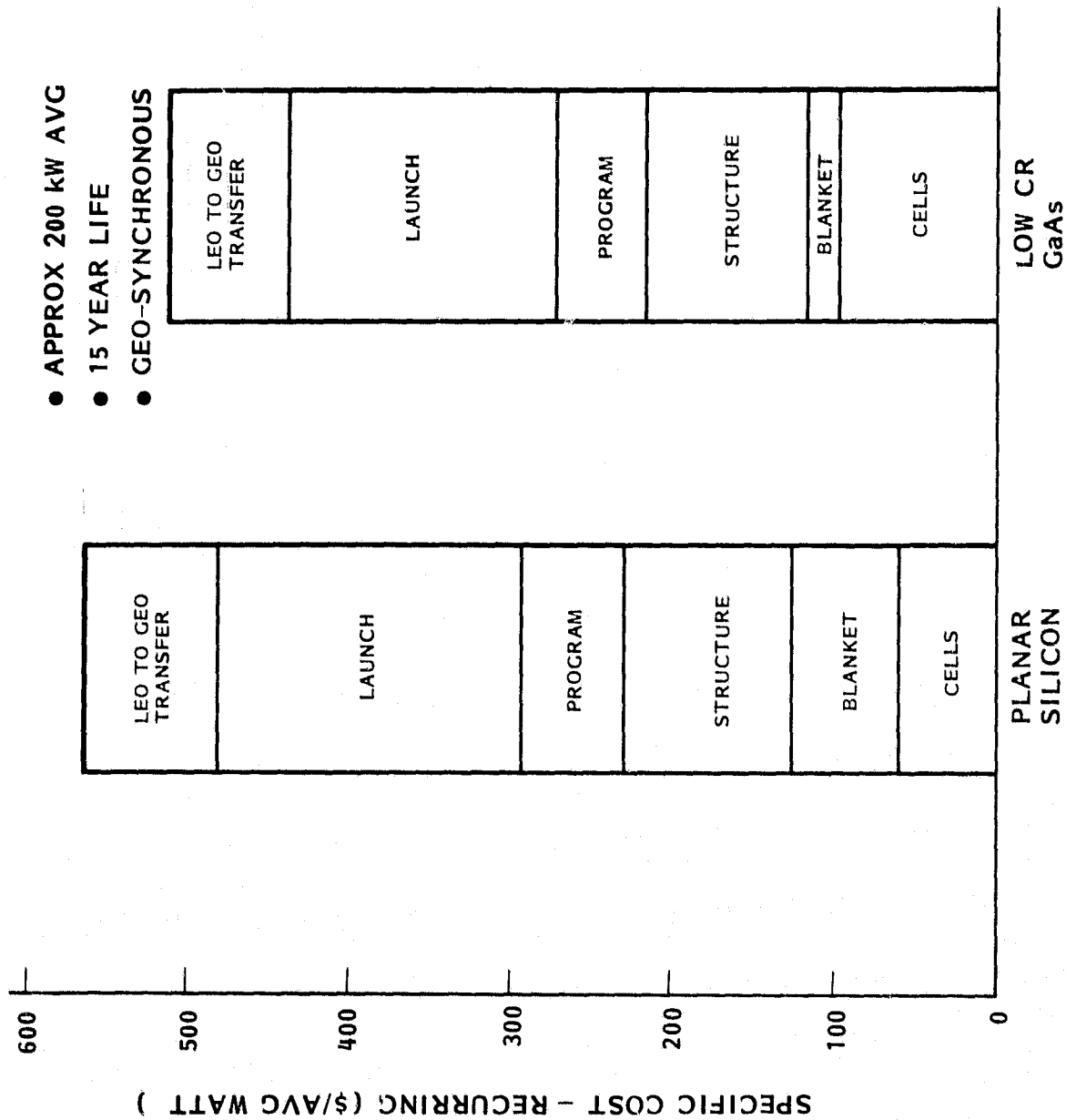
Figure 4-4 Solar Array Specific Cost-Recurring – GEO
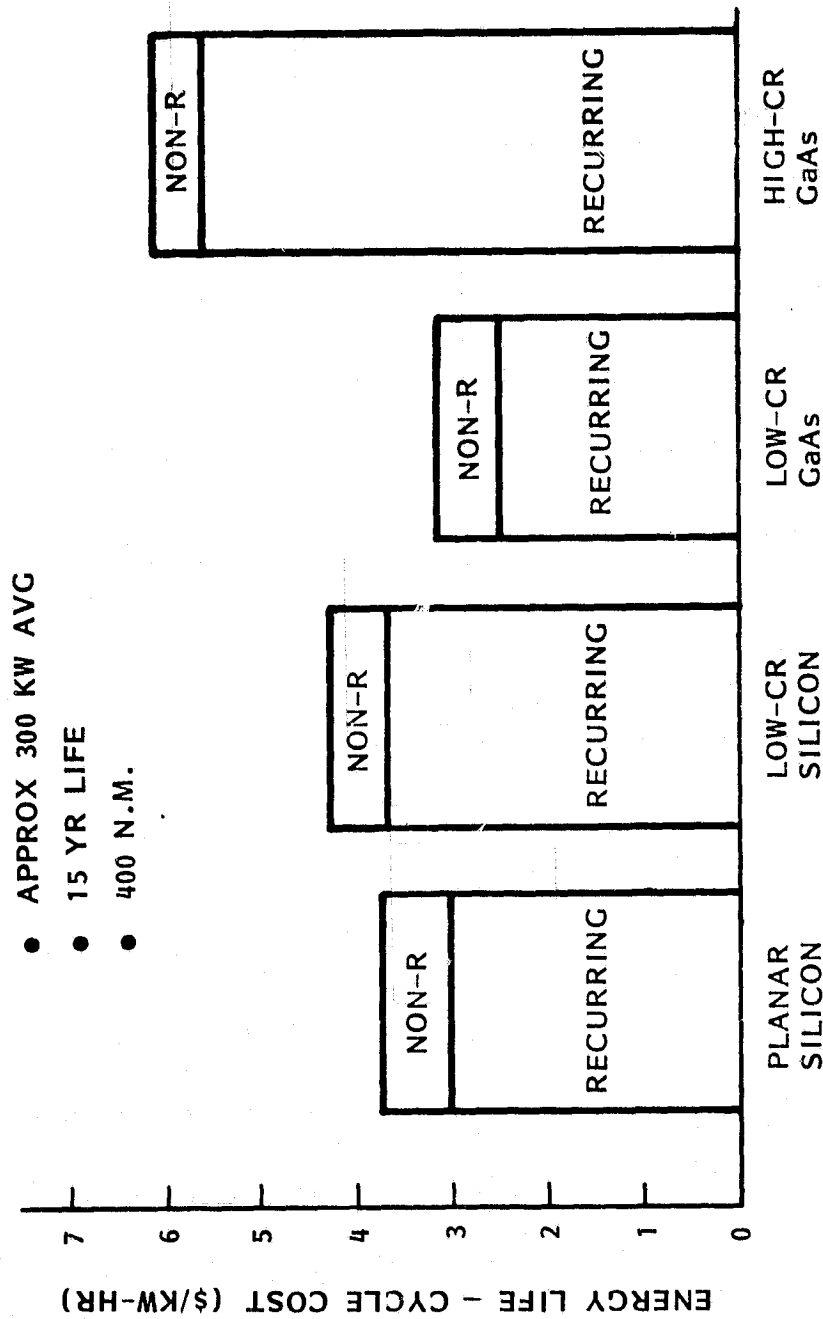
Figure 4-5 Solar Array Energy Life-Cycle Cost

- APPROX 200 kW AVG
- 15 YEAR LIFE
- GEO-SYNCHRONOUS

NON-RECURRING (PLANAR SILICON)

RECURRING (PLANAR SILICON)

NON-RECURRING (LOW-CR GaAs)

RECURRING (LOW-CR GaAs)

PLANAR SILICON

LOW-CR GaAs

ENERGY LIFE-CYCLE COST ($/kW-HR)

7 6 5 4 3 2 1 0
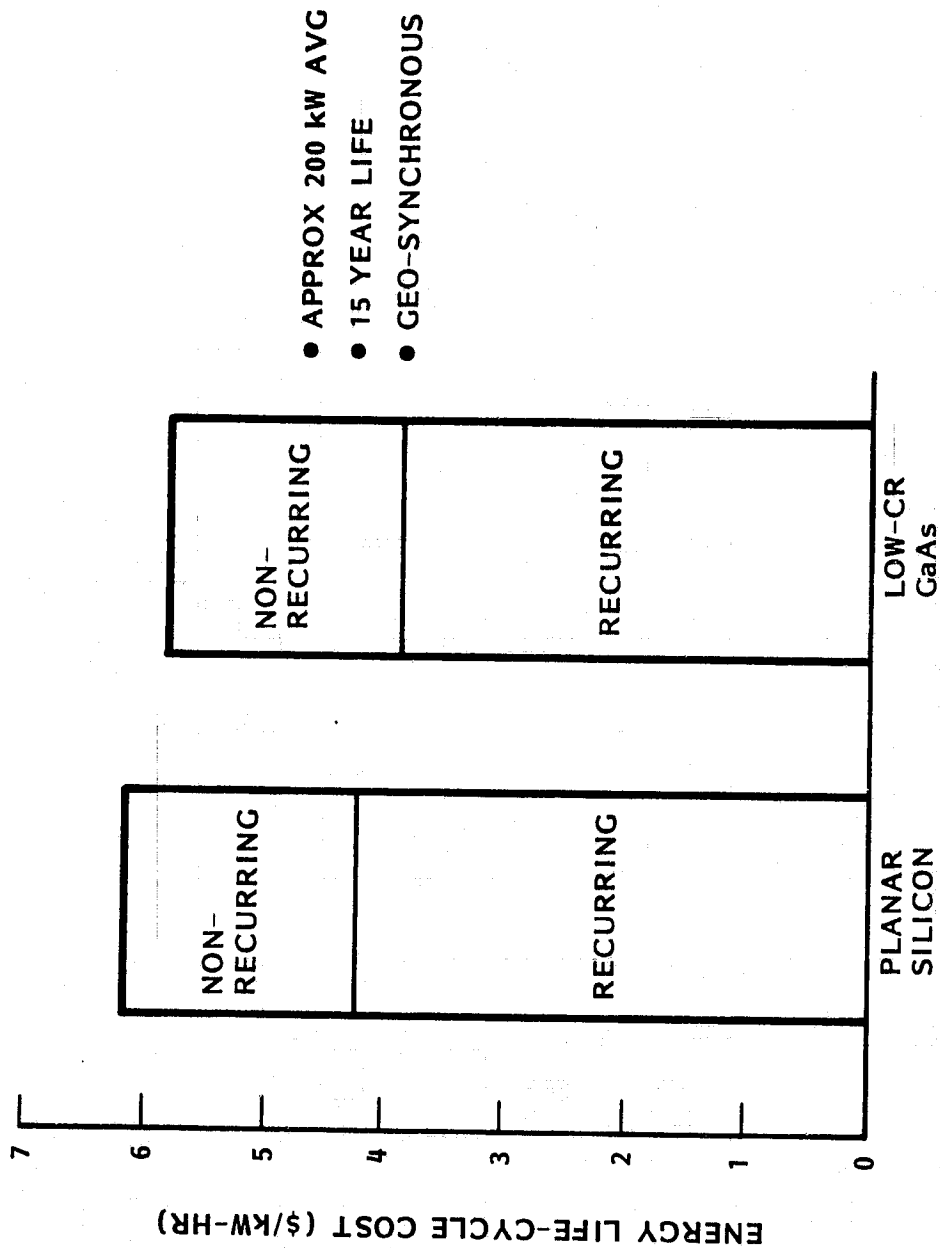
Figure 4-6 Solar Array Energy Life-Cycle Cost

	Specific Cost ($/avg. Watt)		Energy Life-Cycle Cost ($/kW-hr)	
	LEO	GEO	LEO	GEO
planar/silicon	393	206	3.75	6.18
low-CR/silicon	484	--	4.28	--
low-CR/GaAs	326	231	3.16	5.91
high-CR/GaAs	736	--	6.17	--

Looking at LEO only it is instructive to return to a hypothesis made earlier in the selection of representative concepts to be analyzed in depth. GaAs cell technology was considered to be too costly for use on a planar array. Cost and performance figures for the planar array were adjusted to reflect usage of the baseline GaAs cell. Although performance increased by nearly 50% at planar temperatures, the enormous quantities of GaAs cells required boosted total recurring cost by nearly 70%, and resulted in a specific cost of $445/avb. watt, thus confirming the early elimination of this option.

The greatest uncertainty in the cost results given above are contained in the cost prognosis of the GaAs cell. Though the figures indicate a superiority of the low-CR/ GaAs over the planar/silicon, this result depends critically upon GaAs cell cost. It is thus of paramount importance to investigate the sensitivity of the result with respect to GaAs cell cost.

Figure 4-7 plots specific cost of the low-CR/GaAs system against the piece cost of the 2×2 cm^2 baseline GaAs cell. The planar/silicon system specific cost has been drawn in at its value above ($393/avg. watt) as a reference line.

The bold low-CR/GaAs system line descends in cost to the point of "lowest industry prognosis", $12.30/cell, which was used in arriving at the specific cost of $326 cited previously. The cross-over point of the two bold system lines occurs at approx. $25 per GaAs cell. This is the cost at which the low-CR/GaAs system becomes competitive with the planar/silicon system. The two broken low-CR system lines represent system specific cost for GaAs cells of 16% and 20% lab-efficiency, respectively, as opposed to the baseline 18% lab-efficiency. Although a shifting of cross-over points
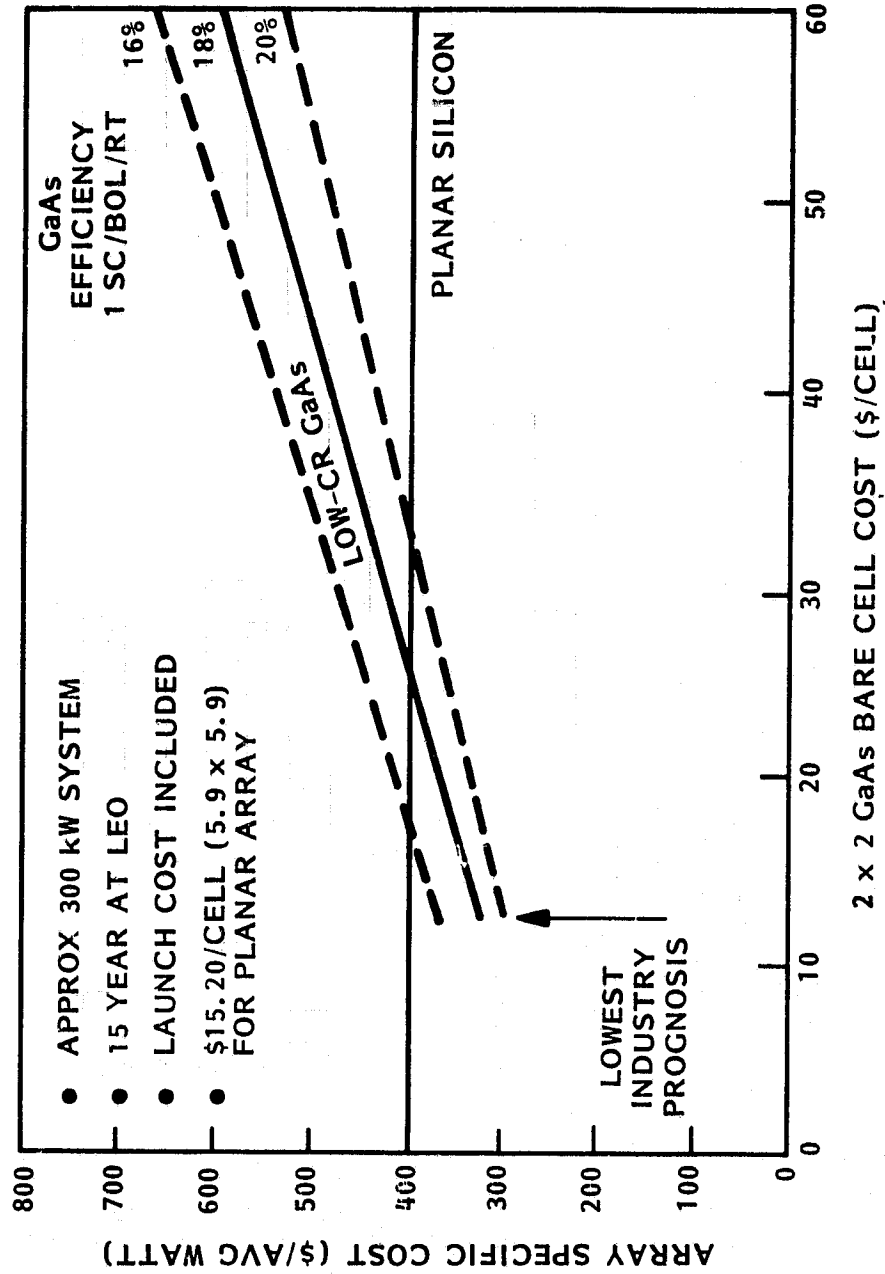
Figure 4-7 Sensitivity of Array System Cost to GaAs Solar Cell Cost

LOCKHEED MISSILES & SPACE COMPANY. INC.

is seen, the cross-over band remains confined to the $20-$30/cell range. Thus, the results of the cost analysis are seen to be relatively insensitive to the efficiency achieved by the GaAs cell. The dominating influence is the cell production cost.

The results of the cost analysis above indicate that it is imprudent at the current stage of technology development to force a selection between a planar/silicon array and a low-CR/GaAs array. The planar/silicon system is particularly attractive due to its low risk to the mission. The low-CR/GaAs system has the potential for being more cost-effective. However, the uncertainty of present GaAs cell cost prognoses does not permit an unequivocal endorsement of this system.

STUDY OF
**MULTI-kW SOLAR ARRAYS
FOR EARTH ORBIT APPLICATION**

Section 5

Summary

NASA   LOCKHEED
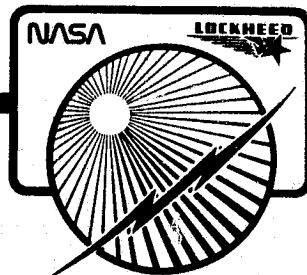
5.0 SUMMARY

This study identifies low cost LEO and GEO Solar Array concepts in the 300 to 1000 kW range which could be reduced to hardware in the mid 80's. Size scaling factors and longer life demands were recognized as the prime drivers for the designs if low life-cycle costs ($/kW-hr) for energy were to be achieved. Technology was identified which requires further development in order to assure component readiness and availability in the needed time frame.

Limited definition of Shuttle capabilities and program requirements has made estimation of all recurring and non-recurring cost elements difficult; however, a serious attempt to at least identify each of these elements associated with delivering a power system into orbit has been made. The cost projections for each of the individual cost elements of the model discussed have been generated from LMSC manufacturing experience and cost analyses for solar arrays (blankets and deploy-ment systems), Cassegrainian antenna systems, and thermal control systems. Extensive use was especially made of existing cost analyses for flexible solar arrays of the SEPS, PEP, and 25 kW PS family, where applicable, including development, manufacturing, assembly, test, QA, and management cost components. The use of such similarity techniques is believed to have given a more realistic system cost projection than, for example, the use of empirical cost formulas.

Cost effectiveness cannot be established on the sole basis of lowest solar array manufactured cost. The cost of delivery to and maintenance on-orbit can easily exceed manufacturing costs and become the cost driver, especially if quality assurance is minimized by acceptance of higher maintainability costs. A risk also exists in projecting on-orbit maintenance costs, because the methods are still very much conceptual.

Drag makeup, shuttle payload vs altitude and inclination, capital investments required to develop materials and processes and system growth schemes all impact the ultimate cost effectiveness which can practically be achieved. Lockheed has approached the task from a total system interinvolvement of cost, design and technology readiness to narrow the practical options to one Planar and two Concentrator (high and low CR) concepts.

LOCKHEED MISSILES & SPACE COMPANY. INC.

Both the LEO and GEO Solar Array configurations can be readied for the 1983-1985
start date with completion of specific near term technology developments; however,
the GEO concept as a system is beyond the 1983 era. This is due to required develop-
ment of an orbital transfer and rendezvous vehicle.

LEO Configuration Discussion

All Planar and Concentrator solar array concepts will be self deployable units. The
planar and the low CR concentrator use a similar and unique stowage and deployment
mechanism to deploy the basic solar array support structure. The solar array blanket
and/or reflectors remain stowed during this operation. When the basic structure is
rigidized a series of extendable longeron masts deploy the solar array blanket/
reflectors into their extended positions. In this condition the arrays are under
adequate tension to compensate for thermal, sun tracking and docking loads when
adding new array modules or experiment platforms. The mast systems are simple
extension mechanisms only. Retraction for retrieval is not an attractive cost
effective consideration.

The solar array blankets for both Planar and Low CR (reflectors included) are of
the fold-up type allowing for high density stowage.

The High CR Cassegrainian concentrator concept is also self deployable as an individual
module using lenticular ribs wrapped around the hub to unfurl the reflectors and
a similar lenticular strut wrapped around the radiator to provide the module
standoffs. The hyperbolic reflector is motor driven to its required position
after both reflectors are unfurled. Remote manipulators and/or EVA will be
required to attach the High CR modules into clusters. Also EVA may be necessary
to assist if the self deployment systems fail or difficulty exists during removal of
the stowed solar array system from the Shuttle bay.

A solar array lifetime of 15 years has been established as baseline. Although no
flight experience verifies this conclusion directly, LMSC is confident that materials
are not the limiting factor but rather the way they are assembled. Development of
high reliability designs will be vital. Proper redundancy will be vital and confirming

developmental tests necessary to reach the required confidence level to support the solar array design selection. Cell radiation degradation is well defined and can be accommodated for the 15 year time period. Drawings of each of the configurations were carried to the preliminary design level to be assured of workable solutions for deployment mechanisms, blankets and for reflectors.

Each solar array when fully deployed is a structurally rigid power generating system. It must however be attached to a SPUS (Solar Power User System) which will provide orbital corrections, drag makeup and sun positioning for the array.

OMS kits and EVA access clearance ports were considered in fitting the solar array stowage lengths within the Shuttle Orbiter cargo bay. An addition to the basic Orbiter is a second RMS for solar array module removal from the Orbiter bay, deployment and docking to the SPUS. RMS stowage does not impact the required solar array volume.

LMSC will use the large area (5.9 x 5.9 cm - 8 mil) silicon solar cell with wraparound contact for the planar and low CR concentrator configurations. This Lockheed-derived cell was selected for its high utilization of the silicon ingot diameter which yields an approximate 20% cost savings, at the array system level, over the conventional 2 x 4 cm cell size. Any weight savings by using thinner cells could reduce performance and greatly increase the handling-breakage problem resulting in increased cost. Since the design is volume limited rather than weight limited, a thinner cell offers no advantage at this time.

The wraparound contact and large area combination provides several obvious assembly advantages. Fewer parts handled reduces assembly time and the rear-side only attachment method eliminates time consuming front-back welding steps. Long term, 15 year equivalent, thermal cycle data is not available for any type of cell, conventional, wraparound, large area or 2 x 4 cm. Lockheed recommends developmental testing on a continuous basis for the next two years to evaluate the large area cell-interconnect-blanket as an assembly. The substantial systems level cost savings warrants such testing at this time.

LOCKHEED MISSILES & SPACE COMPANY, INC.

The gallium arsenide cell selected for the two concentrator versions has several advantages over silicon--higher radiation resistance, a lower temperature coefficient resulting in a higher relative EOL power and 30% greater initial power (18% GaAs as compared to 14% Si). The disadvantage is that no GaAs solar cell has been produced outside of the research laboratory. LMSC takes the position that the need for the GaAs cell exists for systems like the Multi-kW S/A where the ultimate goal is low-cost long-life power systems. Quantities required warrant the development of the GaAs process for mass production. Cell producers and customers agree on a predicted cost for GaAs of 2 to 2.5 times that of silicon and that this is achievable in the 80's. This may be optimistic; however, LMSC is confident this price can be met when the commitment to use gallium arsenide is made. For the purpose of this study the 18% GaAs cell is believed the correct choice and that it can be produced at the price mentioned; however, it may not be ready until 1985.

The 2 x 2 cm - 12 mil conventional contact GaAs cell seems to be the most promising configuration from a brittleness and production capability standpoint. The conventional contacts will necessitate the use of conventional interconnects and adhesive bonding techniques to the blanket. Two design features must be considered: a highly compliant, in-plane (spring-like) interconnect that is unrestrained by the cell bonding adhesive. This combination has proven very successful in long term cycle tests conducted at LMSC amounting to 20,000 LEO type cycles.

The 0211-6 mil microsheet material with low cost coatings will be used on both cell configurations. FEP Teflon will be used for bonding the cover to the cell. The cost ratio of the most expensive cover-adhesive combination, ceria doped microsheet DC 93-500 to 0211 microsheet FEP Teflon was 5.5 to 1 without notable cell performance change.

The Solar Maximum Mission, SMM, is presently flying with FEP Teflon bonded covers, which supports its selection for initial multi-kW missions.

Several thin-film coated reflector materials are available today for use in solar array concentrators. Cold mirror films appear attractive over the more conventional aluminized Kapton materials. The ideal cold mirror reflects wavelengths responsive

to the solar cell and is transparent to the longer heat producing wavelengths. The ultimate conclusion is a cooler operating, higher performance solar cell array.

A proprietary SSR OCLI coating (471/3) on one mil Melinex was selected for the Low Cr concentrator reflector and the High CR primary reflector. The High CR secondary reflector will be a conventional aluminized Kapton in order to optimize the total reflector system. Mass produced SSR material is expected to cost the same as aluminized Kapton.

The cost to customer presented herein is for a delivered, on-orbit, 300 to 400 kW power generation system. This includes cost estimates for engineering and development, and capital investments required by component or assembly facilities, production, and Shuttle supported launch and on-orbit system operation for a 15 year time period.

An expected capital investment, for example, would be expansion of production facilities by the cell vendors to meet high weekly delivery rates required by multi-kW systems. This was estimated to be 2 to 3 million dollars. The real benefit from this capital outlay is more automation and uniformity of product which will probably have an eventual effect on cost reduction in the solar cell.

Including non-recurring and recurring costs, the GaAs Low CR concentrator solar array is the lowest cost at $3.16/kW-Hr ($326/Ave Watt), see Table 5-1, when operational for 15 years. The highest cost was the GaAs High CR concentrator at $6.17/kW-Hr ($736/Ave Watt). The difference was due to two additional launches (about $40 million/launch) required by the High CR system to deliver a comparable power unit to space and the high cost of the module structure. Therefore, on the basis of cost alone the High CR concentrator was eliminated from further consideration. This statement is also true for the Low CR silicon version where higher cost of structure and an additional launch eliminate it as a possibility. At a 25% higher cost than GaAs, $4.28/kW-hr ($484/Ave Watt), the low CR silicon cannot compete with GaAs cell availability and a developed deployable concentrator has not been established; however, these do not appear insurmountable in a 1985-1987 flight readiness time frame.

See Figure 5-1 for the graphical comparison.

LOCKHEED MISSILES & SPACE COMPANY, INC.

TABLE 5-1

SOLAR ARRAY COST/PERFORMANCE SUMMARY - LEO

|	PLANAR	LOW-CR	LOW-CR	HIGH-CR
SOLAR CELL TECHNOLOGY	SILICON	SILICON	GaAs	GaAs
GEOM CR/EFF CR	1/1	5/3.4	5/3.4	125/67.5
GROSS PLANE AREA	39,900 FT^2	125,000 FT^2	62,500 FT^2	82,400 FT^2
GROSS WEIGHT	9790 LB	25,800 LB	13,405 LB	41,850 LB
POWER OUTPUT BOL / 15 YR AVG	427 kW / 311 kW	594 kW / 380 kW	606 kW / 437 kW	576 kW / 384 kW
*SPECIFIC COST	$393/AVG WATT	$484/AVG WATT	$326/AVG WATT	$736/AVG WATT
*ENERGY LIFE-CYCLE COST	$3.63/kW-HR	$4.28/kW-HR	$3.15/kW-HR	$6.22/kW-HR

*1979 DOLLARS

LOCKHEED MISSILES & SPACE COMPANY, INC.
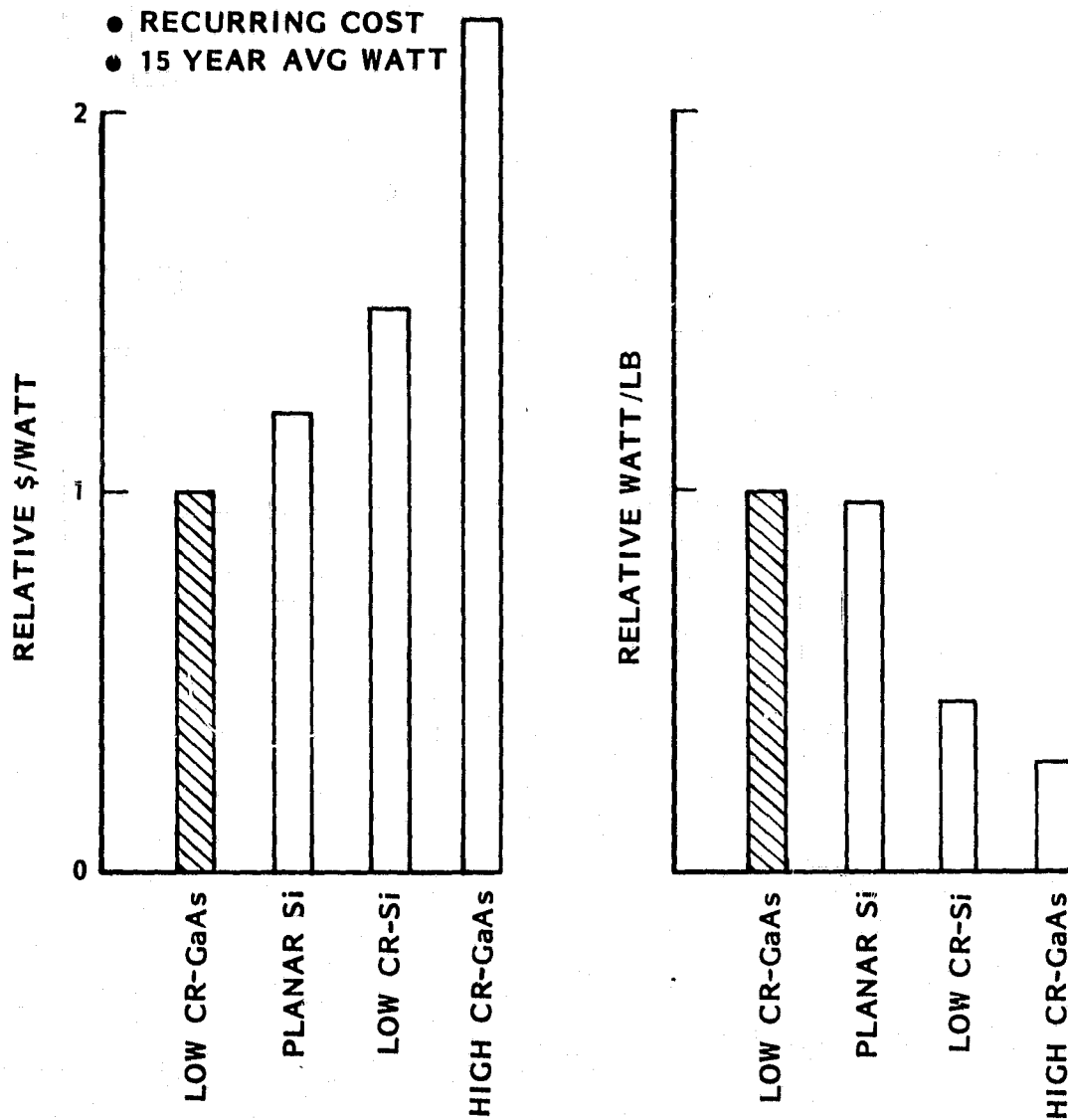
Figure 5-1 Relative Performance Comparison LEO Configurations

LOCKHEED MISSILES & SPACE COMPANY. INC.

The silicon planar configuration exemplifies the design with the least risk when considering 1983 readiness. It may be the lowest cost configuration at $3.75/kW-hr ($393/Ave Watt) if the GaAs cell is not then available.

An alternate to silicon for the planar system would be the use of GaAs when its available price drops to $25/2 x 2 cm cell.

GEO Configuration Discussion

The Low CR Silicon and High CR GaAs solar array concepts were eliminated from GEO cost and performance consideration basically due to the high cost of each system. Intentionally, the LEO and GEO concepts were identically configured. Self-deployment and modularity were directly applicable to both altitude versions without further modification. The only differing point is that the number of modules that can be delivered to GEO is restricted to 4300 lb (IUS) or 8400 lb (LTTV) by the orbital transfer vehicle. It turns out that both GEO configurations are weight-limited, but not volume limited even with the additional volume required by the orbital transfer vehicle in the Shuttle bay.

LMSC has selected the LTTV orbit transfer vehicle to deliver the GEO concept into orbit from a 150 nm drop-off altitude. LTTV payload capability reduces the planar array size by 25% or to three of four basic LEO modules while the Low CR GaAs version is reduced 40% or three of five LEO modules. The power is not directly proportional to size. A 15% further reduction in power is due to the greater predicted radiation degradation expected at GEO.

Table 5-2 compares the Planar and Low CR concepts. Both systems are in the 200 watt EOL average power category for easy comparison. The Low CR is a slight overall favorite again 8.5% and 4.5% improvement, respectively, for specific cost and energy life-cycle costs. Figure 5-2 provides a graphic means of comparing relative $/watt and $/lb for each concept. Again the Low CR indicated a slight improvement over the Planar array. This could be offset by a higher than anticipated GaAs solar cell cost.

TABLE 5-2

SOLAR ARRAY COST/PERFORMANCE SUMMARY – GEO

	PLANAR	LOW-CR
SOLAR CELL TECHNOLOGY	SILICON	GaAs
GEOM CR/EFF CR	1/1	5/3.4
GROSS PLANE AREA	29,925 FT^2	37,500 FT^2
GROSS WEIGHT	7345 LB	8045 LB
POWER OUTPUT BOL / 15 YR AVG	337 kW / 206 kW	375 kW / 231 kW
*SPECIFIC COST	$564/AVG W	$516/AVG W
*ENERGY LIFE-CYCLE COST	$6.18/kW-HR	$5.91/kW-HR

*1979 DOLLARS

LOCKHEED MISSILES & SPACE COMPANY. INC.
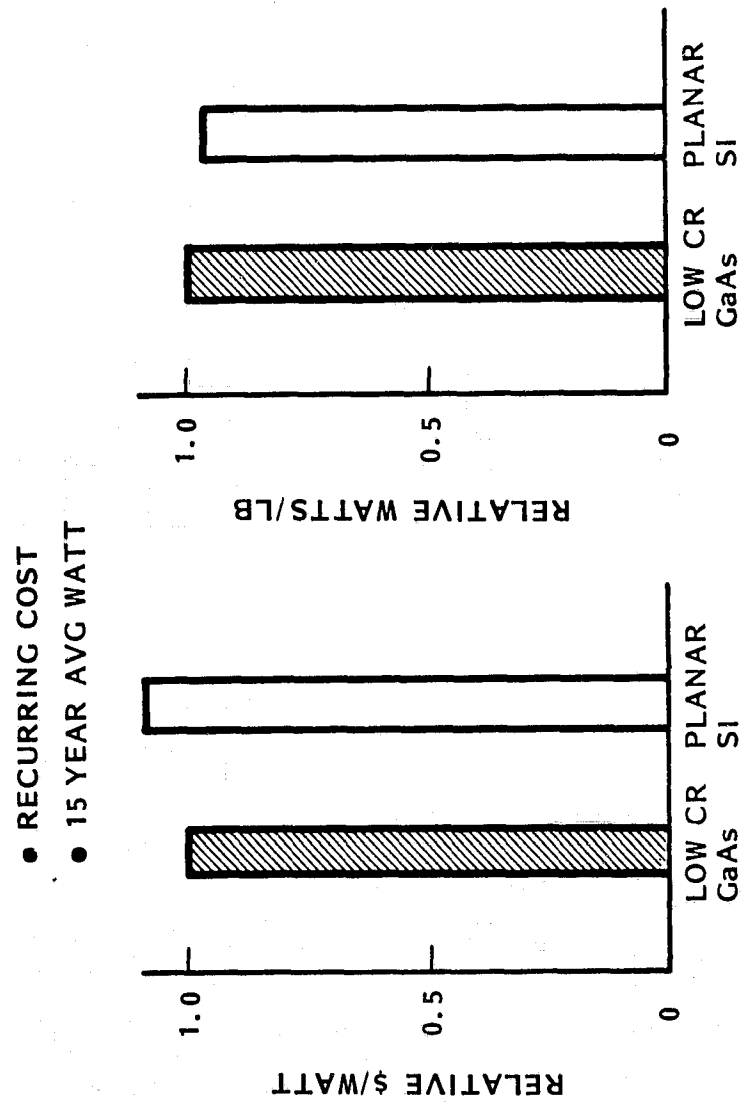
Figure 5-2 Relative Performance Comparison GEO Configuration

Recommended Design Concepts

Lockheed's recommendation, in compliance with the conditions of the Multi-kW Solar Array Study contract, is the low CR concentrator using gallium arsenide solar cells for both LEO and GEO applications.

The recommended concepts are summarized in Tables 5-3 and 5-4.

The technology suggested for the concept is available today. Problems that remain are in the category of design. Risks associated with long life can be minimized by specific technology development over the next three years. Section 6.0 will discuss technologies recommended for further development.

TABLE 5-3

LOW CR CONFIGURATION SUMMARY FOR LEO & GEO

CONCEPT	LOW CR CONCENTRATOR
MODULAR	YES
DEPLOYMENT TECHNIQUE	SELF DEPLOYABLE, MAST/BLANKET
BLANKET STOWAGE	FOLD-UP
EVA REQUIREMENTS	BACKUP REQUIREMENT ONLY
SOLAR CELL	GaAs – 12 MIL (2 x 2 cm)
COVERGLASS	0211 MICROSHEET – 6 MIL
COVER ADHESIVE	FEP TEFLON
REFLECTOR MATERIAL	SPECTRAL SELECTIVE REFLECTOR
GEOMETRIC CR	5
EFFECTIVE CR	3.4

TABLE 5-4

LOW CR COST AND PERFORMANCE SUMMARY FOR LEO & GEO

PARAMETER	LEO	GEO
NO. OF SOLAR CELLS REQ'D	2.0×10^6	1.2×10^6
SYSTEM WEIGHT – LBS	13,405	8,045
GROSS PLANE AREA – FT^2	62,500	37,500
CELL AREA – FT^2	12,656	7,594
POWER (15 YR AVG.) kW	437	231
WATTS/FT^2 (CELL AREA)	34.5	32.9
WATTS/LB	32.6	28.7
SPECIFIC COST $/WATT	326	516
ENERGY LIFE-CYCLE COST $/kW-HR	3.15	5.91

STUDY OF
MULTI-kW SOLAR ARRAYS
FOR EARTH ORBIT APPLICATION

Section 6

Recommended Further Technology

NASA   LOCKHEED
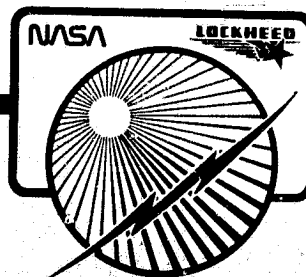
6.0 RECOMMENDED FURTHER TECHNOLOGY

The magnitude of this study is in the realm of the "Step Beyond SEP" category.
Extensive experience has been drawn upon from early programs dating back to the
Large Space Station Solar Array (1970) to the current SEP, PEP and 25 kW Power
System efforts. All have contributed to identifying the Low CR Concentrator design
for Multi-kW applications. Usable ideas were closely examined and designs were
sufficiently detailed to assure that the structure, cell blankets and reflectors would
all inter-relate with a high degree of confidence. However, in considering the array
size and expected life cycle, other elements were exposed where sufficient test or
flight experience did not exist. Short term effects of thermal cycling, for instance,
are fairly well understood but their long term relationship can only be estimated.
Examination of areas where proven designs were not available clearly showed that
present technology could be applied to the needed designs. As an example, the
solar cell and the interconnect can withstand the environment independently but
may not when tested as a bonded assembly.

As such, four areas are suggested where further development is essential in order
to be prepared to meet the conditions of "practicality" and "technology readiness"
by 1983.

LMSC recommends the following major topics as essential to support the selected
Low CR Concentrator conceptual design. Start dates and estimated costs are suggested
where appropriate.

       (a)   Solar cell development - GaAs and large area silicon wraparound
            cells

       (b)   Manufacturing process development and characterization for
            components and assemblies

       (c)   Design and develop blanket assembly with the proposed components

       (d)   Mechanism development to support selected concentrator and
            deployment designs

6.1 SOLAR CELL DEVELOPMENT

Optimization of low cost solar array requires the review of existing solar cell technology and the determination by further development of what portions of that technology have practical application to the Multi-kW Program. Gallium arsenide, large area silicon solar cells and low cost coverglass coatings are prime candidates for development over the next several years.

6.1.1 GaAs Development

- Detailed definition of manufacturing processes of GaAs

- Demonstrate the conversion of the GaAs solar cell from the laboratory level to production using production equipment and personnel

- Determine optimum cell size and thickness to withstand assembly and handling conditions

- Develop production capability that can be sized to deliver Multi-kW quantities required for blanket assembly and develop associated costs

GaAs technology is at the point when this effort can begin. It is suggested that cell contractor efforts begin by June 1980.

6.1.2 Large Area Wraparound Silicon Solar Cells

The silicon solar cell is a viable backup for the GaAs cell in event that production difficulties arise.

- Continue to support wraparound dielectric development and fabrication programs.

- Evaluate optimum cell size relative to ingot size and cell fabrication and handling conditions.

Effort should continue as supported by NASA and Lockheed.

6.1.3 Coverglass - Low Cost Coating Applications

AR coatings account for 50% of the cost of a cover, and higher in the case where microsheet is used as the host material. Motorola, under contract to JPL, has been investigating two low cost coatings which appear to have application. Coating manufacturers should be encouraged by contract to determine feasibility of these and other low cost coatings and their application to space.

6.2 MANUFACTURING AND PROCESS DEVELOPMENT

The adaptability of a solar array component to higher levels of assembly must be verified through environmental testing and the results applied to the final blanket and reflector designs.

The following areas require specific attention in order to properly support the Multi-kW readiness time frame.

6.2.1 GaAs Solar Cell

- Handling - receipt of cell through blanket assembly and test
- Weldability - develop weld schedule for contact pull strength and performance optimization
- Cell performance characterization - conduct electrical/environmental characterization of cell

The starting date for this activity should follow about one year behind cell development. This appears to be close; however, user problems should be fed back to the cell producer in a timely manner.

6.2.2 Large Area Silicon Wraparound Solar Cells

Large area cells are known to cost less per unit area and a reduction in blanket assembly time is indicated; however, the handling, stowage and deployment conditions must be compatible with the cell size. This study discusses only the 5.9 x 5.9 cm cell; however, the optimum size may be larger or smaller as dictated by the overall economics of the solar cell and total blanket assembly.

Several parameters should be expanded over the existing level of effort.

- Weld process development – develop process compatible with required interconnect pull strengths and cell performance optimization

- Handling and blanket fabrication – confirm that the cell can withstand all expected loads, folds, etc.

- Environmental characteristics – the selected cell must be characterized.

6.2.3 Spectral Selective Reflector

The SSR material offers definite advantages to existing reflector materials but requires additional refinement both in coatings and demonstrated producibility. Time phasing must be coordinated with solar cell availability.

- Optimize reflector coatings to specific cell response and to reflector assembly angle of incidence (60°).

- Evaluate degradation of SSR characteristics relative to environmental effects.

6.2.4 Teflon Cover Bonding

The application of FEP Teflon in bonding covers to conventional sized cells is known. Effects are not known for FEP application to large area silicon or GaAs cells. Processes need to be developed and environmental compatibility established. Time phasing must be coordinated with solar cell availability.

6.3 BLANKET TECHNOLOGY

Proper design of the cell-blanket assembly is key to long life capability. Interconnect materials and configuration, adhesive patterns (GaAs cells only), cell laydown and blanket stiffeners must be evaluated as a system relative to handling and operational or environmental stressing.

This effort should begin with blanket-interconnect-stiffener design prior to the delivery of early GaAs 2 x 2 cm cells and large area silicon cells. Suggested areas of development are as follows:

- Develop cell (GaAs)-interconnect – blanket design. Evaluate by test the effect of handling and environment on the final blanket assembly.

- Repeat using large area silicon configuration.

- Continue to develop automated blanket fabrication and cell attachment techniques.

6.4 DEVELOP MECHANISMS

The mechanical and electrical performance of a system must be verified by test. Lockheed recommends that this be accomplished by a full-scale demonstration of a TTP segment--from stowed to operational configuration. The effort described herein should begin by mid 1980.

- Design and fabricate Low-CR Concentrator element(s) to demonstrate stiffening and tension techniques necessary to maintain collector efficiency

- Demonstrate stowage/deployment techniques of array reflector and cell blanket assemblies

- Demonstrate stowage and deployment of array containment structure

- Evaluate improved zero-g simulation techniques for proof testing system deployment

LOCKHEED MISSILES & SPACE COMPANY, INC.